

# Impact Assessment of MGNREGA Farm Ponds Using Remote Sensing

Ramita Sardana

*Department of Computer Science  
Indian Institute of Technology  
Delhi, India  
mcs212857@iitd.ac.in*

Sanjali Agrawal

*Department of Computer Science  
Indian Institute of Technology  
Delhi, India  
cs5180419@iitd.ac.in*

Saketh Vishnubhatla

*Department of Computer Science  
Indian Institute of Technology  
Delhi, India  
saketh181199@gmail.com*

Shruti Kumari

*Department of Computer Science  
Indian Institute of Technology  
Delhi, India  
cs5180420@iitd.ac.in*

**Abstract**—With substantial financial resources being allocated to government programs aimed at providing livelihood benefits to rural communities in India, it becomes crucial to assess the actual impact created by these initiatives. This research focuses on evaluating the impact of Natural Resource Management (NRM) farm ponds constructed under government schemes such as the Mahatma Gandhi National Rural Employment Guarantee Act (MGNREGA), a demand-driven wage employment program. Utilizing remote sensing techniques, we analyze the changes that occur from the pre-intervention to post-intervention period.

The primary objective of our study is to investigate the effects of construction of farm ponds on vegetation indices and cropping intensity over time. To achieve this, we employ various analytical methodologies, including Difference in Differences, Synthetic Controls, and Double ML. Our findings predominantly indicate positive treatment effects in terms of vegetation-based outcome indicators during the Rabi season. However, our analysis of cropping intensity reveals a lack of any discernible positive average treatment effects within our study area. The methodology employed in this study establishes a robust framework for assessing the impact of NRM interventions, thereby enhancing the planning and implementation of future NRM projects.

**Index Terms**—MGNREGA, farm ponds, impact assessment, irrigation, counterfactuals, Propensity Score Matching, Difference-in-Differences, remote sensing, NDVI, Cropping Intensity, Double ML, Synthetic Control

## I. INTRODUCTION

Natural Resource Management (NRM) works are taken up under the government welfare schemes like MGNREGA, PMKVY, etc. Many watershed structures like farm ponds, bunds, check dams, wells, etc. are built under these programs. These structures are designed to support farmers in irrigation and daily agricultural activities, with the goal of providing livelihood benefits.

Evaluating the impact of these structures is crucial to facilitate improved planning for future projects. It is also essential to monitor and analyze the surrounding factors that influence

significant changes and subsequently integrate this valuable data into future planning processes. Unfortunately, at present, there is a dearth of formal methodologies for conducting these assessments.

The availability of high-resolution satellite imagery has provided ample opportunities for monitoring changes in agricultural farmlands. Platforms like Google Earth Engine offer convenient access to download and utilize image datasets from various satellites such as Landsat 7, Landsat 8, Sentinel-2, Sentinel-3, and Sentinel-5. These datasets present valuable resources for research purposes, enabling in-depth analysis and investigation.

This study aims to utilize satellite images to quantitatively assess the changes caused by the farm ponds built in 2017 under the government scheme Mahatma Gandhi National Rural Employment Guarantee Act (MGNREGA), which are observable through remote sensing techniques. Specifically, the research aims to:

- Identify sites from the MGNREGA data available on the MIS database, where planned NRM water-based interventions (farm ponds in our case) were undertaken. [60]
- Monitor pre-post indicators for vegetation and cropping intensity.
- Develop a causal analysis framework to understand the change in outcome indicators.
- Analyze and reflect upon the results obtained from the evaluation and derive key learnings from the study.

In the absence of scientific analysis, the construction of assets can result in wastage of efforts and resources. During a field visit to the Gaya district of Bihar, several discrepancies were identified in the existing assets. One such example is a farm pond depicted in Figure 1, which was constructed without

proper scientific investigation. Unfortunately, this pond proved to be ineffective as it failed to retain water due to the presence of a 5 km long lineament beneath it. Through remote sensing techniques, it was discovered that the water was seeping underground through this lineament, rendering the pond empty. Hence, the entire expenditure invested in constructing the community pond turned out to be futile. Moreover, this had no positive impact on the nearby farms as the water did not remain long enough for utilization.



Figure 1: Community Pond rendered useless due to a lineament below

There are many complexities associated with assessing the impact of farm ponds when we observe from the sky using remote sensing methods, such as:

- Conversion to cropping land: Some farmers who don't find the farm pond useful, may fill it up again with soil for cropping. This can lead to inconsistencies in the data pertaining to the existence of the farm ponds.
- Delineation of farms: It is impossible to predict at what distance or in which farms around the pond, the water will be shared for irrigation through pumps (Figure 2).
- Non-uniformity in usage: The farm pond may be used for other purposes like pisciculture instead of or in addition to irrigation (Figure 7). The impact of farm ponds having other uses is difficult to assess.
- Seasonal Impact: Farm ponds may hold water till the Zaid season or sometimes dry up in the Rabi season itself (as shown in Figure 3). It is difficult to estimate the season in which the farm pond will be used for irrigation of crops.
- Crop Yield Impact : Some farm ponds may help increase the crop yield through protective irrigation in a drought year. However, accurate crop yield data is not available at the farm level.
- Period of impact: Some farmers may immediately start using the farm ponds and grow crops in Rabi/Zaid season. Some farmers wait a year or more before relying on the farm pond for irrigation. Hence, there is a variation in which year(s) the actual impact of the farm pond can be observed.



Figure 2: Farm pond water shared with other farmers through pumps



Figure 3: Farm pond water shared with other farmers through pumps

- Pumping of groundwater into farm ponds: Some farm ponds are filled with groundwater using pumps for fisheries when they dry up. This is a misleading factor in that the farm ponds hold water from rainfall or natural drainage systems.
- Data issues (inaccuracy in geotagging the farm ponds): The geotagged position (latitude/longitude) of the pond may lie on one corner or at a distance from the pond, making it difficult to assess the extent of the farm pond inside the farm.
- Data issues (work type): Some bigger water bodies like Ahars or maintenance works are wrongly mentioned as farm ponds in the work type while digitizing the information in the database.
- Size of farm pond: It is difficult to distinguish bigger farm ponds from smaller ones, and their impact would vary with size. Moreover, some farmers make their own investments to deepen their ponds in order to achieve the intended use, which causes inconsistencies in our data.

The rest of the paper is organized as follows. Section II discusses the related work in the direction of impact assessment and change detection using satellite imagery as input. The next section III describes the datasets being utilized and the methods IV used in the project implementation. Section V discusses the results of the work. Finally, the conclusion is presented in Section VI. The rest of the sections contain the output images of the impact assessment.

## II. RELATED WORK

There have been numerous studies and research conducted to assess the impact of government schemes or the construction of farm ponds/other watershed management structures. Some studies present the implementation of causal inference techniques on observational data to assess the impact of certain developments in an area. Owing to the ease of access of remote sensing data from satellites like Landsat and Sentinel at very good resolutions, some other studies have used satellite data for getting the observed outcome indicators to assess the implementation of some policies/practices in the agricultural domain. Our study combines causal inference techniques with observational data from satellites to assess the impact of the construction of farm ponds under the government scheme of MGNREGA.

Prasad et al. have assessed the hydrological, economic and social impact of farm ponds constructed through system dynamic analysis models [18] [40]. Muralikrishnan et al. [20] have also mentioned the impact of watershed development through farm ponds by using random sampling and interview techniques. Similarly, a study conducted by Fischer et al. [1] assesses the impact of water management on different categories of farmers through interviews and analysis techniques. Another study by Sreedevi et al. [4] assesses the impact of watershed development on crop production and other variables on the site as well as on downstream villages (off-site) through field visits, focused group discussions and analysis methods.

A study specifically on assessing the impact of farm ponds has also been done by Reddy et al. [23] but it uses the survey method with statistical analysis, limited to a particular area and to farm ponds constructed under a different scheme PMKSY.

Even there are some studies sponsored by the Government of India in which the impact assessment of the MGNREGA scheme and assets built under the scheme are published [49] [44], but they find the impact on the livelihood of the rural population and are mostly qualitative in nature. Similarly, there is a study done by GIZ corporation for a qualitative impact assessment of the projects taken under the MGNREGA scheme through interviews and focused group discussions [48]. A study by Center for Study of Science [50] quantifies the climate co-benefits of MGNREGS works but most of the techniques used are manual, including field data collection for the estimation of biomass and soil organic carbon. This kind of approach can be followed for a limited area of interest

and cannot be scaled across regions/states/countries without massive expenditures being involved.

Buxton et al. have conducted a study to assess the impact of bottom-up driven community tree planting programs and their impact around the neighborhood, showing positive spillover effects in NDVI up to 360m around the sites over a decade [2]. Motivated from this work, we have also followed the strategy of distance-based DiD analysis to finalize the buffer size of impact of farm ponds. This is mentioned as ring-buffer analysis section IV-C.

Ugalde et al. [3] have used Difference in Difference (DiD) techniques to evaluate changes in metrics of the effectiveness of a scheme in the Gulf of Mexico, namely PHS (Payments for Hydrological Services), and proved that the impact is different in low and high works density areas. This is the motivation for our Stratified DiD approach.

Ratledge et al. have leveraged remote sensing for local-livelihood measurements (outcome variable) to assess the causal impact of electricity access on the wealth of the community [7]. They compared the techniques of Difference-in-Difference (DiD), Synthetic Control with Elastic Net (SC-EN) and Matrix Completion (MC) and concluded that MC and SC-EN are more robust over DiD in the absence of pre-treatment parallel trends. Overall, they have shown that ML based causal estimators outperform traditional alternatives in assessing causal impact.

A study conducted by Deines et al. aimed to analyze the crop yield outcomes in 6 states of United States and assess the impact of cover crops using Causal Forests [13]. They have leveraged satellite data fused from Landsat and Modis at 30m resolution to train a machine learning model for detecting the presence of cover crops as well as remotely sensed crop phenology for each satellite pixel to estimate pixel-level yields. This is an interesting application of Causal ML and a motivation for us to use this method in our study too.

Giannarakis et al. demonstrate the applicability of causal machine learning, specifically Causal Forest Double Machine Learning (DML), to estimate the impact that two agricultural practices (Crop Rotation and Landscape Crop Diversity) had on an outcome Net Primary Productivity (NPP) and assist in policy evaluation from observational data. Similarly, there is another study by Stetter et al. to assess the heterogenous farm-level impacts of participation in AES (agro-environmental schemes) using Causal Forest DML and aid in policy planning. In our study, we are trying to assess the impact of the MGNREGA policy from observational data so as to aid in policy planning. Hence the methodology of Causal Forests DML is suitable for our study and discussed in Section IV-F.

## III. DATASET

The district Jamui in Bihar, India (Figure 4) was chosen as the study area for our preliminary analysis. It was visually

observed from the satellite images of the year 2015 and year 2018 that there had been an improvement in the vegetation index NDVI in this region. The region consists of 30% forest area and 25% cropped area [9].

A significant portion of agriculture in the district relies on rainfall, with limited irrigation infrastructure. The cultivation of multiple crops in the region remains limited, as the cropping intensity in the district stands at approximately 143%, ranging from a minimum of 108% in the Chakai block to a maximum of 165% in the Jamui block [9]. There is an opportunity to improve irrigation in the region through surface water sources as well as groundwater irrigation methods.

Here, Cropping Intensity is a measure of how many crops are grown in a single agricultural year within a specific field. It can be calculated using the following formula:

$$\text{Cropping Intensity} = 100 * \frac{\text{Gross Cropped Area}}{\text{Net Sown Area}}$$

Gross Cropped Area refers to the total area that is sown at least once during a specific year. This includes counting the same area multiple times for each sowing. It can also be referred to as the total cropped area or total area sown.

Net Sown Area represents the total area that is sown with crops and orchards. If an area is sown multiple times in the same year, it is only counted once when calculating the net sown area.

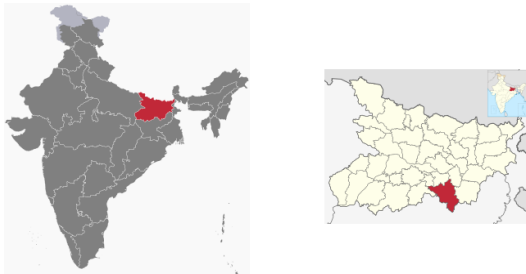


Figure 4: Jamui district in Bihar, India

After the preliminary analysis, the study was expanded to the agro-ecological zone number 13 [75], in which Jamui district lies. There are 38 districts lying in this zone as shown in Figure 5. The region experiences a climate characterized by hot and wet summers, along with cool and dry winters. The average annual rainfall in the area ranges from 1400 to 1800 mm. The soils in the region consist mainly of level to very gently sloping alluvium-derived soils. Rainfed agriculture is predominant in the area, with crops such as rice, maize, pigeonpea, and moong commonly cultivated during the kharif season. In the post-rainy (Rabi) season, crops like wheat, lentil, pea, sesamum, and occasionally groundnut are grown, relying on residual soil moisture supplemented by one or two protective irrigations during critical growth stages.

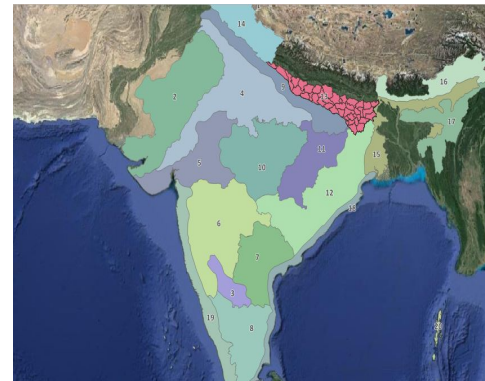


Figure 5: Agro Ecological Zone 13: Eastern plain hot subhumid (moist) eco-region

We have multiple districts within the agro eco region, but we are specifically focusing on districts where the centroid is located inside the region. The reasoning behind this is to avoid analyzing districts that have a small proportion of their area within the region. By excluding such districts, our analysis can be more comprehensive and not limited to a small subset of assets within those districts. For instance, Patna district is mostly situated outside the region, so it has not been included in our considerations.



Figure 6: Agro Ecological Zone 13: Districts

#### A. Preliminary Analysis

The objective of the project is to analyse the impact of farm ponds constructed. We are using the MGNREGA MIS data to get works and metadata done under the MGNREGA, and the geolocation and Asset IDs of the works has been crawled from Bhuvan portal. To verify if the ponds that we are analysing were actually built or not, we sampled some random points from the database for Jamui district. The analysis was motivated by following reasons:

- During the investigation, certain examples were found where the data indicated the presence of ponds, but in reality, these ponds did not exist. This discrepancy suggests that either the ponds were never constructed (potentially indicating corruption cases), or they were filled with mud again due to the farmers' lack of utilization.

There was one such farm pond which was supposedly constructed on government land in Dema village in Tola

Pathra in Gaya. On visiting the location during our field trip, we could not see any trace of farm pond nearby and on asking the local people we came to know that there has no pond been built there in the last few years.

- Even in cases where the ponds did exist physically, they did not necessarily result in any beneficial outcomes for the farmers. This lack of positive impact could be attributed to various factors such as the pond's limited capacity, insufficient rainfall to sustain water levels, or the pond being utilized for other purposes like pisciculture, as depicted in Figure 7. These factors contribute to the ineffectiveness of the ponds in fulfilling their intended purposes and benefiting the farmers.



Figure 7: Farm Pond being used for pisciculture

The preliminary analysis involved the following steps, which are subsequently described in detail:

- Verify the presence of the farm pond after 2017 through Google Earth Pro timeline viewer.
- Analyze the NDVI composite raster image for each season and annual cropping intensity from LULC raster image to visually observe the changes from pre-intervention period (2015) to post-intervention periods (2018, 2019 and 2020).
- Generate, analyze and observe the NDVI time series on some random sample points around the farm pond to check for changes in cropping intensity from pre-intervention period (2015) to post-intervention period (2018) through the number of peaks.
- Statistical tests to establish the difference in the pixel values of NDVI in pre and post intervention periods.

We randomly selected and analyzed 100 ponds out of a total of 485 ponds that were constructed in the year 2017. For this analysis, we utilized the Google Earth Pro timeline viewer to visualize the location of these ponds from before 2017 until the latest available image in 2022 (a sample shown in Figure 8).

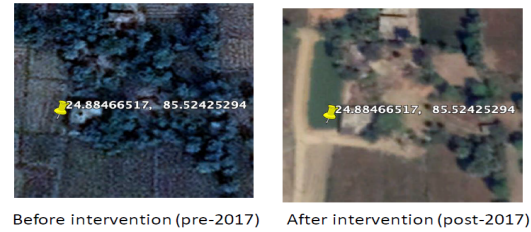


Figure 8: Existence before and after period of intervention

During our analysis, we observed various scenarios among the sampled ponds. Some ponds were built in the year 2017 and remained functional, while others constructed in the same year were never filled with water, rendering them unusable. Additionally, we found instances where ponds existed before 2017 but had dried up, only to be filled again after 2017, suggesting some form of maintenance or restoration.

The results of this analysis are depicted in Figure 9, providing a visual representation of the different scenarios and outcomes observed among the sampled ponds.

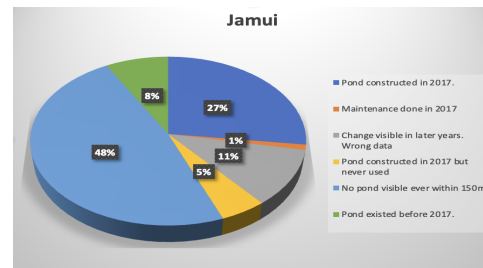


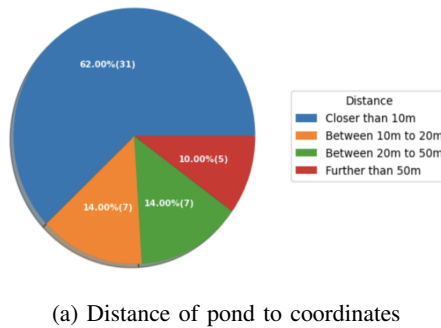
Figure 9: Ponds distribution in Jamui

After considering the availability of a sufficient number of ponds for analysis, we proceeded with the data. However, it is crucial to acknowledge concerns regarding the data's reliability, as approximately 56 percent of the locations exhibit no discernible change before and after 2017. Among these locations, at 8 percent, ponds were observed to exist both before and after 2017, while in the remaining locations, no visible pond boundaries were observed at any point in time. This discrepancy raises doubts about the data's accuracy and reliability, which should be taken into account during the analysis.

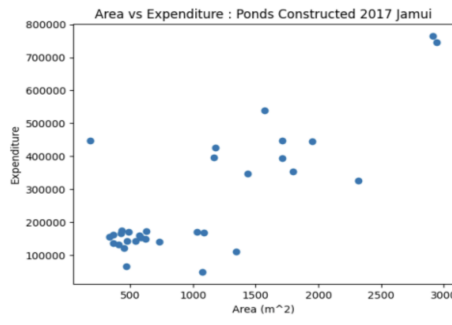
In addition, we utilized the Google Earth Pro ruler tool to calculate the closest distance between the specified coordinates in the data and the nearest farm pond on the rest 44% locations. If a pond was found within a 150-meter radius of the location, it was considered the corresponding pond. Otherwise, it was determined that there was no pond in the vicinity of the specified coordinates.

During workshops with experts from GIZ, it was highlighted that farm ponds of different sizes could have varying impacts.

Consequently, it was suggested to analyze them separately. Since there was no specific column indicating the size of the farm pond in the NREGA data, the column *total expenditure* was used as a proxy for pond size. The area of the farm pond, calculated using the Google Earth Pro ruler, was plotted against the corresponding total expenditure values. The findings presented in Figure 10 indicate that the *total expenditure* column can be reasonably used as a proxy for farm pond size. However, it is important to acknowledge any limitations or assumptions associated with this approach.



(a) Distance of pond to coordinates



(b) Area v/s expenditure in ponds

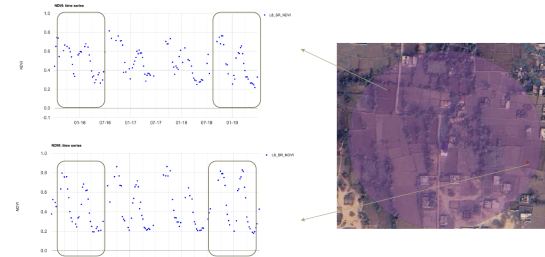
Figure 10: Analysis of Jamui farm ponds of 2017

After validating the data, a preliminary analysis was conducted on the farm ponds that were confirmed to have been built in 2017. A random sampling approach was employed to select farm ponds from Jamui district. This analysis focused on assessing the outcomes related to NDVI (Normalized Difference Vegetation Index) and LULC (Land Use/Land Cover) changes. We observed positive changes in the majority of the farm ponds during the post-intervention years. One such sample farm pond's analysis is shown in Figure 11.

It was also validated and established through multiple statistical tests and plots like Cumulative Distribution (CDF) Plots, KS (Kolmogorov-Smirnov) test, QQ (Quantile Quantile) Plot, KL Divergence test of these sample ponds that the distribution of NDVI values in the pixels around the farm ponds were statistically different in pre and post periods. It was also observed in such tests that there had been statistically significant positive changes in NDVI during Rabi and Zaid seasons after the intervention period. A positive KL divergence was observed in many sample ponds in the Rabi and Zaid seasons. The NDVI



(a) NDVI and LULC Rasters Analysis



(b) NDVI Time series Analysis

Figure 11: Preliminary Manual Analysis of a randomly sampled farm pond

distribution in pre and post period of one such sample farm pond in Jamui district located at (24.52697209, 86.46447384), is shown in Figure 12.

#### B. Dataset Preparation

In these regions, a total of approximately 17 lacs MGNREGA assets were constructed. We focused on interventions related to water structures that could potentially affect vegetation indices in the area. To identify these interventions, we filtered out works whose Work Type included specific keywords determined through manual analysis, like pond, well, tank, etc.. These identified works are referred to as "waterworks" going forward. Out of around 2 lacs waterworks in the region, there were around 1 lac were Farm Ponds.

From our interaction with the Program Officer of MGNREGA in Gaya, we learned that MIS asset creation date, refers to the date when the asset creation job is finished, when the closure of work is done on MIS (which may be anytime later too). Work start date mentioned in the MIS is when the creation of an asset is started after funds allocation. Hence, we used *Work start date* column to extract the year in which the work was done. Around 15000 farm ponds did not have a valid *Work start date* value, hence these were dropped from the analysis. A district wise distribution of total and valid farm ponds is shown in the figure 13. There were 5 districts - Siwan, Saran, Vaishali, Supaul, and Sheohar - which did not have any farm pond with valid *Work start date*, hence these districts would be excluded from our analysis.

The year 2017 was selected as the intervention period for the following reasons:

- Considering the availability of dynamic world and Land-

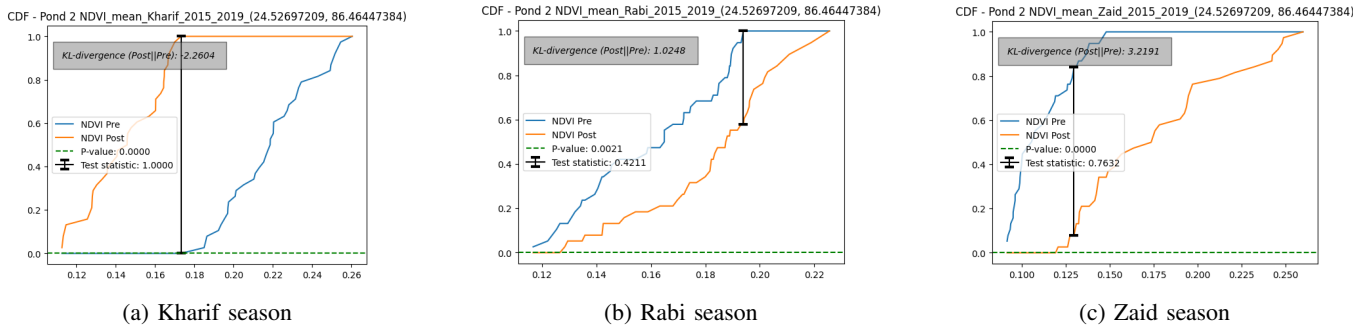


Figure 12: Statistical Analysis of pre vs post period distribution of pixel values of NDVI in 100m buffer around a randomly sampled farm pond at location (24.52697209, 86.46447384) in Jamui district: Positive KL divergence in Rabi and Zaid season

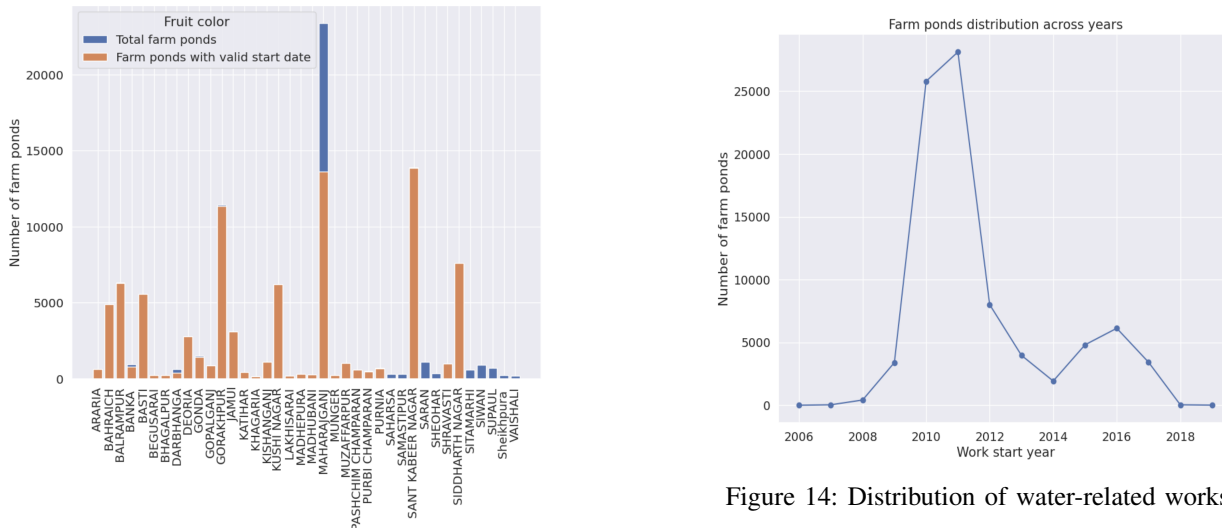


Figure 13: District v/s farm pond distribution

sat 8 images from 2015 onwards, the analysis had to be focused on assets constructed after 2015.

- Due to poor outputs observed in 2015 for IndiaSAT, the decision was made to utilize IndiaSAT data starting from 2016 onwards. As the LULC outputs are available from 2016, it became necessary to establish the base year from hydrological year of 2016-17., hence it was imperative to analyse assets built after 2016.
- The MGNREGA data depicted that maximum farm ponds were built in 2017 (after 2016) as depicted in Figure 14.

We also observed the trends of mean annual precipitation in the agro-ecological zone 13 as shown in Figure 15 and Table I. The district-wise data for the number of large farm ponds constructed along with the annual mean precipitation over the years in each district is presented in Table V in Appendix A. Considering that the treatment period is 2017 and the average annual rainfall is much less in the next year 2018, we expected that the actual impact of the farm ponds could be visible in 2019 onwards.

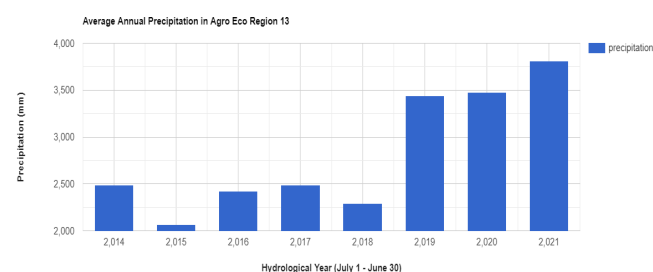


Figure 15: Rainfall trends in AEZ 13

Year	Precipitation (in mm)
2014	2,489.10
2015	2,068.76
2016	2,418.25
2017	2,487.29
2018	2,287.86
2019	3,443.26
2020	3,473.09
2021	3,807.69

Table I: Average annual precipitation in AEZ 13 over the years

We have 3407 farm ponds in the region which were constructed in the year 2017. Our objective is to analyze the impact of these farm ponds through different vegetation indices such as NDVI and cropping intensity. The cropping intensity of an area is the number of crops that are grown in the region in a particular hydrological year. We also met with a couple of farmers whose land's cropping intensity was increased due to the construction of farm ponds on the land. We wanted to focus only on farm ponds which were built on croplands hence we filtered out the ponds which were built either on single, double, or triple cropping intensity lands. Google's Dynamic World does not have these low level classes in their land use land cover classification, hence we are using an improved version of IndiaSat paper [71] which is a work in progress under Professor Aaditeshwar Seth.

Since our analysis is on a 100m buffer around the coordinates of the asset (refer Section IV-C), we take a mode of the LULC class (single, double, triple, or something else) as the class of the particular site. Adopting this methodology, we ended up with only a thousand farm ponds as in most of the buffers there were a lot of built-up pixels (homes of the farmers), trees (big trees in the croplands), or water (the pixels on the farm pond itself), but on analysing these buffers closely it was evident that these were, in fact, in the regions with double cropping intensity as is shown in figure 16a.

In order to mitigate this issue, we masked out all the pixels that did not belong to cropland areas (figure 16b). Next, we determined the most frequently occurring level of cropping intensity within a specified buffer around each farm pond. Lastly, we focused our analysis solely on farm ponds situated within one of the three designated cropland classes.

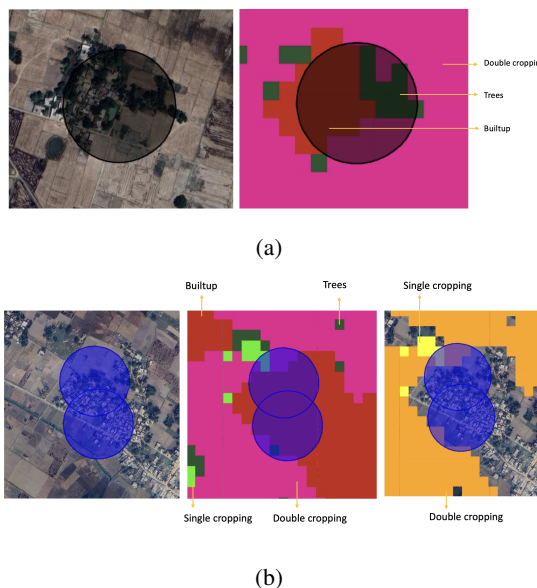


Figure 16: Non cropland pixels in farm pond buffer

We have a total of 2945 farm ponds for our analysis. To analyze only large ponds which might have a reasonable

effect around them, from Figure 10 we can see that, for an expenditure of Rs. 1 lakh, the size of the pond corresponds to  $500m^2$ . So we filtered ponds based on expenditure made on each asset and eliminated ponds with less than Rs. 1 lakh spent. Hence, we ended up with 2136 farm ponds over which we have calculated average treatment effects with various methods. The whole sampling procedure for treated points is shown in Figure 17.

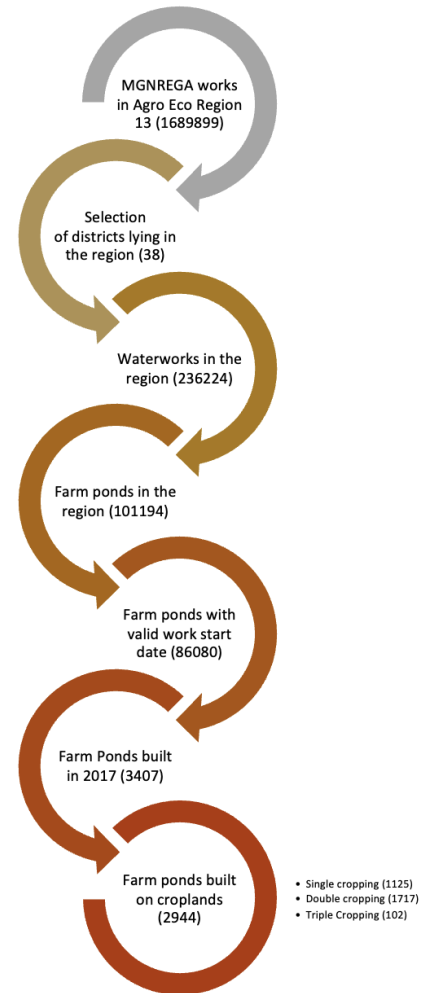


Figure 17: Selection of Farm Ponds for analysis

The subsequent task involves identifying counterfactuals for the treated points. This can be accomplished by acquiring a dataset comprising points where no interventions were implemented. The treated points can then be paired with suitable control points from this dataset, creating a matched sample that serves as the counterfactuals.

A two-level masking process was employed to select control points for sampling, as outlined below-

- **Cropland mask:** To ensure similarity in geography between the treated points and control points, the control

points were sampled exclusively from areas classified as single, double, or triple cropping by IndiaSat. This sampling strategy aimed to match the control points with the treated points based on their cropland classification, thereby creating a more accurate comparison group for evaluating the effects of interventions. The cropland mask for the agro eco region is shown in figure 18

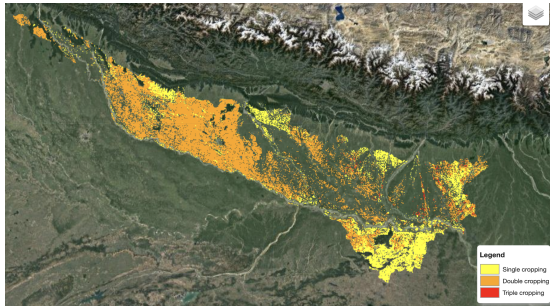


Figure 18: Cropping intensity

- NRM buffers:** To ensure that control points are unaffected by interventions that could impact vegetation indices, a buffer zone of 500 meters was created around all waterworks implemented through the MGNREGA, shown in figure 19. This buffer was established based on field visits and preliminary analysis, which suggested that such waterworks could have a substantial influence on the surrounding area. By masking out the buffers, the control points were selected from areas outside these buffer zones, ensuring they were not subject to any NRM interventions. This approach helps maintain the integrity of the control group and provides a reliable basis for comparison with the treated points.

After masking out the buffers around the waterworks and non-cropland regions, a composite mask is created. This composite mask combines the masked out buffers and areas that are not classified as croplands. From this composite mask, control points are sampled exclusively from regions that are not in close vicinity to any NRM intervention and are located on croplands.

Our objective is to match an asset to a control point that is located in the same block. By matching treated points with corresponding control points from the same block, we can account for potential confounding variables that have not been included in our analysis, as explained in section IV-A1 and strengthen the validity of our analysis.

To ensure a robust matching process, we aim to have a sufficient number of control points available. The number of control points selected is determined by taking the maximum value between 20 and three times the number of treated points within the same block.

Once we have obtained the treated points and control points datasets, we merge them to create a consolidated dataset. This dataset will consist of "n" treated points and approximately

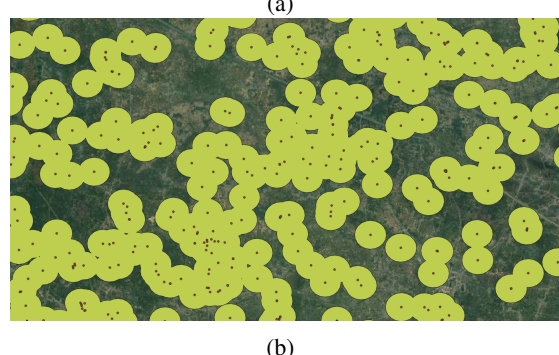


Figure 19: Buffers around waterworks

three times "n" control points. The matching process will be conducted using this dataset, enabling us to proceed with further analysis. This approach allows us to compare the outcomes between the treated and control groups more accurately and draw more reliable conclusions from the data.

#### IV. METHODOLOGY

The research methodology incorporates several approaches to analyze the outcome indices of both the assets and their corresponding counterfactuals or control points. These methods include difference in difference (DiD), stratified DiD, synthetic controls and Double ML models. By employing these methods, we aim to robustly analyze the impacts of the NRM intervention on the sites.

##### A. Counterfactuals

To ensure that the observed impact is attributable to the NRM works and not influenced by external factors such as temporal variations in precipitation, it is crucial to identify suitable comparison locations that share similar characteristics with the asset location, known as counterfactuals. These counterfactuals represent a scenario that would have occurred if a different treatment had been implemented. It represents a "what-if" scenario that allows us to estimate the causal effect of farm ponds by comparing the observed outcomes with the potential outcomes.

As the counterfactuals represent alternate locations where the treatment could have been implemented, they should demonstrate similarities in essential aspects that could potentially influence the outcome of the NRM works. This could in-

clude factors such as topography, vegetation cover, proximity to water sources, and other relevant variables. By selecting counterfactuals that are similar to the asset location in these aspects, it is more likely that both the asset location and the counterfactuals would have been affected by similar external factors, such as rainfall variations, during the evaluation period. After we have a comprehensive dataset of treated and control points, we aim to find corresponding counterfactual for each of the treated points.

### *1) Selection of Confounding Variables and their sources*

The confounding variables, referring to the geographical and socioeconomic variables, were obtained from standard and open sources [59] [3]. In this paper, we have considered geographical variables such as elevation, slope and empirically decided on the following covariates:

- **Elevation:** Elevation is commonly included as a covariate because water usage and management practices are influenced by elevation. Higher elevations often receive more rainfall, which can result in natural water availability and reduce the need for extensive water usage in agricultural practices. Conversely, lower elevation areas may experience less rainfall, requiring additional irrigation and water management efforts to sustain crop growth. Elevation also determined the type of crop being grown in the area.

Shuttle Radar Topography Mission(SRTM) data with a resolution of 1 arc-second(30 m) was used as the data source for elevation. The data can be obtained here for the region of interest. The elevation value for an asset was taken as a mean of elevation values in the 100m buffer around the coordinates of the farm pond.

- **Slope:** The slope of an area plays a crucial role in determining the flow of water. Steeper areas allow for efficient water runoff and reduce the risk of waterlogging. This is beneficial for crop growth as excess water is quickly drained away, preventing damage to the plants' root systems. On the other hand, flatter areas may experience reduced soil erosion due to slower water flow. This can help retain nutrients and topsoil, leading to improved soil fertility. However, flatter areas may face challenges related to water drainage and may require artificial drainage systems to prevent waterlogging. The slope of an area significantly influences crop quality and vegetation indices as it impacts factors such as water availability, soil erosion, and nutrient retention, ultimately affecting the overall health and productivity of crops.

The slope layer was computed from the elevation layer using ee libraries with a resolution of 30m. The slope value for an asset was taken as a mean of elevation values in the 100m buffer around the coordinates of the farm pond.

- **Distance to closest river:** If a site is located near perennial flowing rivers, the presence of a farm pond would have less impact on irrigation since the water requirement is already being fulfilled by the river. Moreover, rivers can also have an impact on soil quality

in their vicinity through processes such as sediment deposition and nutrient enrichment. As a result, areas with comparable distances to rivers may exhibit similar soil characteristics, leading to similarities in crop types and growth patterns. The proximity to rivers can influence both water availability and soil quality, thereby affecting the impact of farm ponds in those areas.

The river layer pan India is obtained from WRIS portal and then the distance to closest river pixel is computed using ee library methods.

- **Flow accumulation:** A catchment area is an expanse of land where surface water resulting from precipitation, such as rain, melting snow, or ice, converges towards a common point at a lower elevation. This water then joins and flows into another water body, such as a river, lake, wetland, sea, or ocean. Hydrological units are categorized based on their size, and various terms are used to describe them, including basin, sub-basin, catchment, sub-catchment, watershed, sub-watershed, and micro-watershed. For example, a river system in a country can be divided into several basins, such as the Ganga Basin or the Godavari Basin, which encompass large areas. Each basin consists of smaller units, such as sub-basins or catchments. At a more localized level, every village or area is typically part of a micro-watershed, which serves as a primary unit for developmental work related to water resource management and conservation. A watershed usually covers an area ranging from approximately 20,000 to 150,000 hectares (ha) and encompasses multiple micro-watersheds, which are typically smaller in size, ranging from 500 to 1,500 ha [70]. These watersheds are each a directed acyclic graph depicting the flow of water. Since these watersheds' size heavily determines the amount of water flowing into all areas, we require a covariate to account for it. Flow accumulation layer stores the number of pixels that drain into each pixel [68] [69]. It is used as an alternative to the size of the catchment area which drains into each pixel.

This layer was computed pan India on a watershed level using the DEM data with D8 algorithm by PySheds library. The watersheds pan India were obtained through the WRIS portal.

- **Distance to closest lineament:** Lineaments are linear geological features that represent underlying geological structures such as faults, fractures, or joints. The proximity of areas to lineaments can have implications for water percolation and retention capacity, which can ultimately affect the effectiveness of water structures built in those areas. When areas are located closer to lineaments, water may have a higher likelihood of directly percolating into the ground along these geological features. This can result in reduced water retention capacity within the soil and limit the effectiveness of water structures, such as ponds or reservoirs, constructed in those areas.

The lineaments map is georeferenced and proximity analysis is carried out. A buffer of 2m is taken to form the

Variable	Primary Source	Resolution	Min	Mean	Max	Std	Normalization Applied
Elevation	SRTM	30m * 30m	29.27	92.63	347.08	51.70	Standard Scalar
Slope	SRTM (GEE)	30m * 30m	0.00	2.25	8.94	0.78	Standard Scalar
Distance To closest Rivers	WRIS	30m * 30m	0.69	2292.80	26440.04	2517.94	Log Normalization
Flow Accumulation	DEM (Pysheds)	30m * 30m	1.00	684.05	1.02e6	20922.84	Log Normalization
Distance to closest Lineaments	Bhuvan	30m * 30m	0.00	2.13e5	1.31e6	4.74e5	Log Normalization
Distance to closest Roads	Geofabrik (OSM)	30m * 30m	0.09	812.03	8992.70	1144.88	Log Normalization
Previous Cropping Intensity	IndiaSat	30m * 30m	1.00	1.65	3.00	0.54	No Normalization
Distance to Upstream Forests	DEM, Dynamic World	10m x 10m	0.00	100.63	979.61	110.45	Log Normalization
Proximity to Water pixels	Dynamic World	10m x 10m	0.00	16.40	315.20	28.91	Log Normalization

Figure 20: Table of all Confounding Variables

binary mask and pixels within the buffer are assigned 10 and those without are 1. Then, the distance to the nearest lineament for all the sites was calculated.

- **Distance to closest road:** The road network layer serves as a valuable indicator of connectivity. Farm ponds that are located in close proximity to roads are generally considered more accessible to farmers and other stakeholders, which, in turn, increases the likelihood of their usage and utilization for various purposes such as irrigation or livestock watering.

To incorporate the road network information, the road network layer was obtained from the geofabrik website. This layer provides information about the road infrastructure in the region of interest. Subsequently, the distance to the nearest road was calculated for all the sites under consideration.

- **Recent cropping intensity:** Since cropping intensity is one of our outcome indices, and we want our counterfactuals and assets to have similar environment pre-intervention, we add recent cropping intensity as a covariate to ensure that only sites with similar cropping intensities before NRM interventions are compared.

We obtain cropping intensity from IndiaSAT LULC at 30m resolution. IndiaSAT provides the following class labels: water, barren, built-up, crop, tree, single-kharif, single-non-kharif, double and triple cropping. Each pixel belongs to one of the following classes. The outputs are generated for every hydrological year (starting from July 30th of an year). To get cropping intensity, a value of 1 is assigned for single-non-kharif and single-kharif, 2 for double and 3 for triple cropping pixels. The value for recent cropping intensity is also taken as a mode of the

cropland pixels in the 100m buffer around the coordinates of the farm pond.

- **Distance to closest upstream forest:** To account for the potential nutrient-rich water runoff from forested areas, a covariate is introduced to quantify the ease of water flowing from upstream forests to a specific site. This covariate takes into consideration the relationship between elevation and water flow direction.

First, the upstream forest area is identified for each site. The forest layer is obtained from Dynamic world. This area comprises the forested regions that have a higher elevation than the site under consideration. This is achieved by filtering out the forest areas with higher elevations using digital elevation model (DEM) data. Once the upstream forest area is determined, the distance between the site and the closest pixel within this upstream forest is computed.

- **Proximity to water:** The layer distance to closest rivers do not account for other water sources such as canals or other water structures which are not built under the NREGA scheme. To factor in the proximity to other water sources, this covariate is computed.

The land use land cover classification layer is obtained from google dynamic world. The LULC is then filtered out to get only the pixels which were classified as water to obtain the water layer. For every pixel, proximity to water sources is computed empirically by considering buffer ranges (in m)

$$B = [100, 200, 400, 800, 1600]$$

Let  $ring(i, pixel)$  denote the ring made by the difference of buffer made by the radius  $B[i]$  and  $B[i - 1]$  around the site, and the weight associated with  $ring(i, pixel)$  be

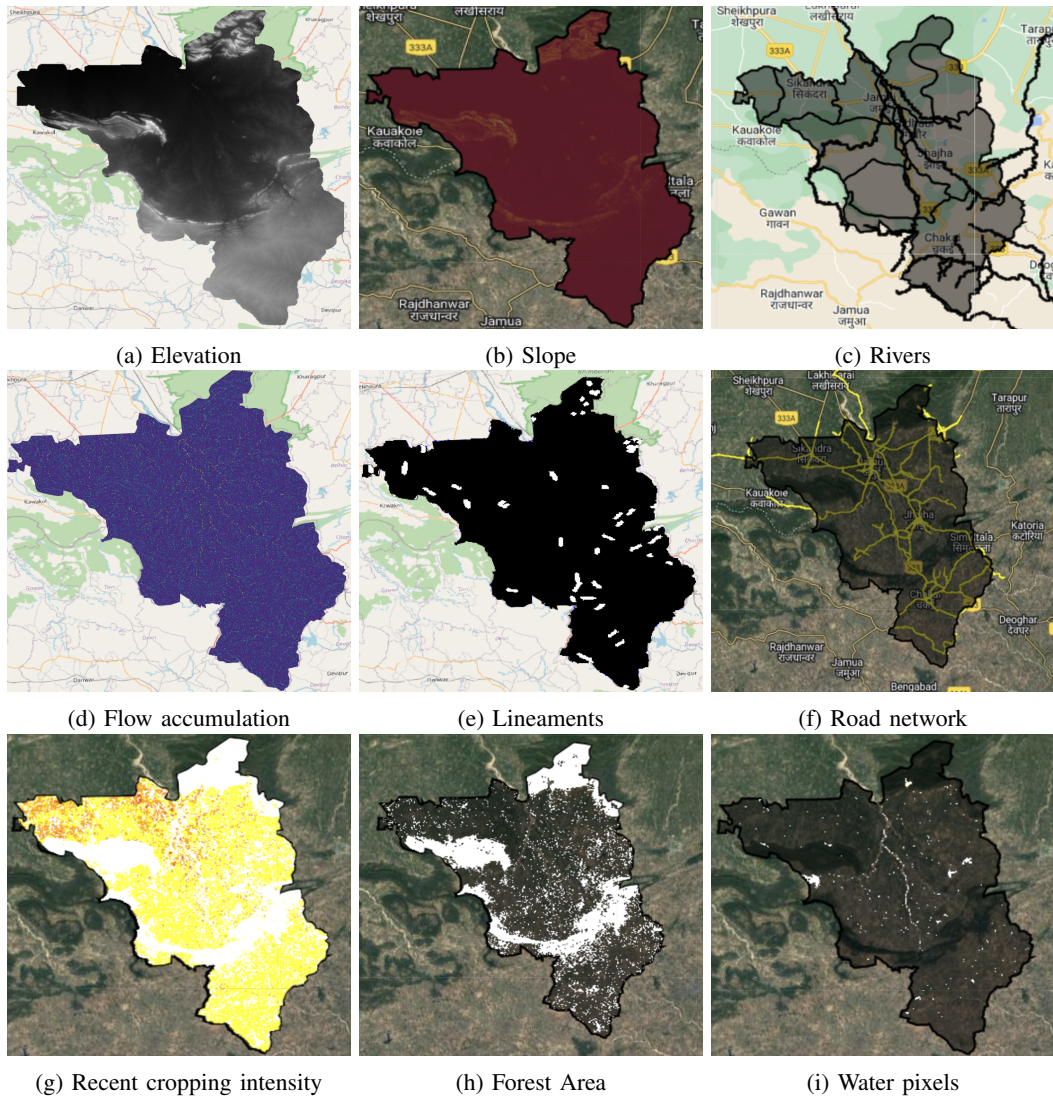


Figure 21: Confounding variable layers for Jamui

$b[i] = 1/B[i]^2$  then the proximity to water is calculated as:

$$p(pixel) = \frac{\sum_{i=1}^4 b[i] * \text{no. of water pixels in } ring(i, pixel)}{\sum_{i=1}^4 b[i]}$$

The variables mentioned above exhibit disparate scales and diverse distributions. For conducting further analysis, it is crucial to consider the collective impact of all these variables. However, due to the variation in scales, certain variables may carry more weight than others simply because of their higher values. Additionally, some variables possess exponential distributions, with the majority of values concentrated around 0 but with a few values exceeding  $10^5$ , such as flow accumulation or distance to rivers.

To address these challenges and ensure fair treatment of variables, normalization techniques specific to the distribution of each variable were implemented. The objective of the normalization process is to ensure comparability and equal consideration of all variables, regardless of their scale or dis-

tribution characteristics and an unbiased analysis. By normalizing the variables appropriately, the analysis can accurately capture their relative importance and contribute to a more comprehensive understanding of the data.

Histograms and Kernel Density Plots were examined to gain insights into the distribution of the data. Based on these observations, two normalization techniques were employed:

- **Standard Scalar Normalization:** Variables that exhibited comparable values and displayed a distribution resembling a normal curve were normalized using this technique. Standard Scalar Normalization transforms the values in a way that sets the mean to 0 and the standard deviation to 1. This ensures that the values fall within the range of -10 to 10, providing a standardized scale for comparison.
- **Log Normalization:** Variables with an exponential distribution or extreme values, such as values ranging from

0 to  $10^5$ , underwent log normalization. By applying log normalization to these variables, the resulting transformed values reflect the relative order of distances rather than the absolute values. This is particularly valuable when dealing with variables that span a wide range (like distance to river or lineaments), as it allows for a more meaningful representation of the underlying order or magnitude. Similar to Standard Scalar Normalization, log normalization brings the values within the range of -10 to 10, promoting uniformity and facilitating meaningful comparisons across variables.

## 2) Propensity Score Matching

The propensity score matching is a method to identify counterfactuals for the subjects that have received a particular treatment.

The propensity score is the estimated probability of receiving a specific treatment based on observed covariates. Subsequently, these propensity scores are utilized to create clusters of data points with similar scores. This matching procedure assists in identifying a group of control points that closely aligns with the characteristics of the treatment point within the group (Figure 22). These control points can then serve as counterfactuals to evaluate the treatment's effects.

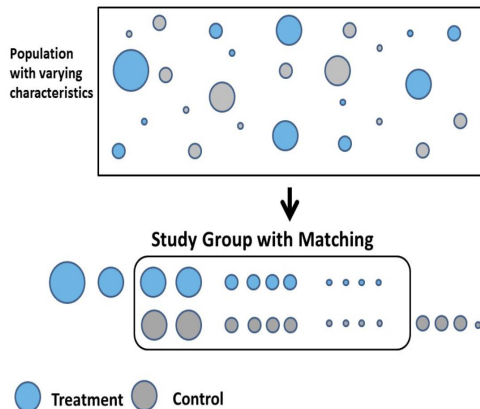


Figure 22: Propensity Score Matching

The following steps were involved:

- **Propensity score estimation:** A classification model is trained, such as logistic regression, in order to estimate the probability of a data point receiving treatment, based on the observed covariates. It is then used to estimate score for each individual.
- **Matching process:** Following this procedure, the data points in the treatment group are matched with corresponding data points in the control group based on their respective propensity scores. The matching process employed is known as kNN matching, which stands for k-nearest neighbor matching. Depending on the specific needs, the matching can take the form of one-to-one matching or one-to-many matching.

Once the balance is achieved, the next step involves calculating the treatment effect by comparing the outcome of interest between the treated and matched control individuals which is discussed later.

### B. Outcome variables

- **Vegetation Index:** There are many vegetation indices that can be easily computed from the satellite bands like Normalized Difference Vegetation Index (NDVI), Green Normalized Difference Vegetation Index (GNDVI), Visible Atmospherically Resistant Index (VARI), Optimized Soil Adjusted Vegetation Index (OSAVI) and Enhanced Vegetation Index (EVI), etc. [22] [64] [65] [66] [67] Some indices which were not found suitable for our study are shown below:

- Atmospherically Resistant Vegetation Index (ARVI): for regions with high content of atmospheric aerosol (e.g. rain, fog, dust, smoke, air pollution)
- Soil Adjusted Vegetation Index (SAVI): Useful for analysis of young crops; for arid regions with sparse vegetation (less than 15% of total area) and exposed soil surfaces.
- Modified Soil-Adjusted Vegetation Index (MSAVI): MSAVI is useful at the very beginning of crop production season – when seedlings start to establish. analysis of plant growth, desertification research, grassland yield estimation, LAI assessment, analysis of soil organic matter, drought monitoring, and analysis of soil erosion
- Normalized Difference Water Index (NDWI): detection of flooded agricultural lands; allocation of flooding on the field; detection irrigated farmland; allocation of wetlands
- Normalized Difference Red Edge Vegetation Index (NDRE): Indicator of crop health
- Red-Edge Chlorophyll Vegetation Index (RECI): most useful at the stage of active vegetation development but are not suitable for the season of harvesting

The following five vegetation indices were found suitable for our initial analysis:

- **Normalized Difference Vegetation Index (NDVI):** NDVI is a vegetation index, which is most suitable to track crop development dynamics since it measures photosynthetically active biomass in plants. NDVI can be used throughout the whole crop production season except when vegetation cover is too scarce, so its spectral reflectance is too low. It can be computed as follows:

$$NDVI = \frac{(NIR - RED)}{(NIR + RED)}$$

NDVI is most accurate in the middle of the season at the stage of active crop growth and is recommended to be used when looking for differences in above-ground biomass in time or across space.

- **Green Normalized Difference Vegetation Index (GNDVI):** GNDVI measures chlorophyll content more accurately than NDVI. It is used to detect wilted or aging crops and measure nitrogen content in leaves when an extreme red channel is not available, monitor vegetation with dense canopies, or at maturity stages.
- **Visible Atmospherically Resistant Index (VARI):** This is perfect for RGB or color images since it works with the whole visible segment of the electromagnetic spectrum (comprising red, green, and blue color bands). Its specific task is to enhance vegetation under strong atmospheric impact while smoothing illumination variations. It is minimally sensitive to atmospheric effects, allowing for vegetation to be estimated in a wide variety of environments. This can be used for crop state assessment when minimum sensitivity to atmospheric effects is required.
- **Optimized Soil Adjusted Vegetation Index (OSAVI):** Soil Adjusted Vegetation Index (SAVI) is an index to mitigate the impact of soil brightness and correct for soil noise effects (soil color, soil moisture, soil variability across regions, etc.). SAVI is particularly useful in circumstances where soil quality varies substantially within a single given area of interest. SAVI can take into account the fact that the soil is either wet or dry, and that the solar inclination angle can vary. OSAVI is Modified SAVI which takes into account the standard value of the canopy background adjustment factor (0.16). OSAVI does not depend on the soil line and can eliminate the influence of the soil background effectively. OSAVI can be used to monitor areas with low-density vegetation with bare soil areas through the canopy. This is mainly used for the calculation of aboveground biomass, leaf nitrogen content, and chlorophyll content.
- **Enhanced Vegetation Index (EVI):** EVI is used to adjust NDVI results to atmospheric and soil noises, particularly in dense vegetation areas, as well as to mitigate saturation in most cases. As a result of the interaction between the soil and the atmosphere, reducing one of them may increase the other. EVI simultaneously corrects soil and atmospheric effects. EVI can be used for analyzing areas of Earth with large amounts of chlorophyll (such as rainforests), and preferably with minimum topographic effects (non-mountainous regions).

These indices were further explored to analyze the trends around a single pond located at (86.54480832, 24.58505145) in Chakai block of Jamui district over the years as shown in Figure 23 and Figure 24. It was observed that almost all the indices show a very similar pattern, but the NDVI curves are smoother than the rest. Observing these trends, NDVI was chosen as the selected

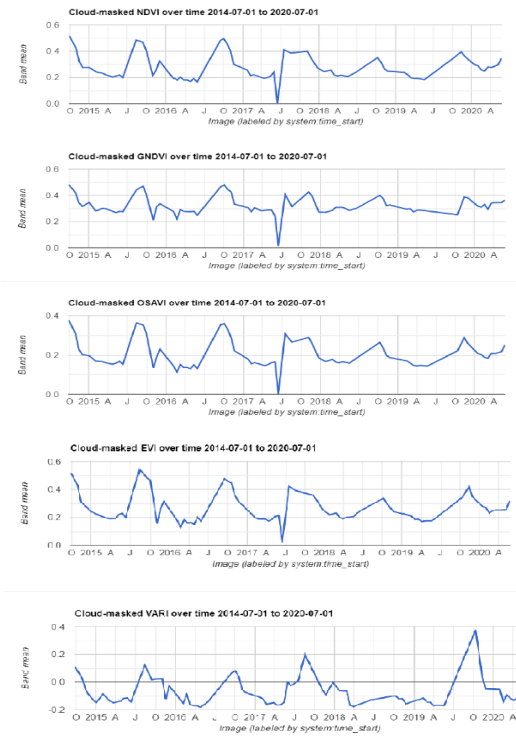


Figure 23: Trends of vegetation indices in 150m buffer around a pond location (86.54480832, 24.58505145) in Chakai block, Jamui district over a period of time

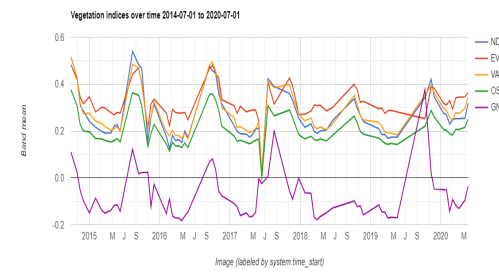


Figure 24: Comparison of vegetation indices in 150m buffer around a pond location (86.54480832, 24.58505145) in Chakai block, Jamui district over a period of time

vegetation index for our study. We conducted our study on temporal mean of NDVI for each of the agricultural season and found that the values were numerically too low in order to be comprehended for analysis. Averaging of NDVI over a full agricultural season followed by averaging over a buffer was almost nullifying Average Treatment Effect (ATE). Moreover, we derived some insights from the field visit that the actual impact of farm ponds would be on the crop yields (Section I), when the ponds have been used for protective irrigation. Hence, Max NDVI has been finally chosen for temporal aggregation in a season, as it closely relates to the crop

yield [33] [42].

To compute the NDVI based outcome indicators, the cloud-free Landsat 8 images of the area of interest for the study periods were acquired from Google Earth Engine (GEE) for this study. The dimensions of the Landsat images are 1800 X 1200 with a resolution of 30 m. The bands from Landsat-8 imagery were used to compute a new band for NDVI in each image.

The outcome NDVI Positive Change is computed as follows:

$$ndvi\_pos\_change_{season} = \frac{100 * count_{buffer}(positive\_ndvi\_pixels)}{count_{buffer}(all\_pixels)}$$

where,

*positive\_ndvi\_pixels* are the pixels with positive values in the composite NDVI difference raster image computed between pre and post intervention periods for each agricultural season. The NDVI values over each pixel is temporally aggregated by max NDVI in the season.

- **Cropping Intensity (CI):** While doing our analysis on the cropping intensity of the Jamui district, we found that almost 90% of the pixels in a buffer of 50m of the ponds, which had no crops earlier, converted to single cropping in the post-year, as depicted in the sample shown in Figure 25. The trend with distance is shown in Figure 26, which depicts that the increase of cropping intensity is more than that in the counterfactuals. This clearly indicates that the farm ponds had a positive impact on the cropping intensity. Thus, this was chosen as one of the outcome variables in our study.

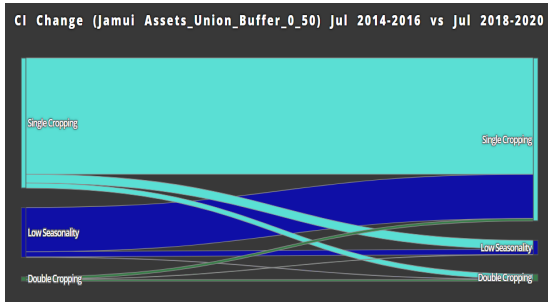


Figure 25: Cropping intensity change in a buffer of 0-50m around the ponds in Jamui district

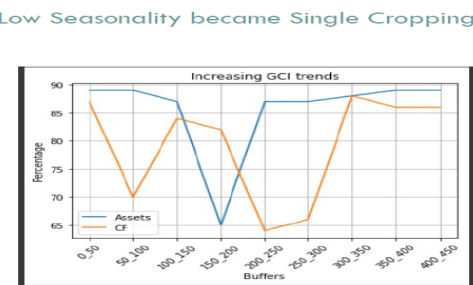


Figure 26: Trends of Increasing Cropping intensity change with distance (Assets vs Counterfactuals)

The outcome CI Positive Change is computed as follows:

$$ci\_pos\_change = \frac{100 * count_{buffer}(positive\_ci\_pixels)}{count_{buffer}(all\_pixels)}$$

where,

*positive\_ci\_pixels* are the pixels with positive values in the composite CI raster difference image in pre and post-intervention periods.

### C. Difference in Differences

The difference-in-differences (DiD) method is a statistical approach utilized to assess the causal impact of a treatment or intervention by examining the changes in outcomes over time between a group receiving the treatment and a control group. At its core, the DiD method aims to establish a counterfactual scenario in which the treatment was not implemented, providing a basis for estimating the treatment effect. By comparing the pre and post-treatment outcomes of both the treated and control groups, the DiD method seeks to isolate the causal effect of the treatment from other potential factors that may influence the outcomes.

In its simplest form, the DiD method calculates the difference between the average change in the outcome variable for the treated group and the average change for the control group. This difference represents an estimation of the treatment effect.

By comparing changes in outcomes over time, the DiD method helps mitigate biases stemming from unobservable factors and provides a more reliable estimation of the causal impact of the treatment.

Mathematically,

$$difference_{asset} = outcome_{post\_intervention}^{asset} - outcome_{pre\_intervention}^{asset}$$

$$difference_{counterfactual} = outcome_{post\_intervention}^{counterfactual} - outcome_{pre\_intervention}^{counterfactual}$$

$$treatment\_effect = difference_{asset} - difference_{counterfactual}$$

We designed a two-period DiD methodology for our analysis [34] and then shifted to analysing effects over multiple years eventually. To compute treatment effects over time, pairwise differences between the target year (2018/2019/2020/2021) and the base year (2016) is taken over assets and counterfactuals.

**Ring buffer analysis:** A distance-based analysis was carried out by constructing 25m buffers (Figure 27) around the farm ponds to find out the range of impact by farm ponds as follows:

- Different buffers of width 25m around assets and their matched counterfactuals are created.
- The difference of NDVI and CI before and after the intervention around asset and counterfactual matching is analyzed.

A buffer of 100 m was finalized by observation as well as after interaction with the farmers during a field trip, considering that

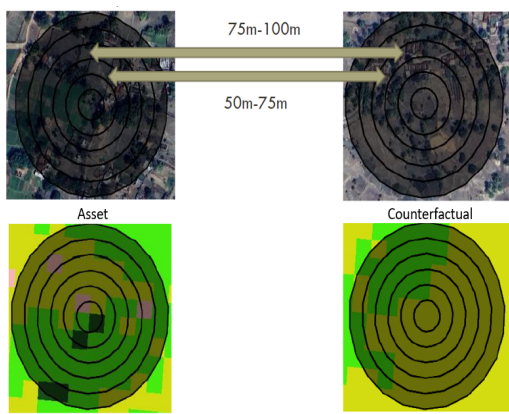


Figure 27: Buffers of 25 m rings around assets and counterfactuals

the water from a farm pond is typically supplied in nearby farms only. The spillover effects can be seen upto 100m as shown in Figure 28, after which they die down.

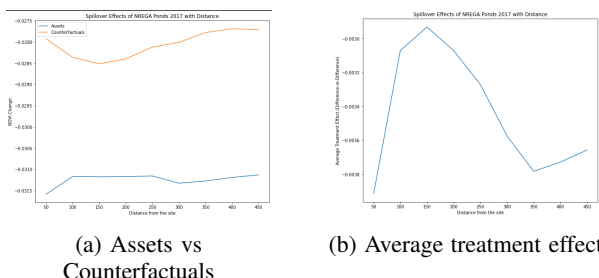


Figure 28: Buffer selection

#### D. Stratified DiD

In the stratified difference-in-differences (DiD) approach, we implement a strict matching process, ensuring that the treatment group is closely matched with comparable counterfactual groups based on their historical cropping intensity. This matching is performed generating three distinct strata: single cropping (asset) - single cropping (counterfactual), double cropping (asset) - double cropping (counterfactual), and triple cropping (asset) - triple cropping (counterfactual). Due to the limited occurrence of triple cropping in the agro-eco region of interest, many asset-counterfactual pairs may not fit into the triple-triple stratum.

Mathematically,

$$\text{treatment\_effect}^{\text{recent\_ci}=i} = \text{difference}_{\text{asset}}^{\text{recent\_ci}=i} - \text{difference}_{\text{counterfactual}}^{\text{recent\_ci}=i}$$

where,

$\text{recent\_ci}$  can take values of 1, 2 or 3 based on the cropping intensity.

Subsequently, we analyze and present the results in a similar manner as the traditional difference-in-differences method, but

separately for each stratum. The primary motivation behind stratifying the dataset is to address the presence of diverse treatment effects. Treatment effects can vary significantly among different subgroups. By employing stratification in our analysis, we are able to detect and examine any discrepancies between the subgroups, allowing for the identification of treatment effects specific to each subgroup.

#### E. Synthetic Control

The Synthetic Control method involves the creation of a synthetic sample from the control group that closely resembles the treated unit [74]. In this method, generally both pre-treatment outcome variables and covariates are utilized for generating suitable matches. The fundamental principle is to ensure similarity between the treated and matched units in terms of their pre-treatment outcomes and covariates, thereby establishing a solid foundation for analysis.

The assignment of weights to each control unit is a crucial aspect of the Synthetic Control method, as these weights determine the extent to which a control unit contributes to approximating the characteristics of the treated unit. Typically, these weights are derived through an optimization process aimed at minimizing the disparity between the pre-treatment outcomes/covariates of the treated unit and the synthetic control group.

To examine treatment effects, a comparison is made between the treated unit and its synthetic counterfactual across multiple time periods after the intervention. By observing the differences between the treated unit and the synthetic control group over time, the impact of the treatment can be assessed. We have used the implementation of Synthetic Control by SparseSC [73]. The core difference between the standard synthetic control and SparseSC implementation is that it leverages a nested optimization equation to not only find optimal weights for generating the synthetic sample but also finds a feature-importance vector for the matching variables. The core parameters required are "features" corresponding to the matching variables and "targets" which usually is post-treatment outcome variables. For our analysis we have considered only covariates discussed in Section IV-A1 as "features" and post-treatment outcome variables as "targets".

The steps involved are as follows:

1. Sample 500 controls from the AEZ of interest.
2. Fit Treated Units on "targets" and "features" to generate weights against each treatment unit.
3. Use the weights to generate synthetic counterfactual by taking a weighted average over the 500 controls.
4. Difference-in-Difference between the asset and synthetic counterfactual to get treatment effects.

#### F. Double Machine Learning (Double ML)

Double Machine Learning (Double ML) is a technique used for causal inference and treatment effect estimation. It is

particularly useful when dealing with high-dimensional data and complex relationships between variables.

The primary goal of Double ML is to estimate the causal effect of a treatment or intervention on an outcome variable while controlling for confounding factors. In observational studies, where researchers cannot randomly assign treatments, confounding variables can distort the estimated treatment effect. Confounding variables are those that are associated with both the treatment and the outcome and can introduce bias if not properly accounted for.

Double ML works as follows:

- Train a model to predict the treatment (in our case, a farm pond is constructed or not) using a set of covariates.
- Train a model to predict the outcome (in our case, NDVI\_POS or CI\_POS) using the same set of covariates.
- Train a model to predict the linear regression of residuals from the outcome model on the residuals from the treatment model.

The crucial aspect of Double ML is that the two machine learning steps are combined in a way that minimizes the bias and overfitting introduced by confounding variables.

### 1) Covariates selection and Instrument variable analysis

The following confounding variables were selected as covariates:

- Block number
- Slope
- Elevation
- Distance to closest river
- Flow Accumulation
- Distance to closest lineament
- Distance to closest road
- Recent Cropping Intensity
- Distance to closest upstream forest
- Proximity to water

Motivated by Deines et al. [13], it was concluded that geospatial information like latitude and longitude may also indicate some impact on the treatment effect. Hence, block number was generated as a categorical variable **by assigning sequential numbers to all the unique block names in the AEZ**. **Block number was added as a covariate** based on the assumption that most of the soil, environment, and climate characteristics are the same throughout the geographical region of a block. Such a confounder was not needed in earlier methods, as the matchings were done at a block level only. To mitigate the effects of unobserved confounders, block numbers would play a critical role. The rest of the covariates have already been discussed in Section IV-A1.

The instrument variable is the one that has a direct causal effect on the treatment variable but not on the outcome variable [41]. All the covariates selected were analyzed and assumed

to affect the treatment as well as the outcome. Hence, it was concluded that our study contains no instrument variables.

### 2) Model Specification

For our study, we used the EconML Python package, which implements numerous Double ML methods. One of the implementation of Double ML methods in this package is LinearDML. It uses an unregularized final linear model and essentially works only when the feature vector is low dimensional i.e. the number of covariates is less. LinearDML also offers confidence intervals by essentially using the StatsModelsLinearRegression as a final model. Hence, LinearDML method was selected after comparison with other methods like CausalForestDML based on the model score which is the mean squared error (MSE) in the final stage model (Figure 29), as it suited our requirements and its performance was better than the others.

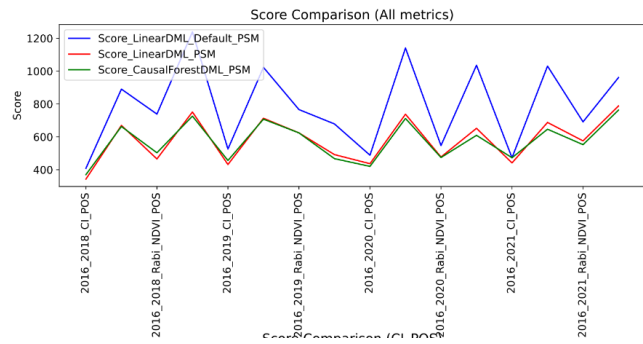


Figure 29: Score Comparison of DML models

In the first stage, a random forest regressor was selected as a model to predict the outcome from covariates. Additionally, because the treatment variable is binary (indicating whether a farm pond was built or not), a random forest classifier was selected as a model to predict the treatment from covariates.

It was observed that random forest models in the first stage drastically reduced the model score when compared to the default models in the first stage of LinearDML i.e. WeightedLassoCV for output prediction and LogisticRegressionCV for treatment prediction, as shown in Figure 29.

In the final stage, the default model used is StatsModelsLinearRegression, which is a part of the LinearDML implementation. StatsModelsLinearRegression extends the scikit-learn LinearRegression estimator and includes features that support inference, allowing for statistical analysis of the results.

To ensure statistical stability, given the limited number of samples in our case, we conducted the analysis with a cross-validation hyperparameter of 6, aiming to achieve reliable results.

### G. Models Validation

DiD-based models heavily depend upon the quality of matchings. Hence, assessing the balance in the matchings from PSM was a critical step to validate our models.

After completing the matching process, the balance between the distributions of the confounding variables in the treatment and control groups is assessed using techniques such as Kernel Density Estimation (KDE), QQ Plots, Pair T-tests and KS Statistics test. This evaluation aims to determine whether the matched individuals exhibit similar distributions. The plots and values for each variable are shown in Figure 34 in Appendix A.

The KDE Plots shows how the treated and counterfactual distributions after the matchings are aligning. Additionally, the QQ plot demonstrates if the values of the treated points and counterfactuals are comparable; i.e. following matchings, the line is more inclined towards 45 degrees. The increased values of KS Statistic implies that the fit between the two plots is good. The distributions are adequate enough for us to proceed even though this is not exactly the case for every variable.

## V. RESULTS AND DISCUSSION

Treatment effects were generated for all the farm ponds in the study area using four different methods: Difference-in-Differences (DiD), Stratified Difference-in-Differences, Synthetic Controls, and Double ML (Table II).

To understand the impact of the interventions, we examined treatment effects over different years compared to the baseline year (2016). This approach was chosen due to the possibility that farm ponds might not be immediately utilized by farmers for irrigation purposes post-intervention. Therefore, a temporal analysis of treatment effects was deemed more appropriate for comprehensive analysis. We have employed different methods to interpret treatment effects over different ponds and find unique advantages with each of the different methods.

### A. Correlation of results from different methods

The Difference-in-difference (DiD) method gives the average treatment effect on the treated points i.e. ATT. Hence the ATT values for different outcome indicators were compared for correlation among all the methods. It was found that the ATT values were positively correlated among all the methods as depicted from the heatmap in Figures 30 and bar plots in Figure 36. The correlation was statistically significant, positive, and very high in all the methods except the stratified DiD for single cropping intensity. The stratified DiD for single cropping intensity shows a weak but positive correlation with the other methods. This is also depicted through the scatter plots of Figure 35 in the Appendix section. The Spearman correlation coefficient is 0.96 for three methods namely, SDID-2, Synthetic control and DML, when compared to DiD.

### B. Analysis of Average Treatment Effect on the Treated (ATT) across AEZ

The aggregated results of ATT from all the methods are shown in Table II and Table III. The statistical significance of the results was computed by performing a Z-test on the treatment effects over all the ponds with all the methods. Our null hypothesis is that the mean of the treatment effect distribution

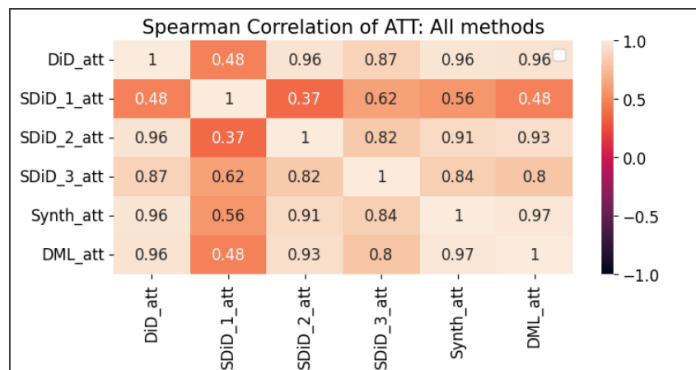


Figure 30: Heatmap for Spearman Correlation of ATT values among all methods

is equal zero. We select the significance-level to be 0.05, and reject the null-hypothesis when the pvalue is below 0.05.

From Table II and Table III, we have the following observations:

- **Cropping Intensity:** Temporal analysis shows negative average treatment effects in the post-treatment years 2018, 2019, 2020, and 2021 when compared to the baseline year of 2016. The results are all statistically significant and these consistent findings hold true across all four analytical methods employed: DiD, stratified DiD, Synthetic Control, and Double ML, across various districts. It is important to note that although an increase in cropping intensity would typically be expected following the construction of farm ponds, this may not always be the case. The primary purpose of these ponds may be protective irrigation rather than directly contributing to an increased cropping intensity.
- **NDVI in Kharif Season:** The treatment effect is mostly negative in the years 2018 and 2019. However, in 2021 we observe a positive average treatment effect on the treated (ATT) on NDVI in Kharif season. The results are mostly significant from DiD and DML methods. Additionally, it is worth noting that the treatment effects based on the DiD variants tend to have a higher magnitude compared to those obtained through the Synthetic Control or Double ML methods.
- **NDVI in Rabi Season:** In contrast, during the Rabi season, the treatment effects on the NDVI POS metric predominantly demonstrate positive values, with the highest being recorded in 2019. This positive trend is encouraging, indicating the effective utilization of ponds during the Rabi season when rainfall alone is typically insufficient for adequate irrigation. All the results are significant from DiD and DML methods. The other methods show some statistically insignificant results.
- **NDVI in Zaid Season:** The treatment effect is mostly negative across all the years from all the methods except Stratified DiD with single cropping intensity. All the

	<b>DiD_att</b>	<b>SDiD_1_att</b>	<b>SDiD_2_att</b>	<b>SDiD_3_att</b>	<b>Synth_att</b>	<b>DML_att</b>
<b>2016_2018_CI_POS</b>	-7.36286	-11.25592	-4.01338	-25.75841	-12.14706	-5.80926
<b>2016_2019_CI_POS</b>	-9.27286	-7.76501	-6.23689	-29.01267	-12.2972	-7.50866
<b>2016_2020_CI_POS</b>	-9.48073	-8.21193	-8.6615	-34.10939	-14.19549	-8.19536
<b>2016_2021_CI_POS</b>	-9.79702	-9.17856	-9.72178	-34.20277	-12.8981	-8.09875
<b>2016_2018_Kharif_NDVI_POS</b>	-3.08718	0.13953	-2.25516	-0.24818	-5.46617	-1.85128
<b>2016_2019_Kharif_NDVI_POS</b>	-1.47145	3.09923	-2.9246	5.2571	-1.97627	-1.4232
<b>2016_2020_Kharif_NDVI_POS</b>	2.58655	4.33335	0.0011	-1.20002	0.28415	-0.12019
<b>2016_2021_Kharif_NDVI_POS</b>	3.11964	8.16678	1.49008	13.76169	0.31986	1.03482
<b>2016_2018_Rabi_NDVI_POS</b>	2.56532	3.25203	0.4365	9.92555	0.22783	0.88056
<b>2016_2019_Rabi_NDVI_POS</b>	6.0836	3.01559	7.22886	6.88538	2.99958	3.71335
<b>2016_2020_Rabi_NDVI_POS</b>	2.4252	0.85436	0.67885	-7.4226	-1.96007	-0.44483
<b>2016_2021_Rabi_NDVI_POS</b>	4.8854	-1.55159	1.77706	3.04622	-0.73221	1.78387
<b>2016_2018_Zaid_NDVI_POS</b>	-3.79016	5.33933	-2.96973	-4.03741	-9.19368	-3.75289
<b>2016_2019_Zaid_NDVI_POS</b>	-2.05835	-1.06037	-2.83334	-7.5936	-3.8205	-0.88131
<b>2016_2020_Zaid_NDVI_POS</b>	-4.22062	3.57265	-4.70304	-11.10439	-4.14885	-0.92346
<b>2016_2021_Zaid_NDVI_POS</b>	-3.32258	3.55804	-4.88947	-4.76227	-5.82398	-3.41585

Table II: Aggregated Treatment Effects over AEZ-13 with various methods

	<b>DiD_pval</b>	<b>SDiD_1_pval</b>	<b>SDiD_2_pval</b>	<b>SDiD_3_pval</b>	<b>Synth_pval</b>	<b>DML_pval</b>
<b>2016_2018_CI_POS</b>	0	0	0	0	0	0
<b>2016_2019_CI_POS</b>	0	0	0	0	0	0
<b>2016_2020_CI_POS</b>	0	0	0	0	0	0
<b>2016_2021_CI_POS</b>	0	0	0	0	0	0
<b>2016_2018_Kharif_NDVI_POS</b>	0.00029	0.90894	0.02983	0.96895	0	0
<b>2016_2019_Kharif_NDVI_POS</b>	0.08063	0.02411	0.00836	0.45371	0.00594	0
<b>2016_2020_Kharif_NDVI_POS</b>	0.00261	0.00112	0.99922	0.83207	0.6898	0.07204
<b>2016_2021_Kharif_NDVI_POS</b>	0.00016	0	0.15245	0.01514	0.63775	0
<b>2016_2018_Rabi_NDVI_POS</b>	0.00031	0.00105	0.63241	0.08445	0.69793	0
<b>2016_2019_Rabi_NDVI_POS</b>	0	0.01468	0	0.22508	0	0
<b>2016_2020_Rabi_NDVI_POS</b>	0.00031	0.4102	0.43271	0.16797	5.00E-05	0
<b>2016_2021_Rabi_NDVI_POS</b>	0	0.13308	0.08128	0.52947	0.20605	0
<b>2016_2018_Zaid_NDVI_POS</b>	2.00E-05	0.00073	0.00611	0.45971	0	0
<b>2016_2019_Zaid_NDVI_POS</b>	0.00095	0.27997	0.00079	0.01329	0	0
<b>2016_2020_Zaid_NDVI_POS</b>	0	0.00311	0	0.05167	0	0
<b>2016_2021_Zaid_NDVI_POS</b>	0.0001	0.00977	4.00E-05	0.34413	0	0

Table III: Statistical significance (p-values rounded to 5 digits) of the treatment effects with Z-test

results are significant from DiD and DML methods. The other methods show some statistically insignificant results.

The distribution of treatment effect estimates for various outcome indicators from all the methods is depicted in the plots from Figure 37 to Figure 48.

As we expected, these results correlate with the fact that the average annual precipitation in the AEZ was quite low in 2018 and increased manifolds in the years 2019, 2020 and 2021, as compared to 2016 as depicted in Figure 15 and Table I. It was expected that the treatment effect should be positive in the later years.

#### C. District Wise ATT analysis

The treatment effects over different districts were aggregated to calculate Average Treatment Effect over the treated units. Using GEE, we have visualized the outcome variables of interest over different years. This is done for each method separately, the visualizations are shown for DiD results over different years for each metric in the Appendix. A sample image for Rabi 2019 is shown in Figure 31.

The advantages of this method of analysis are two-fold: 1)

To notice any geographical trends across the study area where effects in different parts of the region are correlated and 2) It is easier to track changes in treatment effects over the course of time.

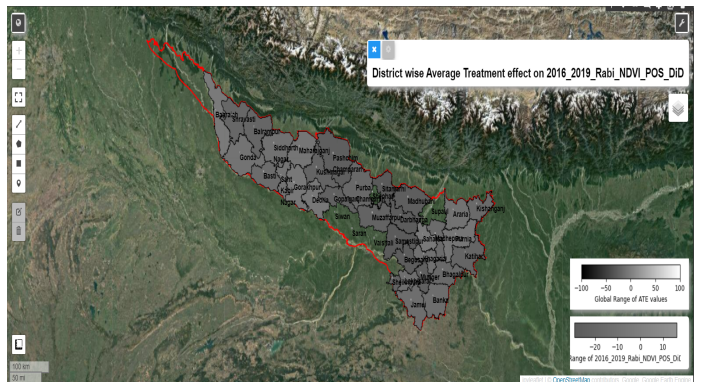


Figure 31: Sample Visualization of District Wise Average Treatment effect on NDVI in Rabi season of 2019

The district-wise ATT values analysis are mentioned in Table VI and Figures 49 to 52 in the Appendix section.

Upon analyzing the treatments across districts, we got the

Year	No. of Districts with Positive ATT (Out of 33)			
	Cropping Intensity (CI)	NDVI Kharif	NDVI Rabi	NDVI Zaid
2018	1	15	23	15
2019	0	18	22	12
2020	4	16	16	14
2021	4	19	21	11

Table IV: No. of districts with Positive ATT

following observations:

- **Cropping Intensity:** All the districts show negative treatment effect on Cropping intensity in all the study years (Table IV, Table VI and Figure 49 in Appendix section). Only Munger, Sitamarhi, and Madhubani districts show a positive treatment effect on CI in the year 2020. It seems, only the farmers in these three districts utilized the farm ponds to increase their cropping pattern. Sitamarhi, and Madhubani are towards the North East, while Munger lies to the South of the Agro-Ecological Zone. Bhagalpur also showed slightly positive ATT in 2020 and 2021 but the magnitude is very low. It showed negative ATT values in 2018 and 2019 as Bhagalpur suffered a drought in the year 2018.
- **NDVI in Kharif season:** As observed from Table IV and Figure 50, we find that around 50% of the districts showed a positive ATT value in Kharif season across all the years, the highest number of districts being in 2021. The magnitudes of ATT in the districts are higher in the year 2020 as compared to 2021, though. The topmost positively impacted districts are Samastipur, Saharsa, Sheikhpura, Khagaria, Gorakhpur, Banka, Munger and Muzaffarpur (Table VI). Katihar faced a drought in 2018, which possibly impacted the treatment effect on NDVI in Kharif season in 2019 and it was negative. Except 2019, Katihar showed positive average treatment effect on NDVI in Kharif season.
- **NDVI in Rabi season:** Around 60-70% of districts showed a positive ATT value in the Rabi season across the 4 post years (2018-2021). The magnitude of treatment effects is high in the year 2019 and 2020. Some districts which showed a positive ATT across all the years include Bahraich, Banka, Bhagalpur, Gorakhpur, Katihar, Purnia and Shravasti (Table VI and Figure 51).
- **NDVI in Zaid season:** There was a positive ATT observed in around 30-40% of the districts in the Zaid season too. However, the magnitude of ATT is quite low in 2018 and 2019. The four districts, namely, Bhagalpur, Khagaria, Saharsa and Sitamarhi show a good impact in the Zaid season of 2020. Samastipur, Khagaria and Madhepura show positive impact in Zaid season of 2021. The rest of the districts show positive but low impacts in the Zaid season (Table VI and Figure 52).

Also analysing effects of assets within each district presents interesting insights. We have plotted box plots for each of district, a reference plot over the district Jamui is shown 32.

This helps us identify the outliers and exploring the ponds that respond greatly to the intervention can provide new insights. For example, we can observe that the medians of treatment effect on NDVI in Rabi 2019, 2020 and 2021 are all above zero, indicating that it was one of the districts which got benefitted by the farm ponds.

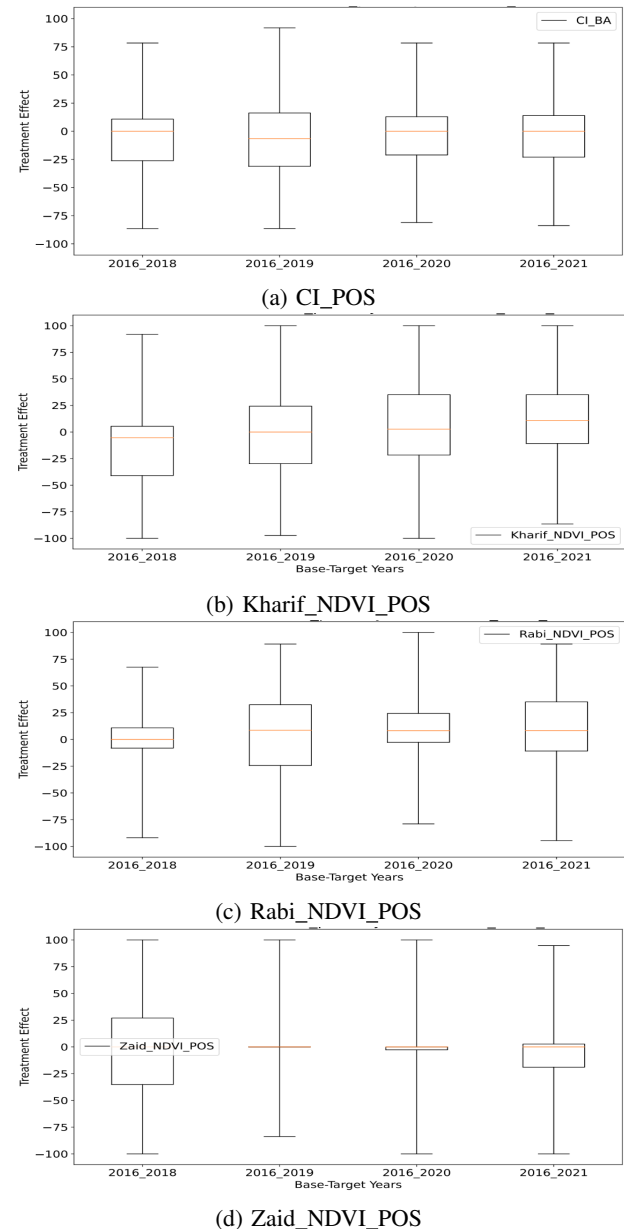


Figure 32: Average Treatment Effects in Jamui District with DiD

#### D. Trend of treatment effects with covariates

We have also analysed how different of these covariates have an impact on the treatment effects with different outcome variables in DiD and DML methods. Some sample images are shown in Figure 33.

The trends in treatment effect predicted by DiD and DML methods with all the covariates for all the metrics are shown in the Appendix section. Following are the observations from these trend plots:

- **Slope:** Considering CI as an outcome, we observe a positive trend of slope over treatment effect with DiD method. As discussed in section IV-A1 this is expected, as higher slope aids in efficient water flow. Though with NDVI in different seasons, a clear trend is not seen in either method, DiD or DML.
- **Elevation:** A clear positive trend is observed with treatment effect on CI as outcome in both the methods, DiD and DML. This could be attributed to the fact that higher elevation areas receive higher rainfall. But over different seasons with NDVI as an outcome, mixed trends are observed with DiD. DML method shows a slightly increasing trends of treatment effect with NDVI in Zaid season and decreasing trends with NDVI in Rabi season. This indicates that higher the elevation, lower is the treatment effect in Rabi season, but more in Kharif/Zaid seasons.
- **Distance to Closest River:** It was expected to have a higher effect as this distance increased. From DiD method, as distance to closest river increased the effect on CI initially decreased before increasing. Though from DML method, a clear increasing trend of treatment effect on CI is observed with distance to closest river. In NDVI Kharif, this covariate shows a slightly positive trend over different years in both the methods (DiD and DML), while with the other seasons we do not have a very clear trend.
- **Flow Accumulation:** With different outcomes we mostly see a positive trend over treatment effects for flow accumulation in DiD method. In contrast, we observe slightly decreasing trends in DML in case of NDVI Kharif and increasing in rest of the outcomes.
- **Distance to Closest Lineament:** For CI, we see a positive trend in both the methods, which is expected because due to low water retention near the lineaments, the effectiveness of the assets is low. For NDVI, we mostly see a flat line except in Kharif where an upward positive trend can be observed in both the methods.
- **Distance to closest road:** Areas with better access to roads might be expected to exhibit better treatment effects though we do no see any such noticeable trend with distance to closest roads in DiD method. In contrast, from DML method, we observe a positive trend with CI and NDVI Zaid, and a slightly negative trend with NDVI Kharif and Rabi.
- **Recent Cropping Intensity:** Since cropping intensity could be 1 (single), 2(double) or 3(triple) the trendline plots do not give much insights.
- **Distance to Closest Upstream Forest:** We see a slight positive trend over different outcomes across multiple years in both the methods, DiD and DML.

- **Proximity to Water:** Over different years for various outcomes mixed trends are observed in DiD and DML. But a clear decreasing trend with CI and NDVI Rabi is observed in DML method, which implies that the treatment effect will decrease if proximity to water increases.

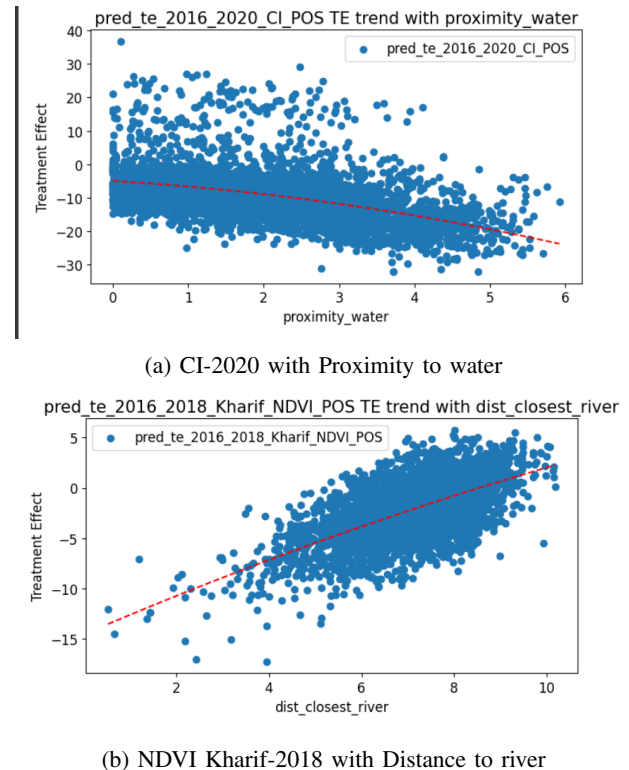


Figure 33: Trends of treatment effect with features in DML method

## VI. CONCLUSION AND FUTURE WORK

We have devised an innovative remote-sensing framework to evaluate the effectiveness of government-constructed farm ponds under the MGNREGA scheme. This framework offers the advantage of complete automation, eliminating the need for on-site visits during monitoring. Understanding the impact of various pond interventions will greatly aid in the informed planning of future government initiatives.

Our results indicate that the NDVI metric predominantly exhibits positive treatment effects during the Rabi season, with convergence across all assessment methods. This is an encouraging result, suggesting that ponds are effectively utilized during the Rabi, which is usually characterized by insufficient rainfall for irrigation. However, we did not observe a positive treatment effect on cropping intensity outcomes across most districts. This could also be attributed to the fact that farm ponds might be used for protective irrigation, thereby increasing crop-yield without any considerable change in cropping patterns. It might also be the case that these farm ponds are used for some other non-irrigation purposes

like pisciculture, hence not showing a positive effect on the cropping intensity.

Nevertheless, it is important to consider certain caveats. As discussed in Section III-A, the accuracy of the data provided by MGNREGA is questionable, significantly influencing the treatment effects observed through different methodologies. This discrepancy could explain the diverging assessments of treatment effects across farm ponds. Secondly, the absence of on-site ground-truth data around the ponds hampers the evaluation of different methods, requiring researchers to rely on derived data for measuring cropping and vegetation indicators. The accuracy of these derived cropping layers greatly impacts the final results in terms of computing treatment effects. Lastly, while our analysis was conducted on agro-ecological region 13, scaling the approach to all AEZs may pose challenges in terms of data preparation and computational requirements.

A common issue when using single satellite measurements for calculations is missing data due to cloud cover. To address this problem, in [76], a multi-satellite composite is created by combining data from LandSAT-7, LandSAT-8, and Sentinel-2 satellites. The composite is generated by calibrating the different satellites onto the same scale using standard calibration coefficients. Such a composite could be utilized in the future to obtain more reliable measurements for various NDVI based outcome indicators.

To address the issue of incorrect markings in the MGNREGA data, we propose developing a land use and land cover (LULC) mask capable of accurately detecting water bodies, including small farm ponds. This approach will enable us to map the precise latitude and longitude coordinates of the ponds mentioned in the database to the nearest water body pixels, thereby rectifying their location.

Additionally, we aim to expand our analysis by incorporating additional outcome variables, such as water levels in the ponds, to further enhance our understanding. Also, this framework developed for site-level assessment could very well be expanded to landscape-level structures like canals, dams etc and this a future direction we are pursuing. The Double ML models learned on past farm ponds can probably be used to predict site assessment for new prospective farm pond locations too.

Currently, we have compiled a comprehensive database of farm ponds, including their treatment effects based on various methodologies. To facilitate monitoring by the government and civil society organizations, we plan to develop a user-friendly dashboard on Google Earth Engine App. This platform will enable easy visualization and access to impact scores by clicking on different ponds of interest. Furthermore, our future endeavors involve developing a prediction model that can provide projected impact scores in real-time based on the latitude and longitude of any selected location.

The code/plots for this project is available at this link.

## ACKNOWLEDGMENT

This project was supported by Indian Institute of Technology, Delhi. We would like to express our sincere gratitude to our project guide and mentor, Professor Aaditeshwar Seth for his continuous guidance and encouragement, without which this project would not have been successful. We would also like to extend our gratitude to ICTD team members Ms. Ashima Mittal, Ms. Shivani Mehta, Ms. Ramneek and Ms. Chahat Bansal for their support.

## REFERENCES

- [1] Fischer, Chloé & Aubron, Claire & Trouvé, Aurélie & Muddu, Sekhar & Ruiz, Laurent. (2022). Groundwater irrigation reduces overall poverty but increases socioeconomic vulnerability in a semiarid region of southern India. *Scientific Reports*. 12. 10.1038/s41598-022-12814-0.
- [2] Buxton, Joshua & Powell, Thomas & Ambler, John & Boulton, Chris & Nicholson, Arwen & Arthur, Rudy & Lees, Kirsten & Williams, Hywel & Lenton, Timothy. (2021). Community-driven tree planting greens the neighbouring landscape. 10.21203/rs.3.rs-334324/v1.
- [3] Von Thaden Ugalde, Juan & Manson, Robert & Congalton, Russell & López Barrera, Fabiola & Jones, Kelly. (2021). Evaluating the environmental effectiveness of payments for hydrological services in Veracruz, México: A landscape approach. *Land Use Policy*. 100. 105055. 10.1016/j.landusepol.2020.105055.
- [4] TK, Sreedevi & Wani, Suhas & Sudi, Raghavendra & MS, Patel & T, Jayesh & SN, Singh & Shah, Tushar. (2006). On-site and Off-site Impact of Watershed Development: A Case Study of Rajasamadhiyala, Gujarat, India. *Global Theme on Agroecosystems Report no. 20*, Patancheru 502 324, Andhra Pradesh, India: International Crops Research Institute for the Semi-Arid Tropic. 2.
- [5] Sirmacek, Beril & Vinuesa, Ricardo. (2022). Remote sensing and AI for building climate adaptation applications. *Results in Engineering*. 15. 100524. 10.1016/j.rineng.2022.100524.
- [6] Zhang, Miao & Wu, Bingfang & Zeng, Hongwei & He, Guojin & Liu, Chong & Tao, Shiqi & Zhang, Qi & Nabil, Mohsen & Tian, Fuyou & Bofana, José & Beyene, Awetahagn & Elnashar, Abdelrazek & Yan, Nana & Wang, Zhengdong. (2021). GCI30: A global dataset of 30m cropping intensity using multisource remote sensing imagery. *Earth System Science Data*. 13. 10.5194/essd-13-4799-2021.
- [7] Ratledge, Nathan & Cadamuro, Gabe & Cuesta, Brandon & Stigler, Matthieu & Burke, Marshall. (2022). Using machine learning to assess the livelihood impact of electricity access. *Nature*. 611. 491-495. 10.1038/s41586-022-05322-8.
- [8] Agaton, Mufubi & Setiawan, Yudi & Effendi, Hefni. (2016). Land Use/Land Cover Change Detection in an Urban Watershed: A Case Study of Upper Citarum Watershed, West Java Province, Indonesia. *Procedia Environmental Sciences*. 33. 654-660. 10.1016/j.proenv.2016.03.120.
- [9] Central Ground Water Board, Department of Water Resources, River Development and Ganga Rejuvenation, Ministry of Jal Shakti, Government of India. *Aquifer mapping and management of ground water resources*. Retrieved May 2023, from [https://cgwb.gov.in/AQM/NAQUIM\\_REPORT/Bihar/Jamui%20district-report%20Final.pdf](https://cgwb.gov.in/AQM/NAQUIM_REPORT/Bihar/Jamui%20district-report%20Final.pdf)
- [10] Athey, Susan & Bayati, Mohsen & Doudchenko, Nikolay & Imbens, Guido & Khosravi, Khashayar. (2017). Matrix Completion Methods for Causal Panel Data Models. *Journal of the American Statistical Association*. 116. 10.1080/01621459.2021.1891924.
- [11] Doudchenko, Nikolay & Imbens, Guido. (2016). Balancing, Regression, Difference-In-Differences and Synthetic Control Methods: A Synthesis. *NBER Working Papers*.

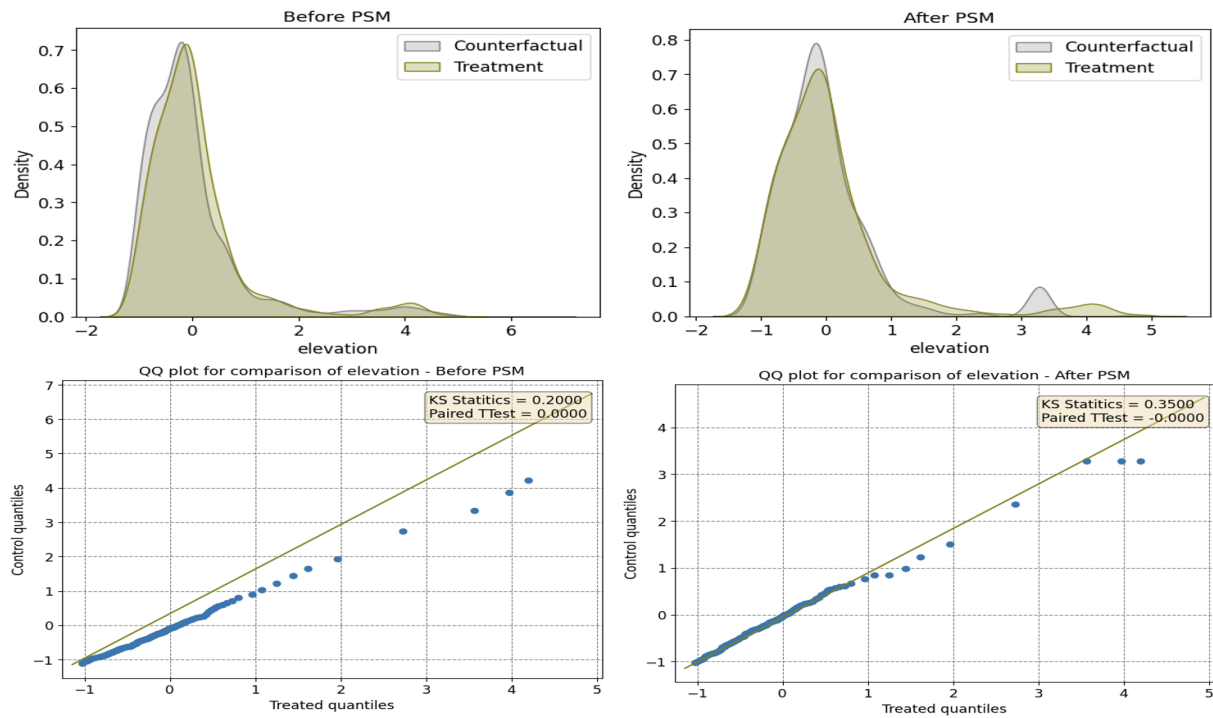
- [12] Egami, Naoki & Yamauchi, Soichiro. (2022). Using Multiple Pre-treatment Periods to Improve Difference-in-Differences and Staggered Adoption Designs. *Political Analysis*. 31. 1-18. 10.1017/pan.2022.8.
- [13] Deines, Jillian & Guan, Kaiyu & Lopez, Bruno & Zhou, Qu & White, Cambria & Wang, Sheng & Lobell, David. (2022). Recent cover crop adoption is associated with small maize and soybean yield losses in the United States. *Global change biology*. 29. 10.1111/gcb.16489.
- [14] Athey, Susan & Wager, Stefan. (2019). Estimating Treatment Effects with Causal Forests: An Application.[Preprint]
- [15] Giannarakis, Georgios & Sitokonstantinou, Vasileios & Lorilla, Roxanne & Charalabos, Kontoes. (2022). Towards assessing agricultural land suitability with causal machine learning. [Preprint]
- [16] Stetter, Christian & Mennig, Philipp & Sauer, Johannes. (2022). Using Machine Learning to Identify Heterogeneous Impacts of Agri-Environment Schemes in the EU: A Case Study. *European Review of Agricultural Economics*. 49. 723-759. 10.1093/erae/jbab057.
- [17] Prasad, Pooja & Sohoni, Milind A. (2018). Farmponds for Horticulture: Boon or Curse? Analysing Impact on Farm Profitability, Resource Sustainability and Social Welfare. Centre for Technology Alternatives for Rural Areas (CTARA), IIT Bombay. <https://www.cse.iitb.ac.in/~sohoni/TD463/poojaFPpaper.pdf>
- [18] Ali, Ammar & Sayl, Ass.Prof & Abed, Rasha & Abdeladhim, Mohamed & Wesseling, Jan & Riksen, Michel & Fleskens, Luuk & Karim, Usama & Ritsema, Coen. (2018). A GIS-based approach for identifying potential sites for harvesting rainwater in the Western Desert of Iraq. *International Soil and Water Conservation Research*. 6. 10.1016/j.iswcr.2018.07.003.
- [19] Ministry of Rural Development, Government of India. (2017). Handbook - Preparation of Gram Panchayat INRM Plan for Mission Water Conservation under MGNREGA. National Resource Training Team (NRTT) orientation workshop, Hyderabad.
- [20] Krishnan, Murali & Kakade B. & Premlatasingh & Peer, Quadri Javeed Ahmad. (2017). Impact and constraints of farm pond based watershed development in the Hassan district of Karnataka. *Chemical Science Review and Letters*. ISSN 2278-6783. [https://chesci.com/wp-content/uploads/2017/01/V6i21\\_59\\_CS122048023\\_Javid\\_365-370.pdf](https://chesci.com/wp-content/uploads/2017/01/V6i21_59_CS122048023_Javid_365-370.pdf)
- [21] Karmeshu, Neha, Trend Detection in Annual Temperature & Precipitation using the Mann Kendall Test – A Case Study to Assess Climate Change on Select States in the Northeastern United States (2012). Master of Environmental Studies Capstone Projects. 47. [https://repository.upenn.edu/mes\\_capstones/47](https://repository.upenn.edu/mes_capstones/47)
- [22] Jinru, Xue & Su, Baofeng. (2017). Significant Remote Sensing Vegetation Indices: A Review of Developments and Applications. *Journal of Sensors*. 2017. 1-17. 10.1155/2017/1353691.
- [23] Reddy, P.V.R.M. & Shankar, M. & Reddy, B. & Naik, Y. & Prasad, Yerra & Rekha, D.V.S.R.L.. (2020). Farm Pond Impact Analysis of PMKSY-Watersheds Project in Srikakulam District of Andhra Pradesh. *International Journal of Current Microbiology and Applied Sciences*. 9. 1719-1729. 10.20546/ijcmas.2020.912.204.
- [24] Collignon, Bernard. (2020). A new tool for the remote sensing of groundwater tables: satellite images of pastoral wells. *Open Geospatial Data Software and Standards*. 5. 10.1186/s40965-020-00077-3.
- [25] Fathy, I., Abd-Elhamid, H.F., Zeleňáková, M., & Kaposztásová, D. (2019). Effect of Topographic Data Accuracy on Watershed Management. *International Journal of Environmental Research and Public Health*, 16.
- [26] Rajasekhar, M., Sudarsana Raju, G., & Siddi Raju, R. (2019). Assessment of groundwater potential zones in parts of the semi-arid region of Anantapur District, Andhra Pradesh, India using GIS and AHP approach. *Modeling Earth Systems and Environment*, 5, 1303 - 1317.
- [27] Pande, Dr. Chaitanya & Khadri, Syed & Moharir, Dr. Kanak & Patode, R. (2018). Assessment of groundwater potential zonation of Mahesh River basin Akola and Buldhana districts, Maharashtra, India using remote sensing and GIS techniques. 4. 965–979. 10.1007/s40899-017-0193-5.
- [28] Yağmur, Nur & Tanik, Aysegul & Tuzcu Kokal, Aylin & Musaoglu, Nebiye & Erten, Esra & Bilgilioğlu, Bahar. (2020). Opportunities provided by remote sensing data for watershed management: Example of Konya closed basin. *International Journal of Engineering and Geosciences*. 5. 10.26833/ijeg.638669.
- [29] Sekhar M, Tomer SK, Thiyaku S, Giriraj P, Murthy S, Mehta VK. Groundwater Level Dynamics in Bengaluru City, India. *Sustainability*. 2018; 10(1):26. <https://doi.org/10.3390/su10010026>
- [30] Choudhary, Karan & Goel, Inka & Bisen, P. & Sanapala, Mamatha & Ray, Shibendu & K, Chandrasekar & Murthy, C. & Seshaiah, Mullapudi. (2015). Use of Remote Sensing Data for Drought Assessment: A Case Study for Bihar State of India During Kharif, 2013. 10.1007/978-3-319-10217-7\_28
- [31] Upadhyaya, Deepa & Evans, Jonathan & Muddu, Sekhar & Kumar, Sat & Al Bitar, Ahmad & Yeggina, Subash & S., Thiyaku & Morrison, Ross & Fry, Matthew & Tripathi, Sachchida & Mujumdar, M. & Goswami, Mangesh & Ganeshi, Naresh & Nema, Manish & Jain, Sharad & Angadi, S & Yenagi, Basavaraj. (2021). The Indian COSMOS Network (ICON): Validating L-Band Remote Sensing and Modelled Soil Moisture Data Products. *Remote Sensing*. 13. 537. 10.3390/rs13030537.
- [32] Senthilkumar, M. & Gnandasundar, Devadasan & Arumugam, Rethinam. (2019). Identifying groundwater recharge zones using remote sensing & GIS techniques in Amaravathi aquifer system, Tamil Nadu, South India. *Sustainable Environment Research*. 29. 10.1186/s42834-019-0014-7.
- [33] Lobell, David & Thau, David & Seifert, Christopher & Engle, Eric & Little, Bertis. (2015). A scalable satellite-based crop yield mapper. *Remote Sensing of Environment*. 164. 10.1016/j.rse.2015.04.021.
- [34] Wing, Coady & Simon, Kosali & Bello-Gomez, Ricardo. (2018). Designing Difference in Difference Studies: Best Practices for Public Health Policy Research. *Annual Review of Public Health*. 39. 10.1146/annurev-publhealth-040617-013507.
- [35] Egami, Naoki & Yamauchi, Soichiro. (2022). Using Multiple Pre-treatment Periods to Improve Difference-in-Differences and Staggered Adoption Designs. *Political Analysis*. 31. 1-18. 10.1017/pan.2022.8.
- [36] López Felices, Belén & Aznar-Sánchez, José A. & Velasco Muñoz, Juan & Piquer-Rodríguez, María. (2020). Contribution of Irrigation Ponds to the Sustainability of Agriculture. A Review of Worldwide Research. *Sustainability*. 12. 5425. 10.3390/su12135425.
- [37] Gajbhiye, K.S., & Mandal, C (2000). Agro-ecological zones, their soil resource and cropping systems. *National Bureau of Soil Survey and Land Use Planning*, Nagpur
- [38] Athey, Susan & Tibshirani, Julie & Wager, Stefan. (2019). Generalized random forests. *Annals of Statistics*. 47. 1179-1203. 10.1214/18-AOS1709.
- [39] Schafer, Joseph & Kang, Joseph. (2009). Average Causal Effects From Nonrandomized Studies: A Practical Guide and Simulated Example. *Psychological methods*. 13. 279-313. 10.1037/a0014268.
- [40] Prasad, Pooja & Damani, Om & Sohoni, Milind. (2022). How can resource-level thresholds guide sustainable intensification of agriculture at farm level? A system dynamics study of farm-pond based intensification. *Agricultural Water Management*. 264. 107385. 10.1016/j.agwat.2021.107385.
- [41] Pokropek, Artur. (2016). Introduction to instrumental variables and their application to large-scale assessment data. *Large-scale Assessments in Education*. 4. 10.1186/s40536-016-0018-2.
- [42] Reed, Bradley & Brown, Jesslyn & VanderZee, Darrel & Loveland, Thomas & Merchant, James & Ohlen, Donald. (1994). Measuring Phenological Variability From Satellite Imagery. *Journal of Vegetation Science - J VEG SCI*. 5. 703-714. 10.2307/3235884.

- [43] Brown, Christopher & Brumby, Steven & Guzder-Williams, Brookie & Birch, Tanya & Hyde, Samantha & Mazzariello, Joseph & Czerwinski, Wanda & Pasquarella, Valerie & Haertel, Robert & Ilyushchenko, Simon & Schewhr, Kurt & Weisse, Mikaela & Stolle, Fred & Hanson, Craig & Guinan, Oliver & Moore, Rebecca & Tait, Alexander. (2022). Dynamic World, Near real-time global 10 m land use land cover mapping. *Scientific Data*. 9. 251. 10.1038/s41597-022-01307-4.
- [44] Panda, Manoj & Jha, Brajesh & Mandal, Amit & Pal, Vivek & Sharma, Aakanksha & Choudhury, Atrayee & Kumar, Deepak. (2018). Rapid assessment of natural resource management component under MGNREGA and its impact on sustainable livelihoods. Ministry of Rural Development, Government of India.
- [45] Prodanovic, Dusan & Stanić, Milos & Milivojević, Vladimir & Simić, Zoran & Arsic, Milos. (2023). DEM-based GIS algorithms for automatic creation of hydrological models data.
- [46] Cramb, Rob & Purcell, T.. (2001). How to Monitor and Evaluate Impacts of Participatory Research Projects: A Case Study of the Forages for Smallholders Project.
- [47] Shinde, M. & Gorantiwar, Sunil & Smout, Ian. (2011). Application of Watershed-Based Tank System Model for Rainwater Harvesting and Irrigation in India. *Journal of Irrigation and Drainage Engineering*. 137. 659-667. 10.1061/(ASCE)IR.1943-4774.0000313.
- [48] Sunil Kumar, Rajesh Kumar Pant, Basant Kumar Mishra and Sonal Kulshreshtha. (2019). Impact Assessment of Environmental Benefits through MGNREGA project. Deutsche Gesellschaft für Internationale Zusammenarbeit (GIZ) GmbH. [https://www.giz.de/en/downloads/Synopsis\\_Impact%20Assessment\\_MGNREGA-EB.pdf](https://www.giz.de/en/downloads/Synopsis_Impact%20Assessment_MGNREGA-EB.pdf)
- [49] Ministry of Rural Development, Government of India. *Study to Assess the Impact of MGNREGS*. Retrieved May 2023, from <https://rural.nic.in/en/press-release/study-assess-impact-mgnregs>
- [50] Center for Study of Science, Technology and Policy, India. *A framework for quantifying the Climate co-benefits of MGNREGS Works*. Retrieved March 2023, from <https://cstep.in/publications-details.php?id=2316>
- [51] Austin, Peter. (2011). An Introduction to Propensity Score Methods for Reducing the Effects of Confounding in Observational Studies. *Multivariate behavioral research*. 46. 399-424. 10.1080/00273171.2011.568786.
- [52] Rosenbaum, Paul & Rubin, Donald. (1983). The Central Role of the Propensity Score in Observational Studies For Causal Effects. *Biometrika*. 70. 41-55. 10.1093/biomet/70.1.41.
- [53] Jacob, Daniel. (2021). CATE meets ML: Conditional average treatment effect and machine learning. *Digital Finance*. 3. 10.1007/s42521-021-00033-7.
- [54] Amit Sharma & Emre Kiciman. (2018). *Tutorial on Causal Inference and Counterfactual Reasoning*. Retrieved February 2023, from <https://causalinference.gitlab.io/kdd-tutorial/>
- [55] Haaya Naushan, Apr 2021, *Causal Machine Learning for Econometrics: Causal Forests*. Retrieved 23 January 2023, from <https://towardsdatascience.com/causal-machine-learning-for-econometrics-causal-forests-5ab3aec825a7>
- [56] Matteo Courthoud, Jul 2022, *Understanding AIPW, the Doubly-Robust Estimator*. Retrieved 24 January 2023, from <https://towardsdatascience.com/understanding-aipw-ed4097dab27a>
- [57] Stanford Graduate School of Business, Jan 2022, *Conditional Average Treatment Effects: Forests*. Retrieved 24 January 2023, from <https://www.youtube.com/watch?v=fNjToAQ9v3g>
- [58] Stanford Graduate School of Business, Jan 2022, *Robust Estimation of Treatment Heterogeneity*. Retrieved 24 January 2023, from <https://www.youtube.com/watch?v=0GK6IZut6K8>
- [59] Datameet & CIS. (2017). *Open Water Data in India*. <https://datameet-pune.github.io/open-water-data/docs/open-water-data-paper.pdf>
- [60] Baba Amte Centre for People's Empowerment, Samaj Pragati Sahayog. (2006). *National Rural Employment Guarantee Act Watershed Works Manual*. Retrieved February 2023, from [https://nrega.nic.in/Netnrega/Data/SPS\\_Watershed\\_Works\\_Manual\\_Eng.pdf](https://nrega.nic.in/Netnrega/Data/SPS_Watershed_Works_Manual_Eng.pdf)
- [61] *How to download Satellite Images from the USGS, ESA and Google Earth Engine*. Retrieved March 2022, from <https://www.youtube.com/watch?v=uQvlTQoUWuQ>
- [62] *Google Earth Engine Guide: Supervised Classification*. Retrieved March 2022, from <https://developers.google.com/earth-engine/guides/classification>
- [63] *Google Earth Engine API Reference*. Retrieved April 2022, from <https://developers.google.com/earth-engine/apidocs/>
- [64] Abderrazak, Bannari & Morin, D. & Bonn, F. & Huete, Alfredo. (1996). A review of vegetation indices. *Remote Sensing Reviews*. 13. 95-120. 10.1080/02757259509532298.
- [65] Pooja, Vinod & Deshmukh, Ratnadeep & Randive, Priyanka. (2018). *Vegetation Indices for Crop Management: A Review*.
- [66] Kateryna Sergieieva. (2022). *Vegetation Indices To Drive Digital Agri Solutions*. Retrieved November 2022, from <https://eos.com/blog/vegetation-indices/>
- [67] MicaSense. *Overview of Agricultural Indices*. Retrieved November 2022, from <https://support.micasense.com/hc/en-us/articles/227837307-Overview-of-Agricultural-Indices>
- [68] L. Wang & H. Liu. (2006). *An efficient method for identifying and filling surface depressions in digital elevation models for hydrologic analysis and modelling*, International Journal of Geographical Information Science, 20:2, 193-213, DOI: 10.1080/13658810500433453 MicaSense.
- [69] O'Callaghan, J.F. & Mark, D.M. (1984). *AThe Extraction of Drainage Networks from Digital Elevation Data*. *Computer Vision, Graphics and Image Processing*, 28, 328-344., [http://dx.doi.org/10.1016/S0734-189X\(84\)80011-0](http://dx.doi.org/10.1016/S0734-189X(84)80011-0)
- [70] Micro watershed atlas of India , Soil and Land Use Survey of India, Dept. of Agriculture and Cooperation, Ministry of Agriculture, Govt. of India, New Delhi. <https://slus.iacnet.nic.in/mwa.pdf>
- [71] Bansal, Chahat & Om, Hari & Jain, Mayank & A., Omprakash & Mehta, Shivani & Singh, Deepanshu & Baheti, Harshavardhanshushil & Singh, Suyash & Seth, Aaditeshwar. (2021). IndiaSat: A Pixel-Level Dataset for Land-Cover Classification on Three Satellite Systems - Landsat-7, Landsat-8, and Sentinel-2. 147-155. 10.1145/3460112.3471953.
- [72] A. Kline & Y. Luo, PsmPy: A Package for Retrospective Cohort Matching in Python, 2022 44th Annual International Conference of the IEEE Engineering in Medicine & Biology Society (EMBC), 2022, pp. 1354-1357, doi: 10.1109/EMBC48229.2022.9871333.
- [73] Brian Quistorff, Matt Goldman, and Jason Thorpe (2020) Sparse Synthetic Controls: Unit-Level Counterfactuals from High-Dimensional Data, Microsoft Journal of Applied Research, 14, pp.155-170.
- [74] Alberto Abadie, Alexis Diamond & Jens Hainmueller (2010) Synthetic Control Methods for Comparative Case Studies: Estimating the Effect of California's Tobacco Control Program, *Journal of the American Statistical Association*, 105:490, 493-505, DOI: 10.1198/jasa.2009.ap08746.
- [75] Sehgal, J., Mandal, D.K., Mandal, C. and Vadivelu, S. (1992): Agro-Ecological Regions of India. Second Edition, Tech. Bull. No. 24, NBSS and LUP. 130p.
- [76] Zhang, M., Wu, B., Zeng, H., He, G., Liu, C., Tao, S., Zhang, Q., Nabil, M., Tian, F., Bofana, J., Beyene, A. N., Elnashar, A., Yan, N., Wang, Z., and Liu, Y.: GCI30: A global dataset of 30m cropping intensity using multisource remote sensing imagery, *Earth Syst. Sci. Data*, 13, 4799–4817, <https://doi.org/10.5194/essd-13-4799-2021>, 2021.

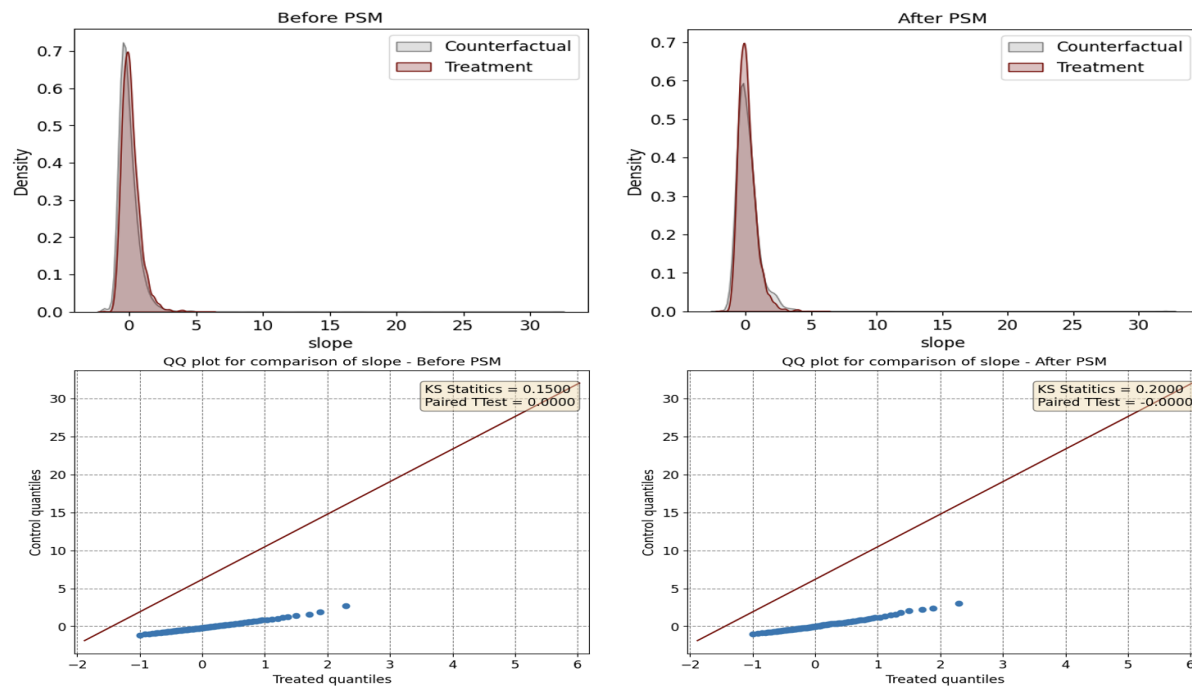
## APPENDIX

District	Number of Large Farm Ponds	Annual Mean Precipitation in the District in Hydrological Year								
		2014	2015	2016	2017	2018	2019	2020	2021	
Araria	50	2611.14	2767.61	3376.27	2950.92	2658.73	3961.59	4592.72	6063.71	
Bahraich	123	2917.26	1883.68	2349.12	2102.15	3091.17	3295.74	2580.62	2931.41	
Balrampur	72	1982.35	2151.58	2994.80	2391.42	2290.28	3290.65	2658.17	2181.27	
Banka	63	2453.37	2161.70	2269.59	2734.69	1836.74	3025.27	2832.18	2709.60	
Basti	46	2220.44	1394.26	2028.26	2283.03	2188.12	3634.72	2841.14	3008.24	
Begusarai	14	2155.33	1920.08	2047.27	1991.75	1528.67	2849.28	3048.32	2966.58	
Bhagalpur	14	2399.73	2260.57	2408.93	2720.05	1915.40	3145.68	3295.00	3212.53	
Darbhanga	34	2127.30	2159.59	2375.53	2270.25	1749.92	3133.34	3697.26	4184.70	
Deoria	106	2120.59	1500.12	1844.38	2109.98	2007.61	3779.45	3303.52	3373.70	
Gonda	9	2357.92	1517.34	2109.25	2116.42	2553.18	3478.10	2659.37	2837.97	
Gopalganj	102	2113.58	1735.20	1776.20	1944.59	1829.85	3519.46	3462.05	3224.84	
Gorakhpur	114	2201.93	1418.66	2007.97	2414.25	2107.20	3821.22	3406.49	3552.99	
Jamui	403	2413.89	2032.42	2234.60	2530.53	1649.49	2862.08	2749.94	2642.65	
Katihar	33	2583.57	2580.17	2825.20	3048.35	2231.58	3702.13	4022.70	4536.31	
Khagaria	4	2268.65	2142.96	2231.31	2362.18	1659.75	2976.70	3354.57	3204.90	
Kishanganj	87	3504.80	3856.02	4074.90	4003.51	3432.34	4898.92	5731.00	7950.30	
Kushinagar	91	2628.75	1950.57	2442.69	2790.00	2825.73	3848.69	3998.94	3918.68	
Lakhisarai	6	2237.70	1911.07	2099.41	2141.35	1555.16	2789.24	2839.46	2814.00	
Madhepura	17	2312.82	2327.10	2694.66	2581.66	2039.65	3297.90	3829.18	4142.21	
Madhubani	9	2160.59	2342.17	2709.07	2441.08	2157.38	3260.88	3783.86	4726.46	
Maharajganj	226	2929.06	2061.05	2869.09	3454.13	3091.00	3941.68	4238.80	4455.12	
Munger	14	2292.24	2051.01	2160.28	2434.69	1652.39	2900.75	2983.83	2803.50	
Muzaffarpur	66	2071.25	1945.60	1993.59	1910.12	1642.05	3229.26	3662.82	3772.54	
Pashchim Champaran	47	3003.31	2440.05	2863.26	3415.49	3126.54	4045.12	4582.99	4752.18	
Purba Champaran	93	2345.89	2137.29	2249.27	2388.11	2117.40	3551.27	3949.72	4124.76	
Purnia	53	2561.32	2605.27	3011.60	2957.82	2332.71	3738.48	4201.57	5237.44	
Saharsa	1	2268.38	2265.39	2510.54	2466.80	1774.24	3087.97	3672.42	4005.20	
Samastipur	1	2151.45	1966.37	2123.12	1975.05	1468.11	2986.49	3278.74	3528.21	
Sant Kabir Nagar	30	2271.59	1458.88	2046.25	2459.84	2225.52	3793.53	3241.98	3378.58	
Shravasti	14	2909.92	1893.12	2405.81	2297.56	3031.37	3407.15	2604.85	2980.84	
Siddharth Nagar	193	2735.19	1825.52	2524.60	2903.73	2827.74	3916.26	3564.18	3782.52	
Sitamarhi	1	2294.49	2294.41	2572.07	2481.70	2169.12	3476.62	4019.69	4667.71	

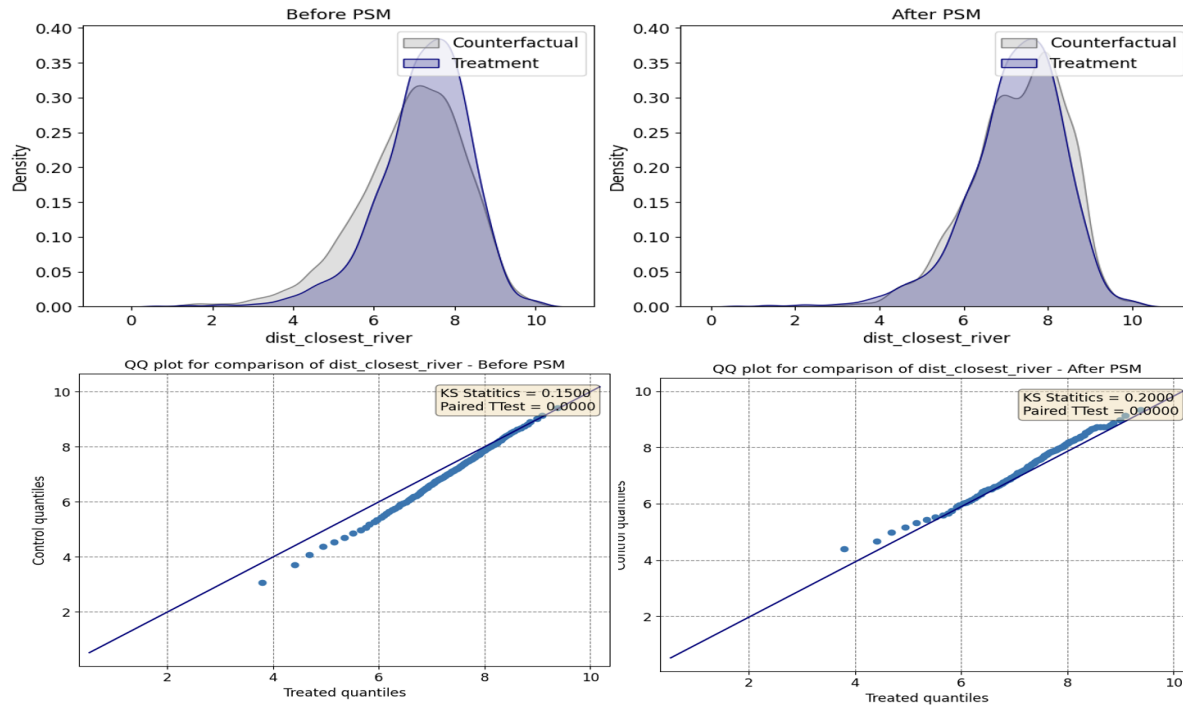
Table V: District-Wise Annual Mean Rainfall and No. of Farm Ponds Constructed



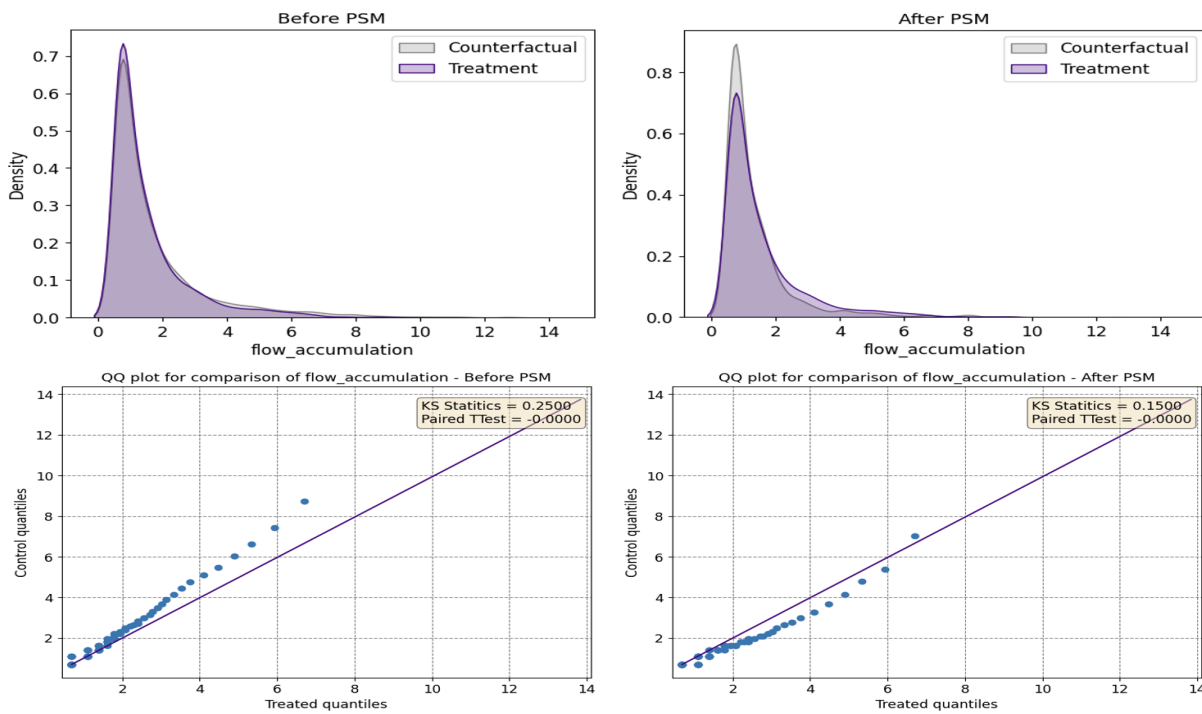
(a) Analysing matchings wrt elevation



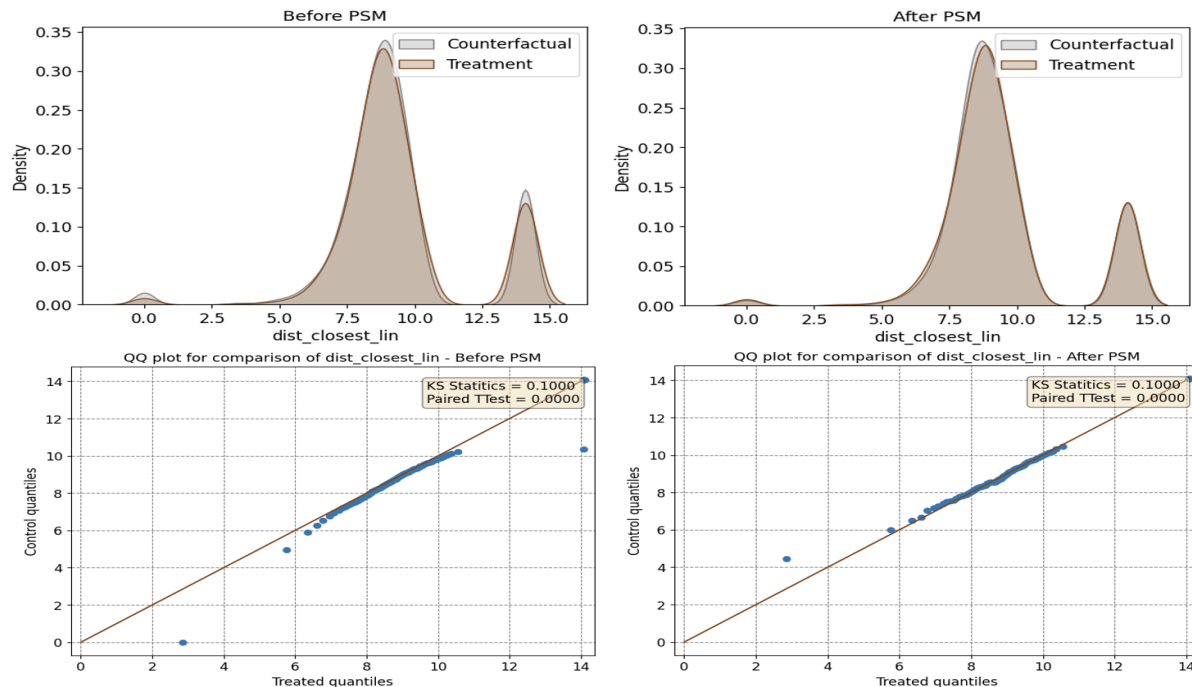
(b) Analysing matchings wrt slope



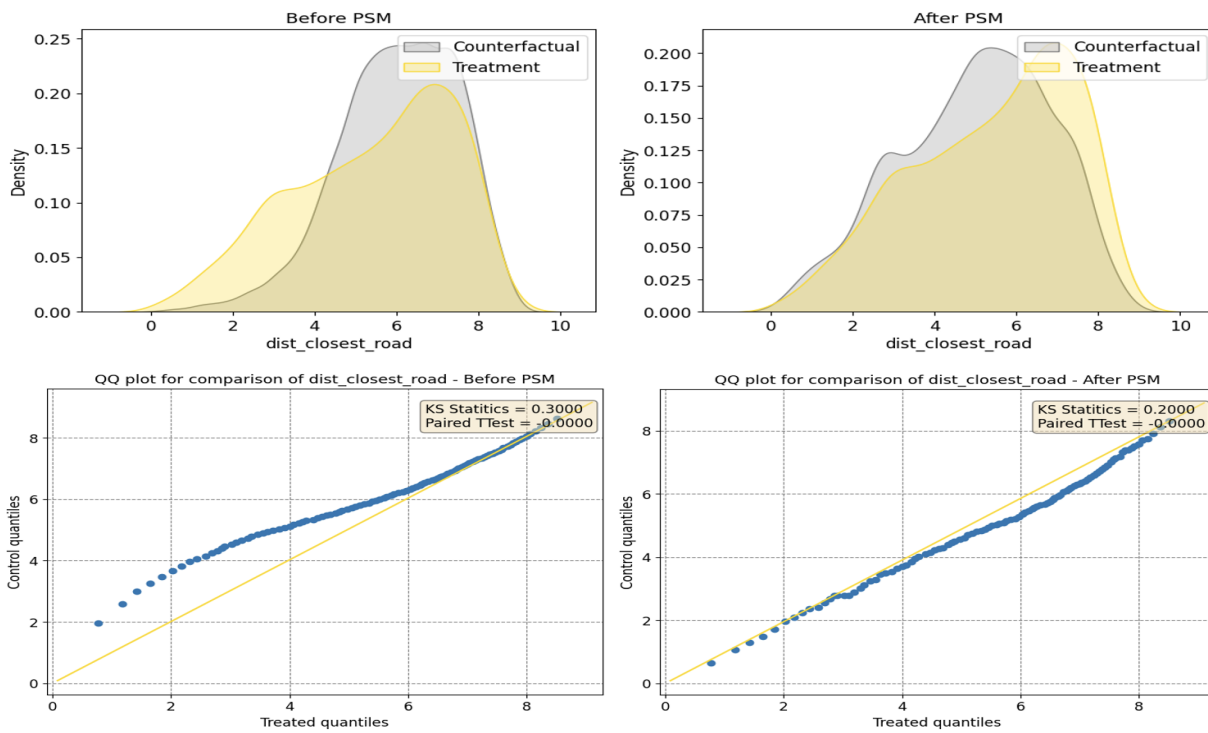
(c) Analysing matchings wrt distance to rivers



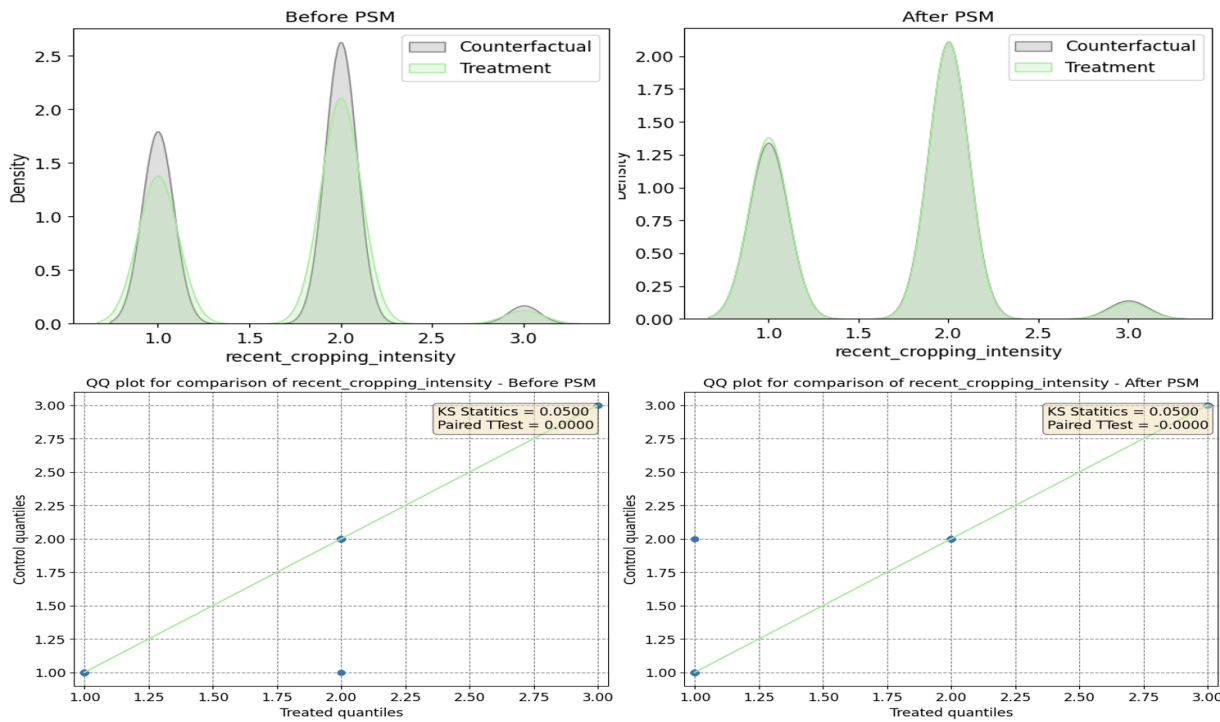
(d) Analysing matchings wrt flow accumulation



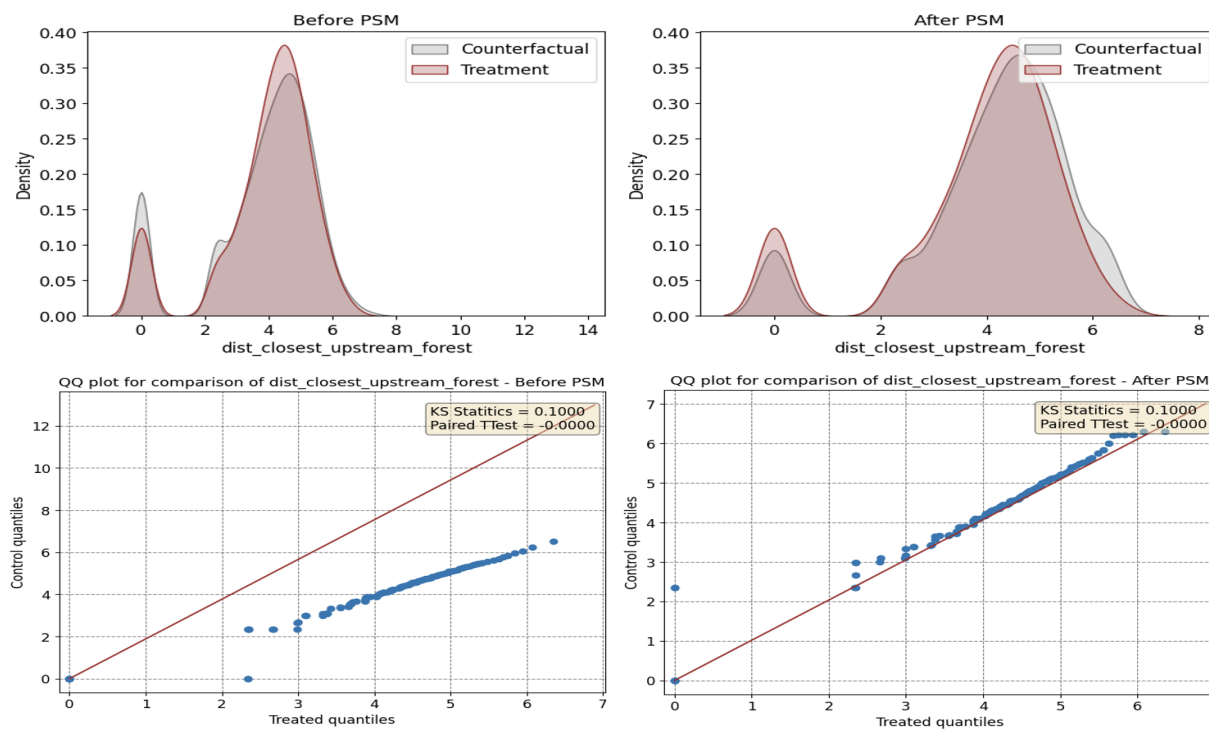
(e) Analysing matchings wrt distance to lineaments



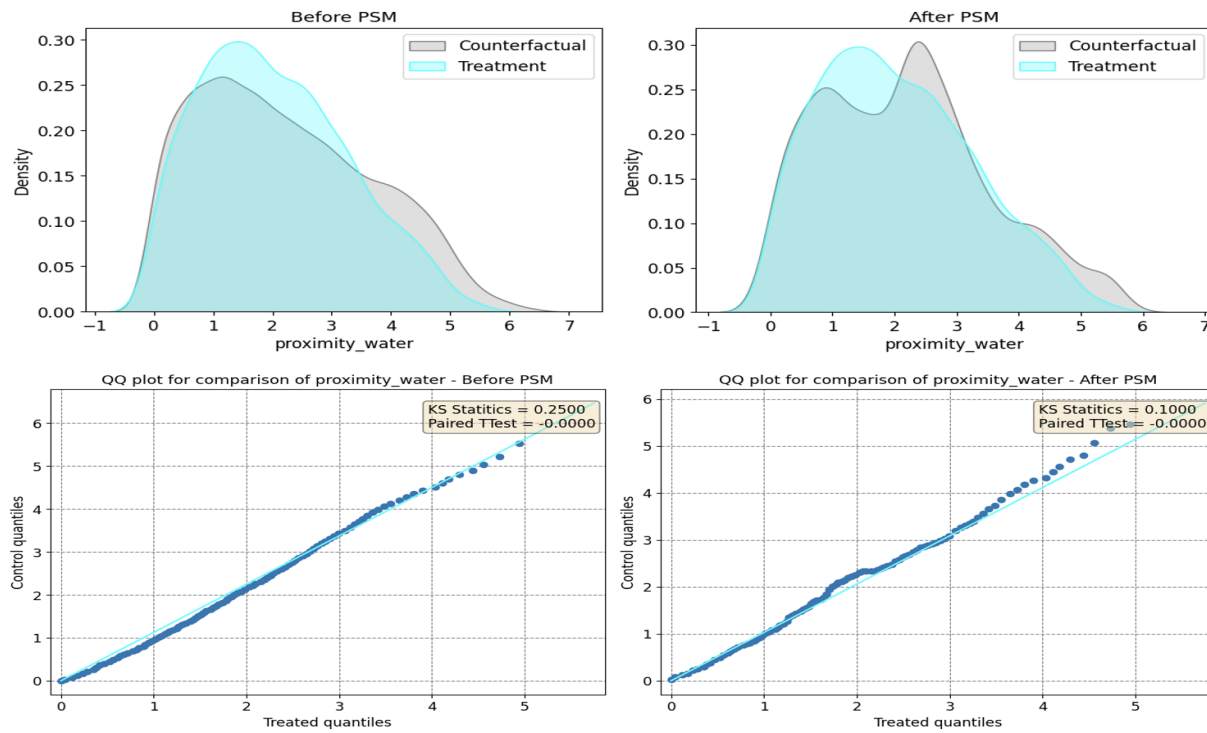
(f) Analysing matchings wrt distance to roads



(g) Analysing matchings wrt recent cropping intensity



(h) Analysing matchings wrt distance to closest upstream forest



(i) Analysing matchings wrt proximity to water

Figure 34: PSM distributions analysis

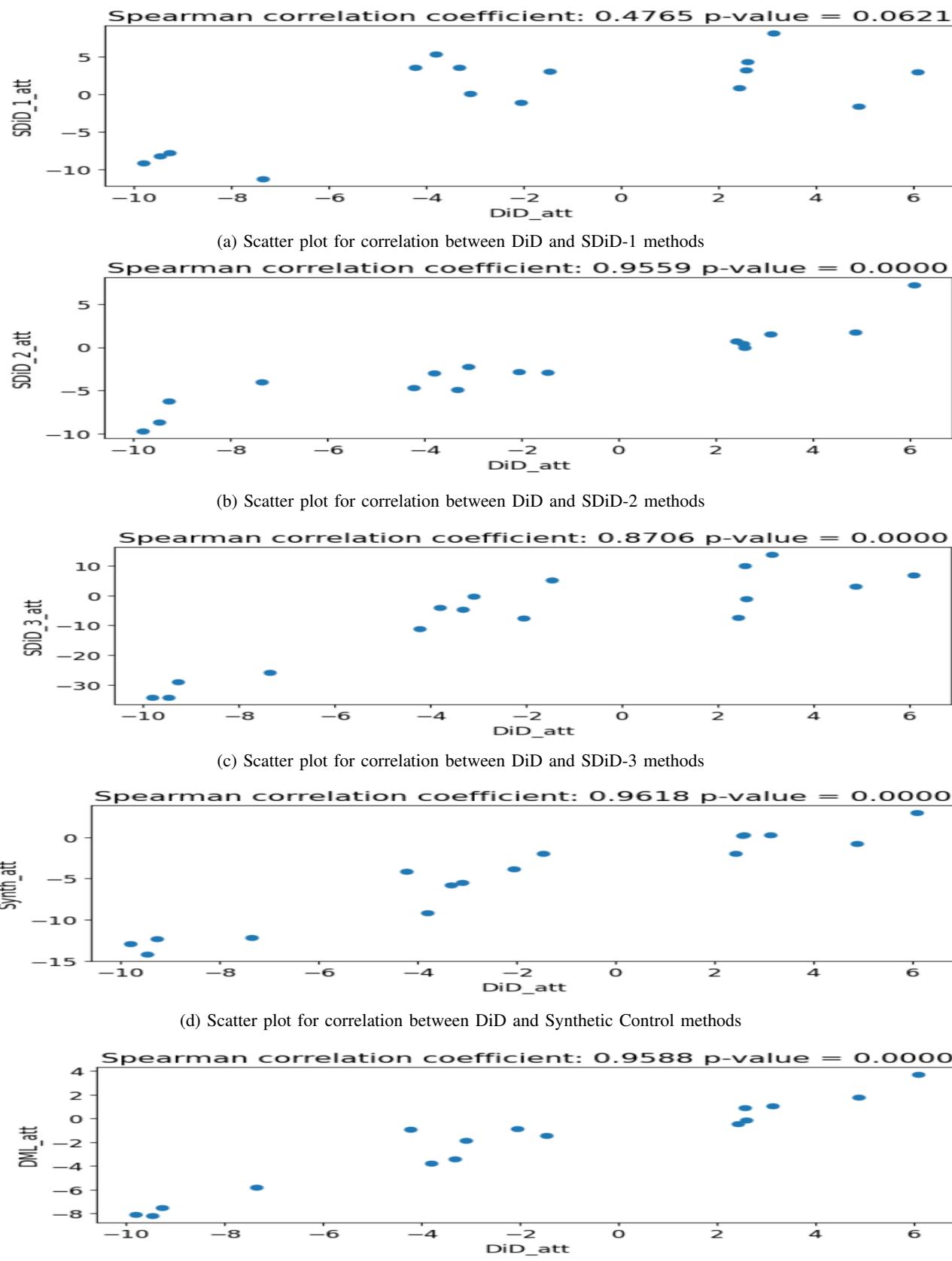


Figure 35: Correlation of ATT values of DiD method with all the methods

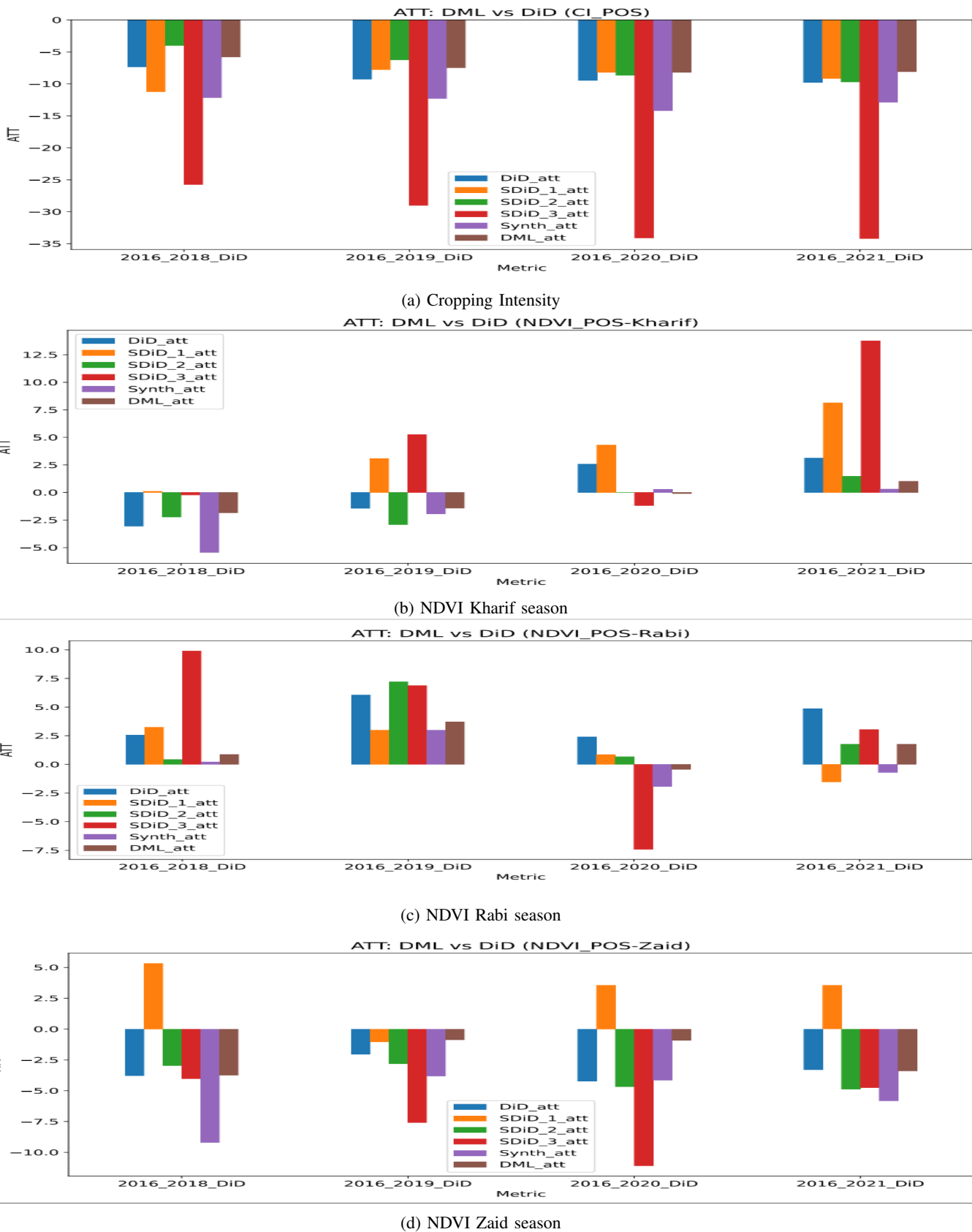


Figure 36: Average Treatment Effects on the treated (ATT) comparison of all methods

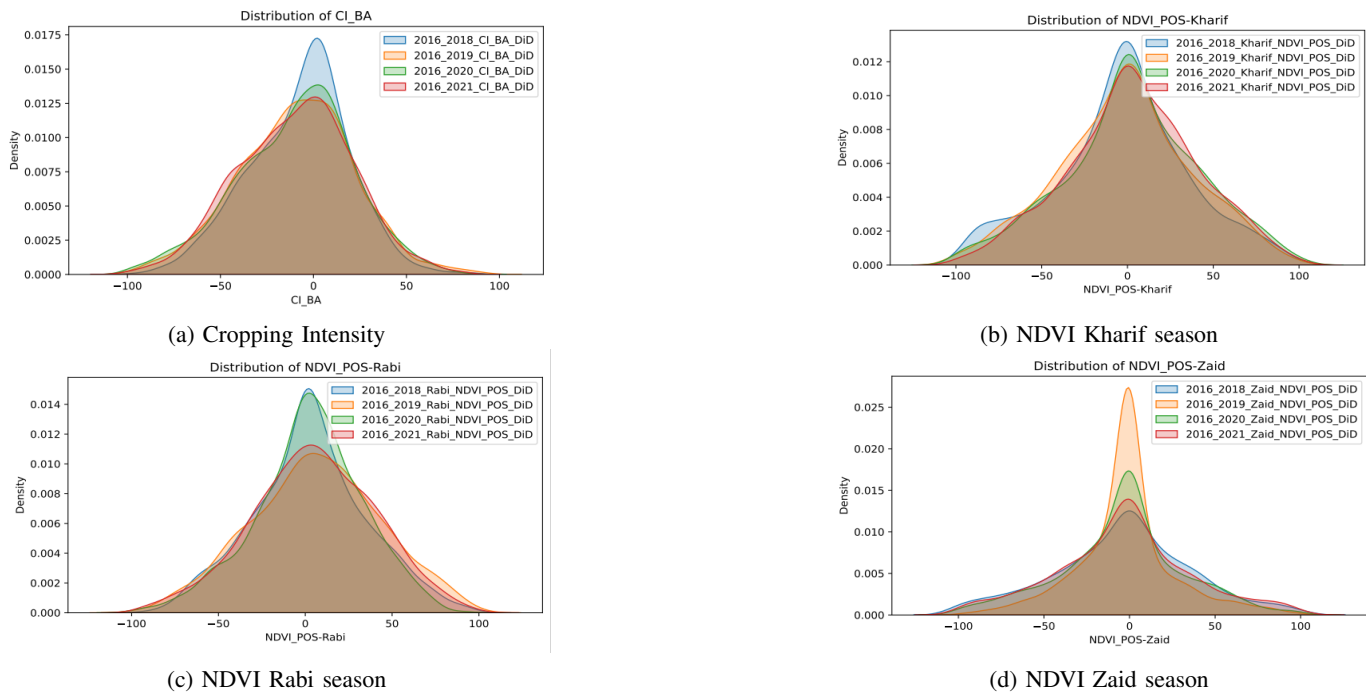


Figure 37: Distribution of Average Treatment Effects (ATE) - DiD

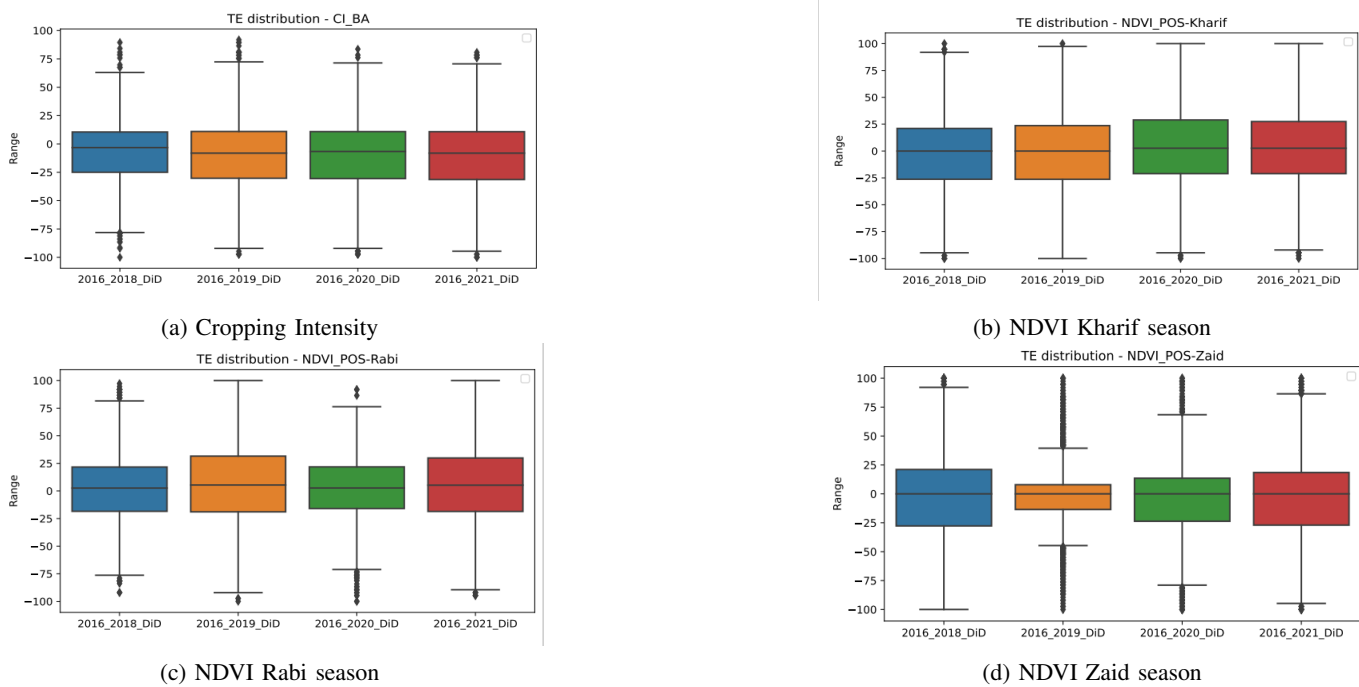


Figure 38: Distribution of Treatment Effects (TE) - DiD method

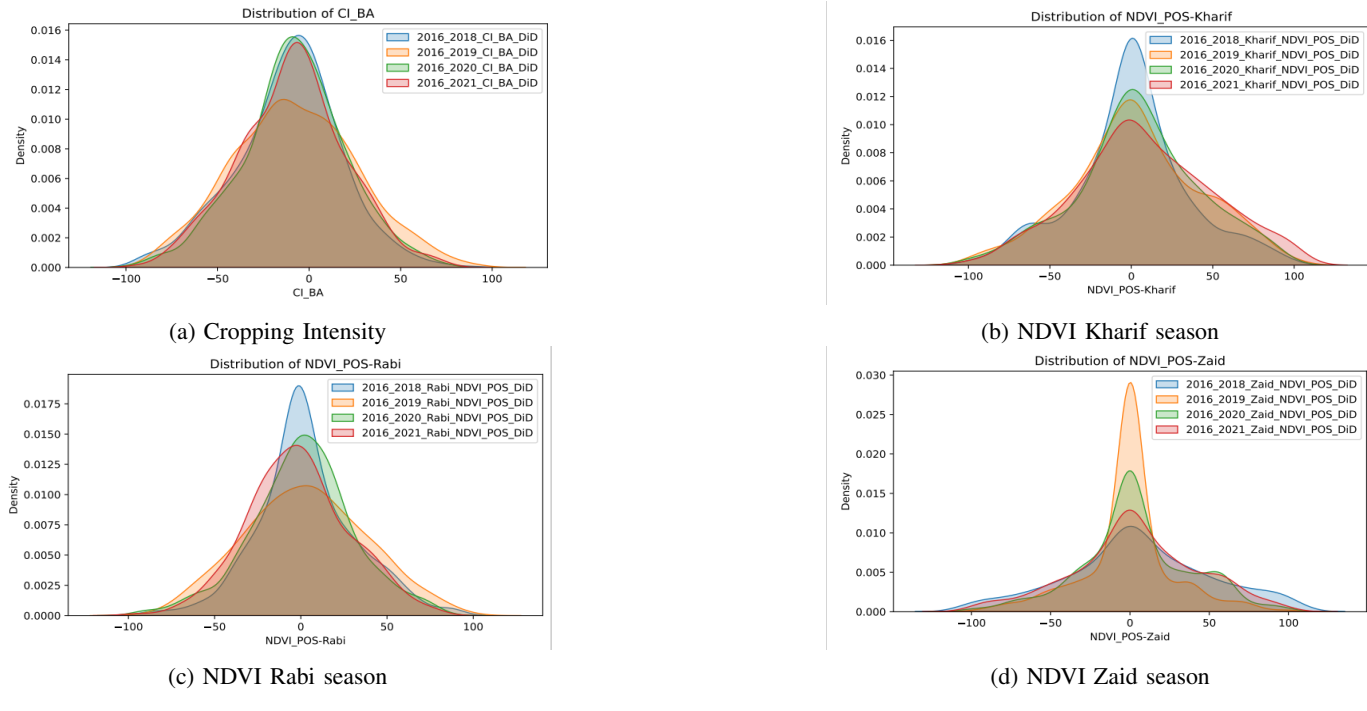


Figure 39: Distribution of Average Treatment Effects (ATE) - Stratified DiD (single cropping)

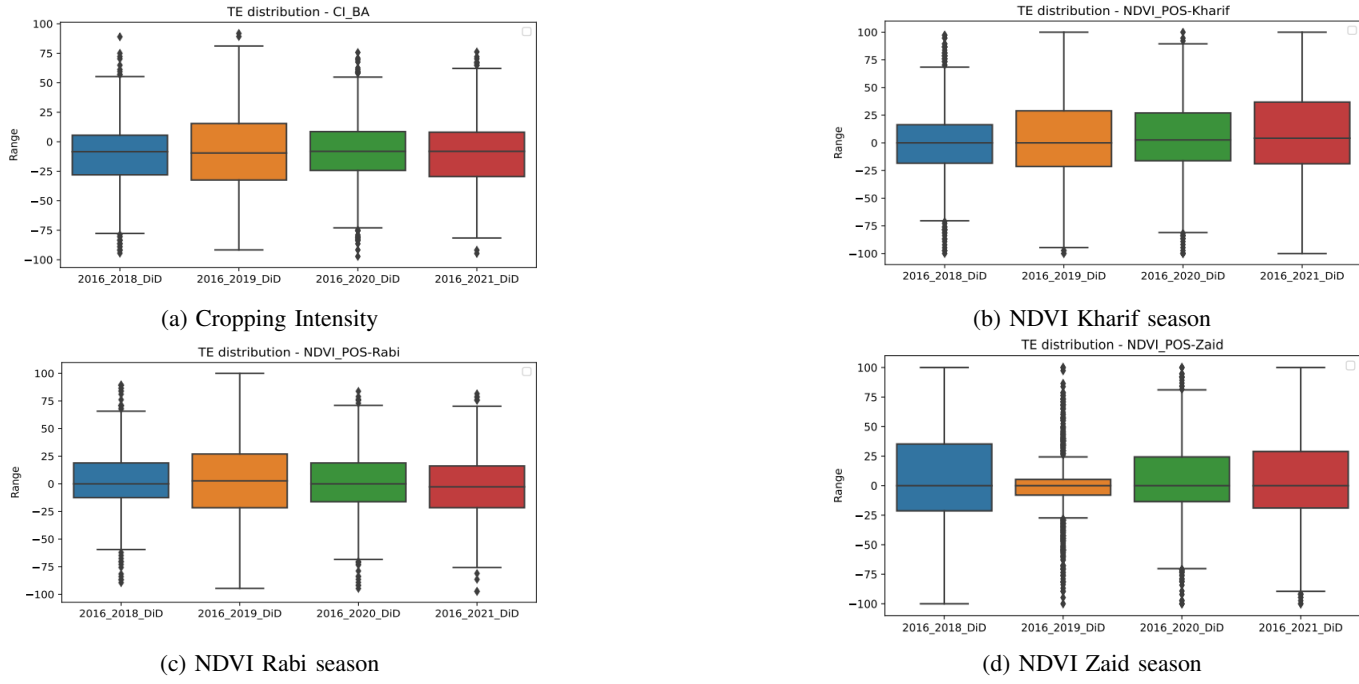


Figure 40: Distribution of Treatment Effects (TE) - Stratified DiD (single cropping) method

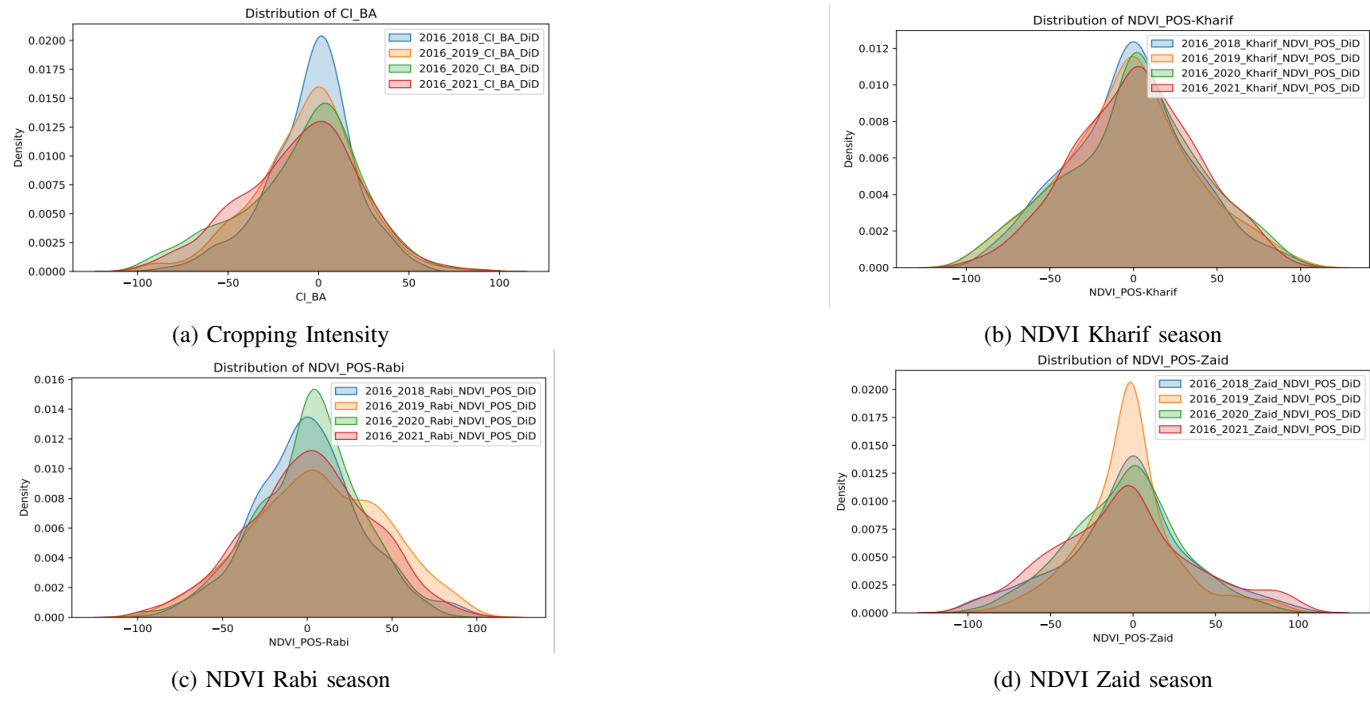


Figure 41: Distribution of Average Treatment Effects (ATE) - Stratified DiD (double cropping)

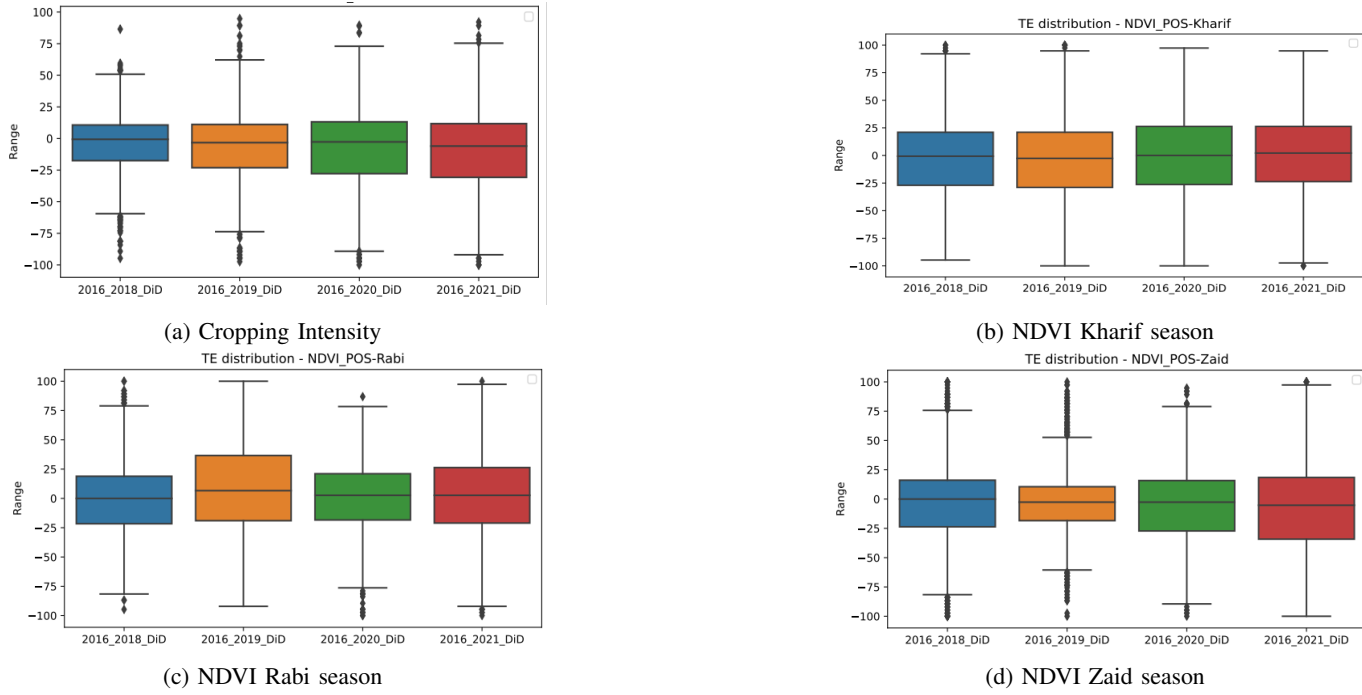


Figure 42: Distribution of Treatment Effects (TE) - Stratified DiD (double cropping) method

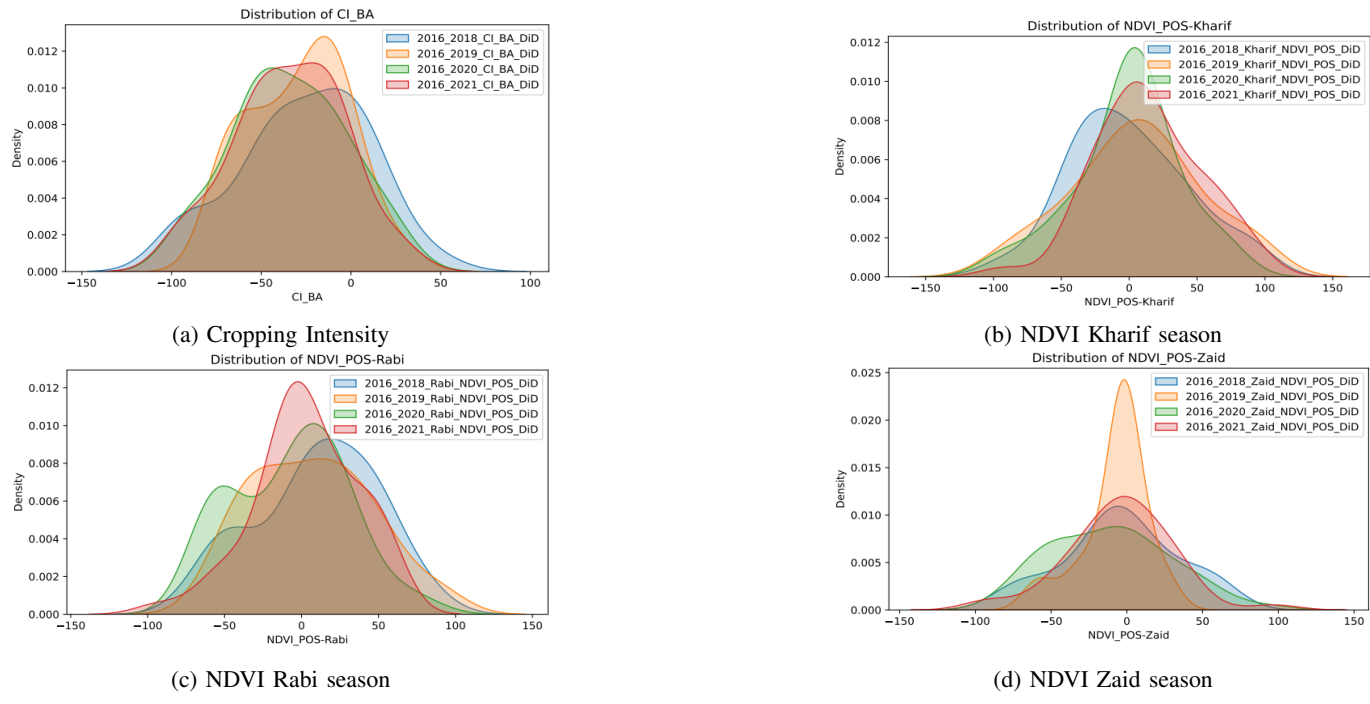


Figure 43: Distribution of Average Treatment Effects (ATE) - Stratified DiD (triple cropping)

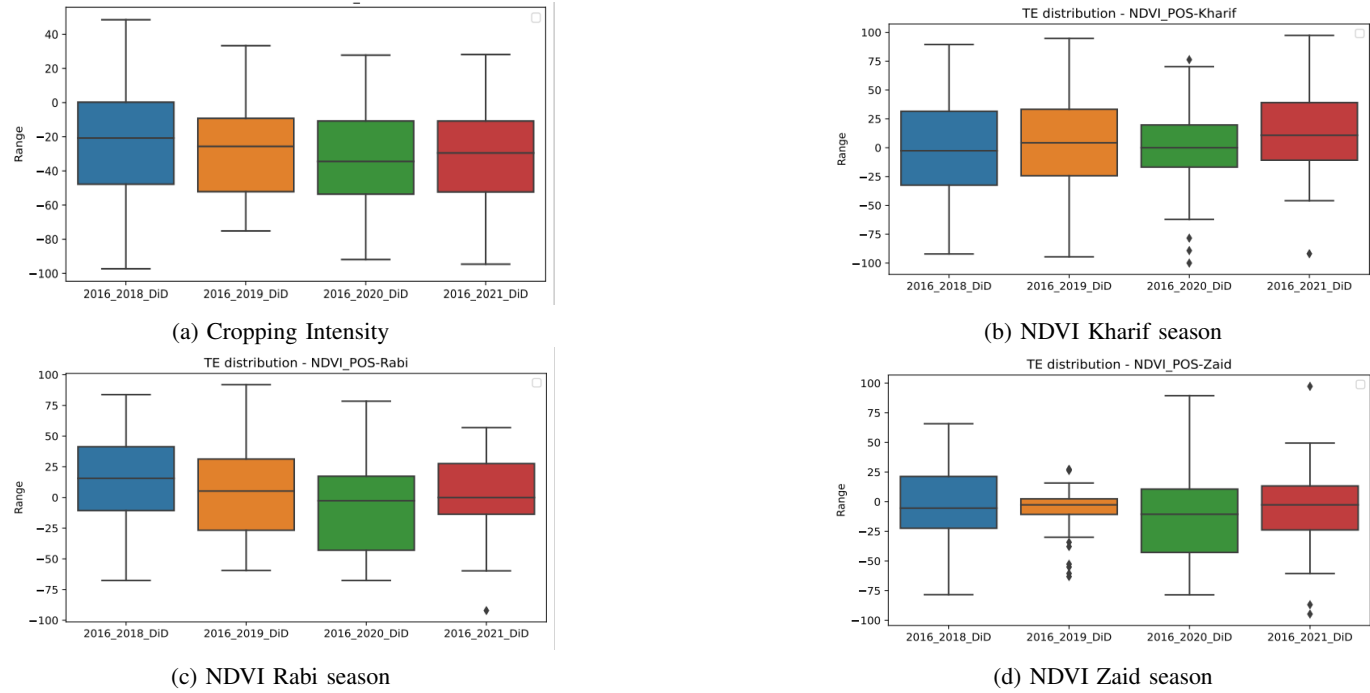


Figure 44: Distribution of Treatment Effects (TE) - Stratified DiD (triple cropping) method

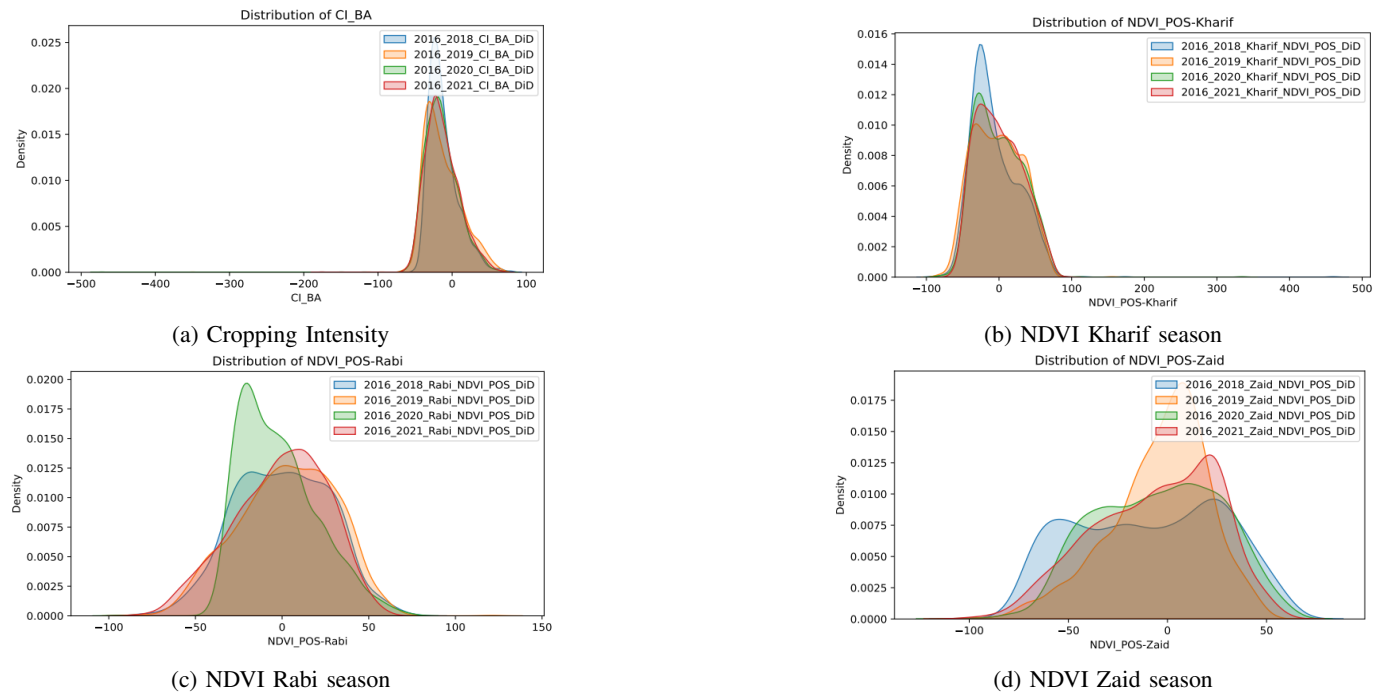


Figure 45: Distribution of Average Treatment Effects (ATE) - Synthetic Control

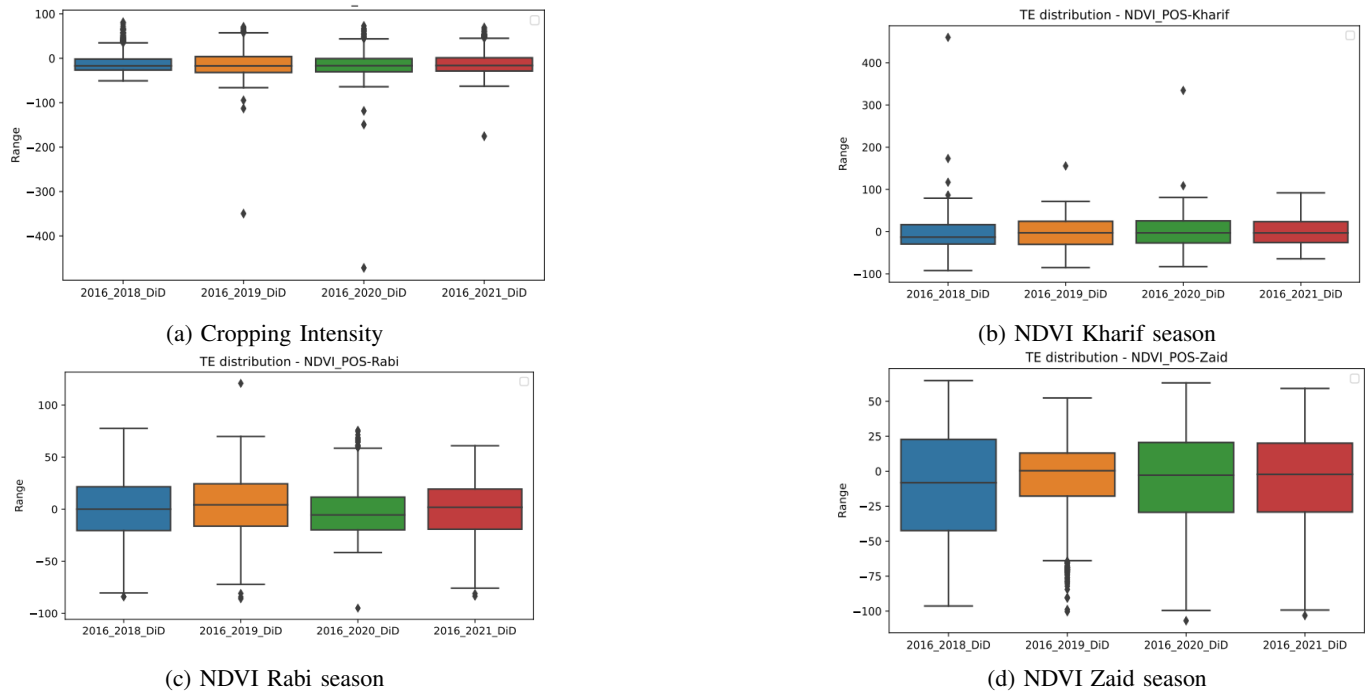


Figure 46: Distribution of Treatment Effects (TE) - Synthetic Control method

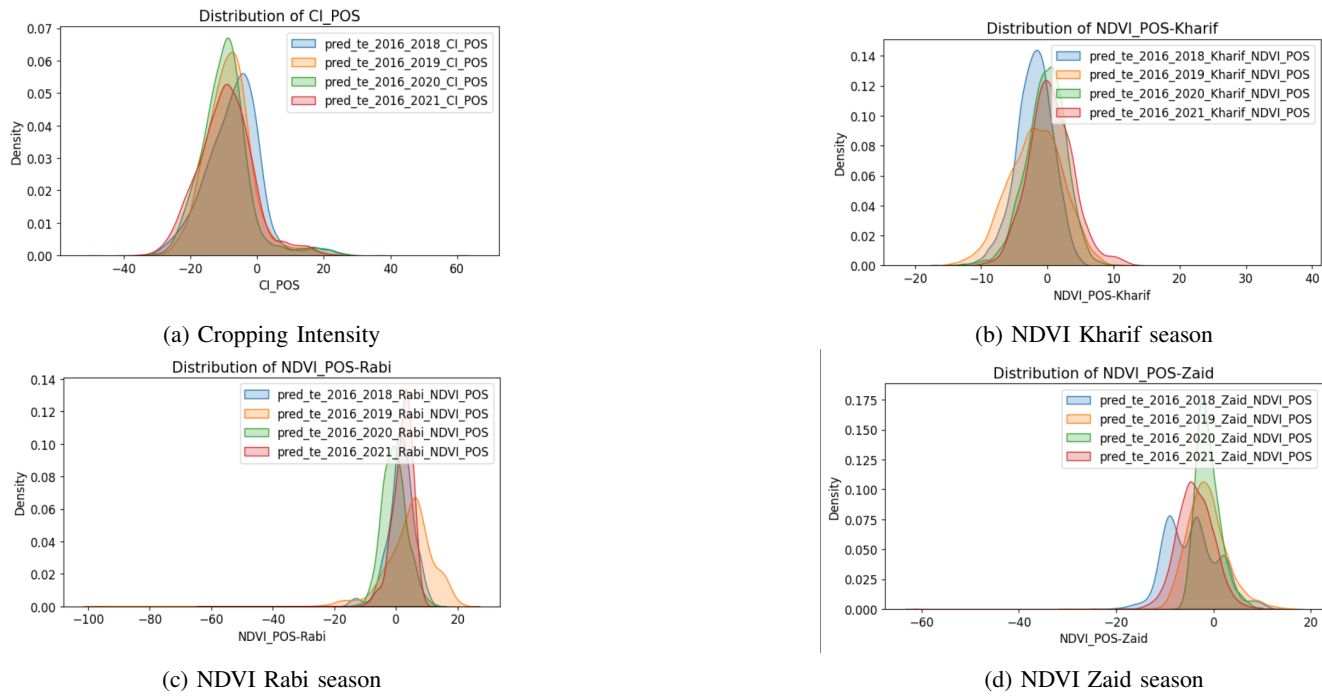


Figure 47: Distribution of Treatment Effects - Double ML method

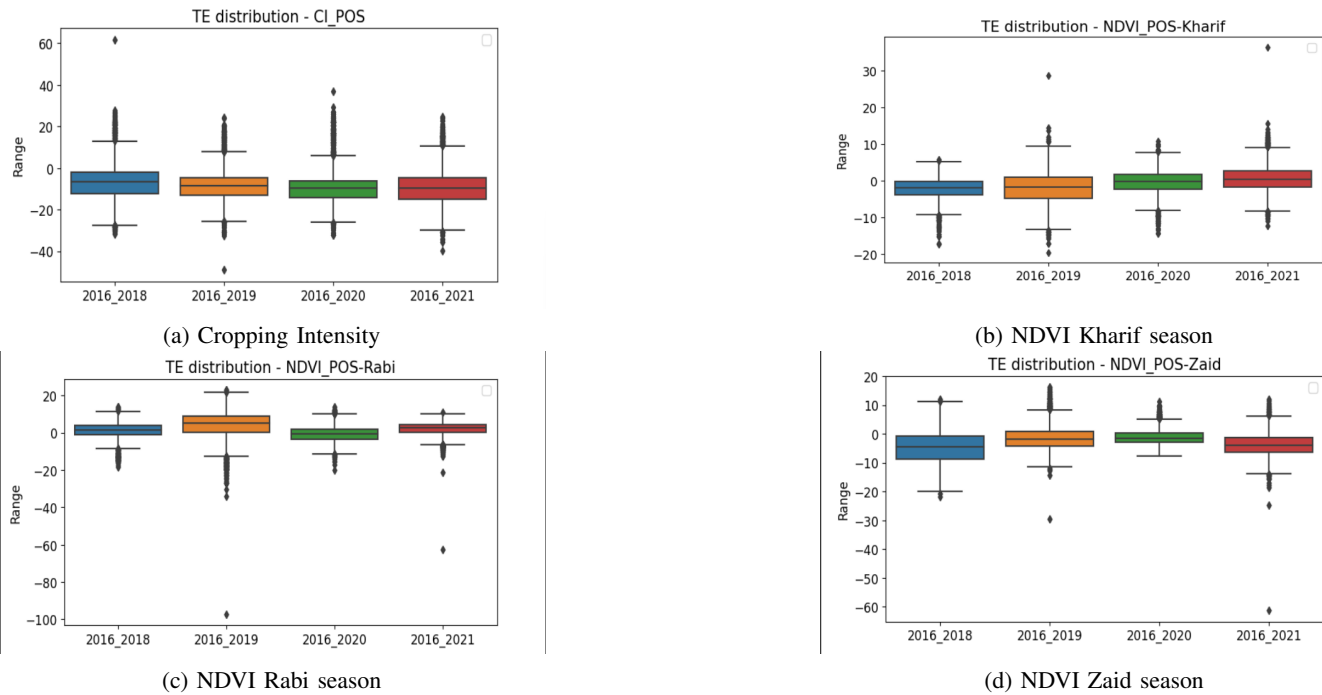


Figure 48: Distribution of Treatment Effects (TE) - Double ML method

District	2018 CI	2019 CI	2020 CI	2018 KH	2019 KH	2020 KH	2018 Ra	2019 Ra	2020 Ra	2018 Zd	2019 Zd	2020 Zd	2021 Zd
araria	-30.44	-18.01	-22.49	-27.92	-9.77	-7.55	-7.47	-10.20	2.39	-0.32	8.62	-4.41	-13.95
bahadarpur	-2.28	-6.14	-10.88	4.37	1.20	-9.61	9.26	2.79	6.73	-0.84	6.60	-1.36	-1.99
bahadarpur	-6.83	-3.25	-13.15	-5.79	-13.25	-5.29	-2.26	-7.33	0.88	-3.41	-2.42	-0.06	-4.93
banka	-4.30	-4.84	-1.10	0.12	17.74	0.06	13.19	11.76	3.02	3.35	0.62	0.47	1.99
basti	-2.27	-9.47	0.37	6.55	1.01	4.60	2.07	3.16	1.34	-7.29	-3.71	0.19	-0.14
begusarai	-18.97	-5.97	-9.36	4.06	6.90	2.51	-2.50	7.93	3.27	-8.95	10.09	0.67	-4.33
bhagalpur	-2.98	-15.64	0.76	0.37	-5.67	9.04	-6.18	-2.28	10.93	2.19	15.88	0.67	24.51
darbhanga	-1.39	-14.73	-21.57	-11.36	-11.15	4.96	3.97	3.77	-10.09	-11.59	-11.44	-12.71	-7.99
deoria	-2.24	-14.40	-14.55	-10.66	-0.25	0.83	10.53	5.17	4.83	14.00	-1.32	8.18	-4.73
gonda	-12.92	-5.22	-10.35	-19.89	-5.56	8.48	-21.01	-13.09	11.04	-7.70	-3.41	0.21	-7.13
gopalganj	-6.13	-8.96	-8.57	-10.72	-9.16	-3.57	-2.08	-5.84	2.21	-2.87	-2.44	-8.62	-3.46
gorakhpur	-7.49	-13.72	-23.94	19.70	1.61	18.32	15.68	9.92	14.15	10.73	5.53	4.60	3.35
janauj	-5.43	-6.23	-3.33	-15.31	-1.24	5.86	11.61	-2.32	3.99	9.15	10.33	-4.35	-0.75
kathua	-17.16	-14.98	-14.12	-19.01	6.90	-2.59	1.12	4.12	11.37	0.74	6.03	5.42	-12.48
khagaria	-18.03	-8.78	-16.79	-11.61	13.94	1.05	19.73	22.96	-4.61	5.51	-36.05	-9.15	-6.20
kishanganj	-16.73	-6.41	-19.48	-20.87	-1.51	-3.39	-1.04	-3.61	-4.07	2.69	-3.22	3.58	-7.24
kushinagar	-10.47	-2.72	-11.32	-10.91	-6.35	-3.01	-0.90	0.58	13.19	-1.04	7.83	6.81	0.75
lakhisarai	-2.34	-25.62	-18.35	-3.33	-22.78	-2.00	-15.50	16.27	4.51	-9.23	1.47	9.99	0.56
madhepura	-4.17	-5.69	-7.44	-8.16	-13.85	-18.13	-11.09	-8.02	-1.80	3.10	8.18	-4.07	5.27
madhubani	3.52	-6.52	5.69	-1.12	-3.48	2.87	-17.34	-12.60	-9.58	-8.13	-1.43	2.00	8.79
maharajganj	-3.26	-6.81	-4.73	-4.05	-4.83	3.48	14.60	3.71	1.89	12.59	-1.64	8.42	-12.80
munger	-3.13	-3.02	6.14	2.23	18.57	-13.10	21.57	17.28	10.79	-3.20	15.41	6.44	29.17
nuzaffarpur	-7.96	-8.78	-15.78	-11.73	11.18	2.17	6.84	5.81	-1.50	-1.38	-3.70	3.32	-14.02
paschim champaran	-24.56	-24.33	-20.95	-23.11	-12.85	-25.64	0.08	-9.61	1.32	-4.85	5.77	-2.73	-10.17
purnia	-8.22	-3.99	-5.75	-8.25	2.60	-0.92	-13.11	-10.28	15.10	1.95	-0.24	1.03	3.88
saharsa	-19.18	-15.76	-22.63	-21.38	-9.47	-7.08	-16.36	-7.79	18.35	12.71	0.95	10.41	-1.53
samastipur	-46.88	-59.46	-53.60	-46.70	65.36	56.76	35.53	6.76	5.44	15.11	-54.69	-62.38	3.95
sant kabir nagar	-30.37	-37.80	-37.80	-44.94	66.25	91.89	62.16	37.73	-8.11	-28.41	-5.135	-50.11	38.05
sheikhpura	-8.09	-18.29	-24.16	-14.65	-0.15	8.05	-0.86	8.23	1.22	11.52	5.25	-14.28	-25.69
shrawasti	-3.83	-34.31	-32.43	-8.11	29.73	21.62	-20.41	36.70	18.92	-2.70	52.63	21.62	-21.05
siddharth nagar	-7.98	-11.15	-9.22	-11.22	-3.97	-7.77	-5.80	-23.34	2.11	1.67	0.63	4.32	7.88
sitamarhi	-5.41	-0.29	6.83	-22.22	16.22	9.46	18.42	-13.51	3.69	9.23	-0.93	2.71	-9.05
Positive Count	1	0	4	4	15	18	16	19	23	22	16	21	15
Average of Positive ATT	3.522078469	0	4.85527252	0.77117479	18.91398695	14.00551825	14.8065478	11.5565661	7.743484	7.2667626	9.81844513	7.0339258	9.178373

Table VI: District Wise ATT values for all Metrics (Green Rows showing Positive ATT with Yellow being the top 10% values)

(Yellow Rows showing Negative ATT with Green being the top 10% values)

(Yellow Rows showing Neutral ATT)

(Green Rows showing Neutral ATT)

(Yellow Rows showing Negative ATT)

(Green Rows showing Neutral ATT)

(Yellow Rows showing Negative ATT)

(Green Rows showing Neutral ATT)

(Yellow Rows showing Negative ATT)

(Green Rows showing Neutral ATT)

(Yellow Rows showing Negative ATT)

(Green Rows showing Neutral ATT)

(Yellow Rows showing Negative ATT)

(Green Rows showing Neutral ATT)

(Yellow Rows showing Negative ATT)

(Green Rows showing Neutral ATT)

(Yellow Rows showing Negative ATT)

(Green Rows showing Neutral ATT)

(Yellow Rows showing Negative ATT)

(Green Rows showing Neutral ATT)

(Yellow Rows showing Negative ATT)

(Green Rows showing Neutral ATT)

(Yellow Rows showing Negative ATT)

(Green Rows showing Neutral ATT)

(Yellow Rows showing Negative ATT)

(Green Rows showing Neutral ATT)

(Yellow Rows showing Negative ATT)

(Green Rows showing Neutral ATT)

(Yellow Rows showing Negative ATT)

(Green Rows showing Neutral ATT)

(Yellow Rows showing Negative ATT)

(Green Rows showing Neutral ATT)

(Yellow Rows showing Negative ATT)

(Green Rows showing Neutral ATT)

(Yellow Rows showing Negative ATT)

(Green Rows showing Neutral ATT)

(Yellow Rows showing Negative ATT)

(Green Rows showing Neutral ATT)

(Yellow Rows showing Negative ATT)

(Green Rows showing Neutral ATT)

(Yellow Rows showing Negative ATT)

(Green Rows showing Neutral ATT)

(Yellow Rows showing Negative ATT)

(Green Rows showing Neutral ATT)

(Yellow Rows showing Negative ATT)

(Green Rows showing Neutral ATT)

(Yellow Rows showing Negative ATT)

(Green Rows showing Neutral ATT)

(Yellow Rows showing Negative ATT)

(Green Rows showing Neutral ATT)

(Yellow Rows showing Negative ATT)

(Green Rows showing Neutral ATT)

(Yellow Rows showing Negative ATT)

(Green Rows showing Neutral ATT)

(Yellow Rows showing Negative ATT)

(Green Rows showing Neutral ATT)

(Yellow Rows showing Negative ATT)

(Green Rows showing Neutral ATT)

(Yellow Rows showing Negative ATT)

(Green Rows showing Neutral ATT)

(Yellow Rows showing Negative ATT)

(Green Rows showing Neutral ATT)

(Yellow Rows showing Negative ATT)

(Green Rows showing Neutral ATT)

(Yellow Rows showing Negative ATT)

(Green Rows showing Neutral ATT)

(Yellow Rows showing Negative ATT)

(Green Rows showing Neutral ATT)

(Yellow Rows showing Negative ATT)

(Green Rows showing Neutral ATT)

(Yellow Rows showing Negative ATT)

(Green Rows showing Neutral ATT)

(Yellow Rows showing Negative ATT)

(Green Rows showing Neutral ATT)

(Yellow Rows showing Negative ATT)

(Green Rows showing Neutral ATT)

(Yellow Rows showing Negative ATT)

(Green Rows showing Neutral ATT)

(Yellow Rows showing Negative ATT)

(Green Rows showing Neutral ATT)

(Yellow Rows showing Negative ATT)

(Green Rows showing Neutral ATT)

(Yellow Rows showing Negative ATT)

(Green Rows showing Neutral ATT)

(Yellow Rows showing Negative ATT)

(Green Rows showing Neutral ATT)

(Yellow Rows showing Negative ATT)

(Green Rows showing Neutral ATT)

(Yellow Rows showing Negative ATT)

(Green Rows showing Neutral ATT)

(Yellow Rows showing Negative ATT)

(Green Rows showing Neutral ATT)

(Yellow Rows showing Negative ATT)

(Green Rows showing Neutral ATT)

(Yellow Rows showing Negative ATT)

(Green Rows showing Neutral ATT)

(Yellow Rows showing Negative ATT)

(Green Rows showing Neutral ATT)

(Yellow Rows showing Negative ATT)

(Green Rows showing Neutral ATT)

(Yellow Rows showing Negative ATT)

(Green Rows showing Neutral ATT)

(Yellow Rows showing Negative ATT)

(Green Rows showing Neutral ATT)

(Yellow Rows showing Negative ATT)

(Green Rows showing Neutral ATT)

(Yellow Rows showing Negative ATT)

(Green Rows showing Neutral ATT)

(Yellow Rows showing Negative ATT)

(Green Rows showing Neutral ATT)

(Yellow Rows showing Negative ATT)

(Green Rows showing Neutral ATT)

(Yellow Rows showing Negative ATT)

(Green Rows showing Neutral ATT)

(Yellow Rows showing Negative ATT)

(Green Rows showing Neutral ATT)

(Yellow Rows showing Negative ATT)

(Green Rows showing Neutral ATT)

(Yellow Rows showing Negative ATT)

(Green Rows showing Neutral ATT)

(Yellow Rows showing Negative ATT)

(Green Rows showing Neutral ATT)

(Yellow Rows showing Negative ATT)

(Green Rows showing Neutral ATT)

(Yellow Rows showing Negative ATT)

(Green Rows showing Neutral ATT)

(Yellow Rows showing Negative ATT)

(Green Rows showing Neutral ATT)

(Yellow Rows showing Negative ATT)

(Green Rows showing Neutral ATT)

(Yellow Rows showing Negative ATT)

(Green Rows showing Neutral ATT)

(Yellow Rows showing Negative ATT)

(Green Rows showing Neutral ATT)

(Yellow Rows showing Negative ATT)

(Green Rows showing Neutral ATT)

(Yellow Rows showing Negative ATT)

(Green Rows showing Neutral ATT)

(Yellow Rows showing Negative ATT)

(Green Rows showing Neutral ATT)

(Yellow Rows showing Negative ATT)

(Green Rows showing Neutral ATT)

(Yellow Rows showing Negative ATT)

(Green Rows showing Neutral ATT)

(Yellow Rows showing Negative ATT)

(Green Rows showing Neutral ATT)

(Yellow Rows showing Negative ATT)

(Green Rows showing Neutral ATT)

(Yellow Rows showing Negative ATT)

(Green Rows showing Neutral ATT)

(Yellow Rows showing Negative ATT)

(Green Rows showing Neutral ATT)

(Yellow Rows showing Negative ATT)

(Green Rows showing Neutral ATT)

(Yellow Rows showing Negative ATT)

(Green Rows showing Neutral ATT)

(Yellow Rows showing Negative ATT)

(Green Rows showing Neutral ATT)

(Yellow Rows showing Negative ATT)

(Green Rows showing Neutral ATT)

(Yellow Rows showing Negative ATT)

(Green Rows showing Neutral ATT)

(Yellow Rows showing Negative ATT)

(Green Rows showing Neutral ATT)

(Yellow Rows showing Negative ATT)

(Green Rows showing Neutral ATT)

(Yellow Rows showing Negative ATT)

(Green Rows showing Neutral ATT)

(Yellow Rows showing Negative ATT)

(Green Rows showing Neutral ATT)

(Yellow Rows showing Negative ATT)

(Green Rows showing Neutral ATT)

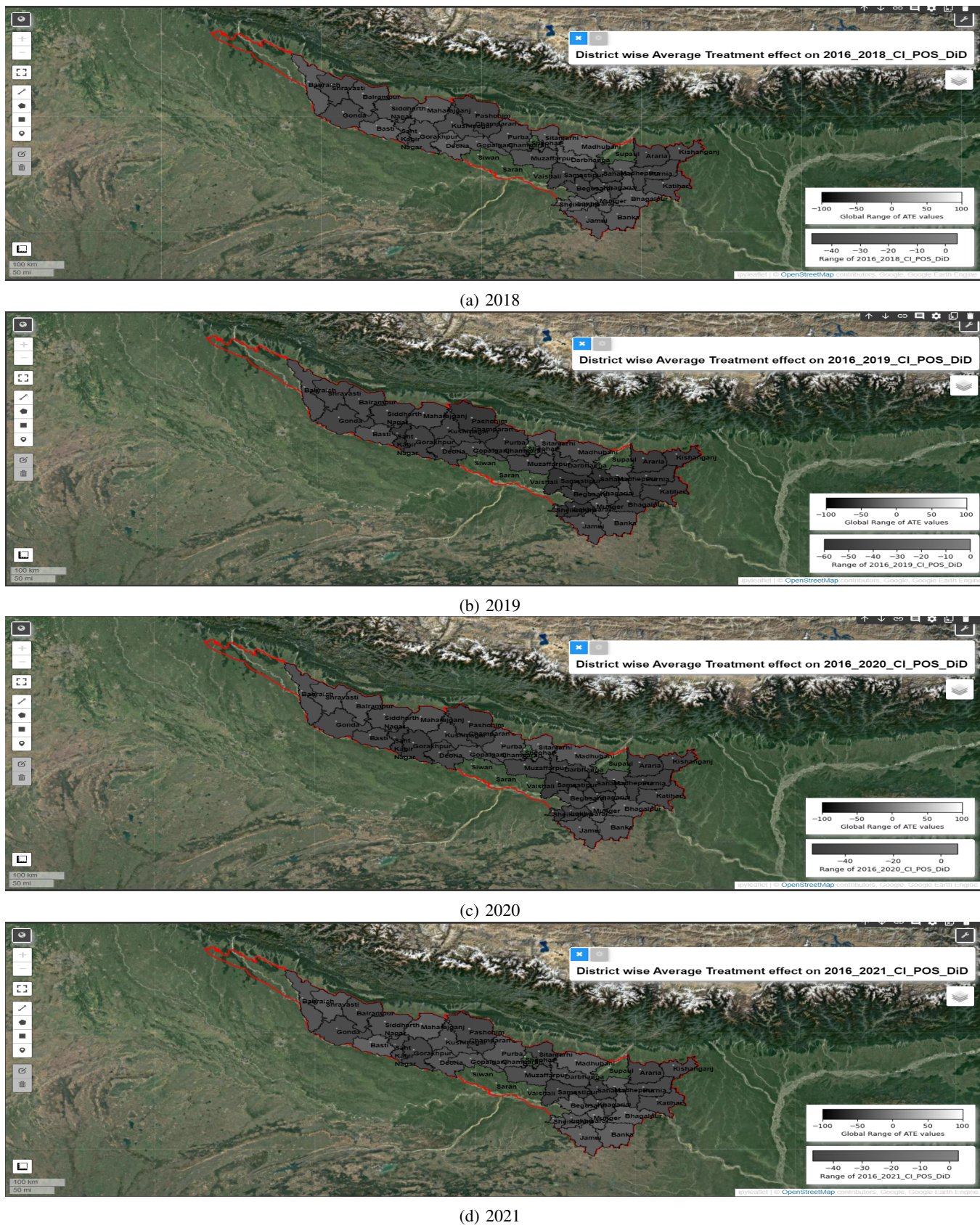


Figure 49: District-wise ATT (Average Treatment Effect on the treated) from DiD for Cropping Intensity

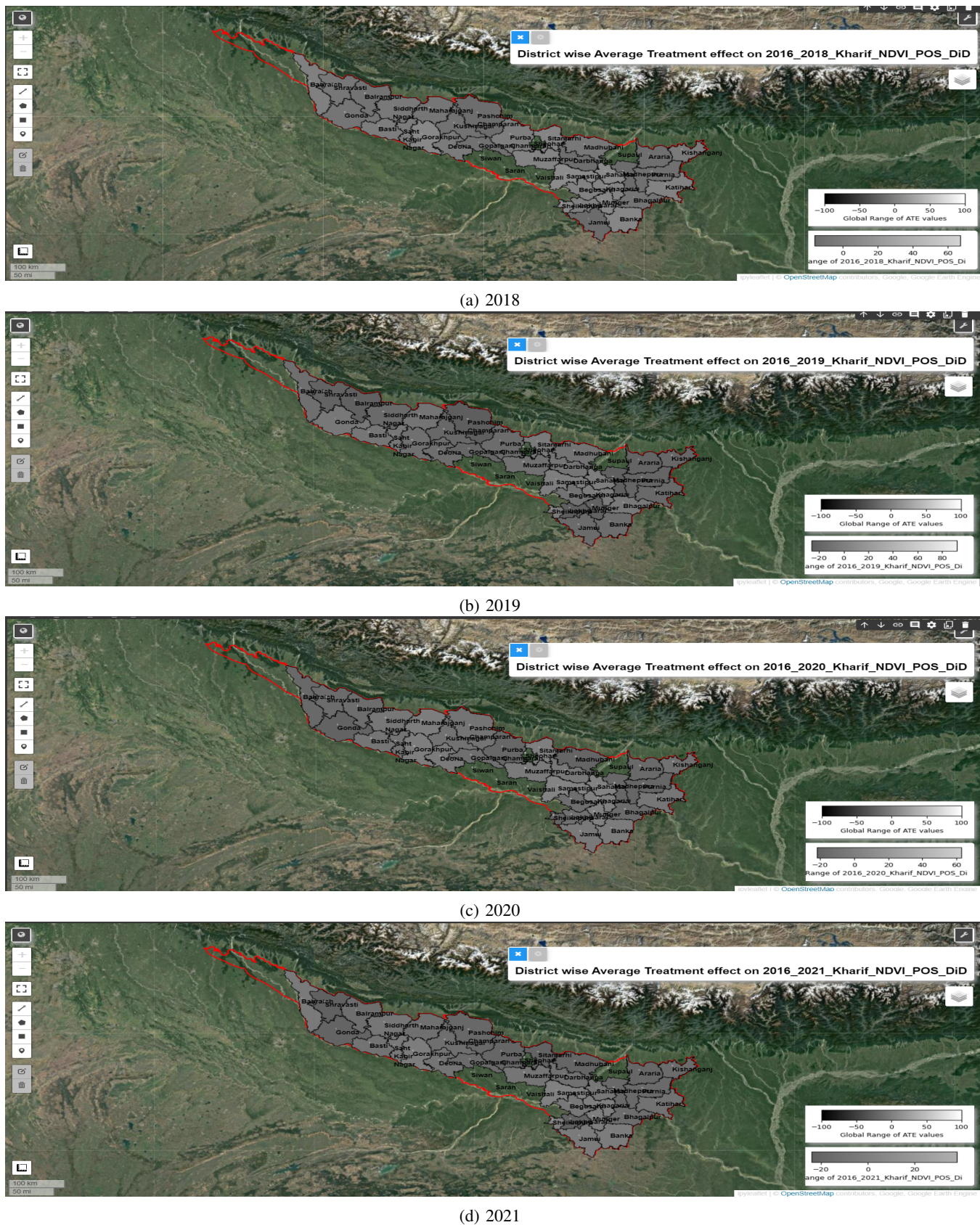


Figure 50: District-wise ATT (Average Treatment Effect on the treated) from DiD for Kharif

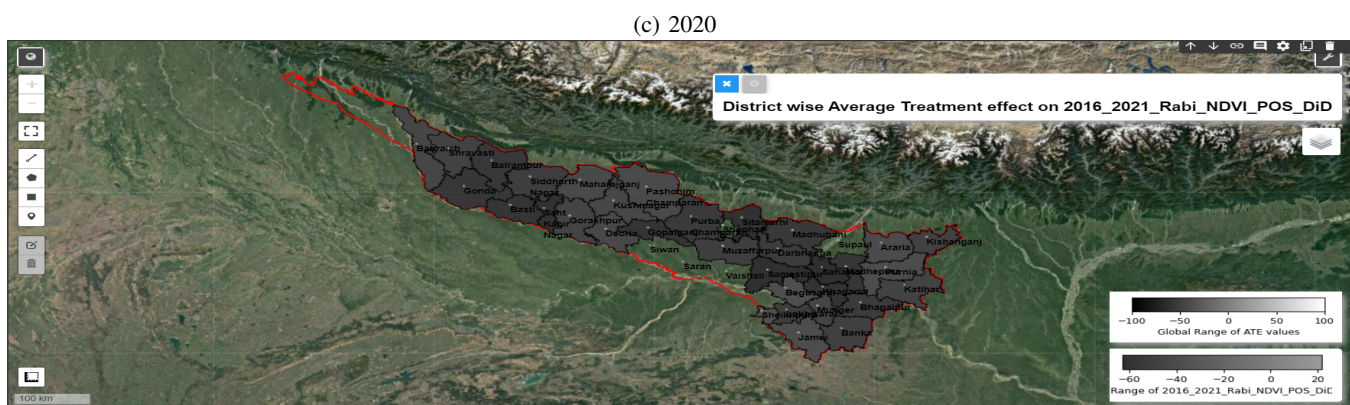
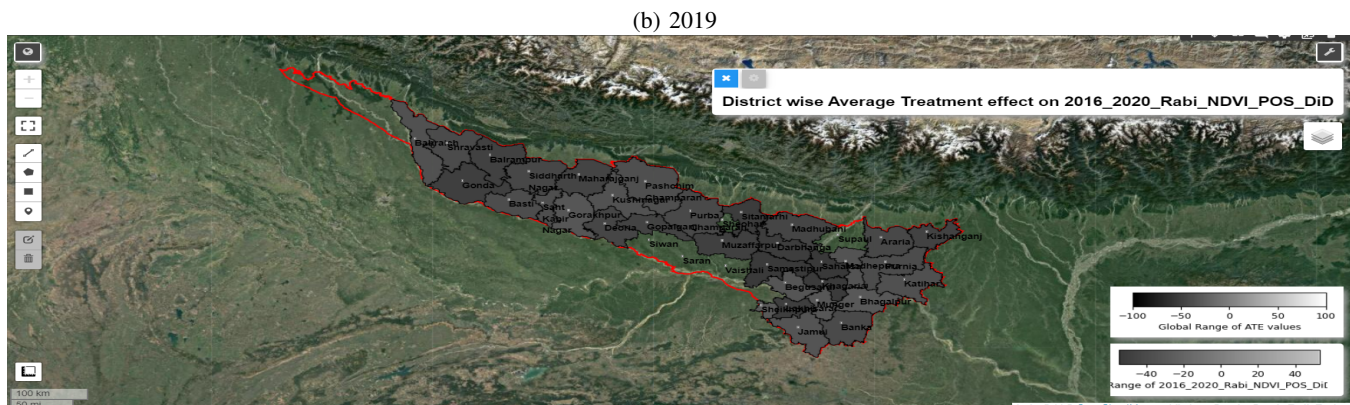
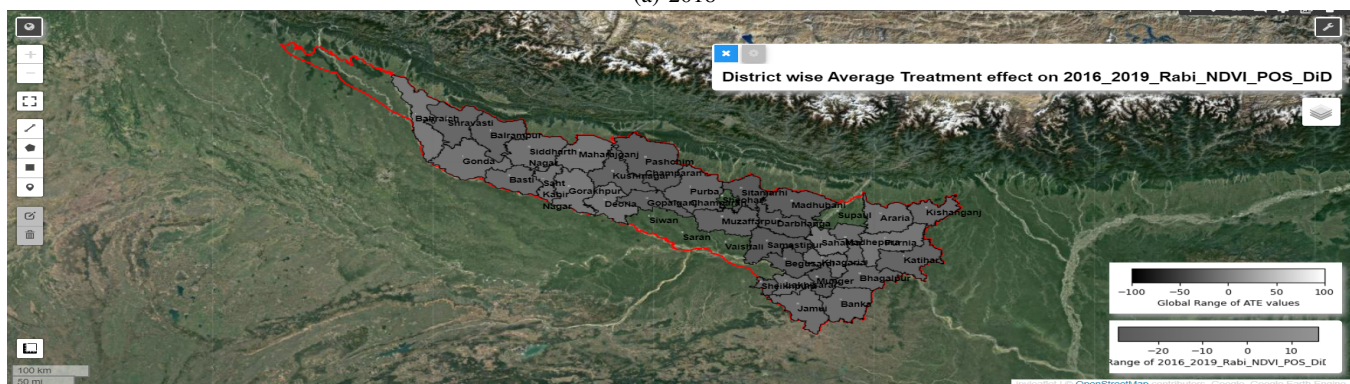
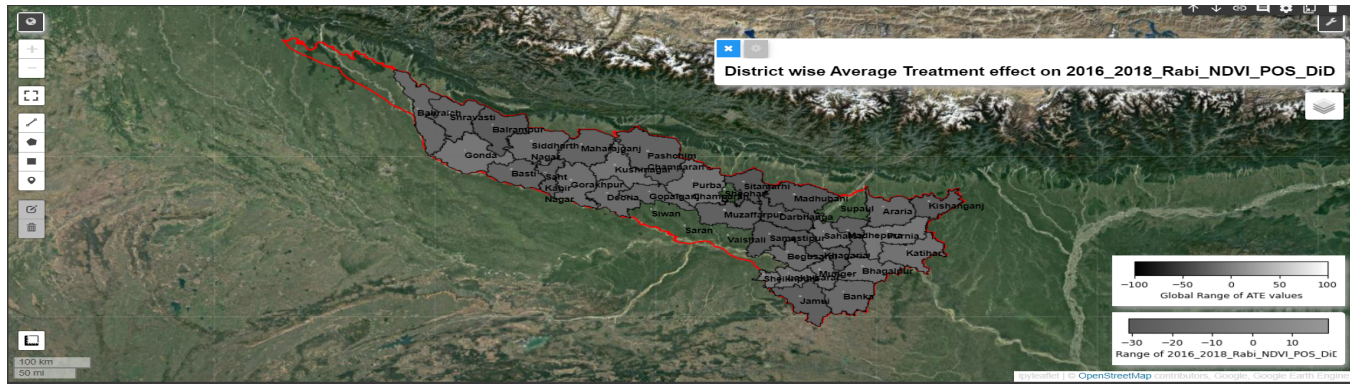


Figure 51: District-wise ATT (Average Treatment Effect on the treated) from DiD for Rabi

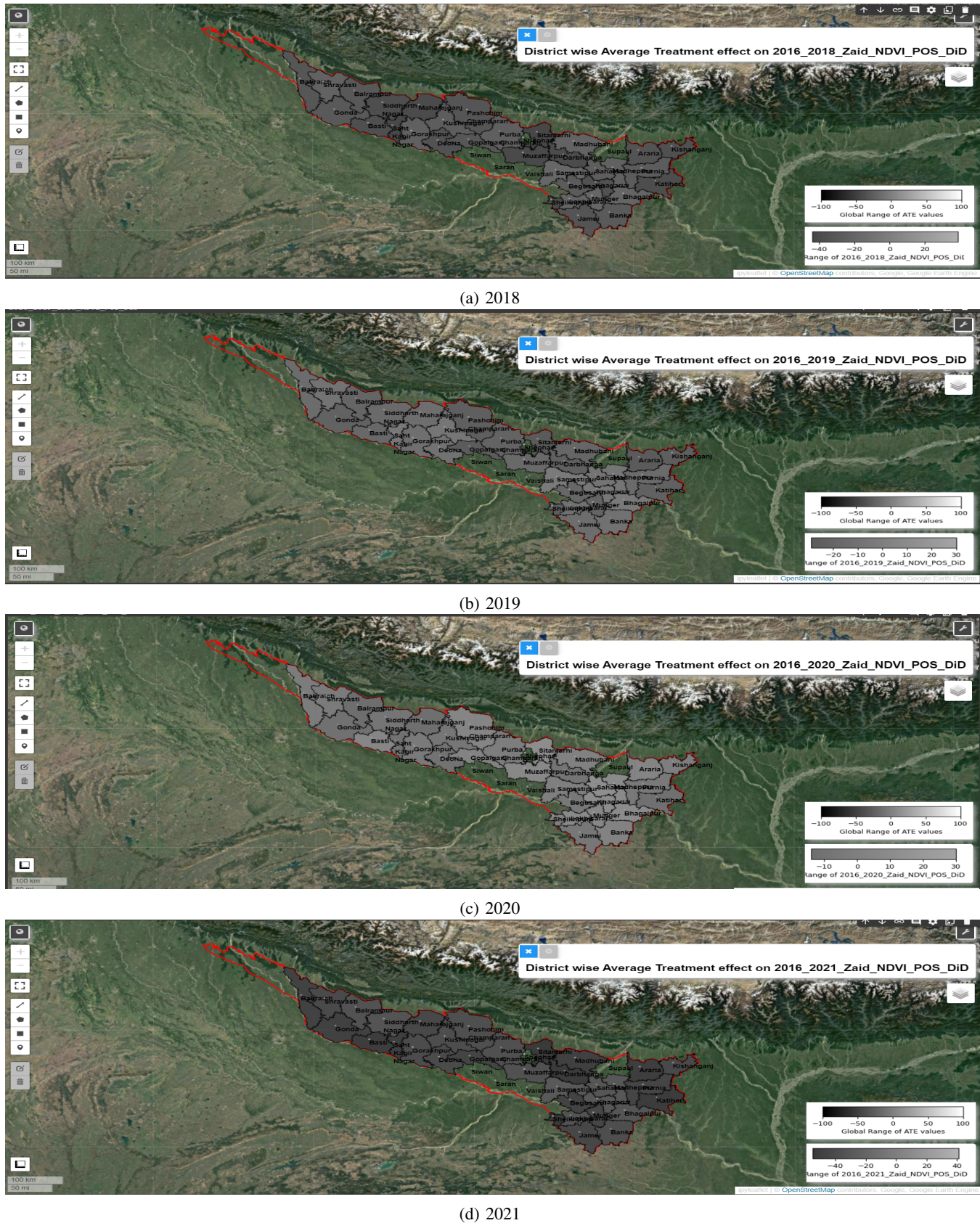


Figure 52: District-wise ATT (Average Treatment Effect on the treated) from DiD for Zaid

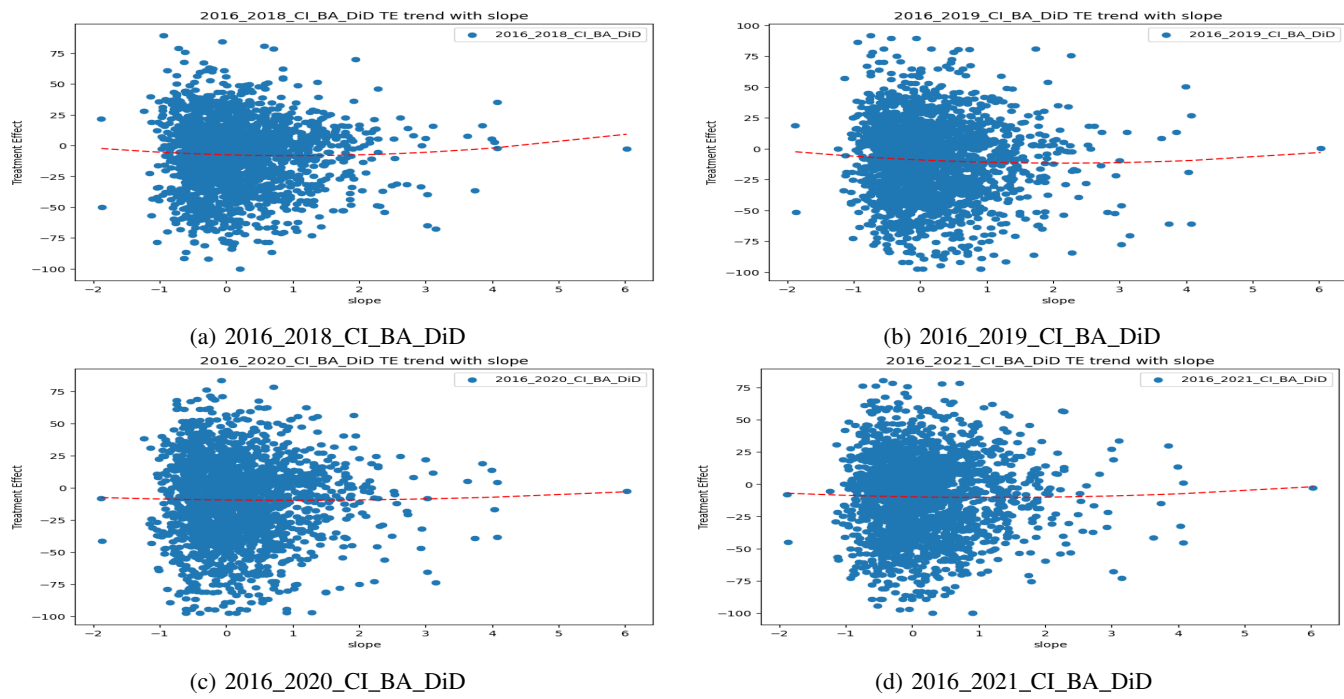


Figure 53: Trend of treatment effect (from DiD) on CI wrt covariate slope

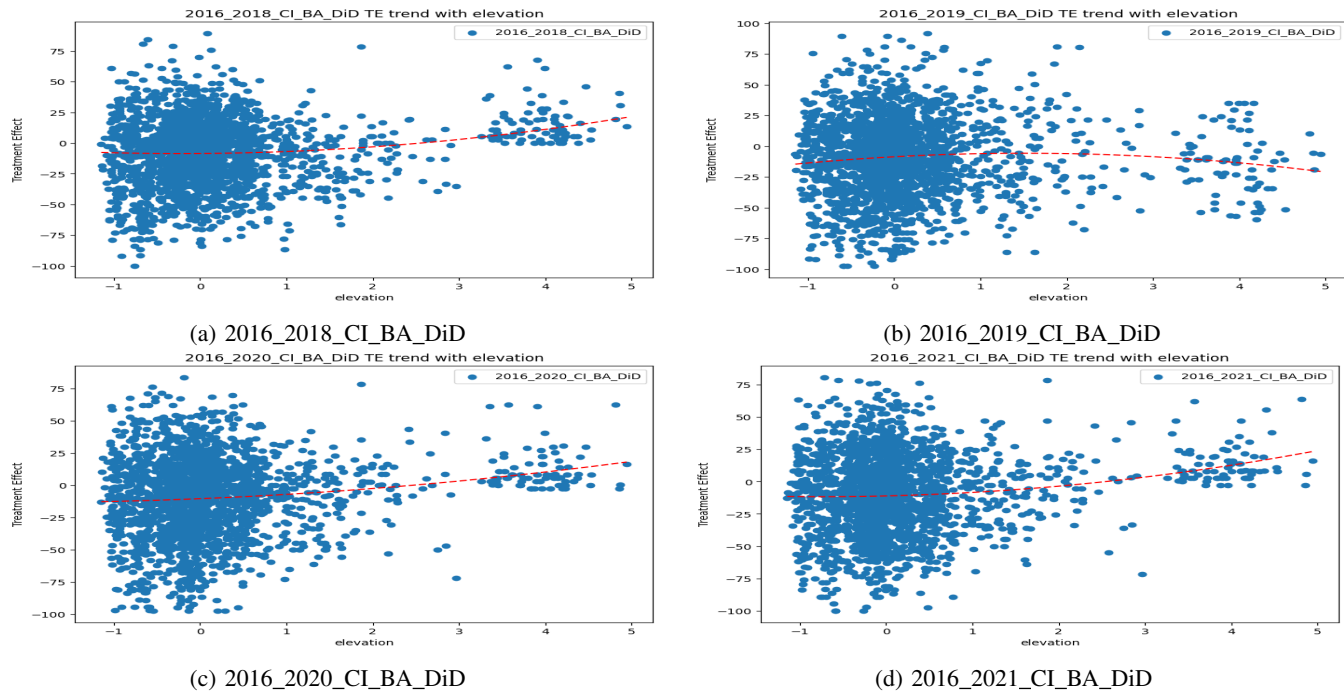


Figure 54: Trend of treatment effect (from DiD) on CI wrt covariate elevation

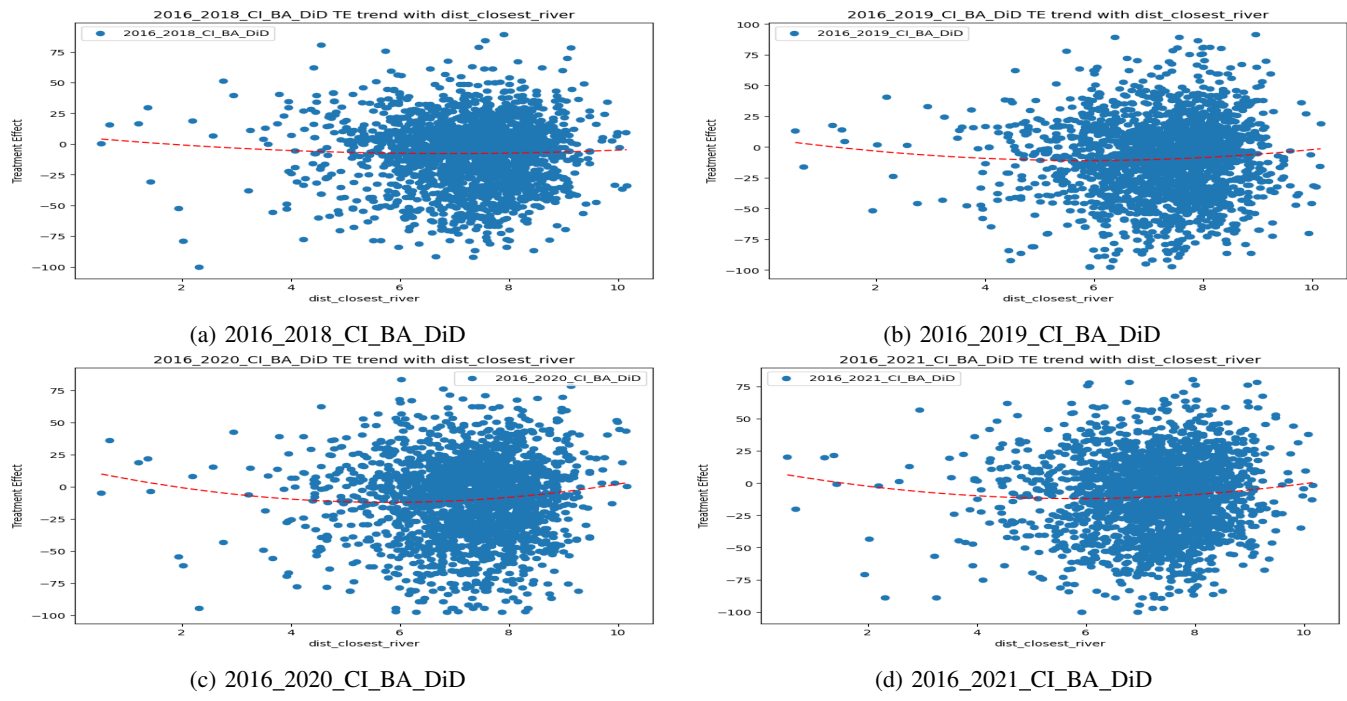


Figure 55: Trend of treatment effect (from DiD) on CI wrt covariate dist\_closest\_river

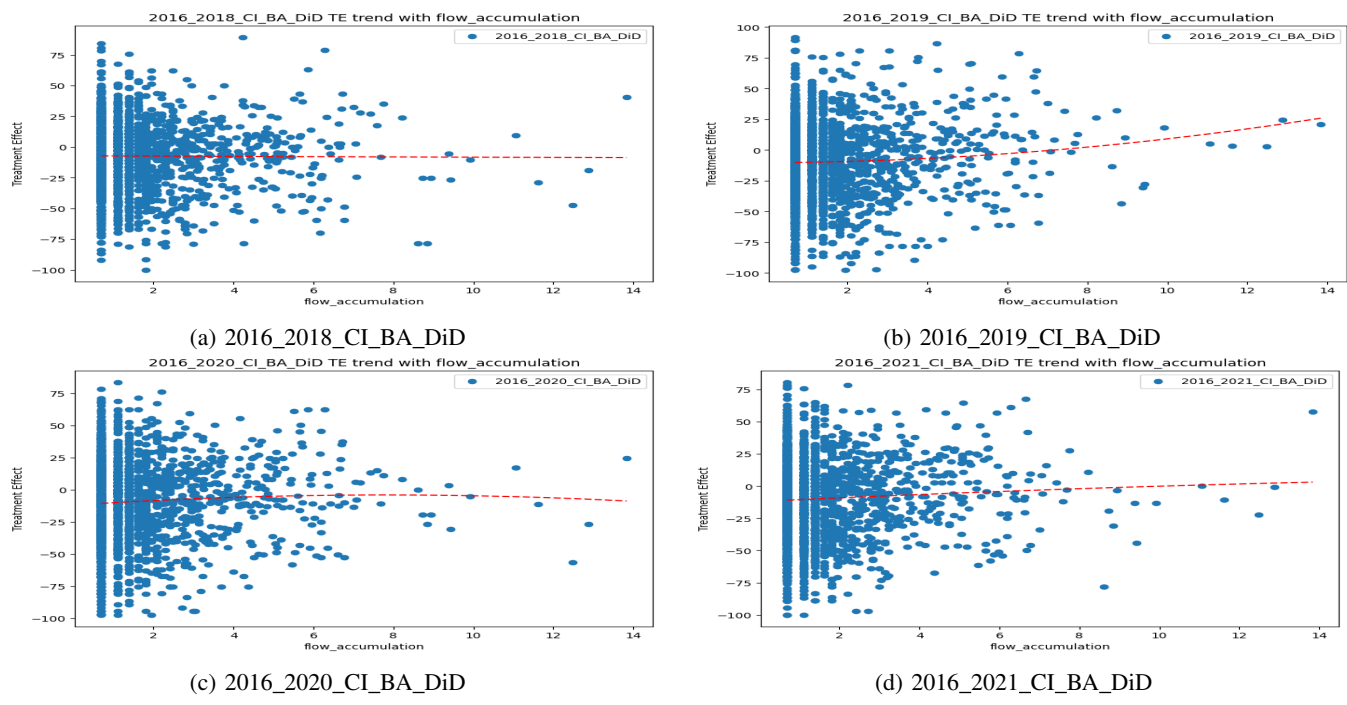


Figure 56: Trend of treatment effect (from DiD) on CI wrt covariate flow\_accumulation

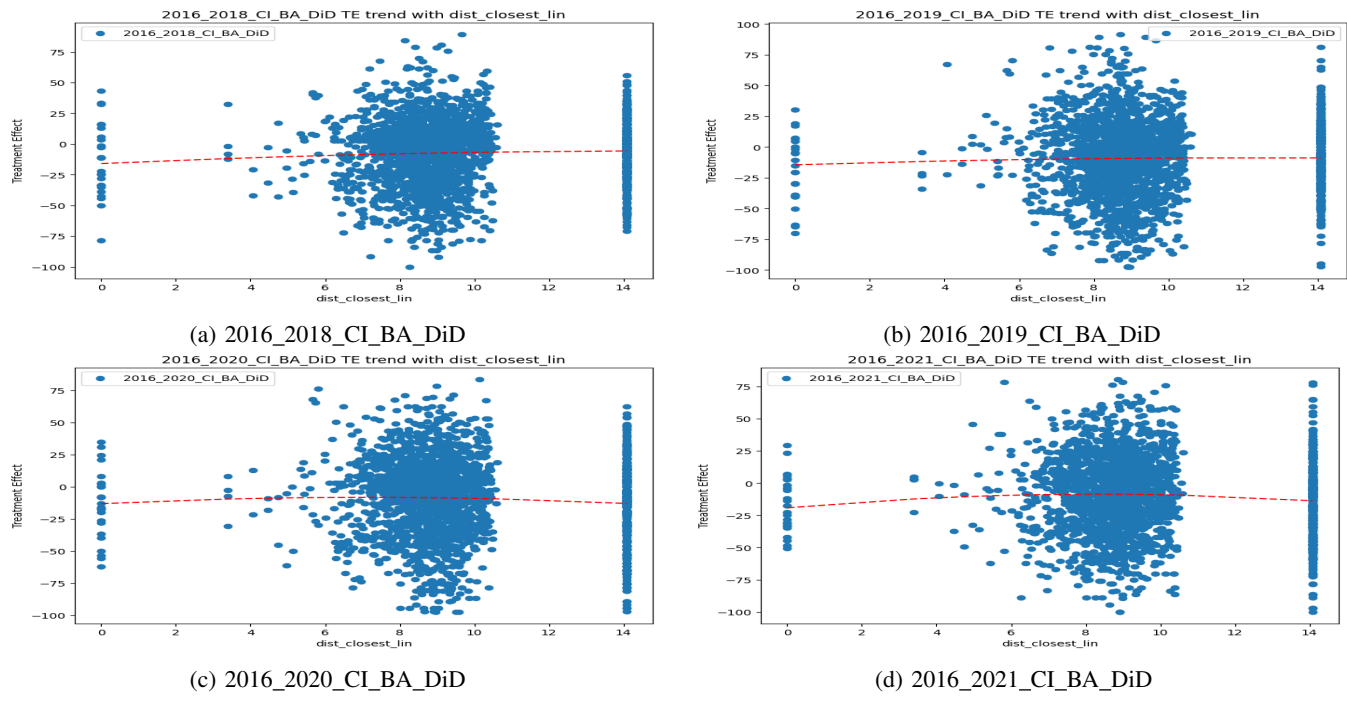


Figure 57: Trend of treatment effect (from DiD) on CI wrt covariate dist\_closest\_lin

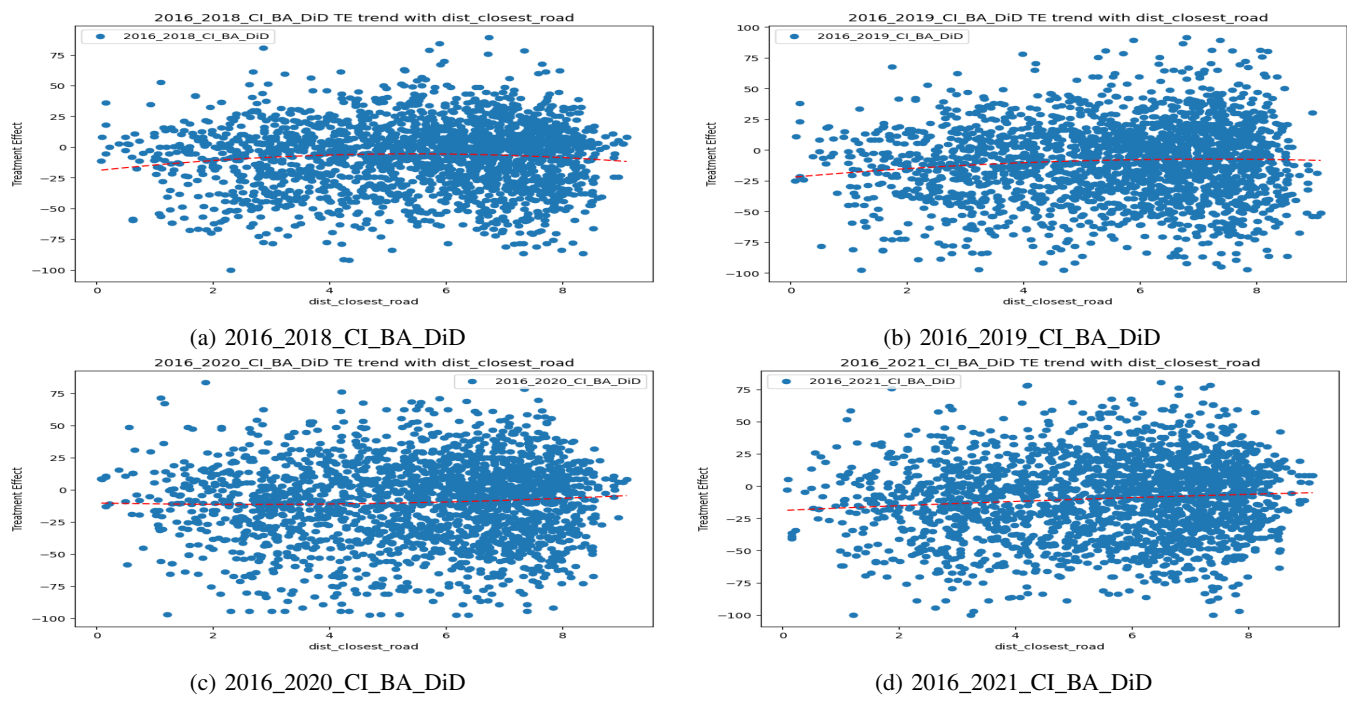


Figure 58: Trend of treatment effect (from DiD) on CI wrt covariate dist\_closest\_road

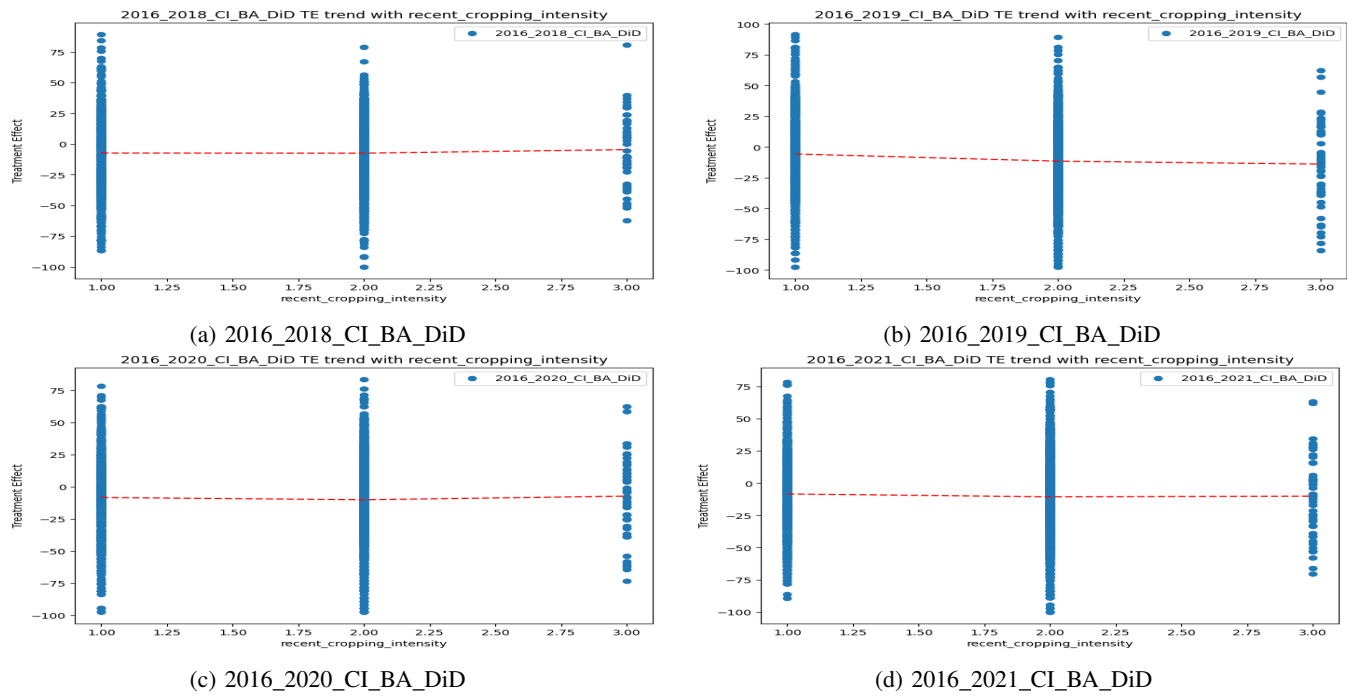


Figure 59: Trend of treatment effect (from DiD) on CI wrt covariate recent\_cropping\_intensity

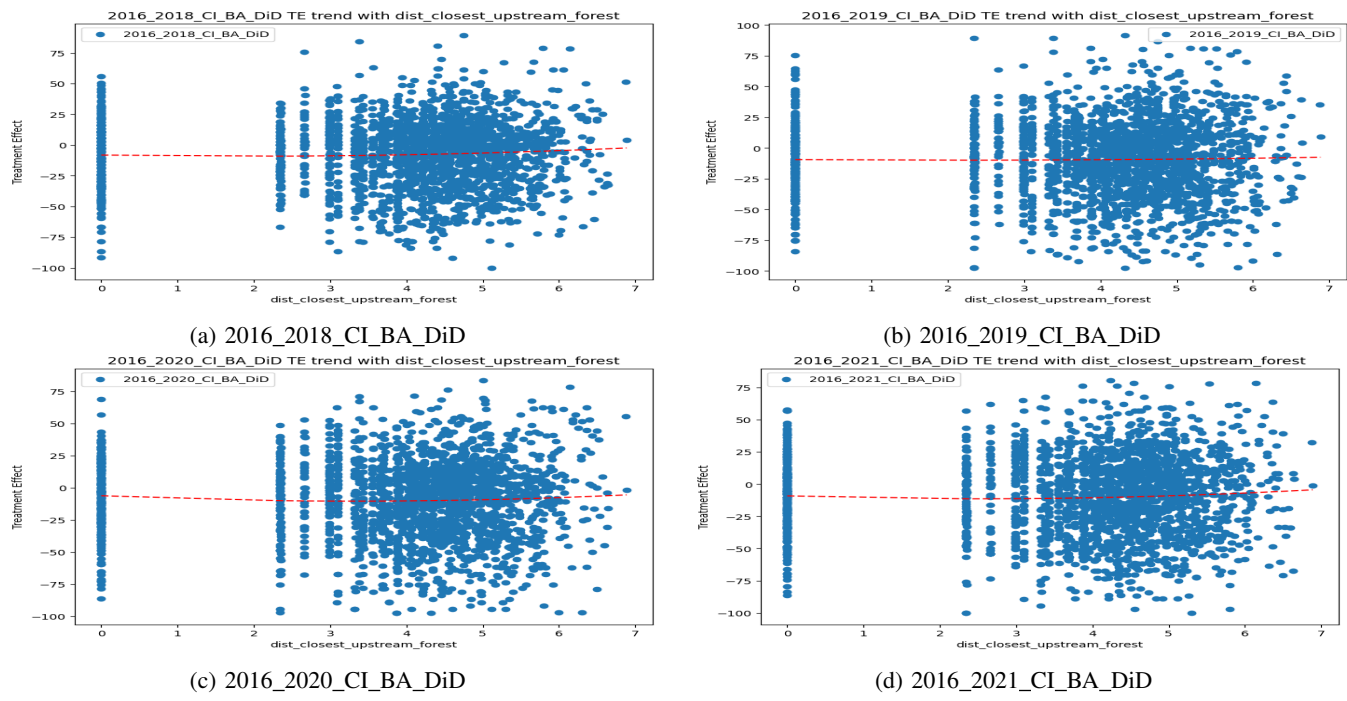


Figure 60: Trend of treatment effect (from DiD) on CI wrt covariate dist\_closest\_upstream\_forest

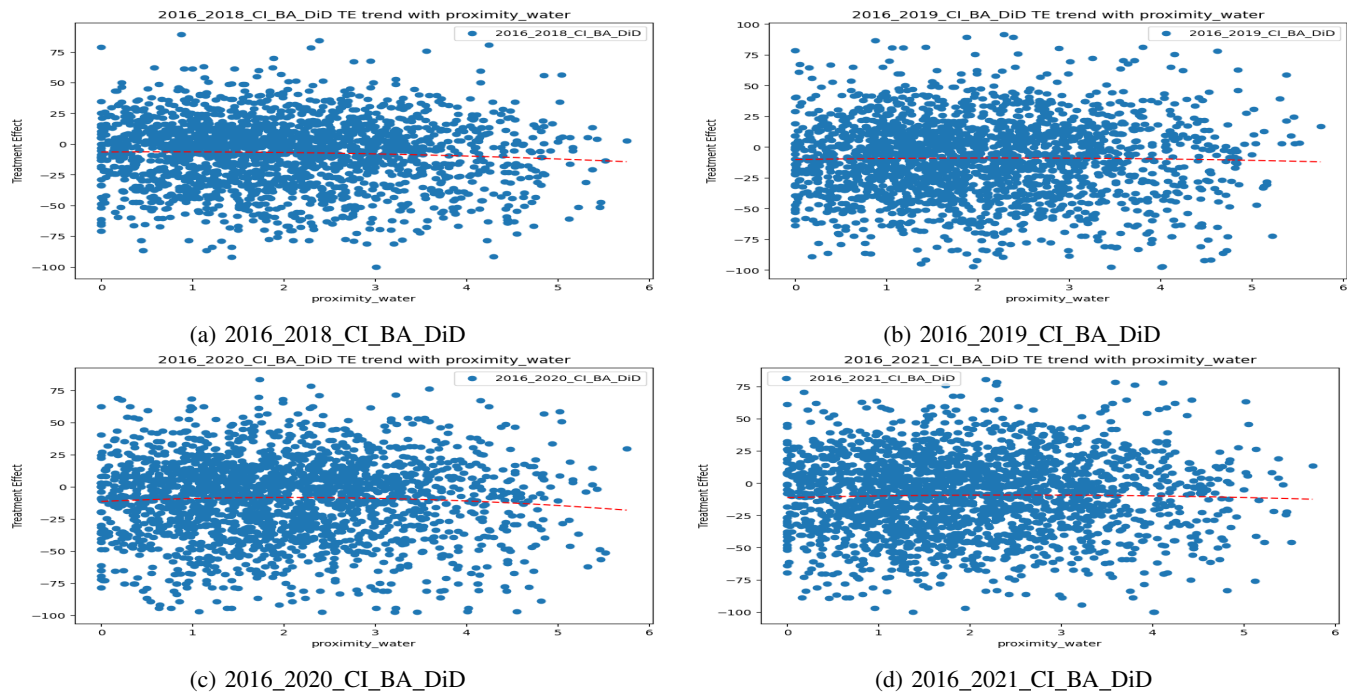


Figure 61: Trend of treatment effect (from DiD) on CI wrt covariate proximity\_water

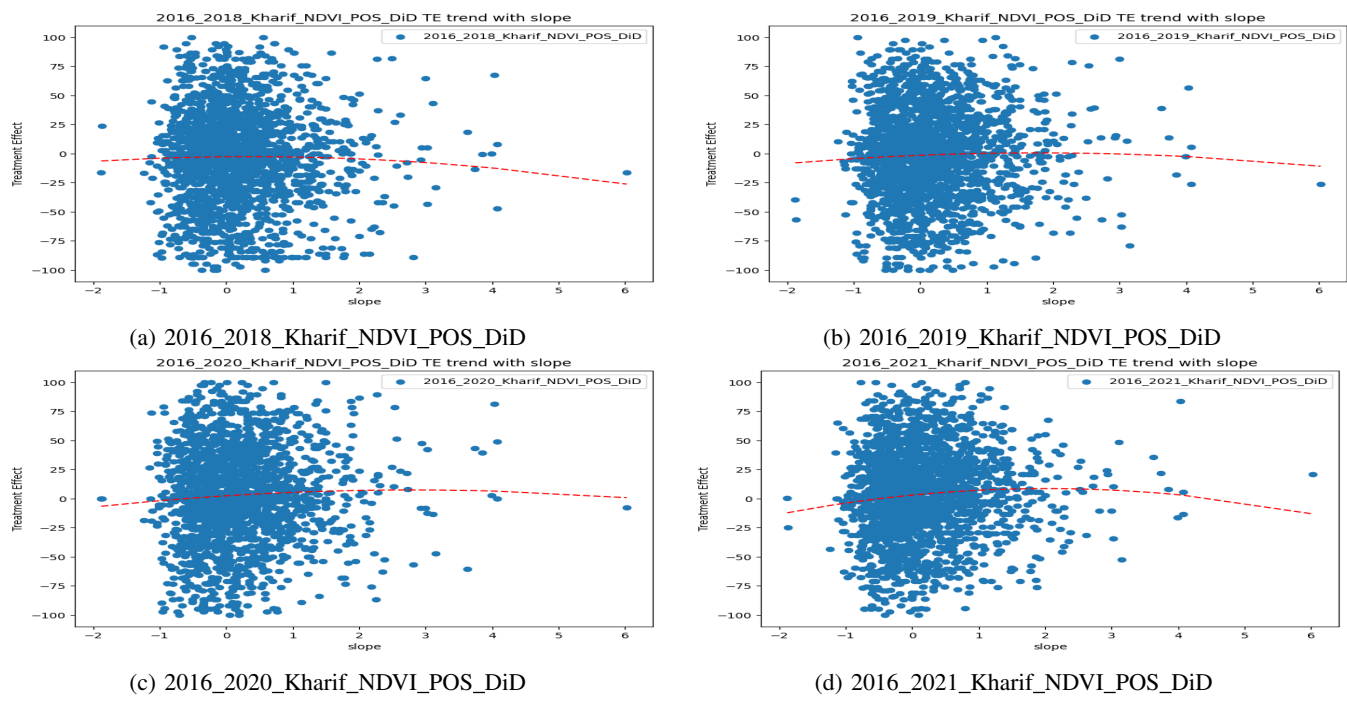


Figure 62: Trend of treatment effect (from DiD) on NDVI Kharif wrt covariate slope

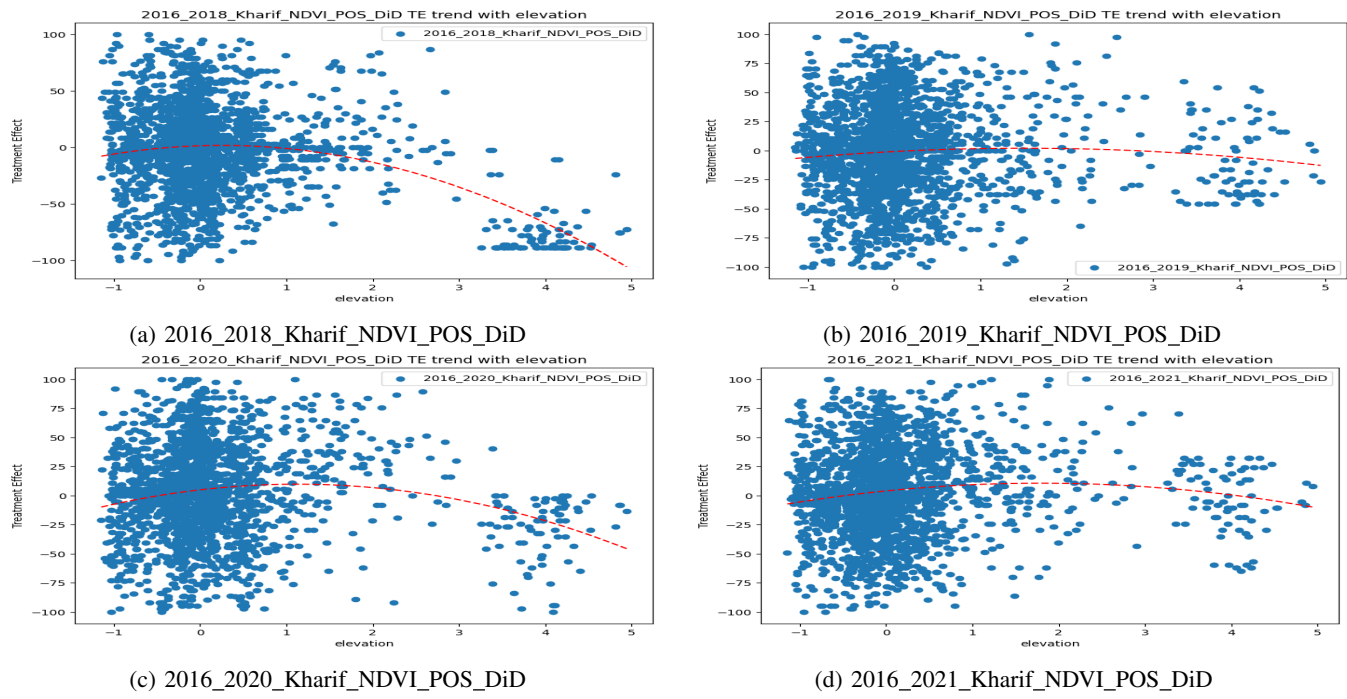


Figure 63: Trend of treatment effect (from DiD) on NDVI Kharif wrt covariate elevation

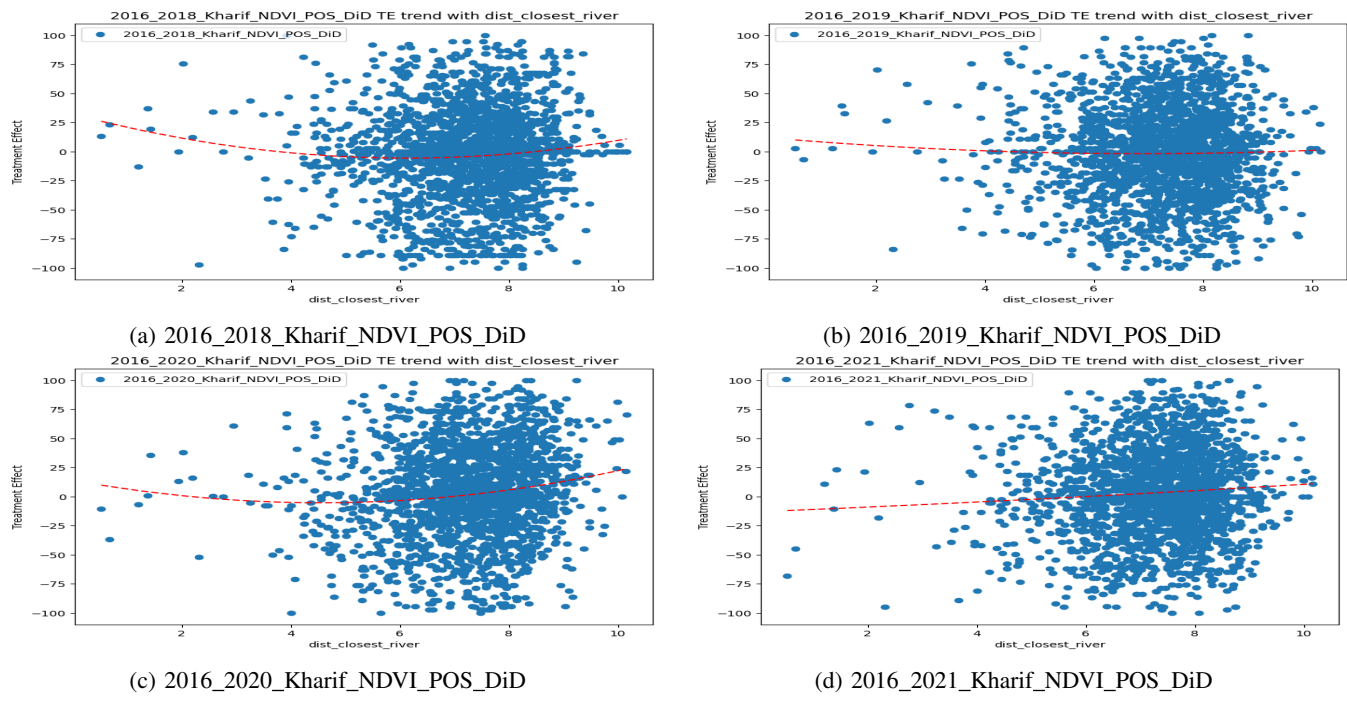


Figure 64: Trend of treatment effect (from DiD) on NDVI Kharif wrt covariate dist\_closest\_river

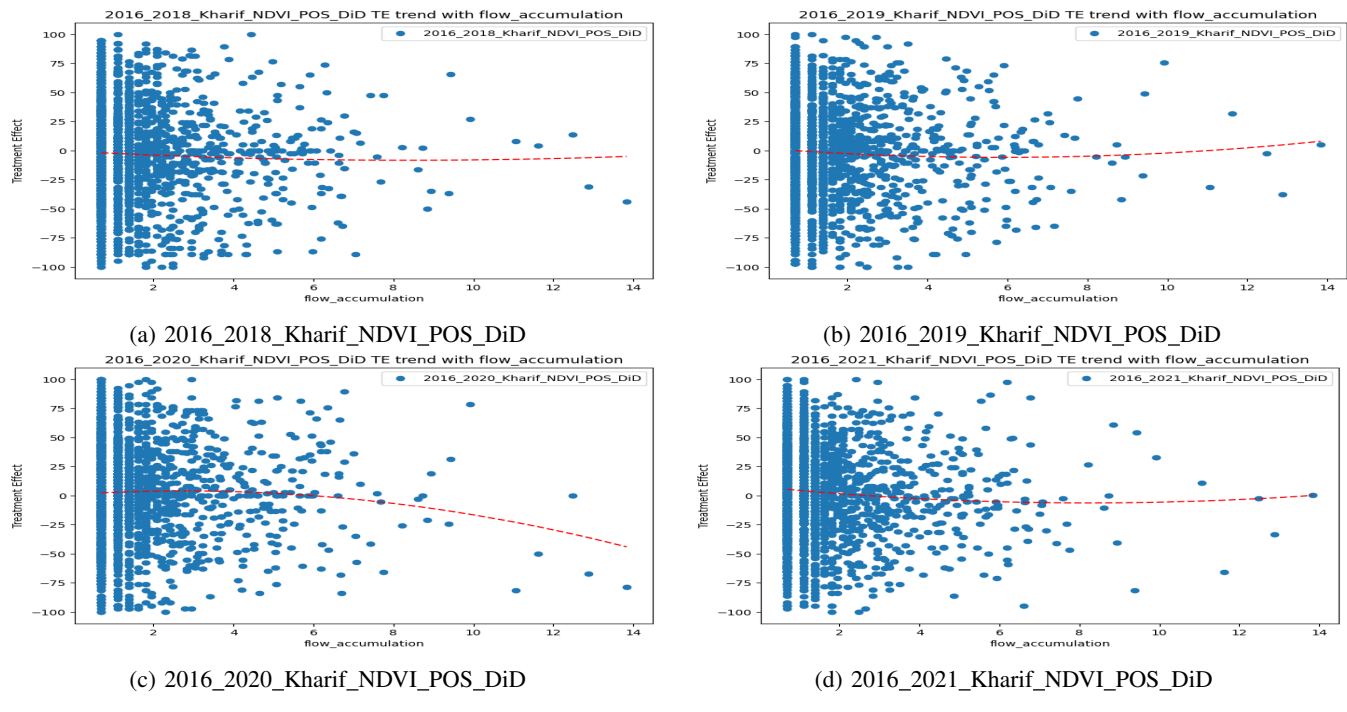


Figure 65: Trend of treatment effect (from DiD) on NDVI Kharif wrt covariate flow\_accumulation

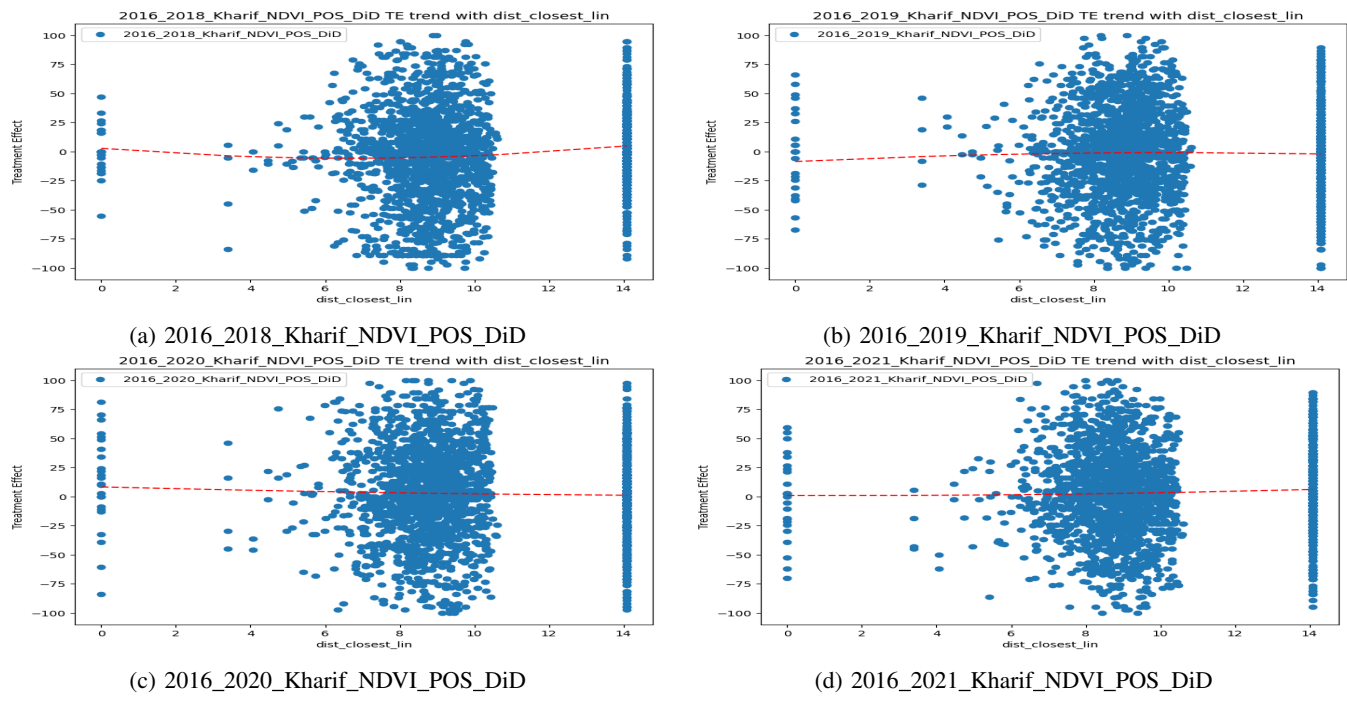


Figure 66: Trend of treatment effect (from DiD) on NDVI Kharif wrt covariate dist\_closest\_lin

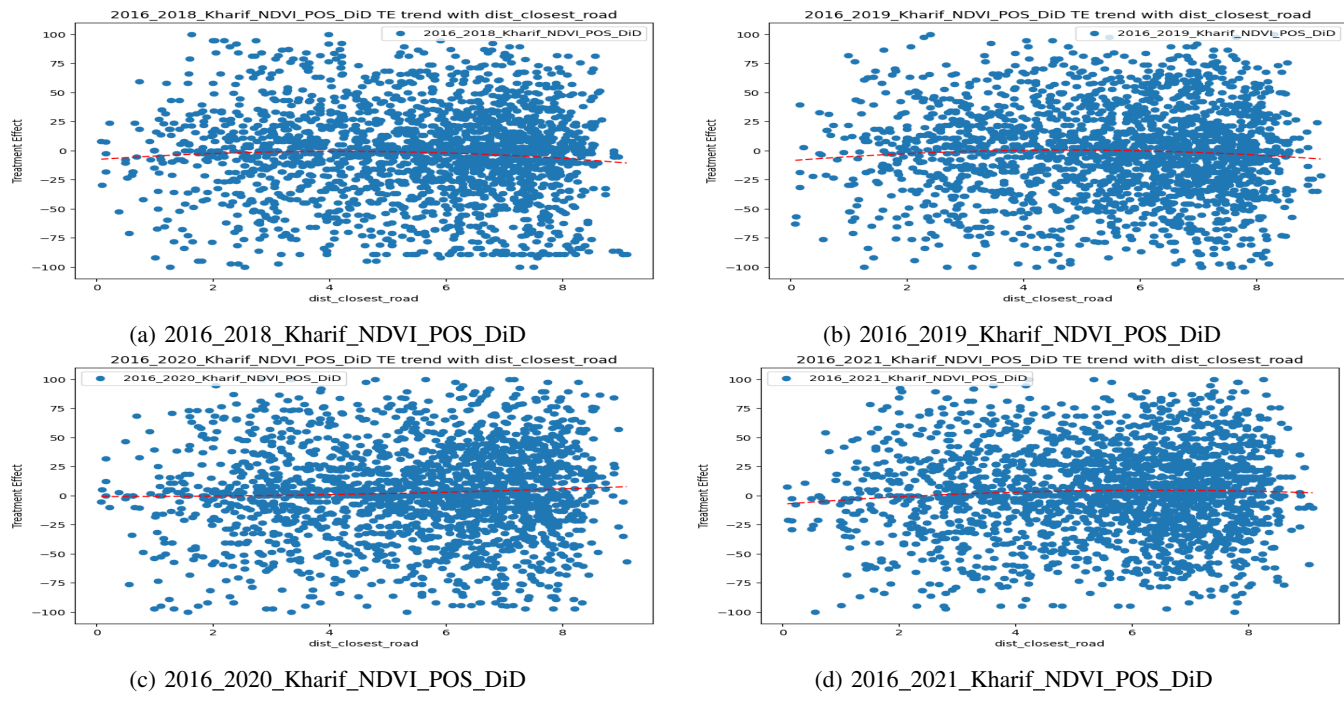


Figure 67: Trend of treatment effect (from DiD) on NDVI Kharif wrt covariate dist\_closest\_road

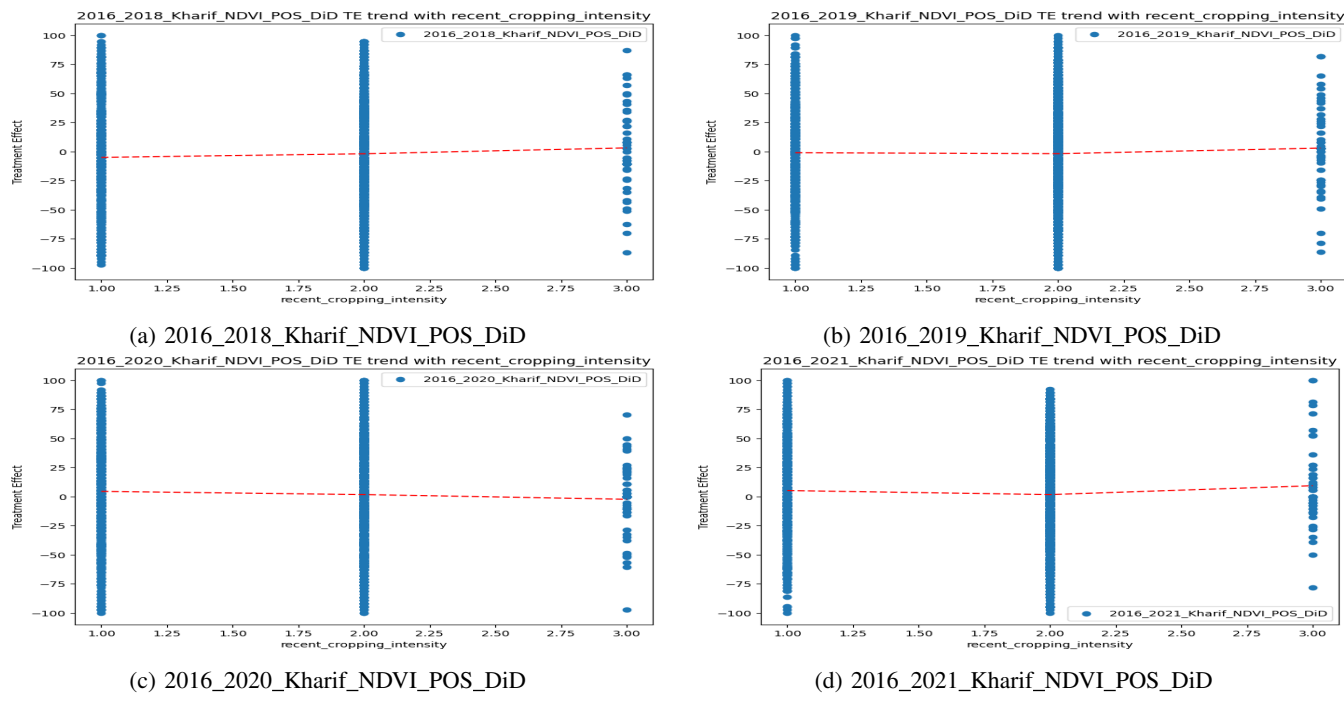


Figure 68: Trend of treatment effect (from DiD) on NDVI Kharif wrt covariate recent\_cropping\_intensity

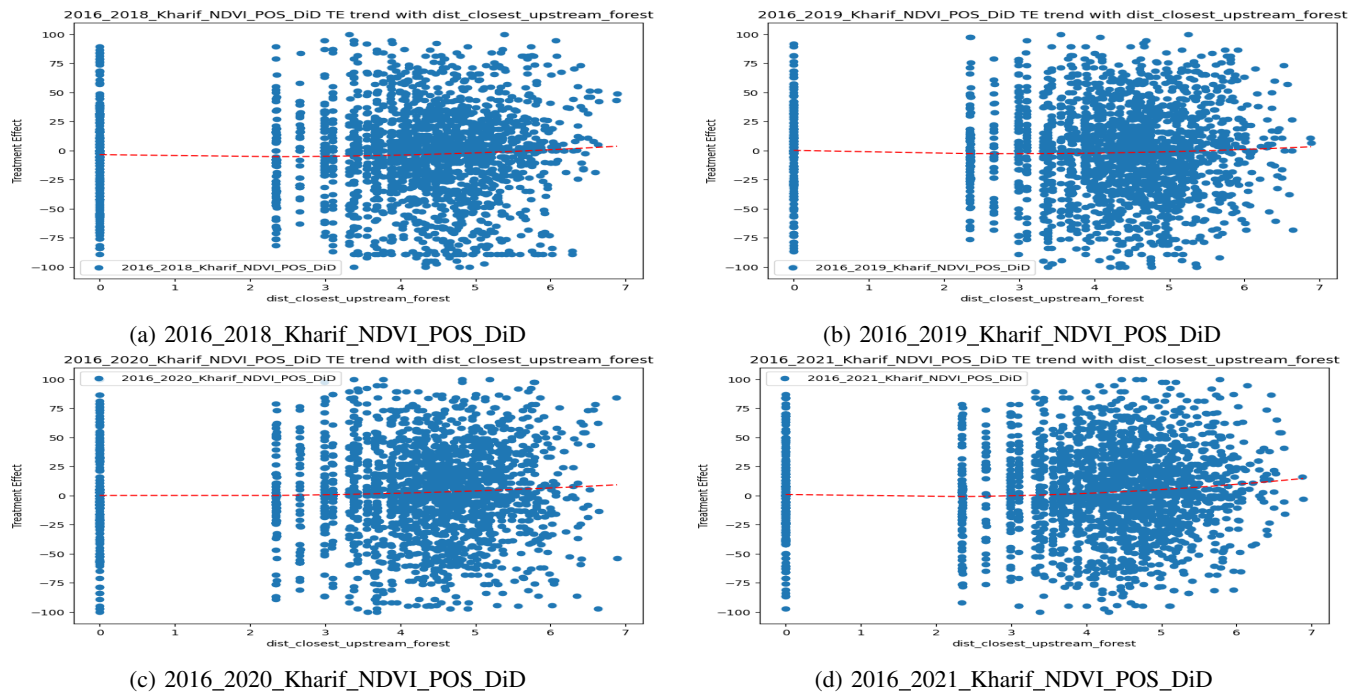


Figure 69: Trend of treatment effect (from DiD) on NDVI Kharif wrt covariate dist\_closest\_upstream\_forest

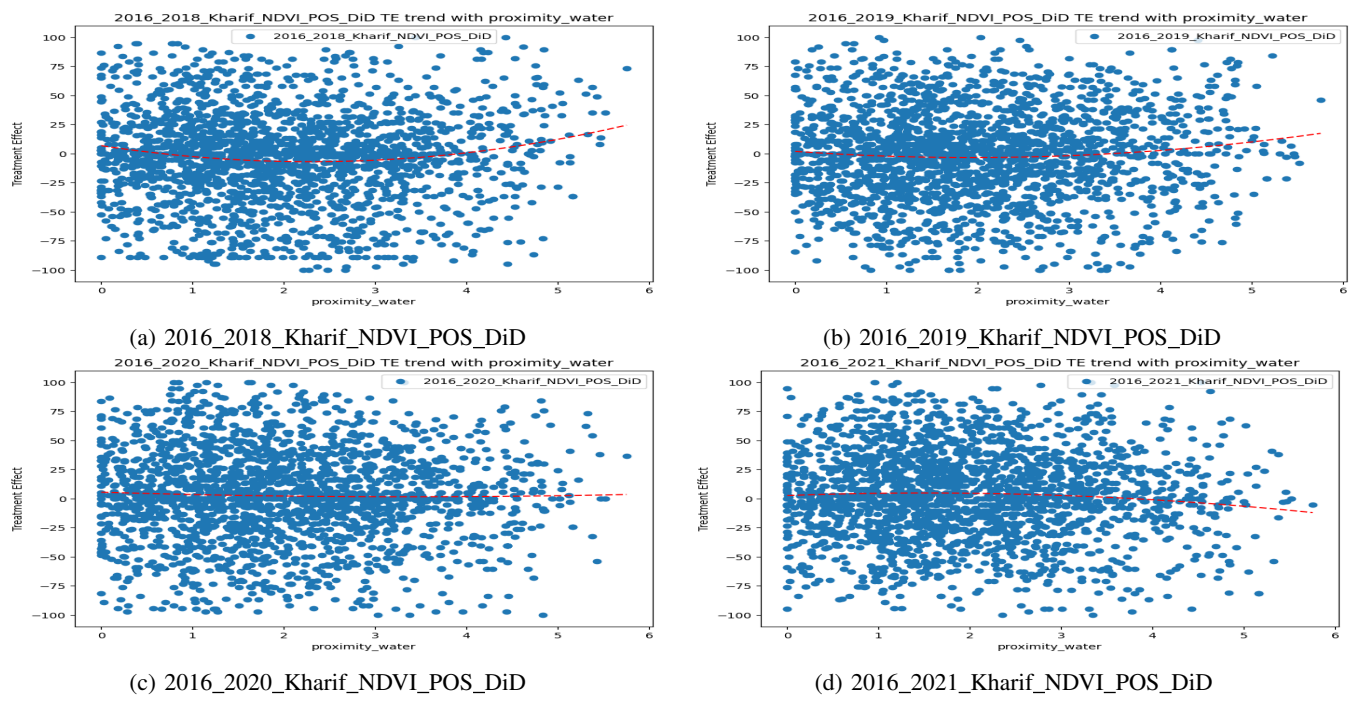


Figure 70: Trend of treatment effect (from DiD) on NDVI Kharif wrt covariate proximity\_water

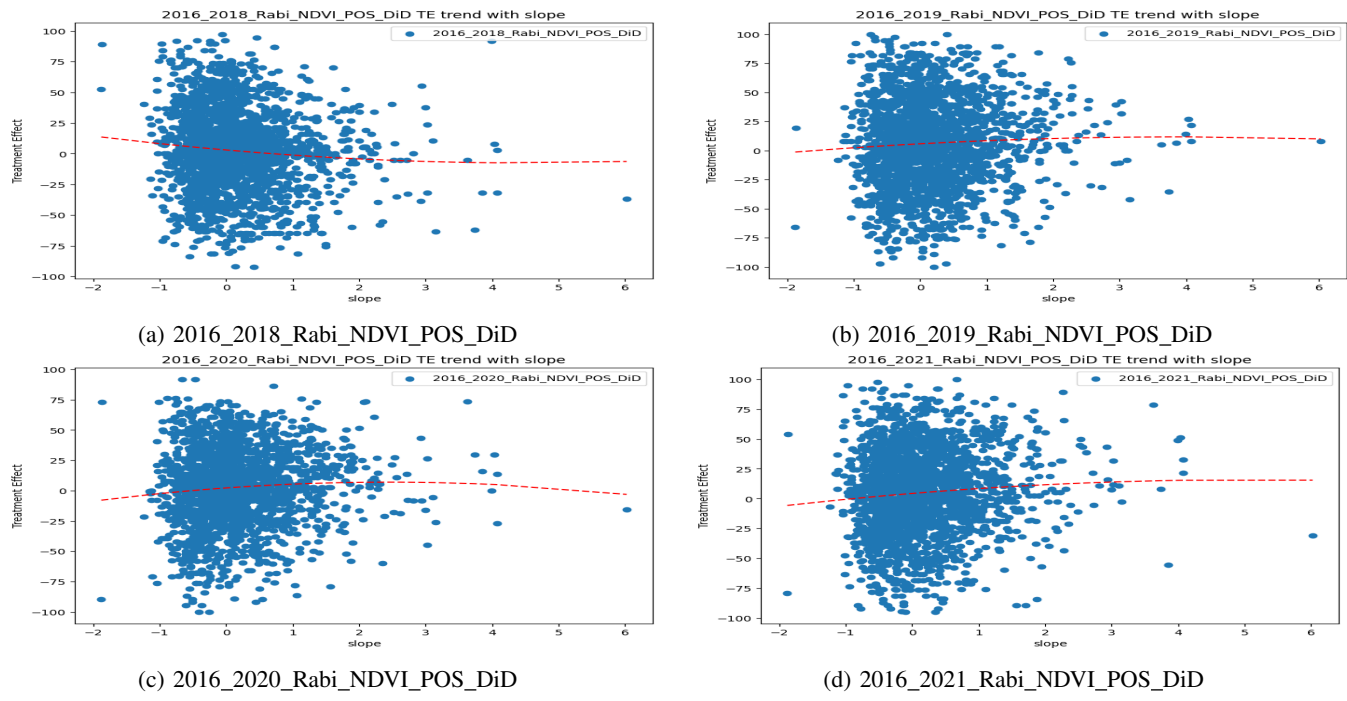


Figure 71: Trend of treatment effect (from DiD) on NDVI Rabi wrt covariate slope

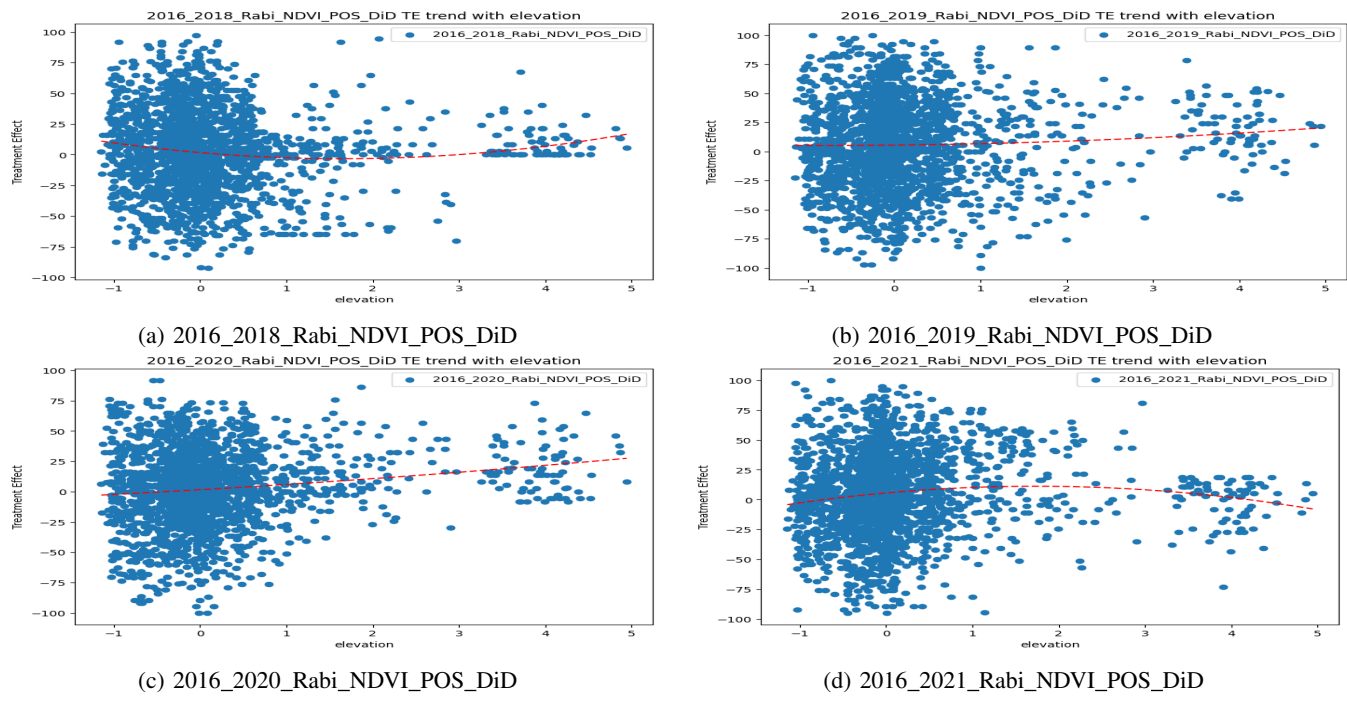


Figure 72: Trend of treatment effect (from DiD) on NDVI Rabi wrt covariate elevation

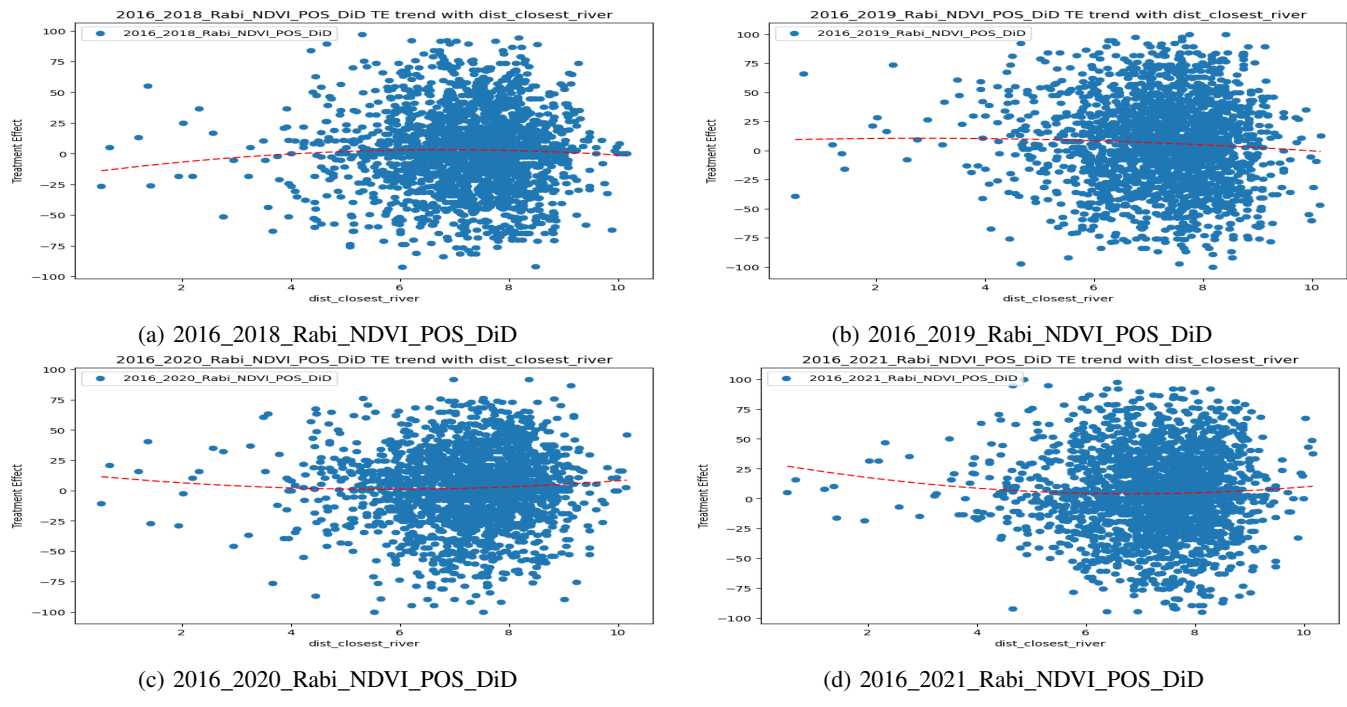


Figure 73: Trend of treatment effect (from DiD) on NDVI Rabi wrt covariate dist\_closest\_river

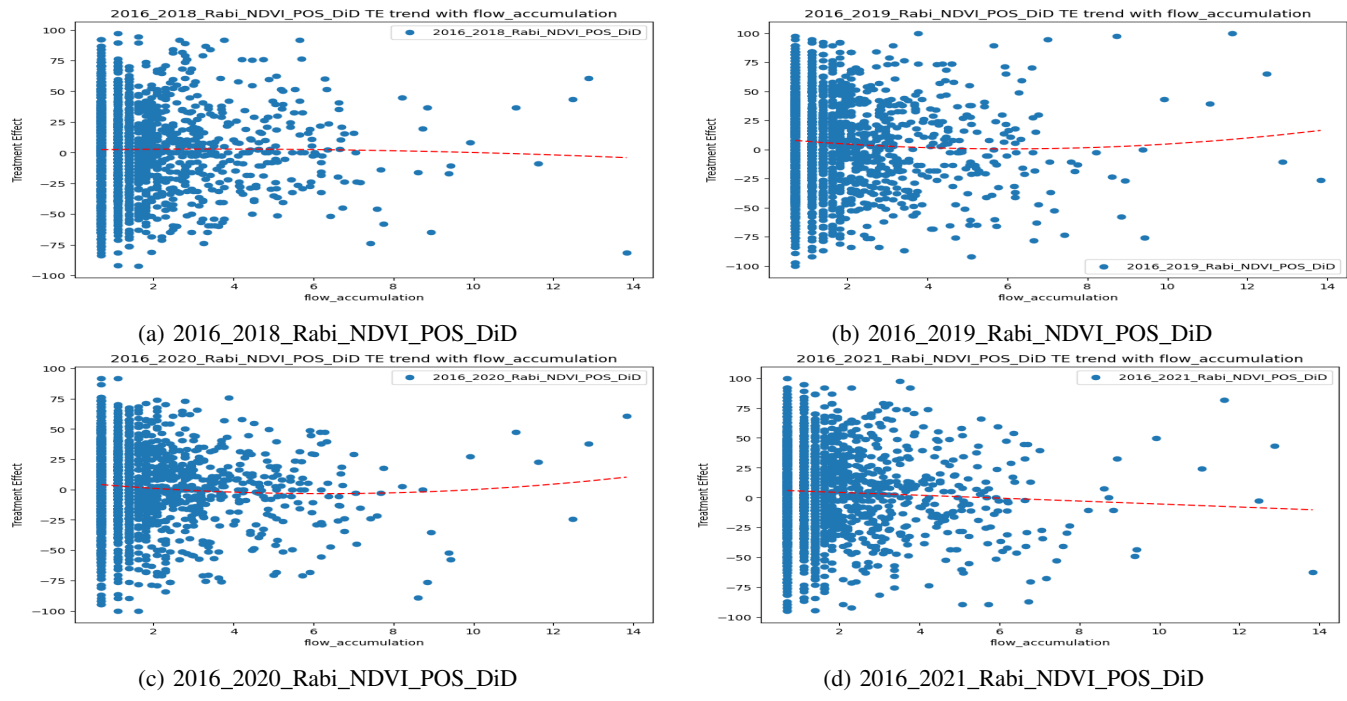


Figure 74: Trend of treatment effect (from DiD) on NDVI Rabi wrt covariate flow\_accumulation

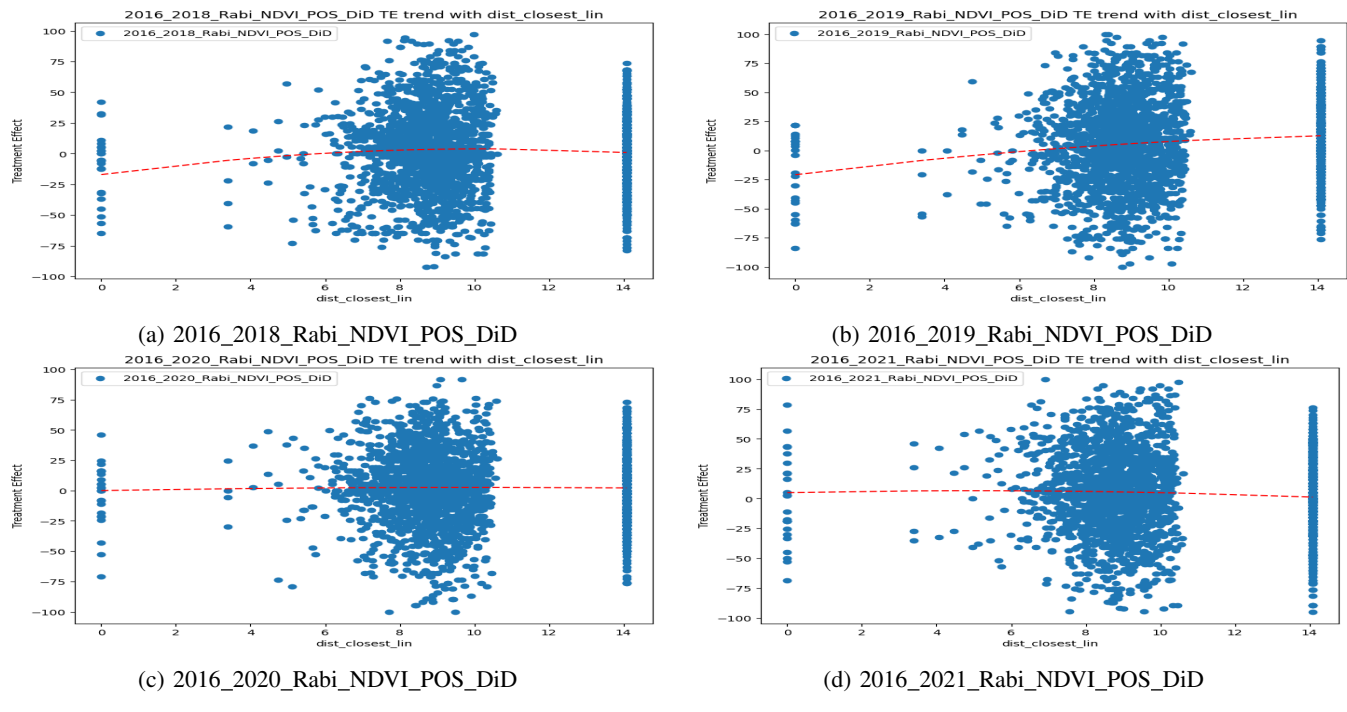


Figure 75: Trend of treatment effect (from DiD) on NDVI Rabi wrt covariate dist\_closest\_lin

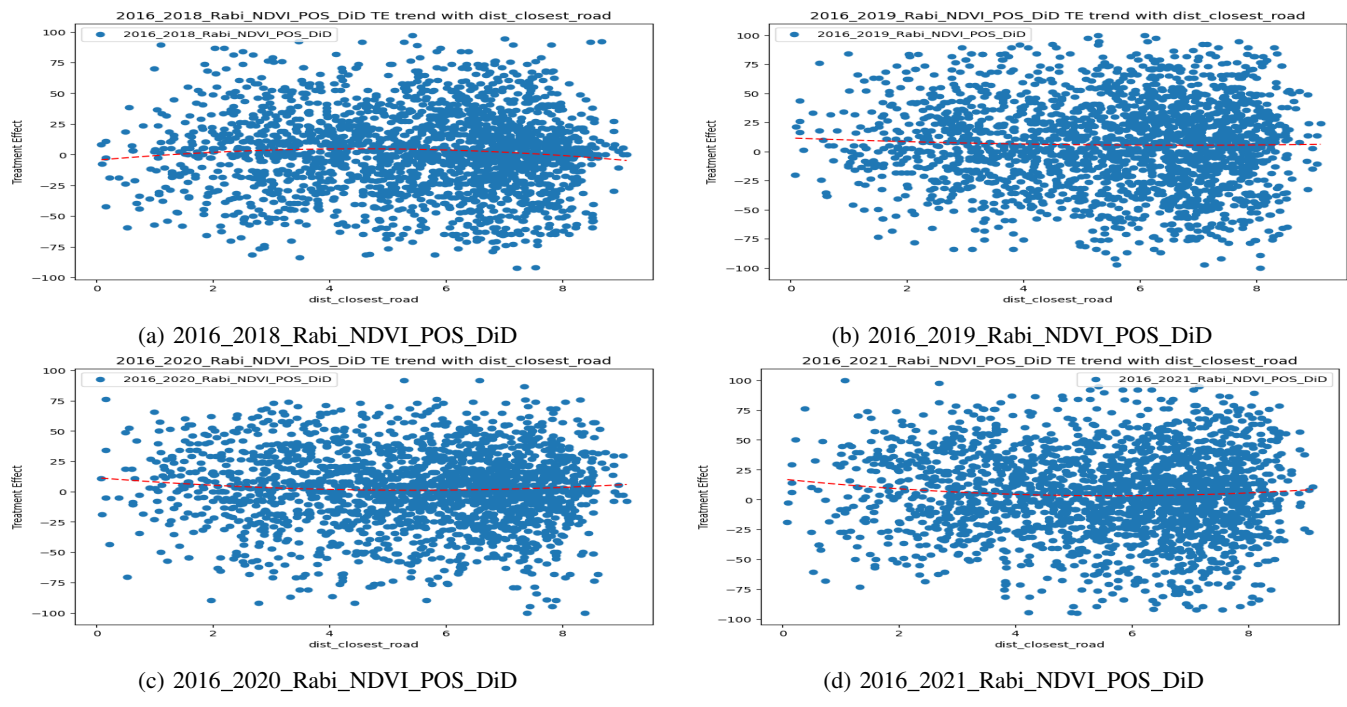


Figure 76: Trend of treatment effect (from DiD) on NDVI Rabi wrt covariate dist\_closest\_road

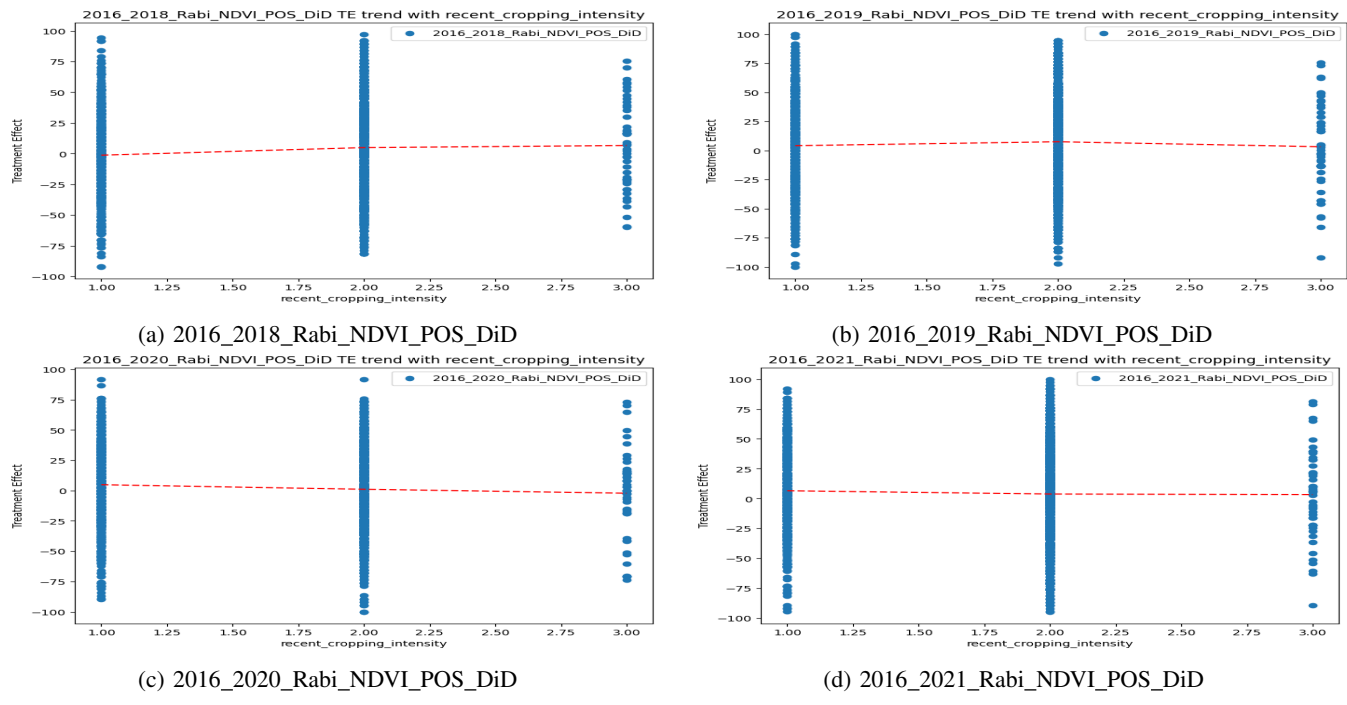


Figure 77: Trend of treatment effect (from DiD) on NDVI Rabi wrt covariate recent\_cropping\_intensity

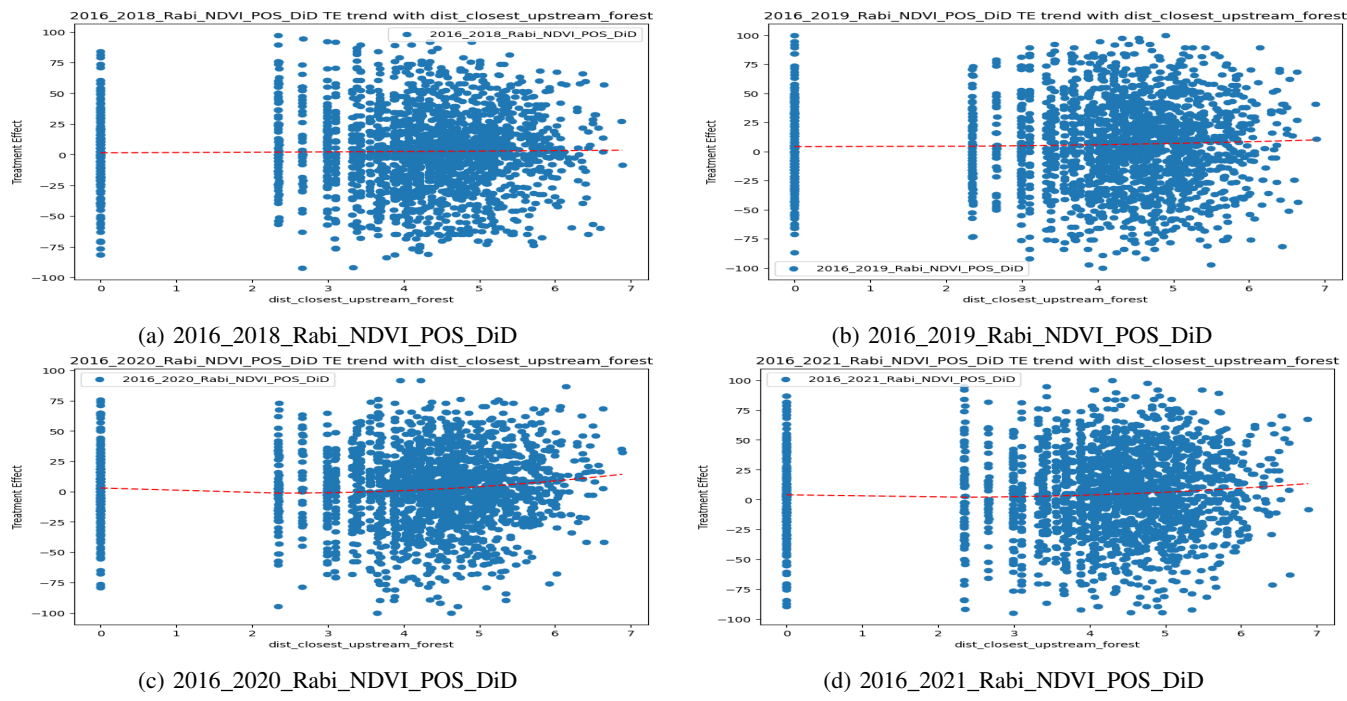


Figure 78: Trend of treatment effect (from DiD) on NDVI Rabi wrt covariate dist\_closest\_upstream\_forest

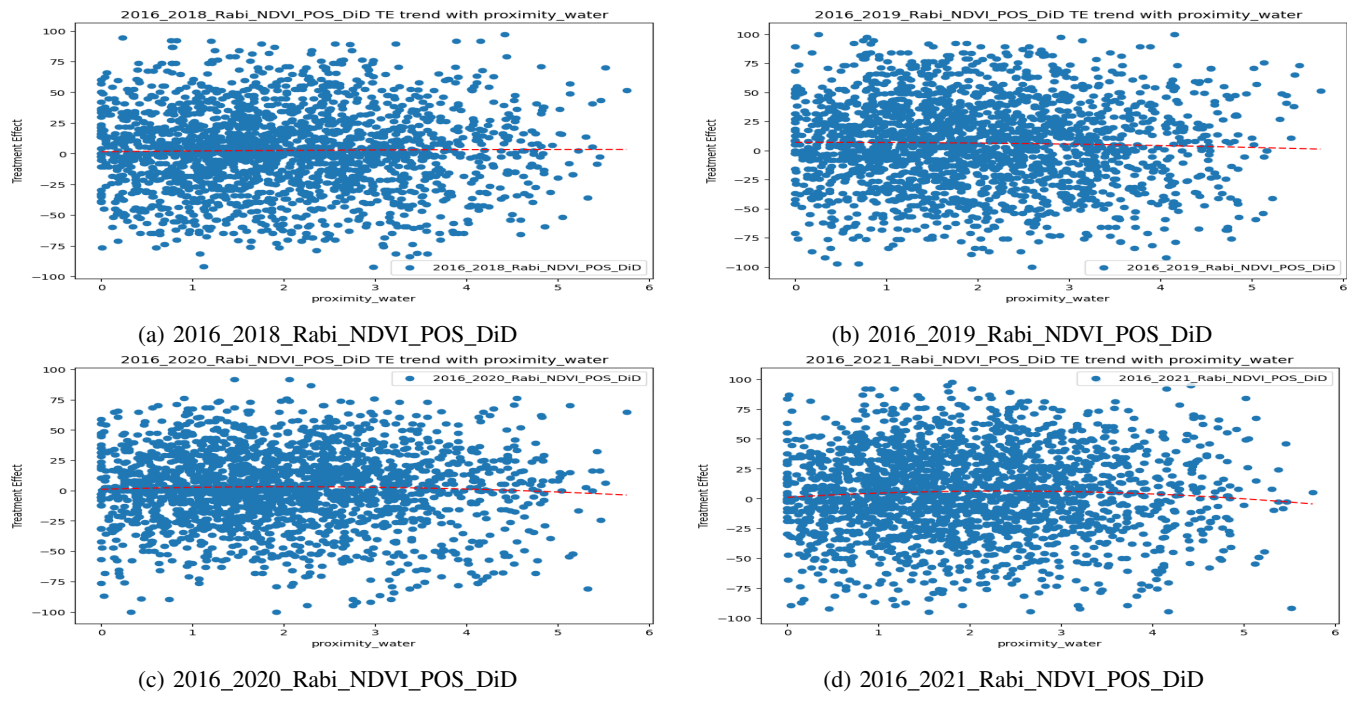


Figure 79: Trend of treatment effect (from DiD) on NDVI Rabi wrt covariate proximity\_water

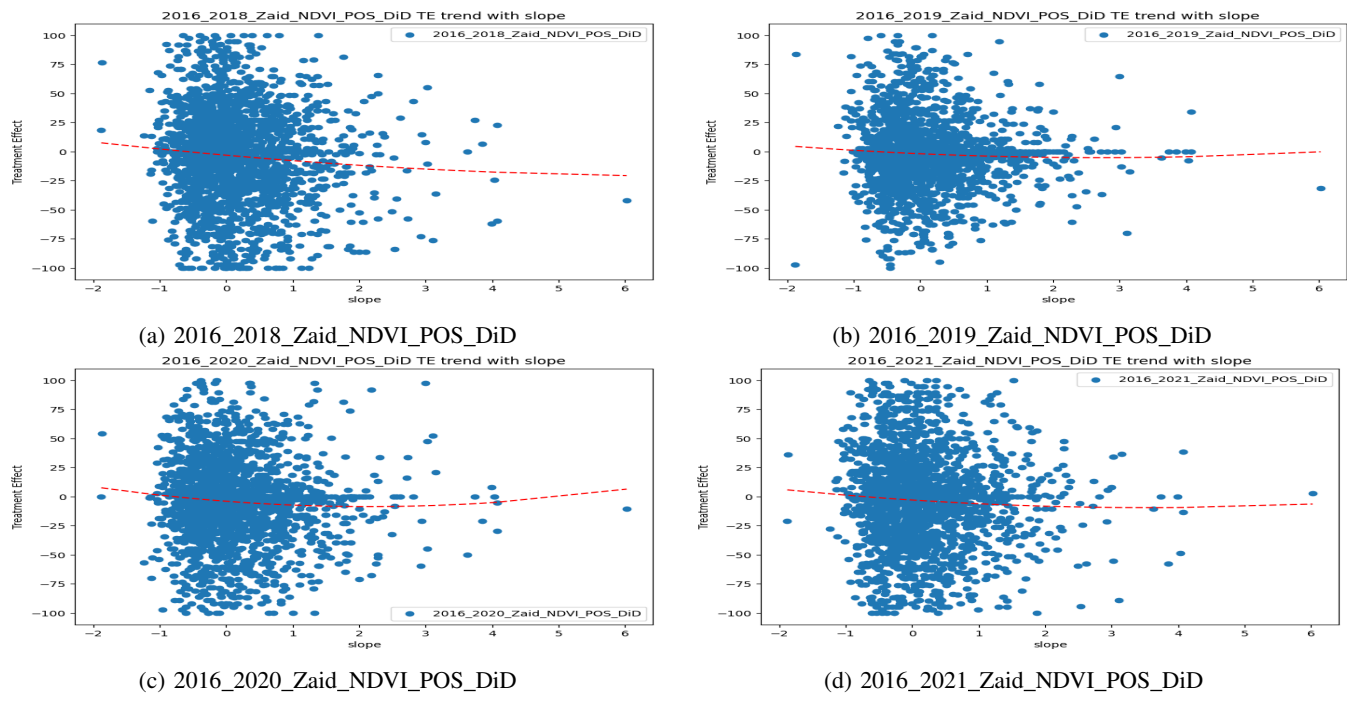


Figure 80: Trend of treatment effect (from DiD) on NDVI Zaid wrt covariate slope

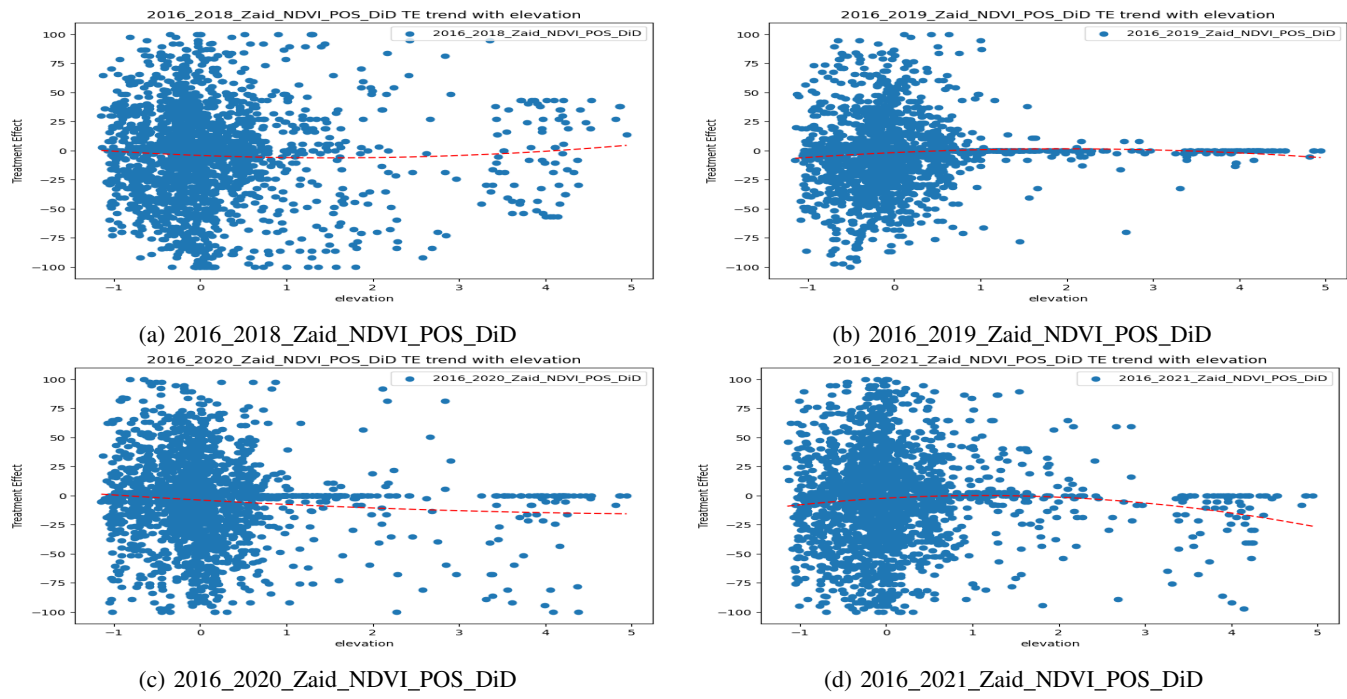


Figure 81: Trend of treatment effect (from DiD) on NDVI Zaid wrt covariate elevation

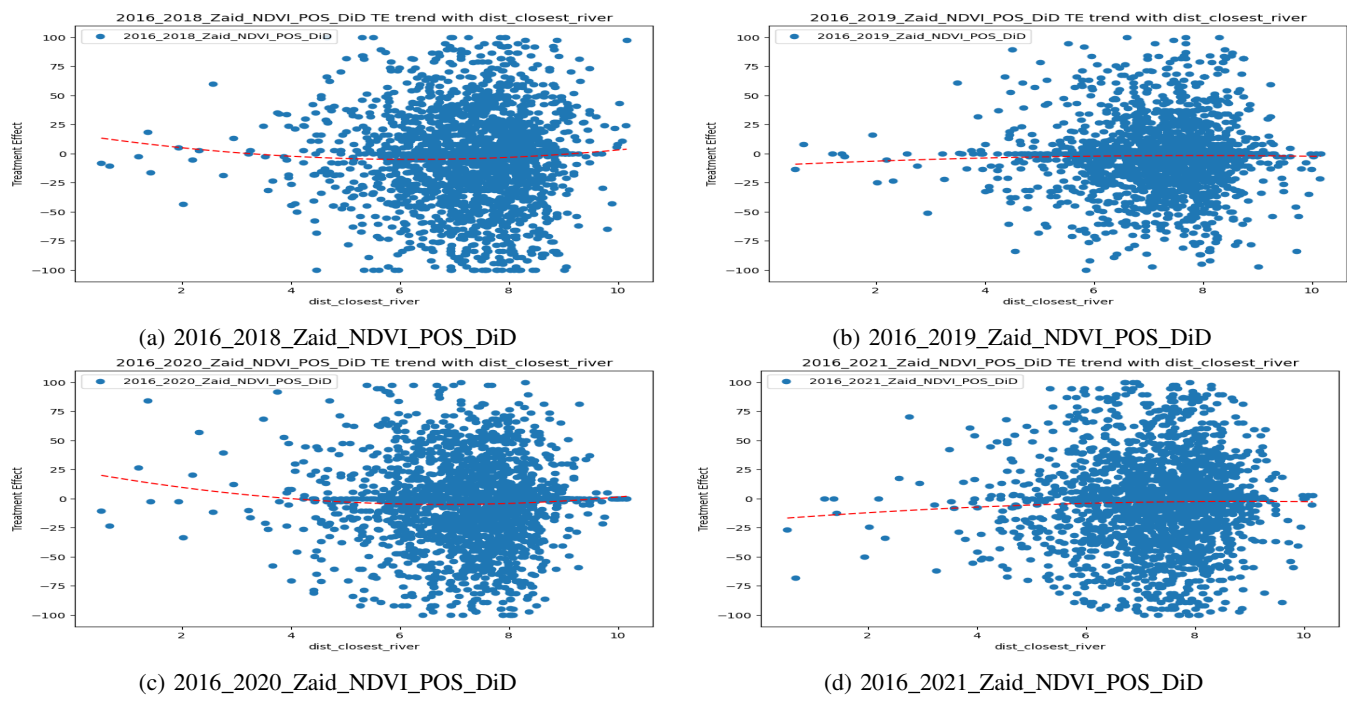


Figure 82: Trend of treatment effect (from DiD) on NDVI Zaid wrt covariate dist\_closest\_river

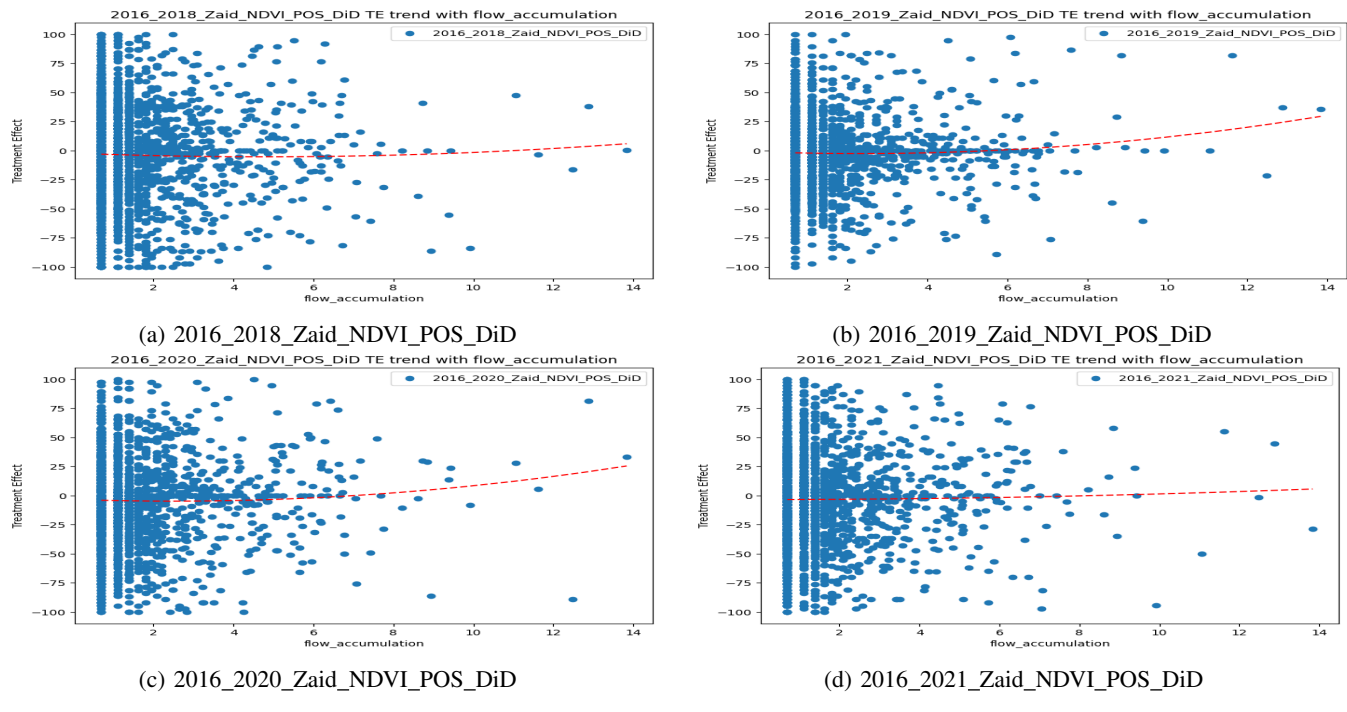


Figure 83: Trend of treatment effect (from DiD) on NDVI Zaid wrt covariate flow\_accumulation

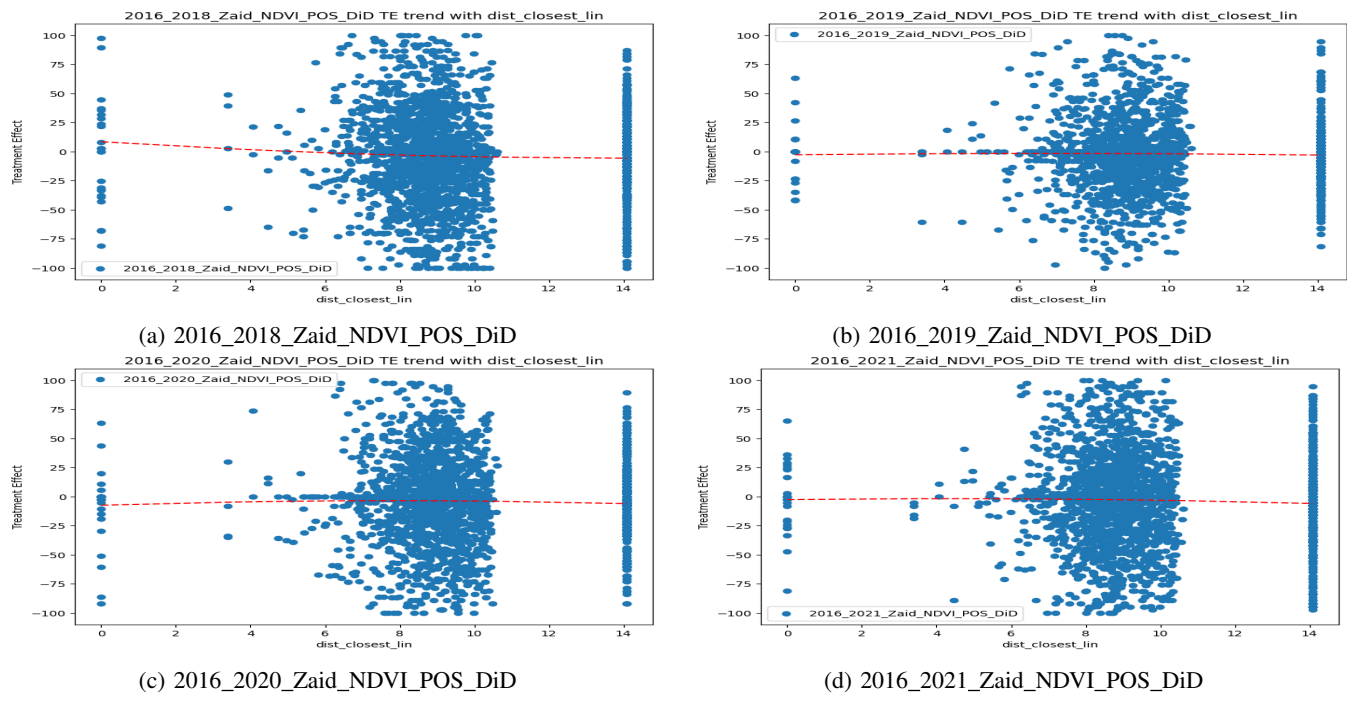


Figure 84: Trend of treatment effect (from DiD) on NDVI Zaid wrt covariate dist\_closest\_lin

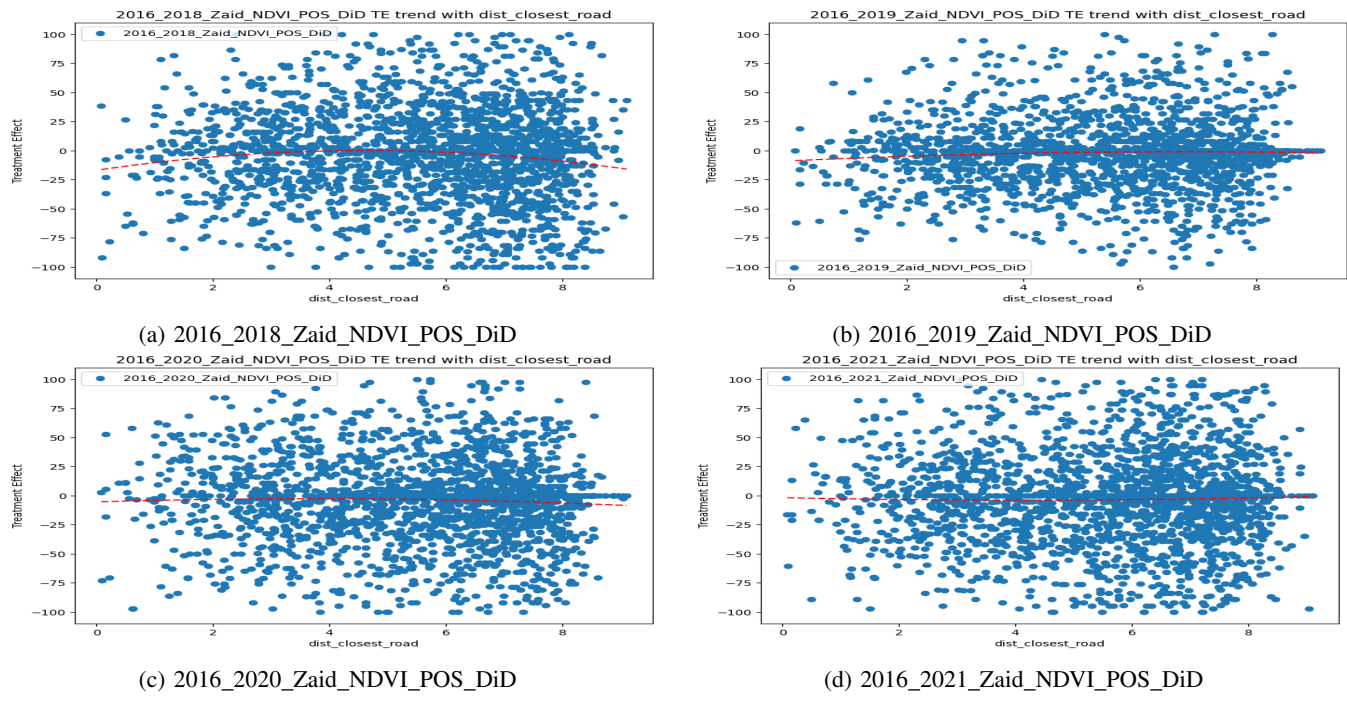


Figure 85: Trend of treatment effect (from DiD) on NDVI Zaid wrt covariate dist\_closest\_road

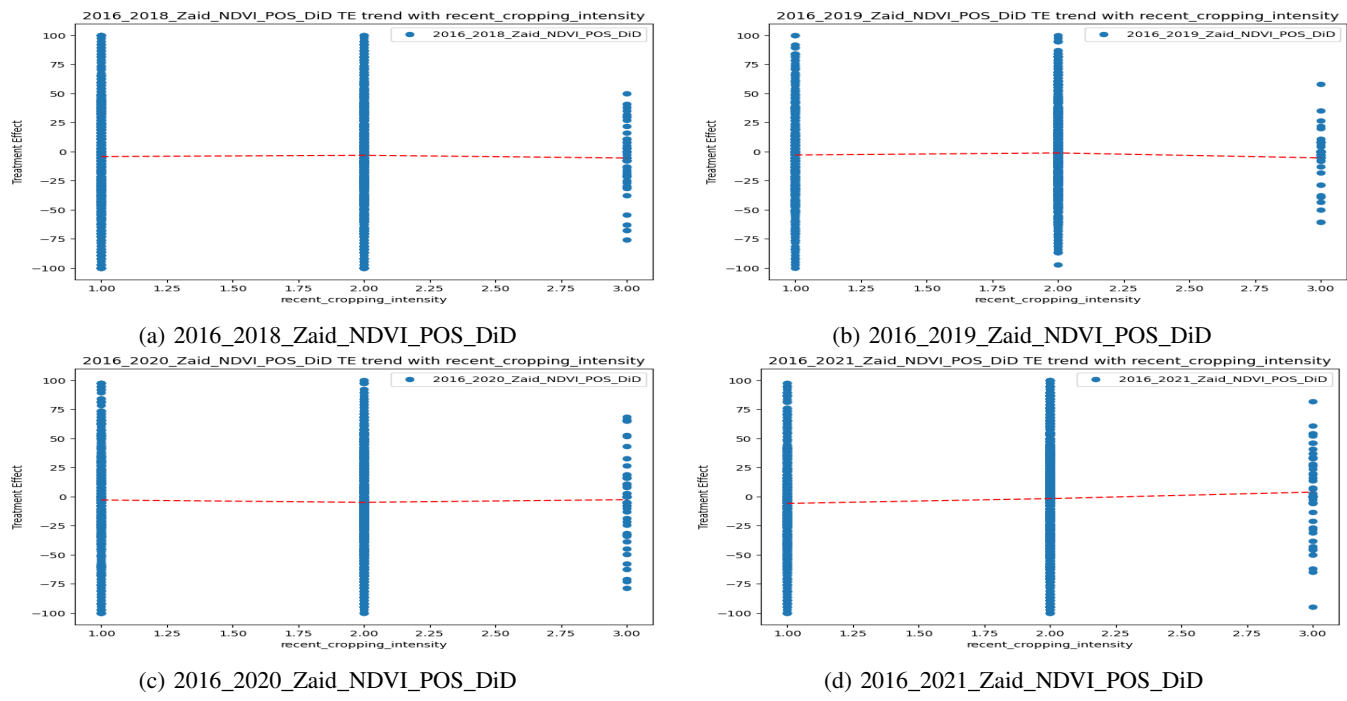


Figure 86: Trend of treatment effect (from DiD) on NDVI Zaid wrt covariate recent\_cropping\_intensity

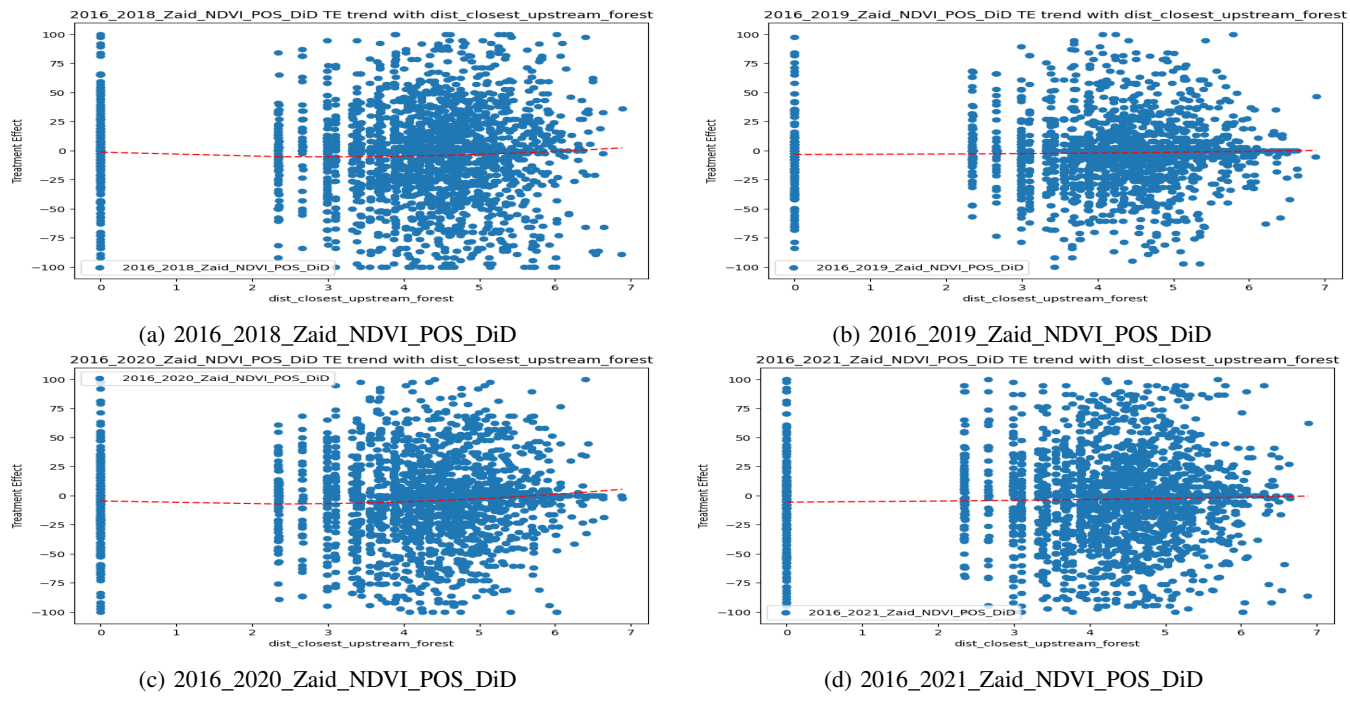


Figure 87: Trend of treatment effect (from DiD) on NDVI Zaid wrt covariate dist\_closest\_upstream\_forest

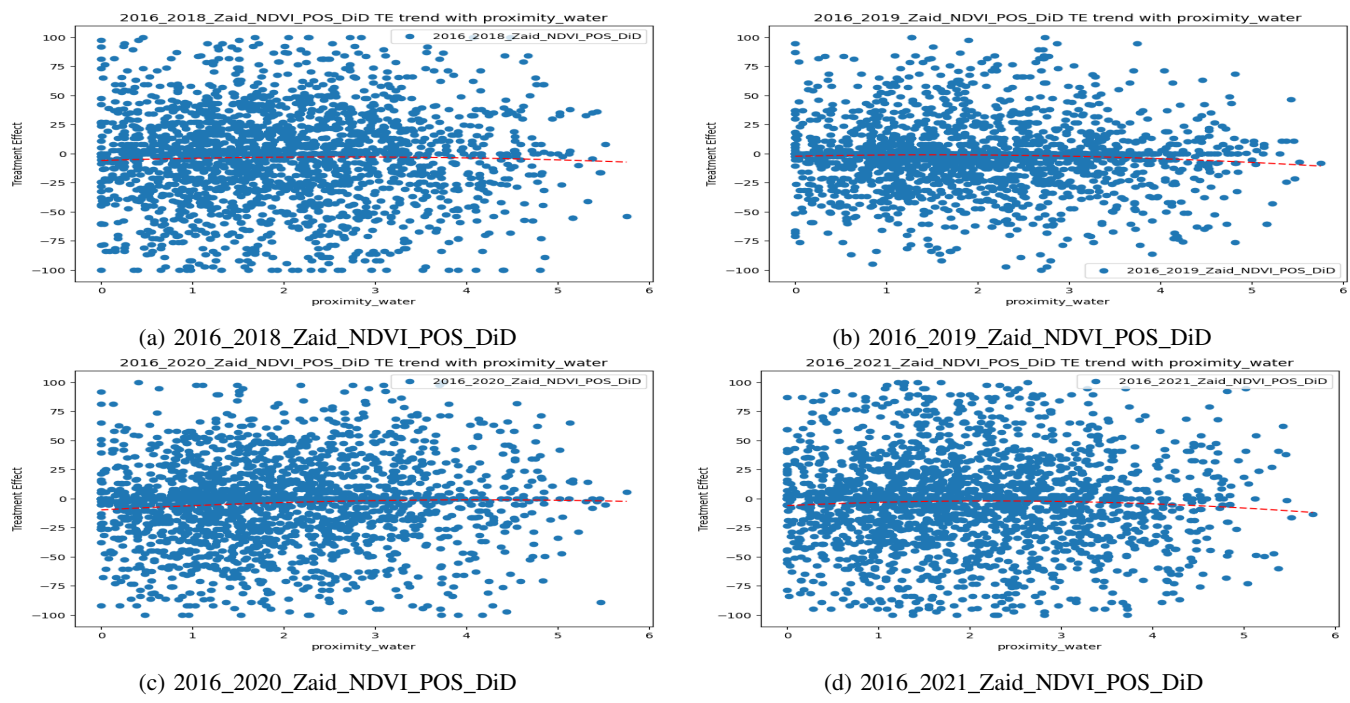


Figure 88: Trend of treatment effect (from DiD) on NDVI Zaid wrt covariate proximity\_water

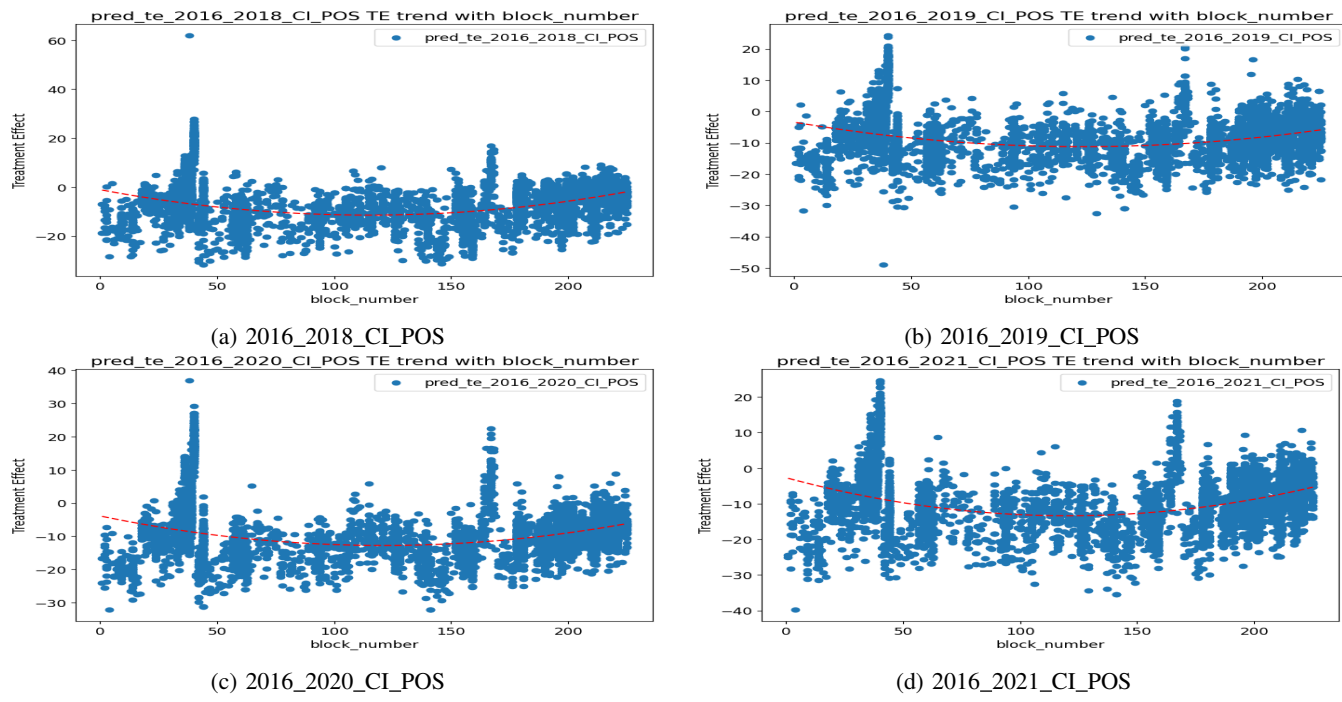


Figure 89: Trend of treatment effect (from DML) on CI wrt covariate block\_number

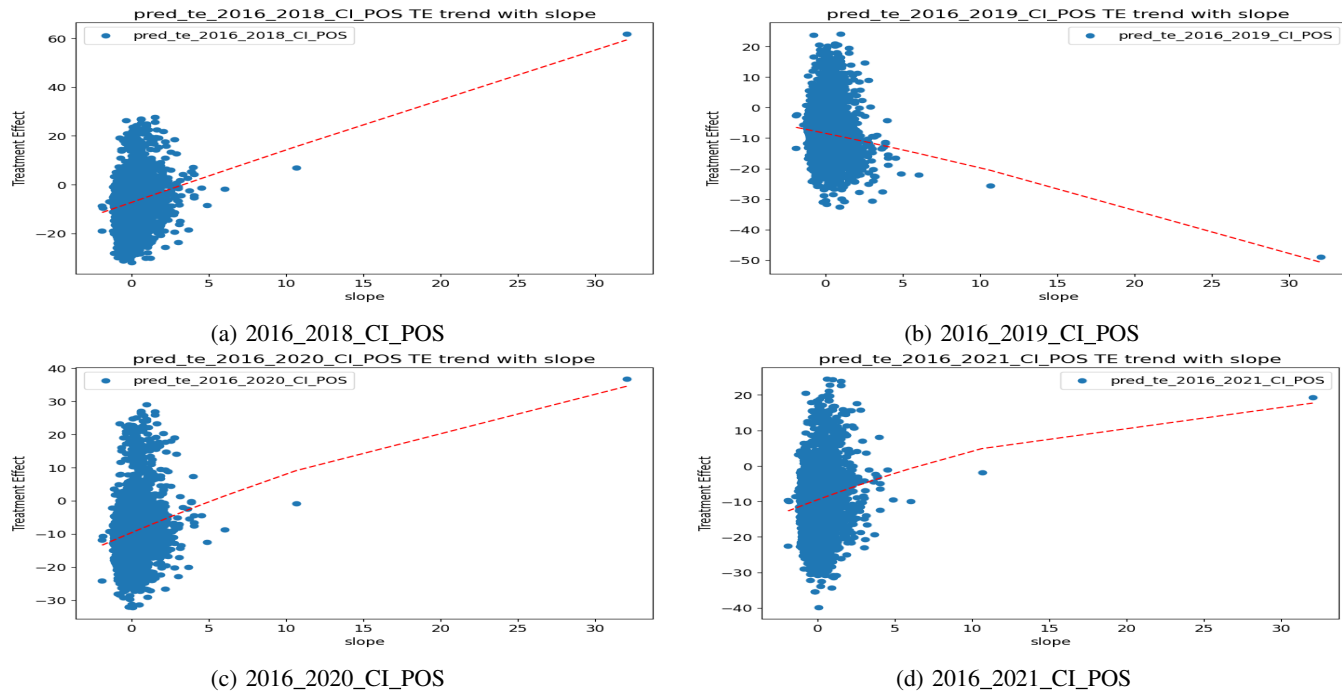


Figure 90: Trend of treatment effect (from DML) on CI wrt covariate slope

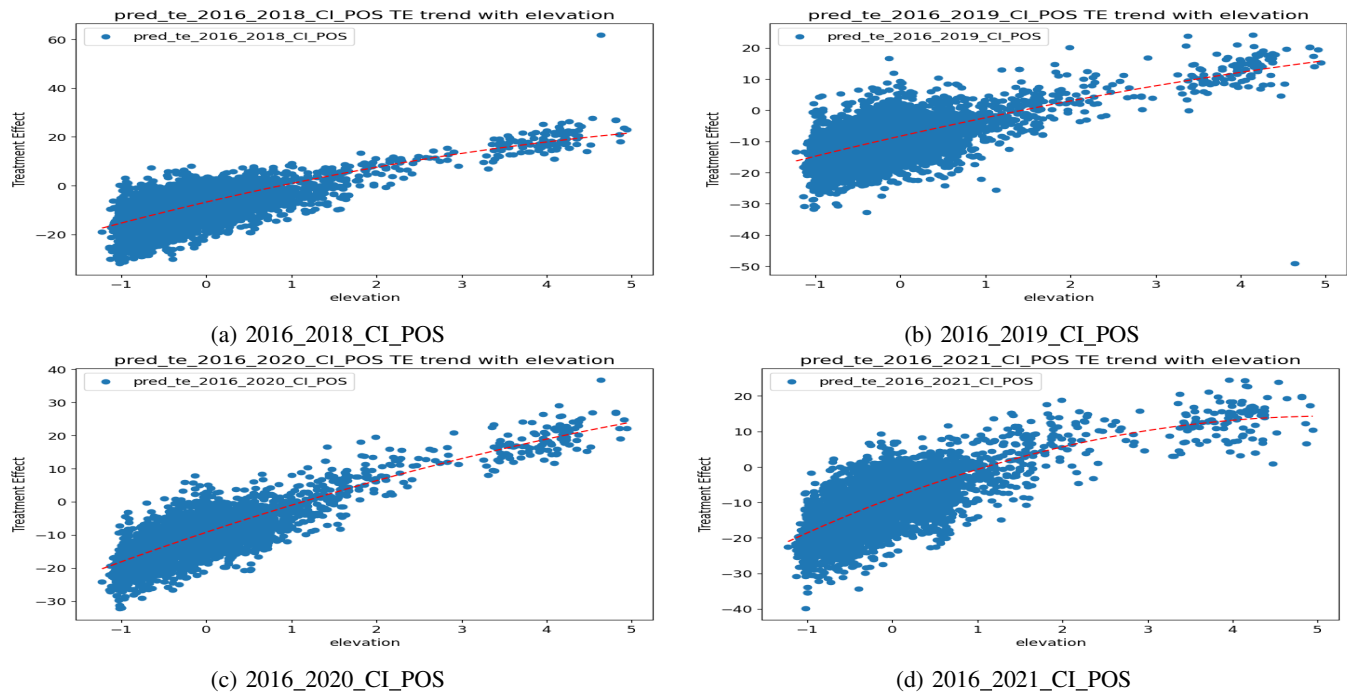


Figure 91: Trend of treatment effect (from DML) on CI wrt covariate elevation

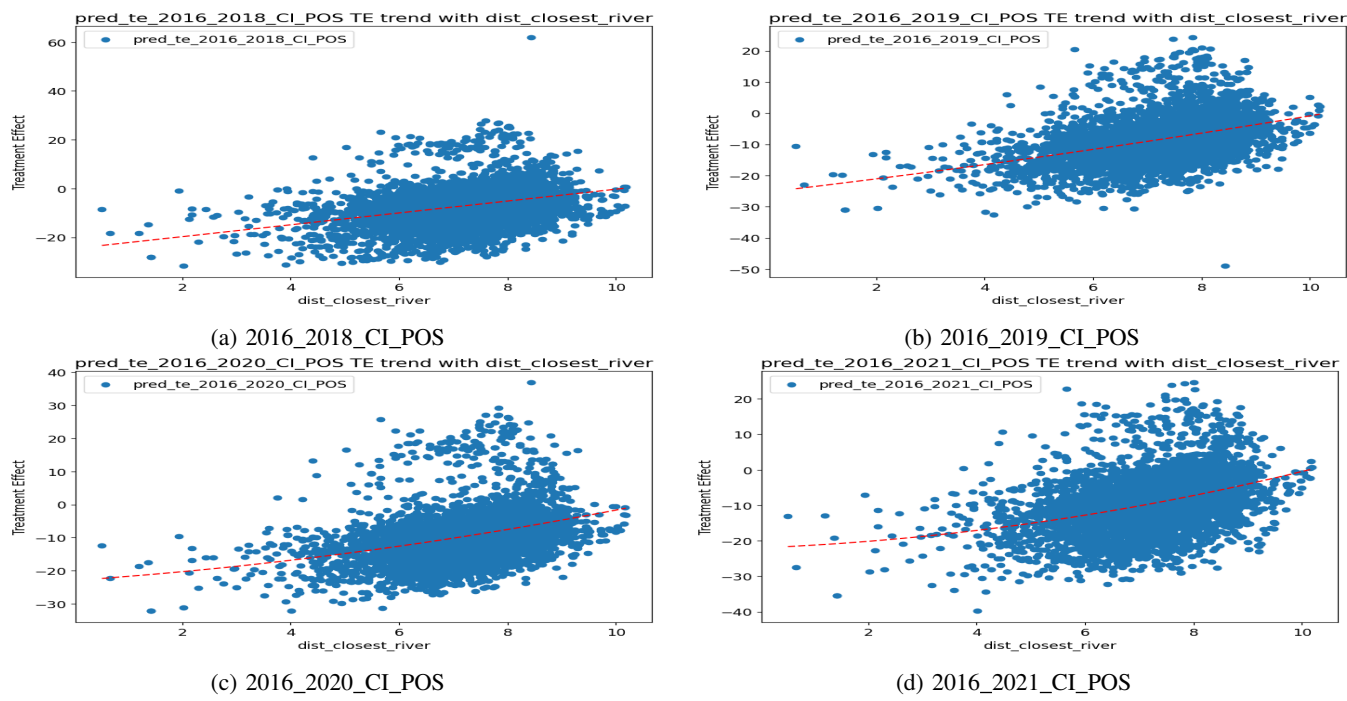


Figure 92: Trend of treatment effect (from DML) on CI wrt covariate dist\_closest\_river

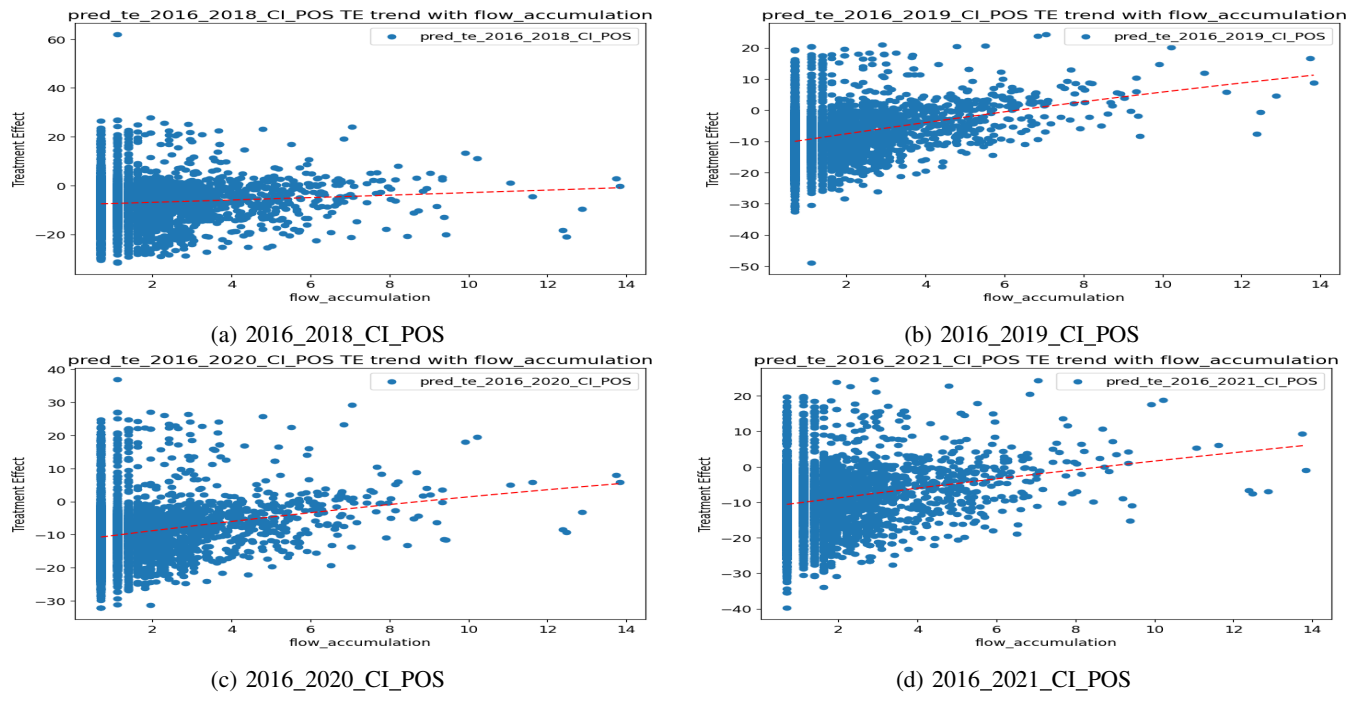


Figure 93: Trend of treatment effect (from DML) on CI wrt covariate flow\_accumulation

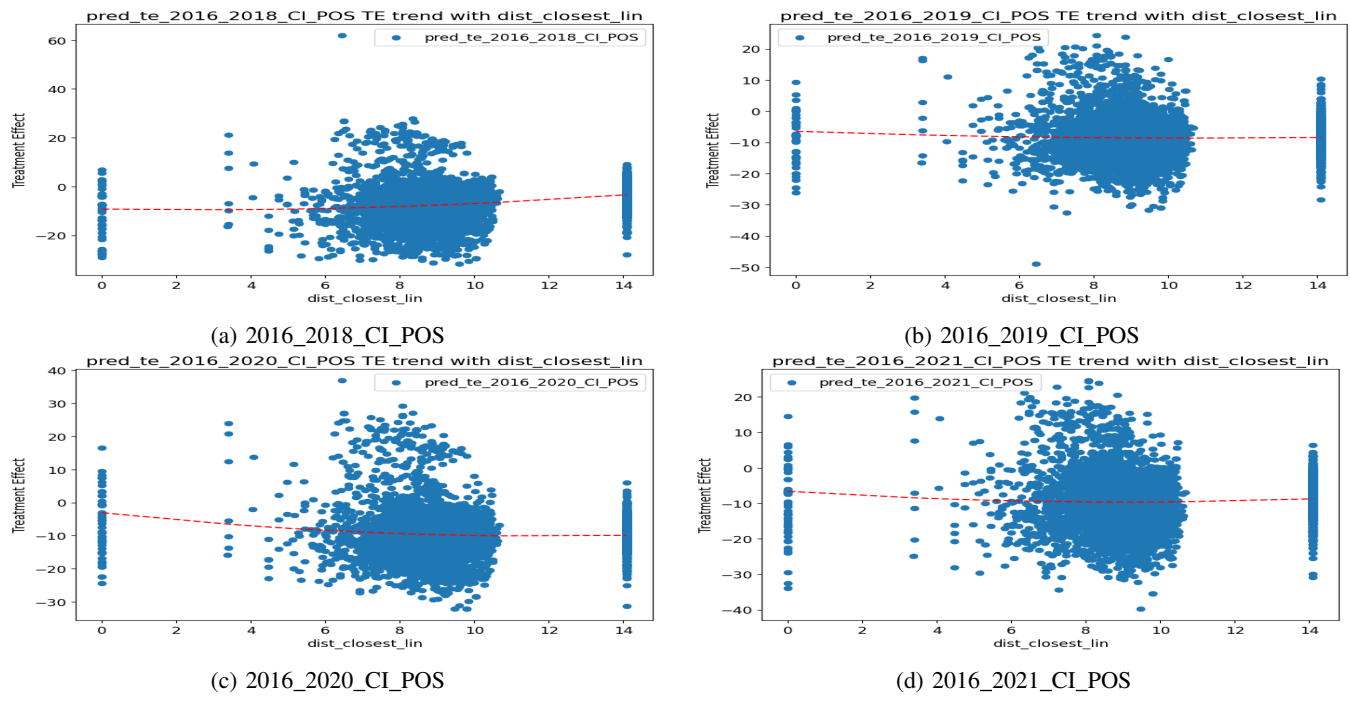
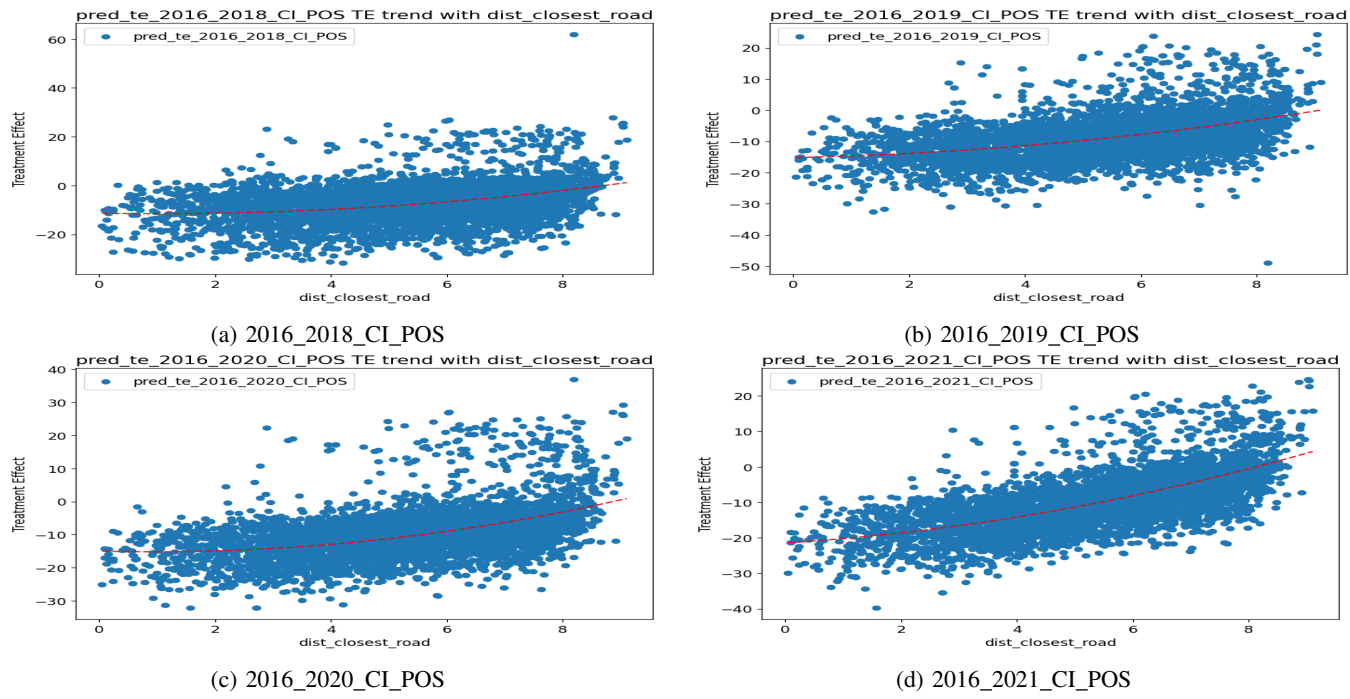
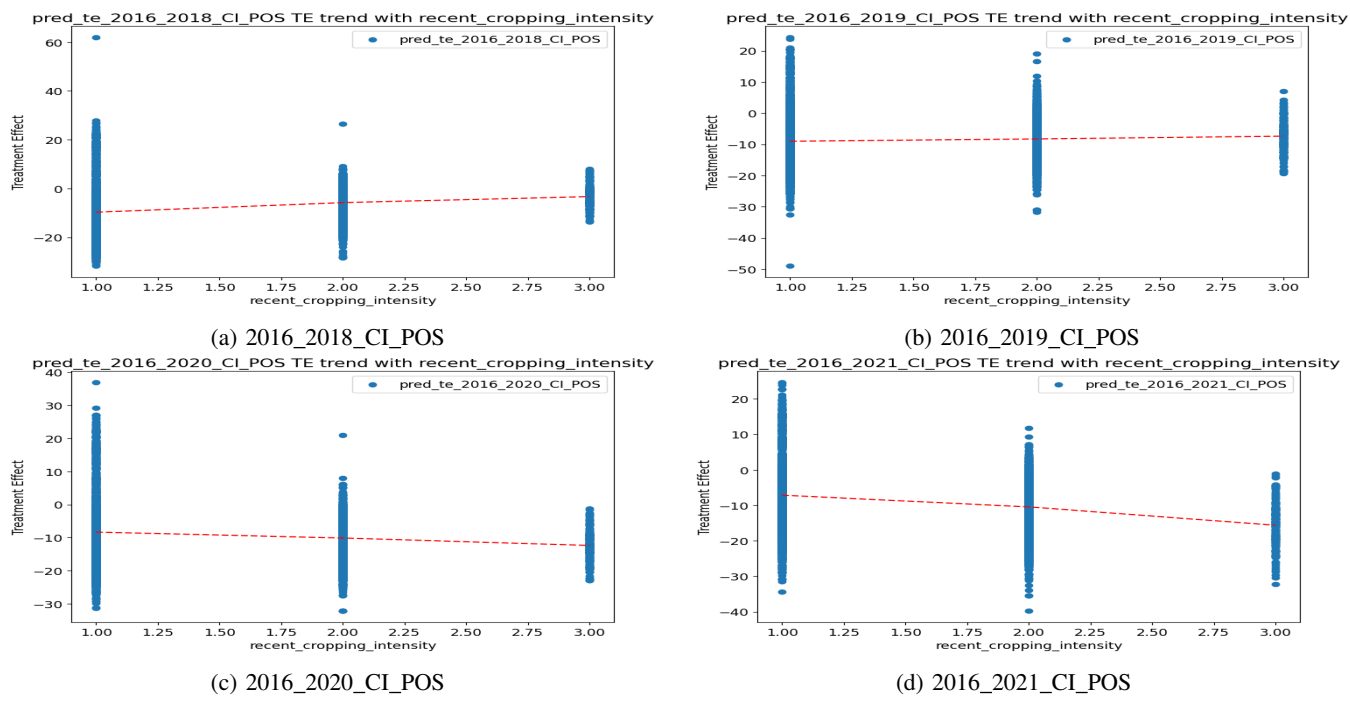


Figure 94: Trend of treatment effect (from DML) on CI wrt covariate dist\_closest\_lin

Figure 95: Trend of treatment effect (from DML) on CI wrt covariate `dist_closest_road`Figure 96: Trend of treatment effect (from DML) on CI wrt covariate `recent_cropping_intensity`

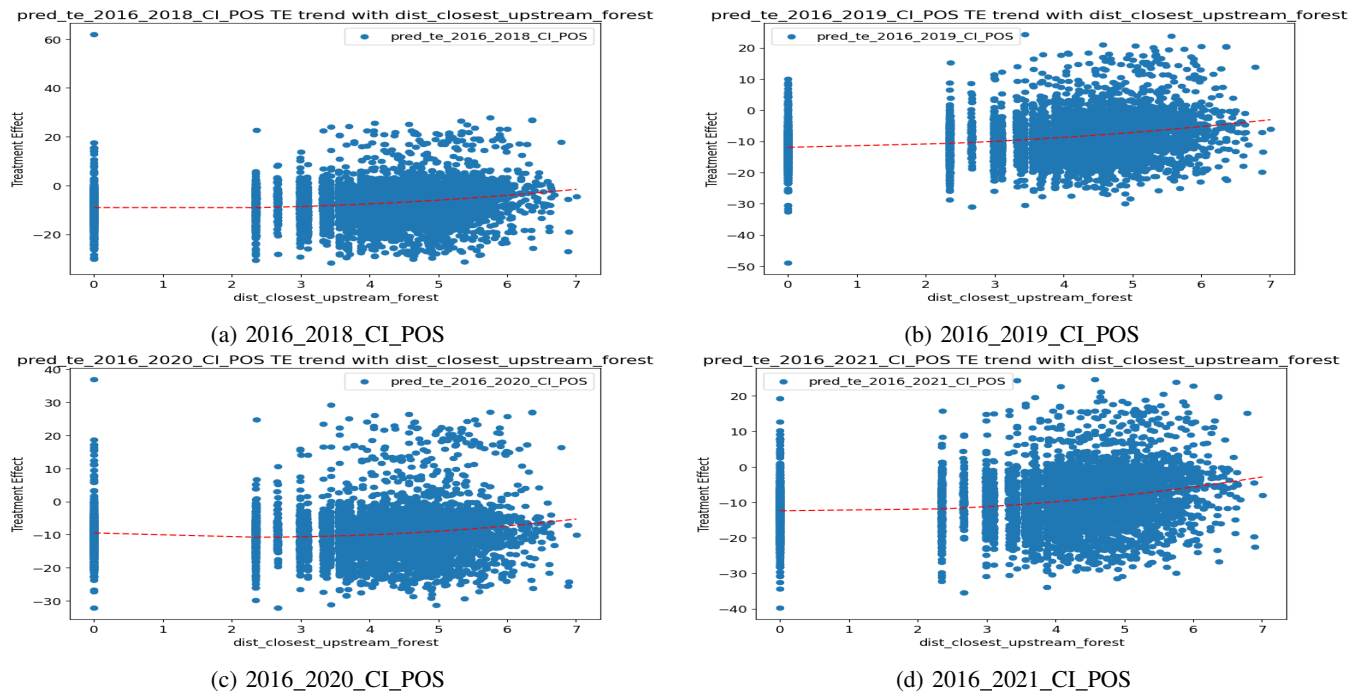


Figure 97: Trend of treatment effect (from DML) on CI wrt covariate dist\_closest\_upstream\_forest

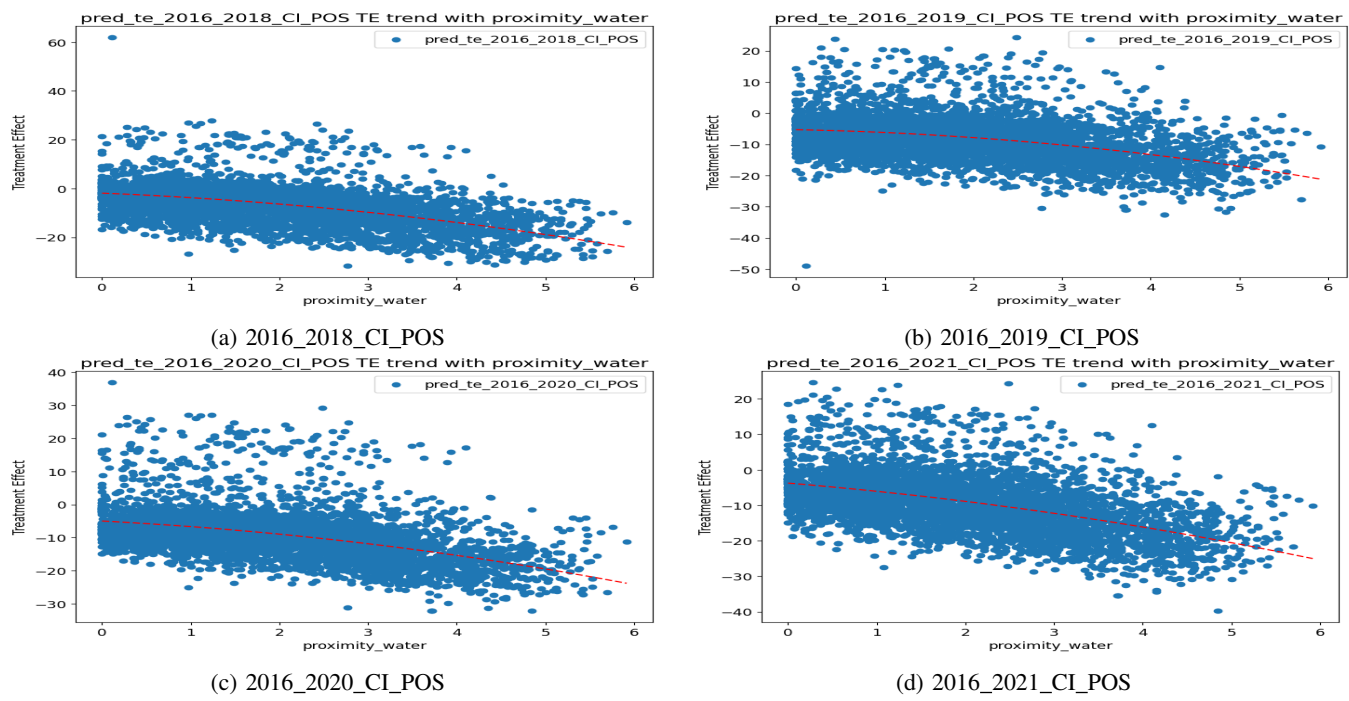


Figure 98: Trend of treatment effect (from DML) on CI wrt covariate proximity\_water

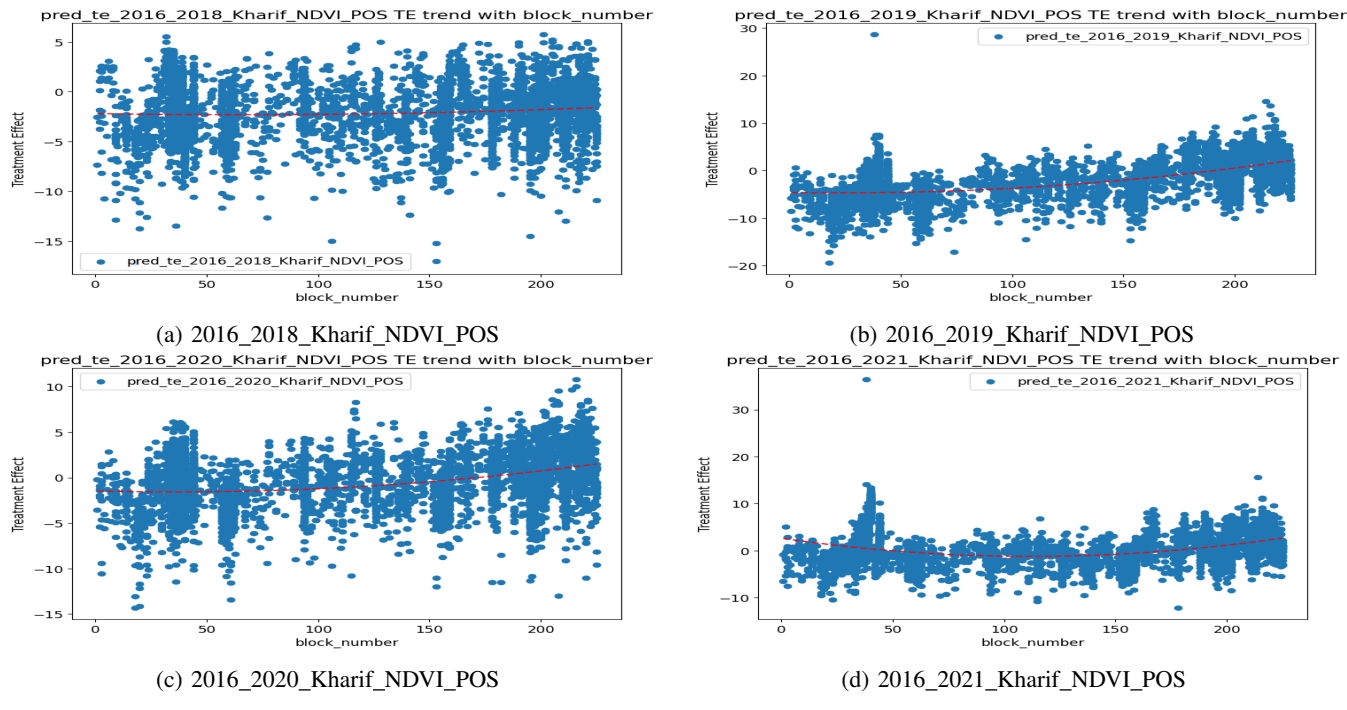


Figure 99: Trend of treatment effect (from DML) on NDVI Kharif wrt covariate block\_number

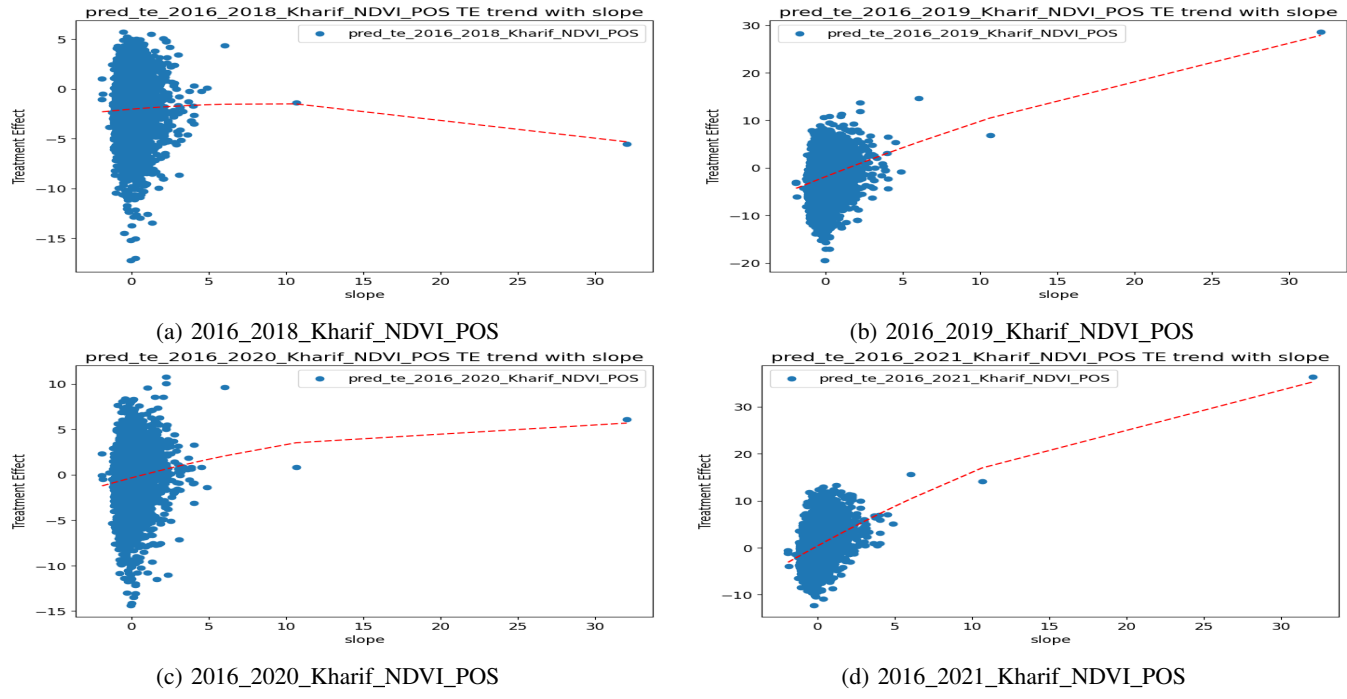


Figure 100: Trend of treatment effect (from DML) on NDVI Kharif wrt covariate slope

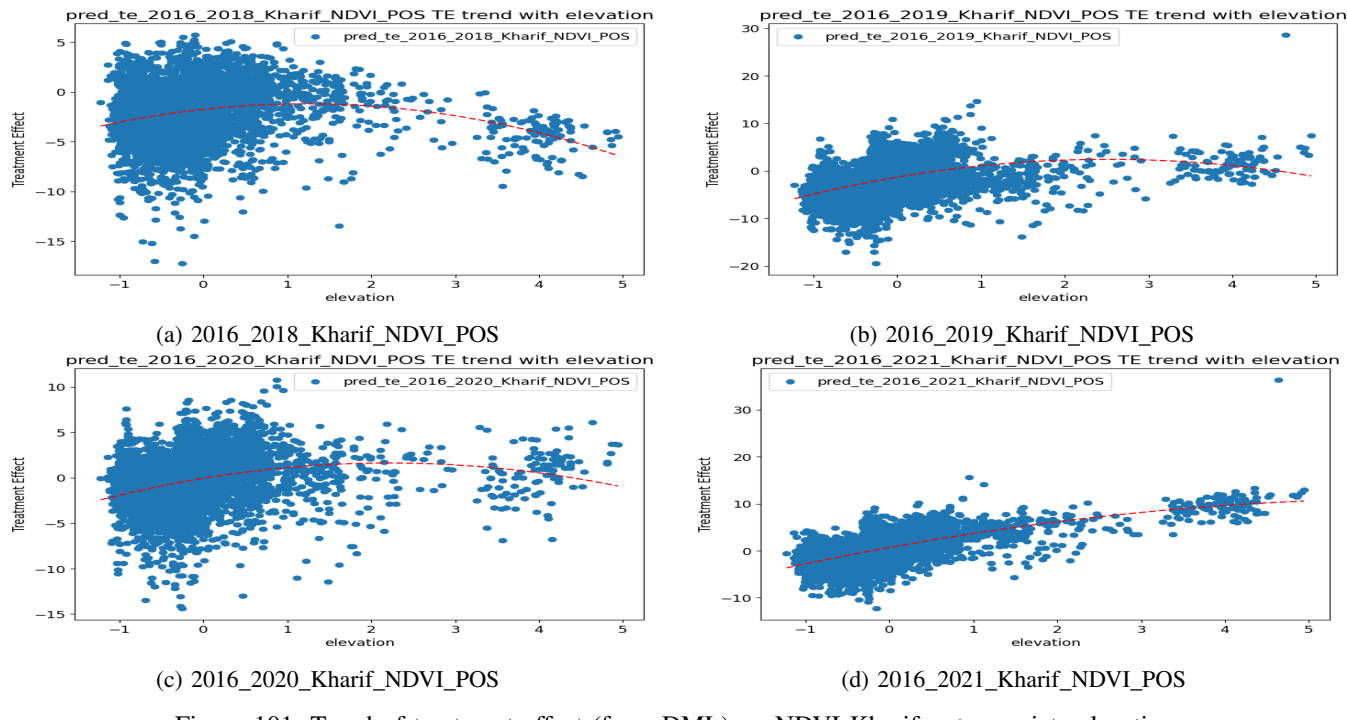


Figure 101: Trend of treatment effect (from DML) on NDVI Kharif wrt covariate elevation

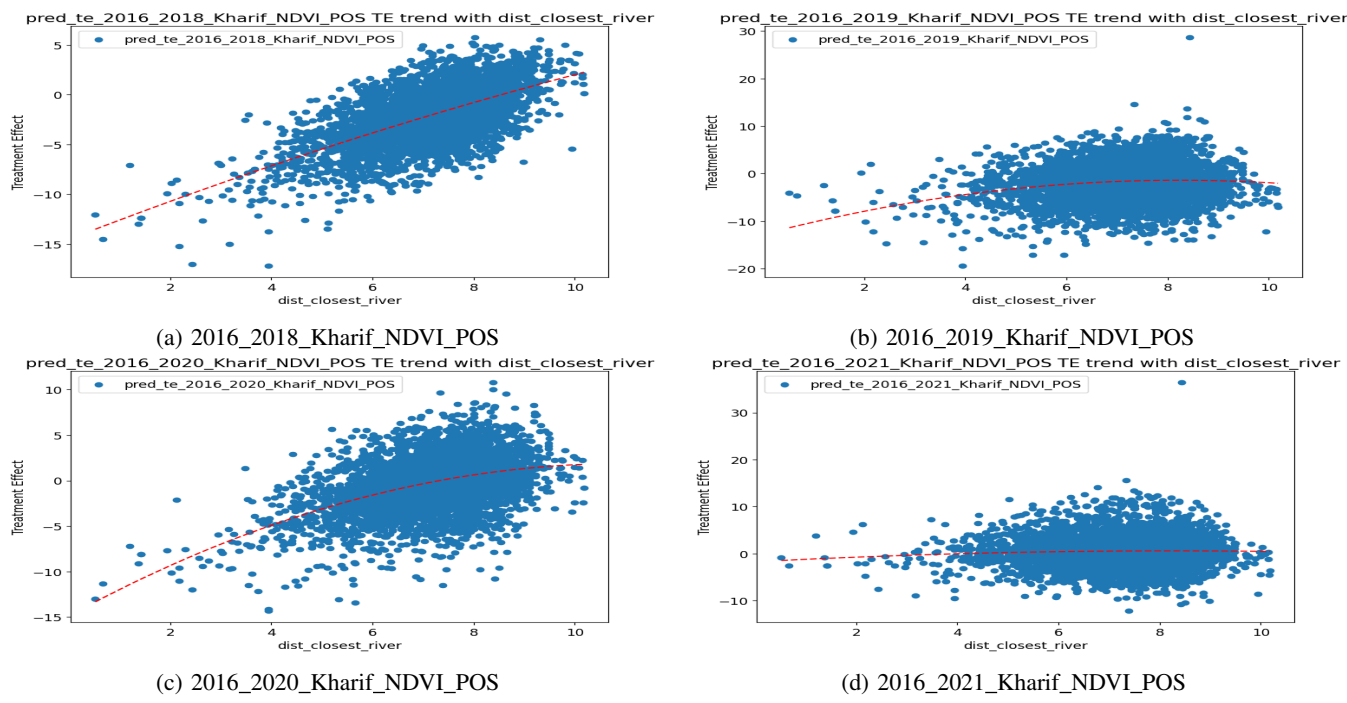


Figure 102: Trend of treatment effect (from DML) on NDVI Kharif wrt covariate dist\_closest\_river

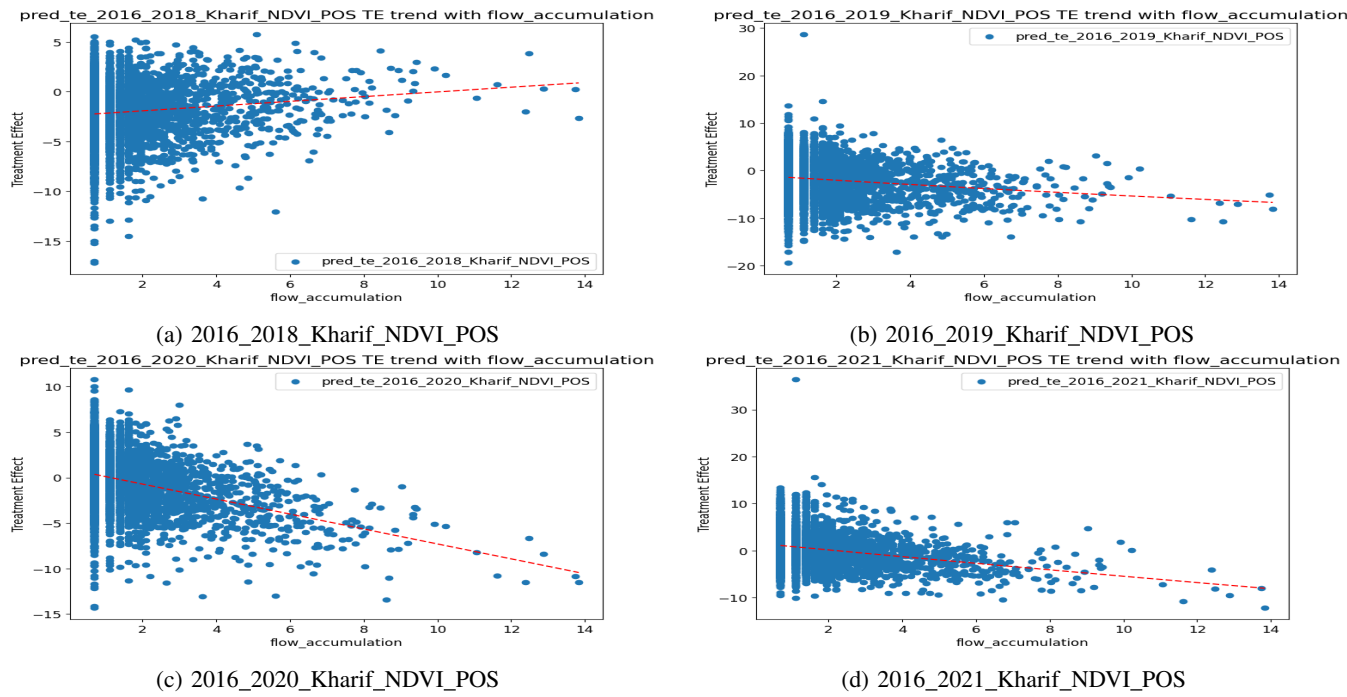


Figure 103: Trend of treatment effect (from DML) on NDVI Kharif wrt covariate flow\_accumulation

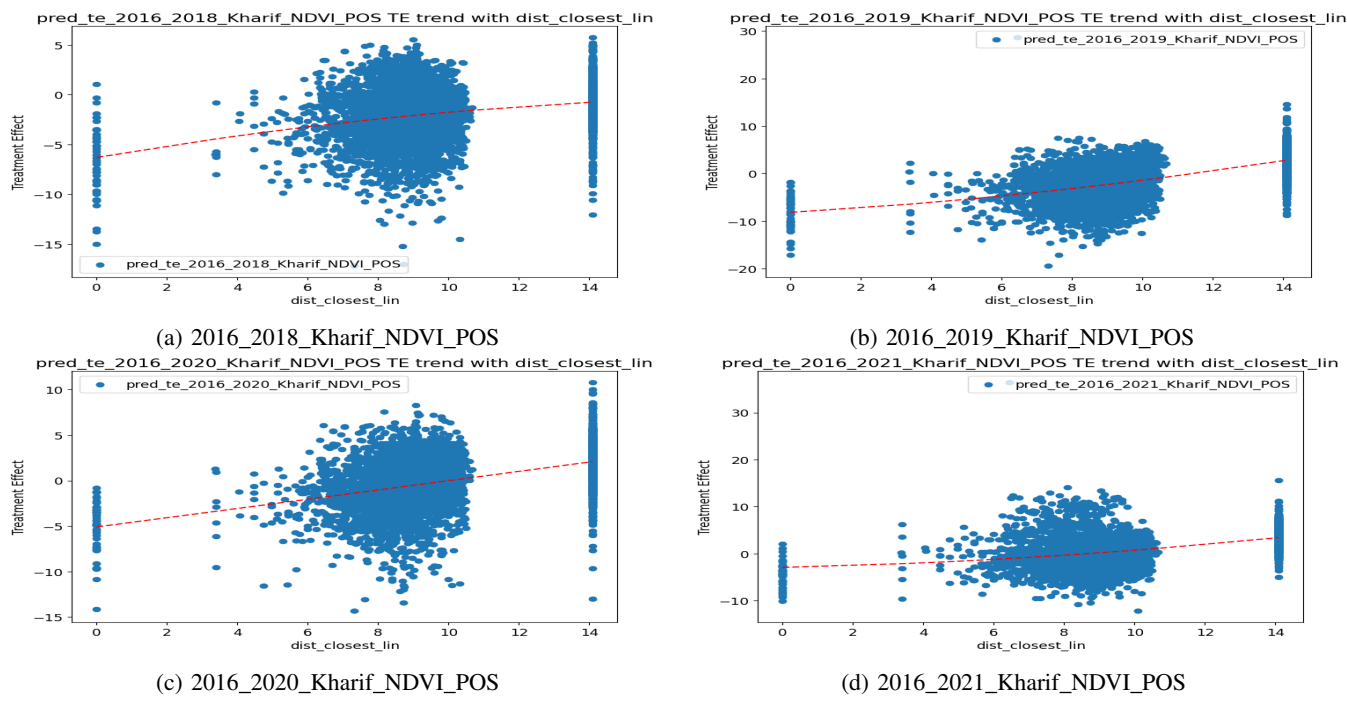


Figure 104: Trend of treatment effect (from DML) on NDVI Kharif wrt covariate dist\_closest\_lin

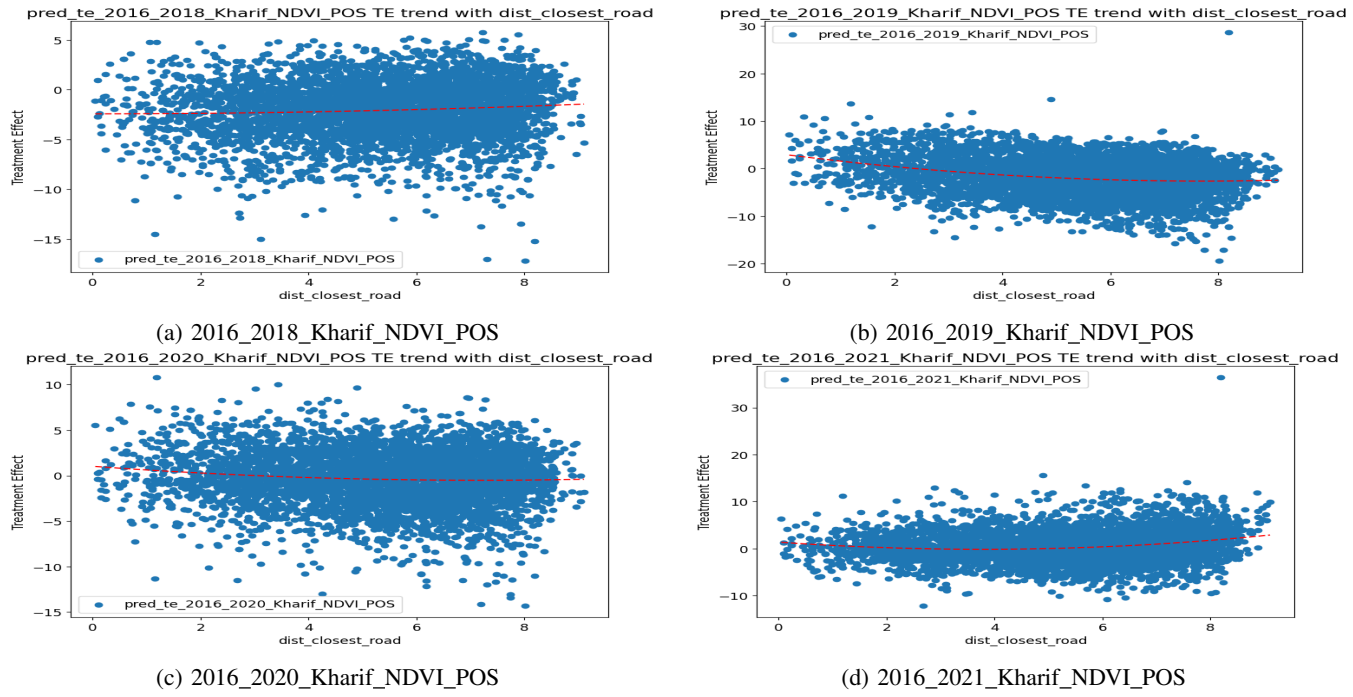


Figure 105: Trend of treatment effect (from DML) on NDVI Kharif wrt covariate dist\_closest\_road

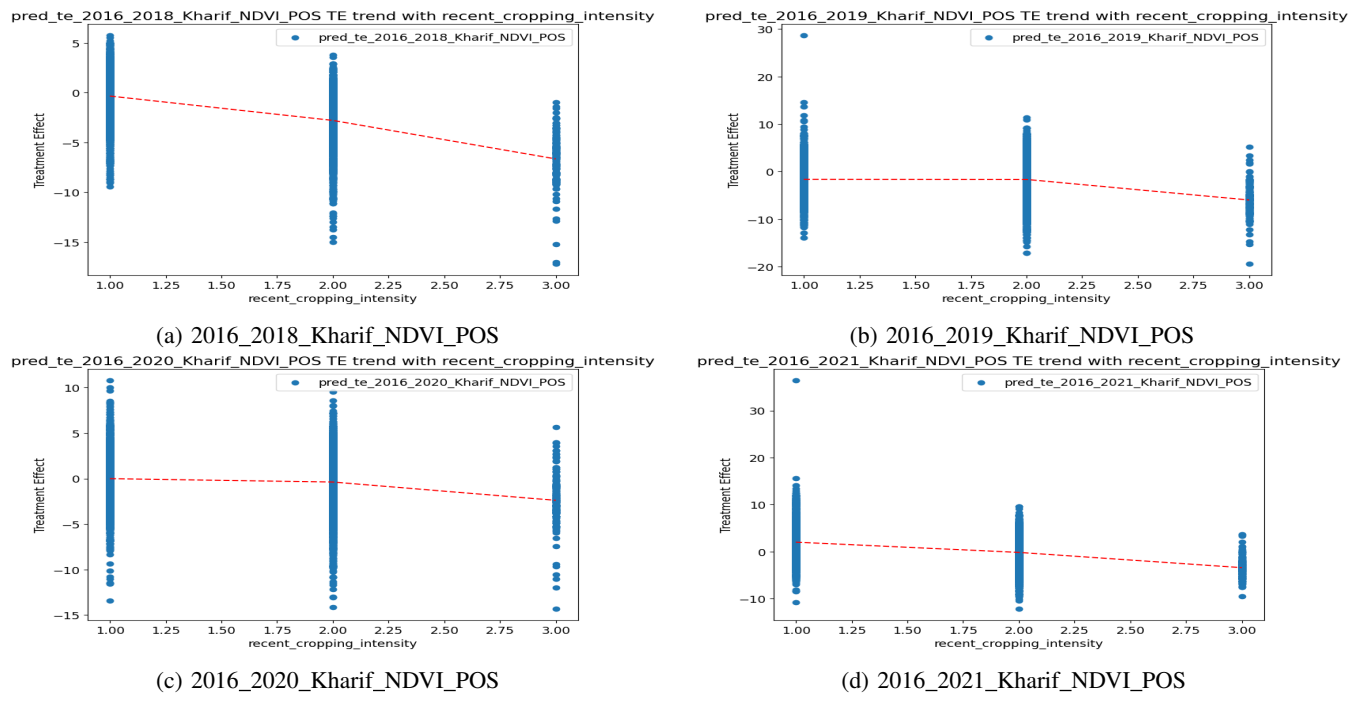


Figure 106: Trend of treatment effect (from DML) on NDVI Kharif wrt covariate recent\_cropping\_intensity

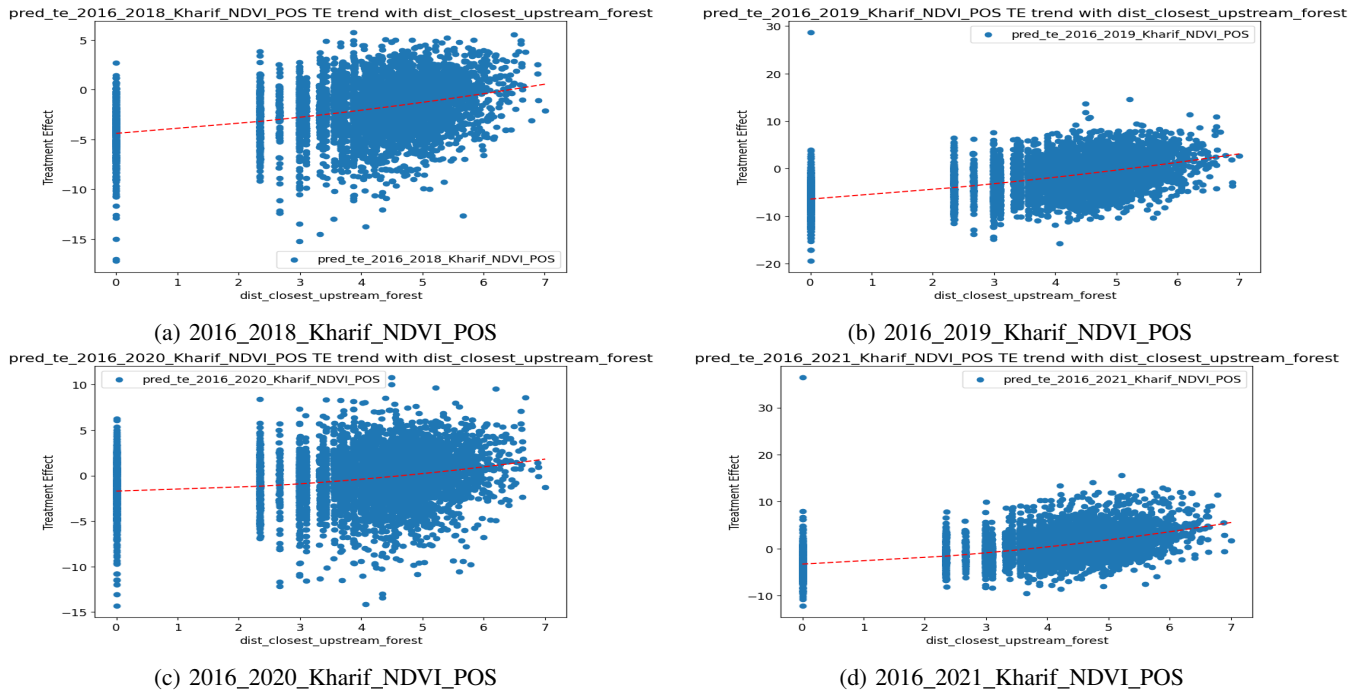


Figure 107: Trend of treatment effect (from DML) on NDVI Kharif wrt covariate dist\_closest\_upstream\_forest

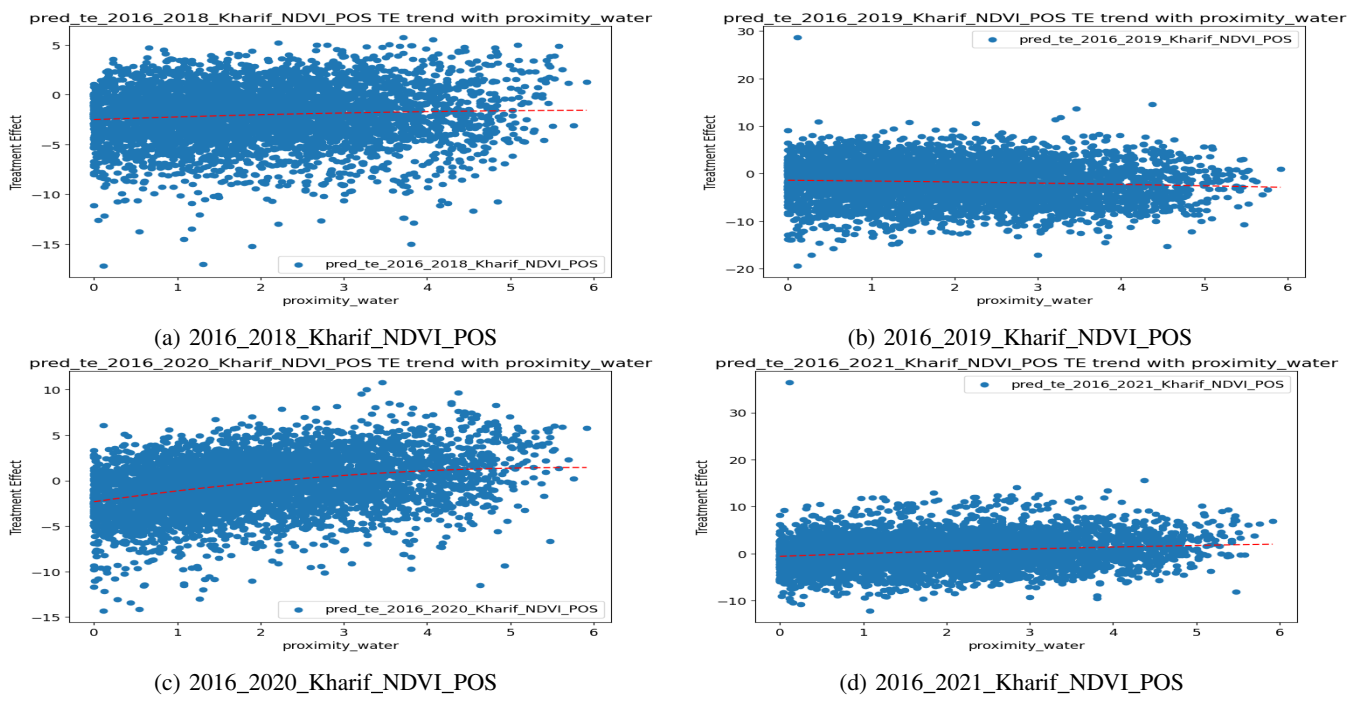


Figure 108: Trend of treatment effect (from DML) on NDVI Kharif wrt covariate proximity\_water

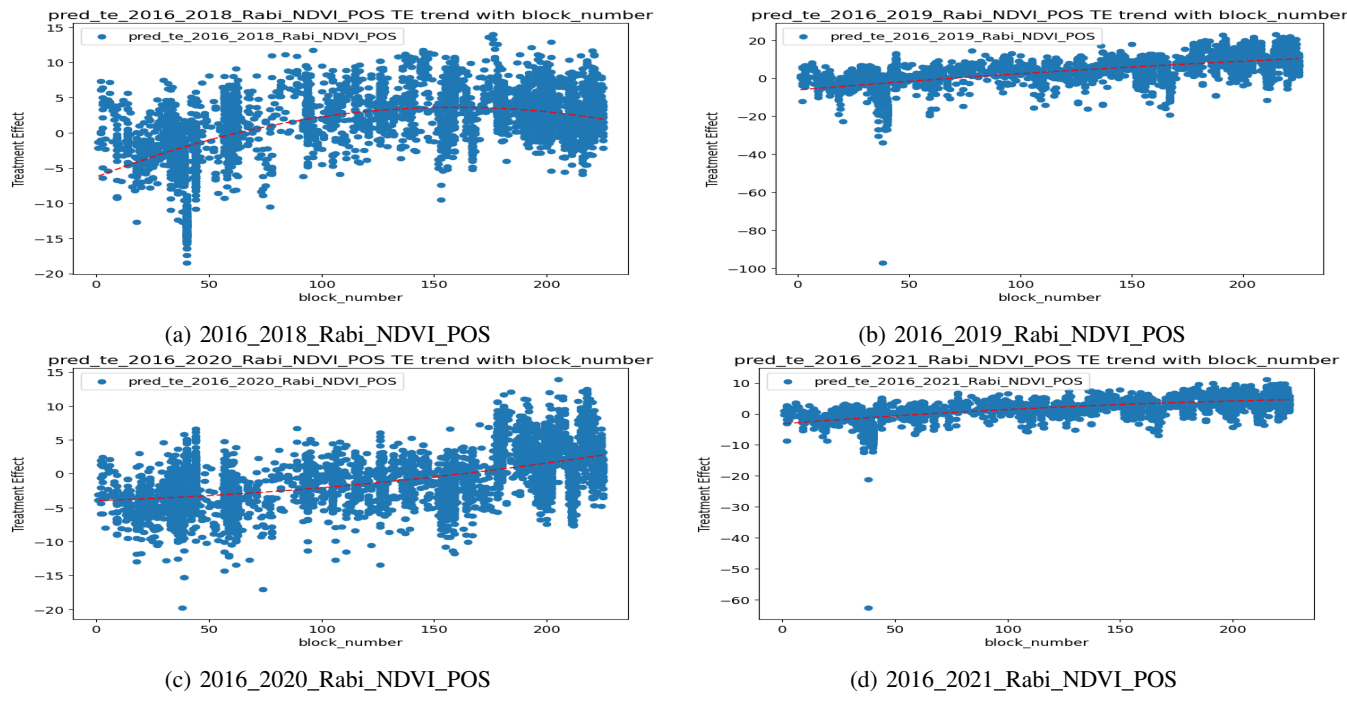


Figure 109: Trend of treatment effect (from DML) on NDVI Rabi wrt covariate block\_number

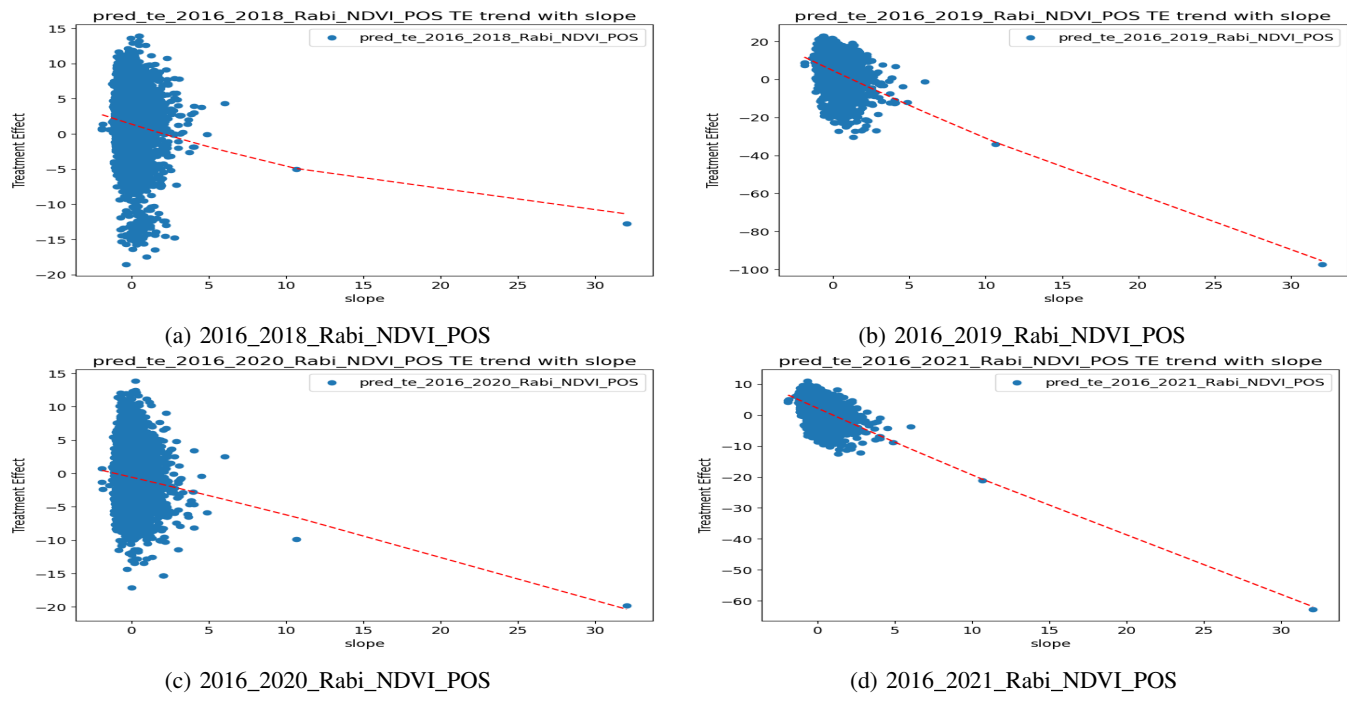


Figure 110: Trend of treatment effect (from DML) on NDVI Rabi wrt covariate slope

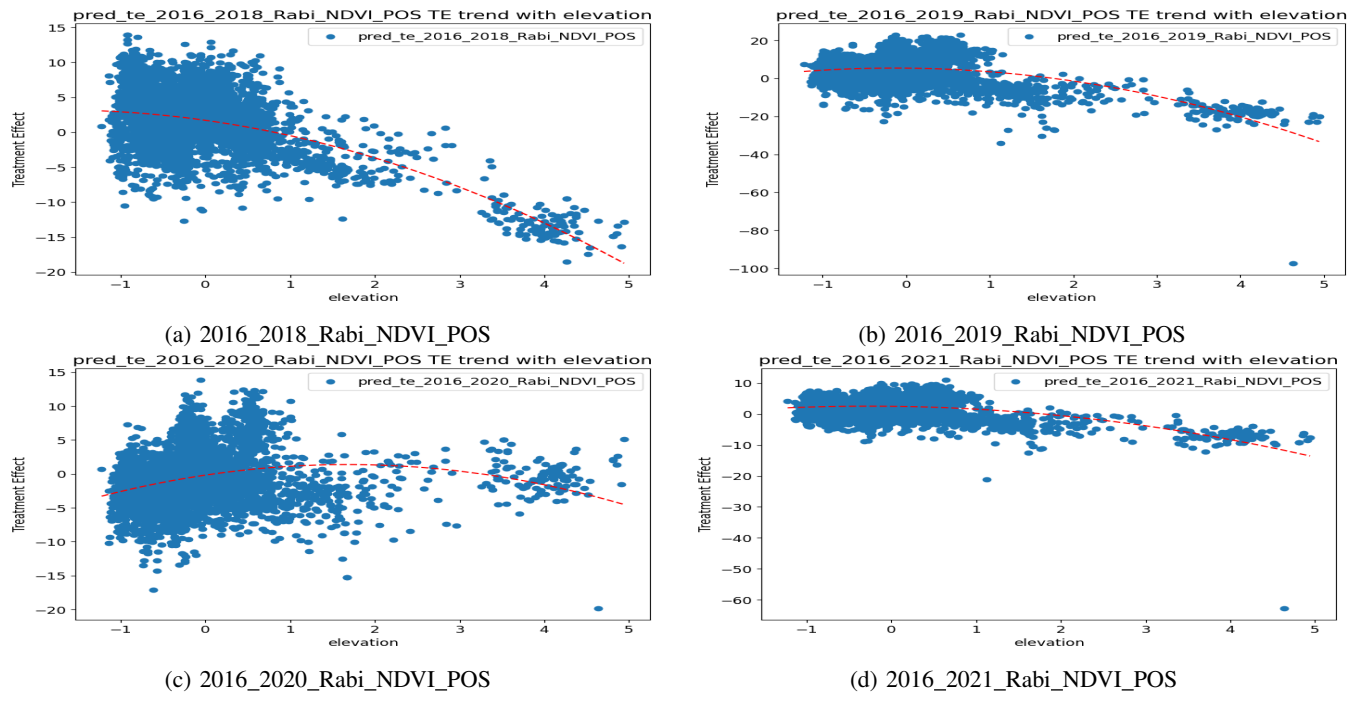


Figure 111: Trend of treatment effect (from DML) on NDVI Rabi wrt covariate elevation

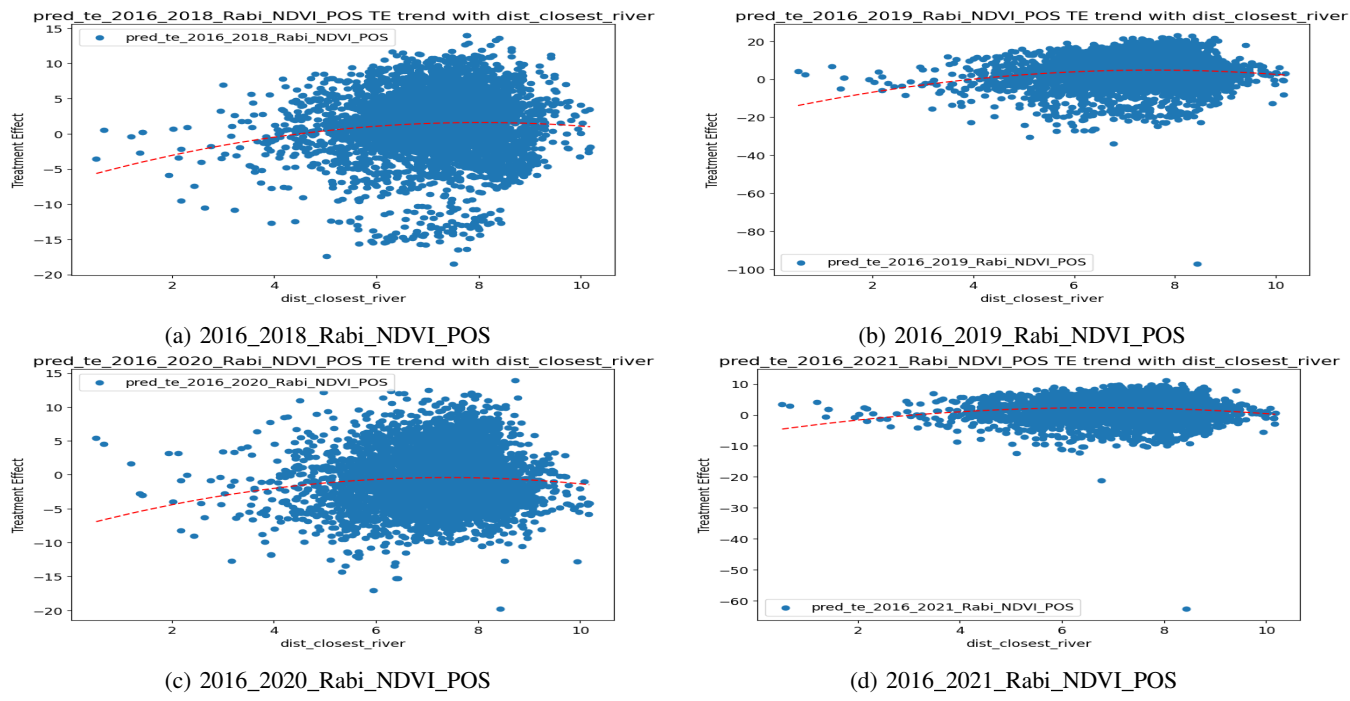


Figure 112: Trend of treatment effect (from DML) on NDVI Rabi wrt covariate dist\_closest\_river

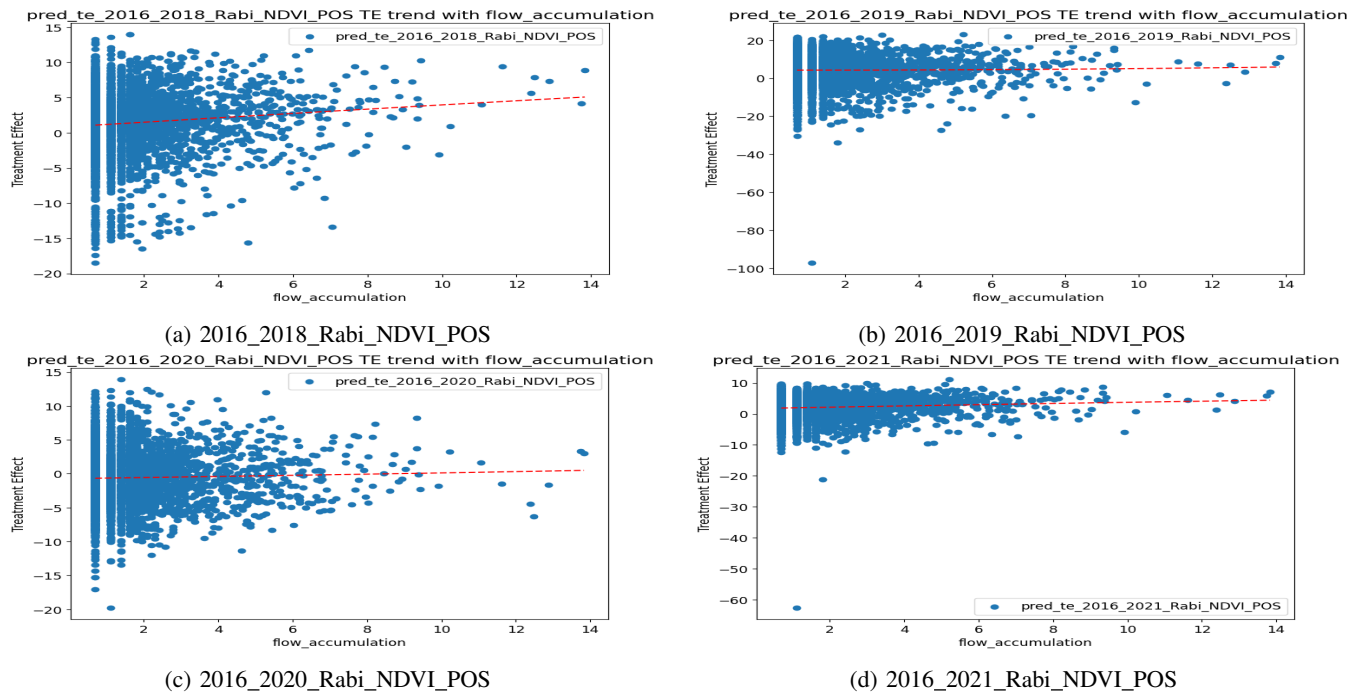


Figure 113: Trend of treatment effect (from DML) on NDVI Rabi wrt covariate flow\_accumulation

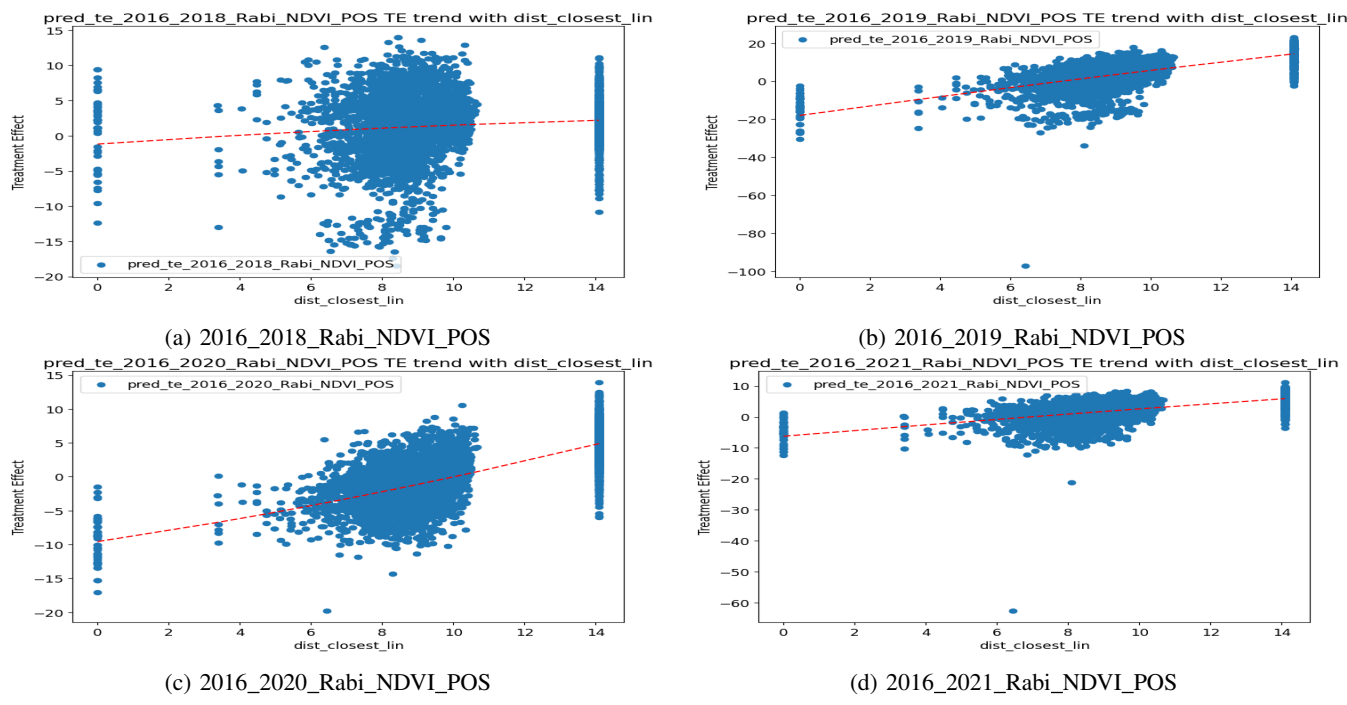


Figure 114: Trend of treatment effect (from DML) on NDVI Rabi wrt covariate dist\_closest\_lin

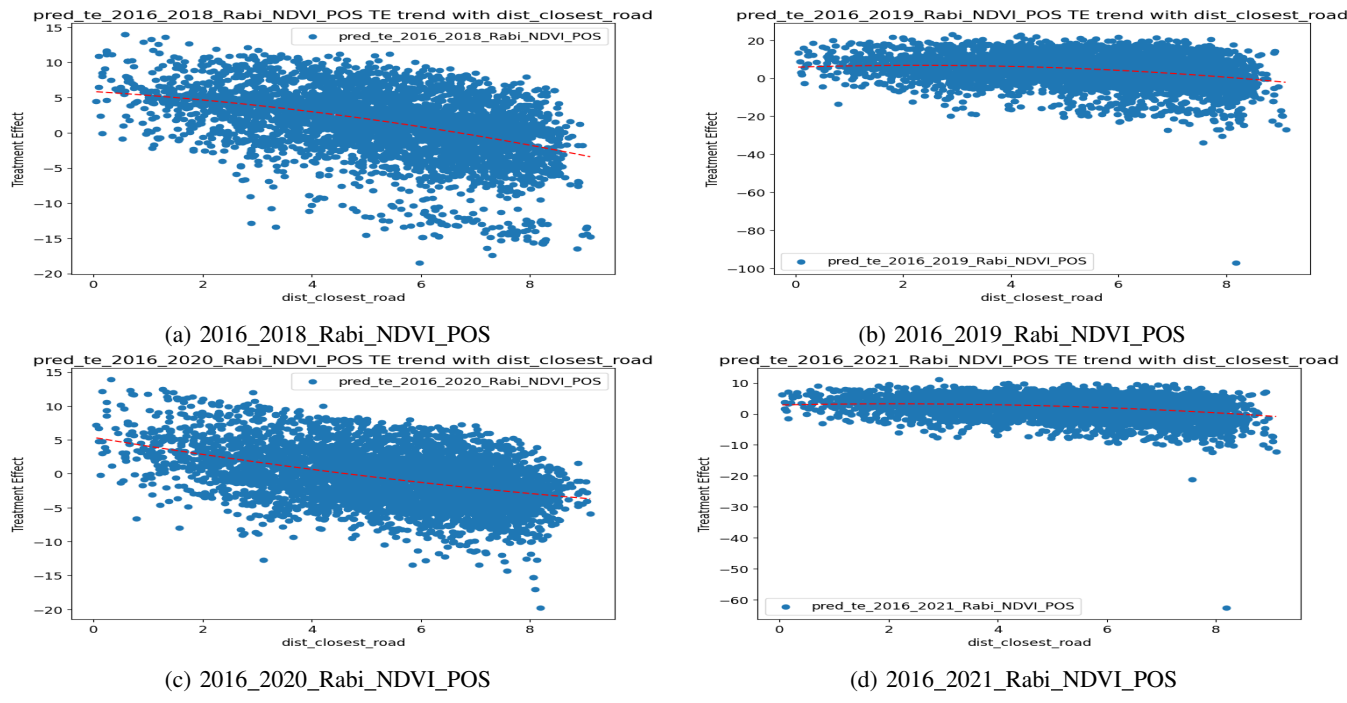


Figure 115: Trend of treatment effect (from DML) on NDVI Rabi wrt covariate dist\_closest\_road

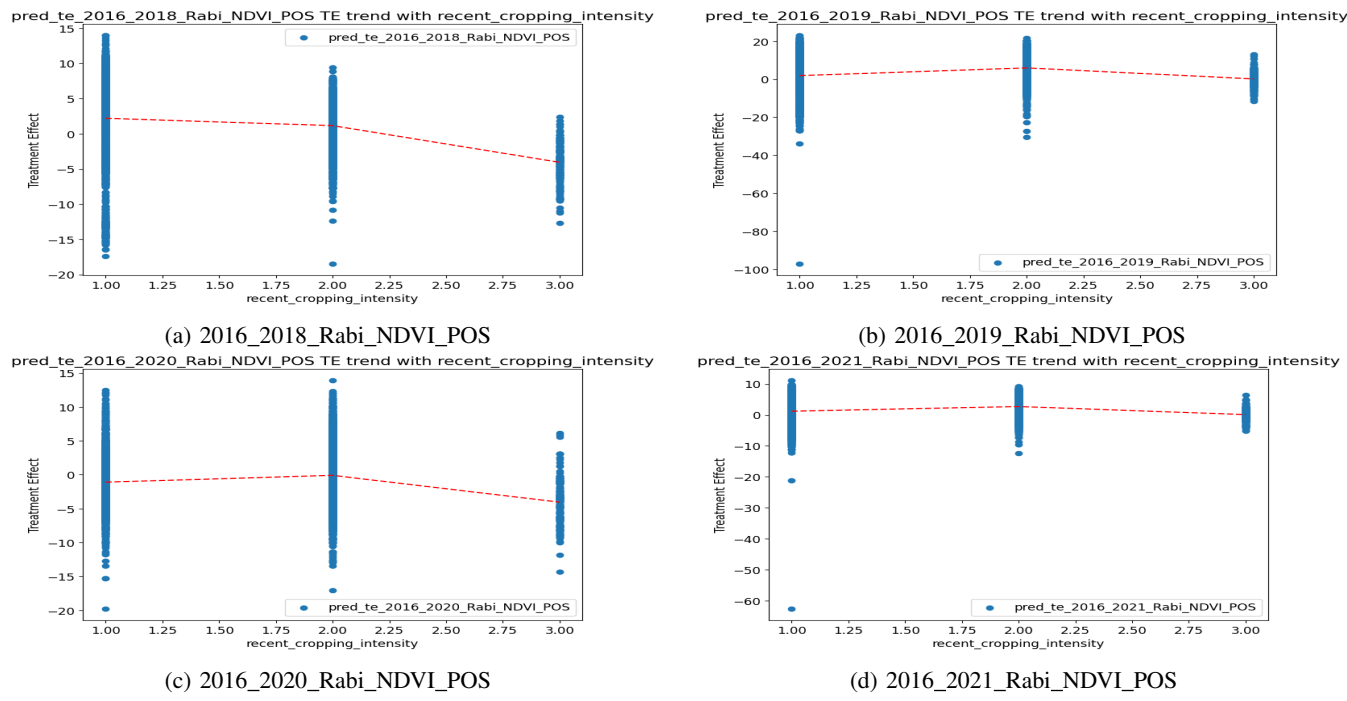


Figure 116: Trend of treatment effect (from DML) on NDVI Rabi wrt covariate recent\_cropping\_intensity

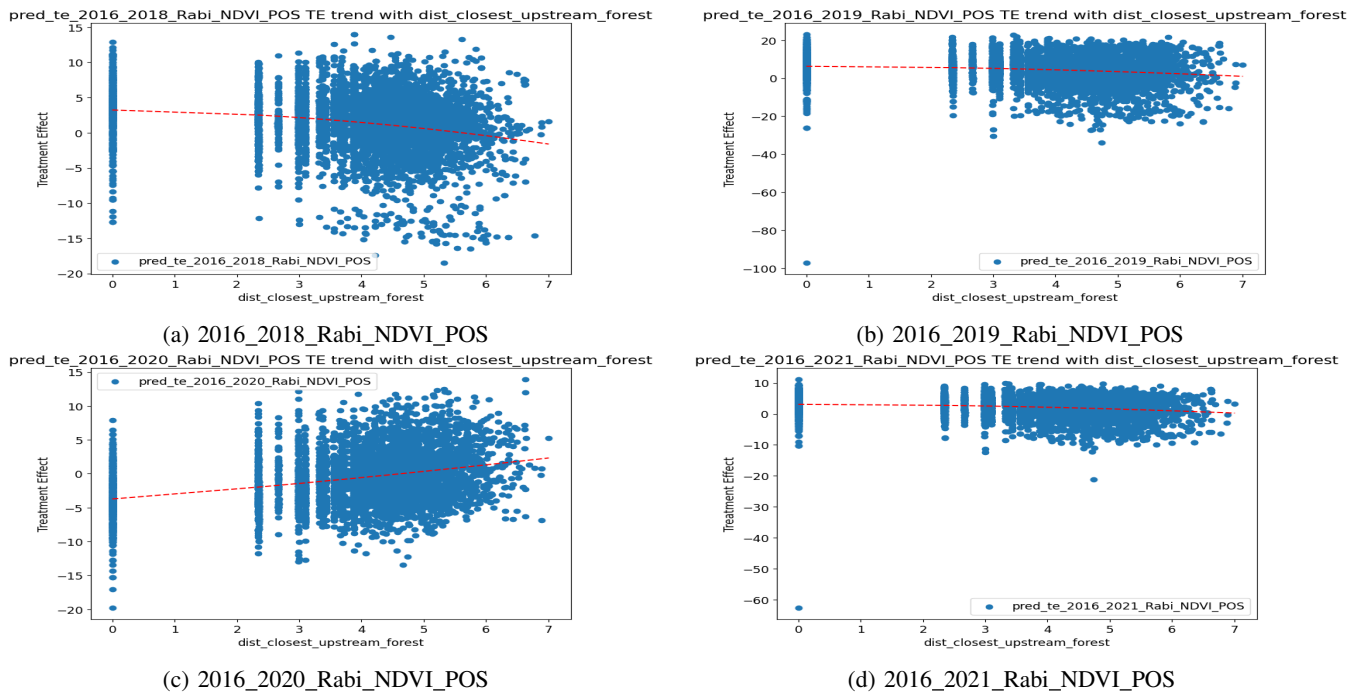


Figure 117: Trend of treatment effect (from DML) on NDVI Rabi wrt covariate dist\_closest\_upstream\_forest

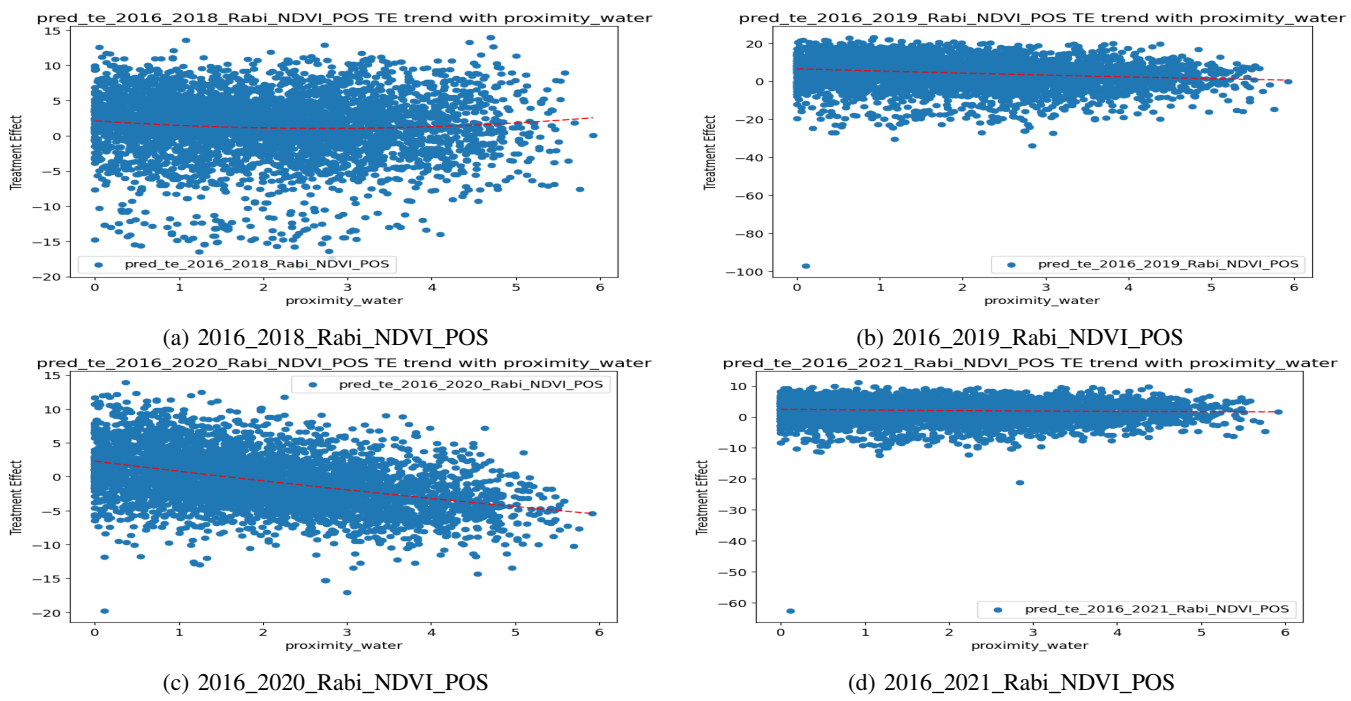


Figure 118: Trend of treatment effect (from DML) on NDVI Rabi wrt covariate proximity\_water

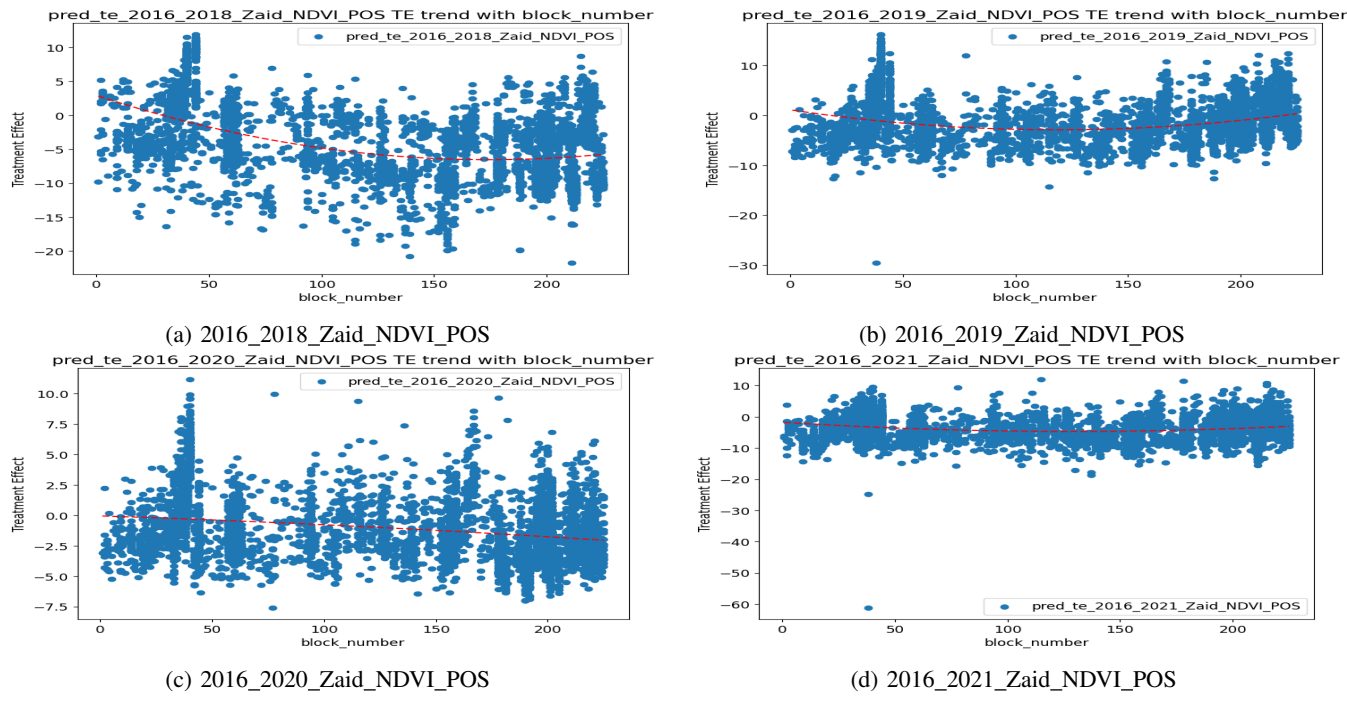


Figure 119: Trend of treatment effect (from DML) on NDVI Zaid wrt covariate block\_number

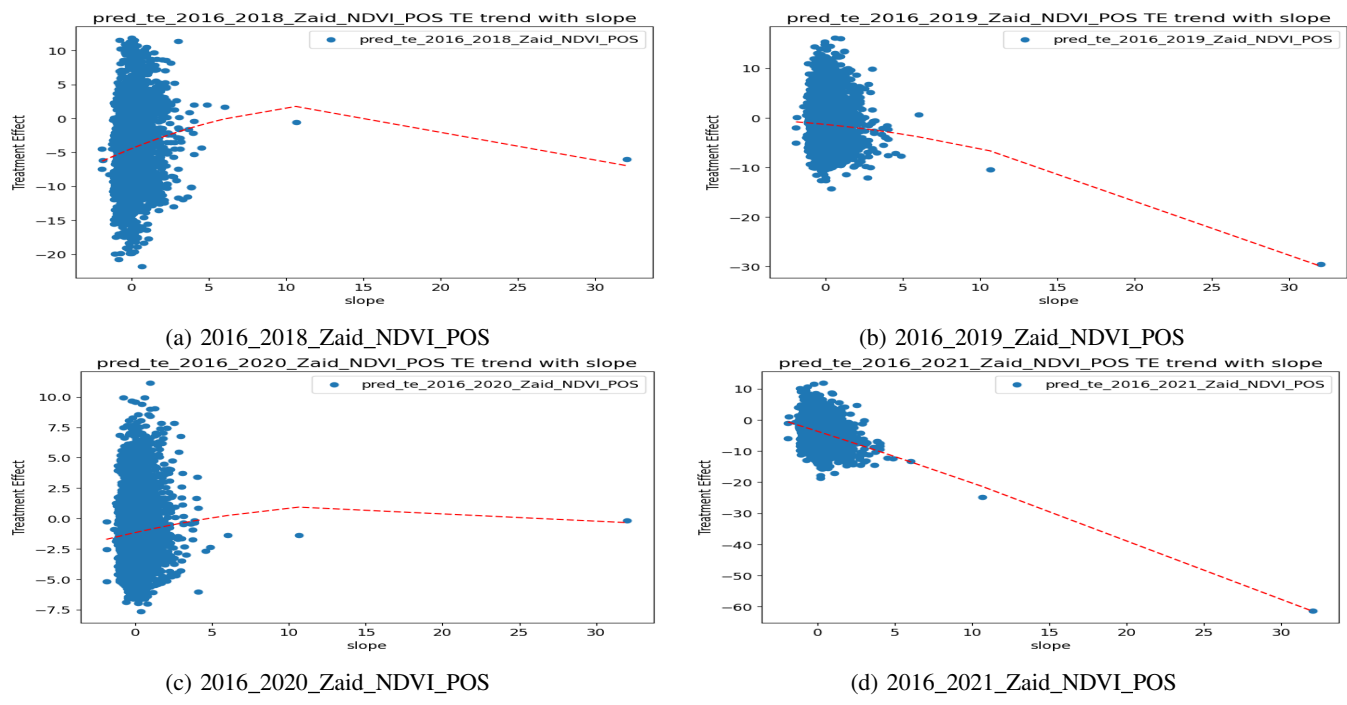


Figure 120: Trend of treatment effect (from DML) on NDVI Zaid wrt covariate slope

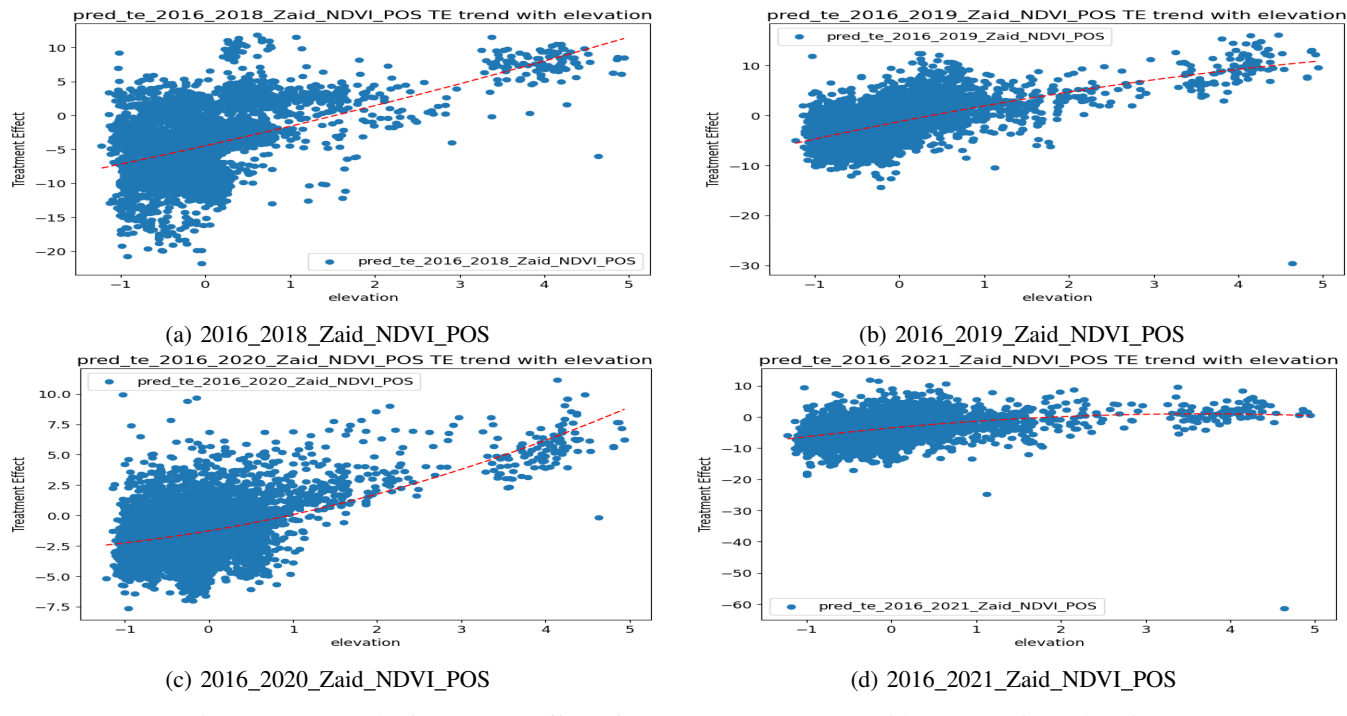


Figure 121: Trend of treatment effect (from DML) on NDVI Zaid wrt covariate elevation

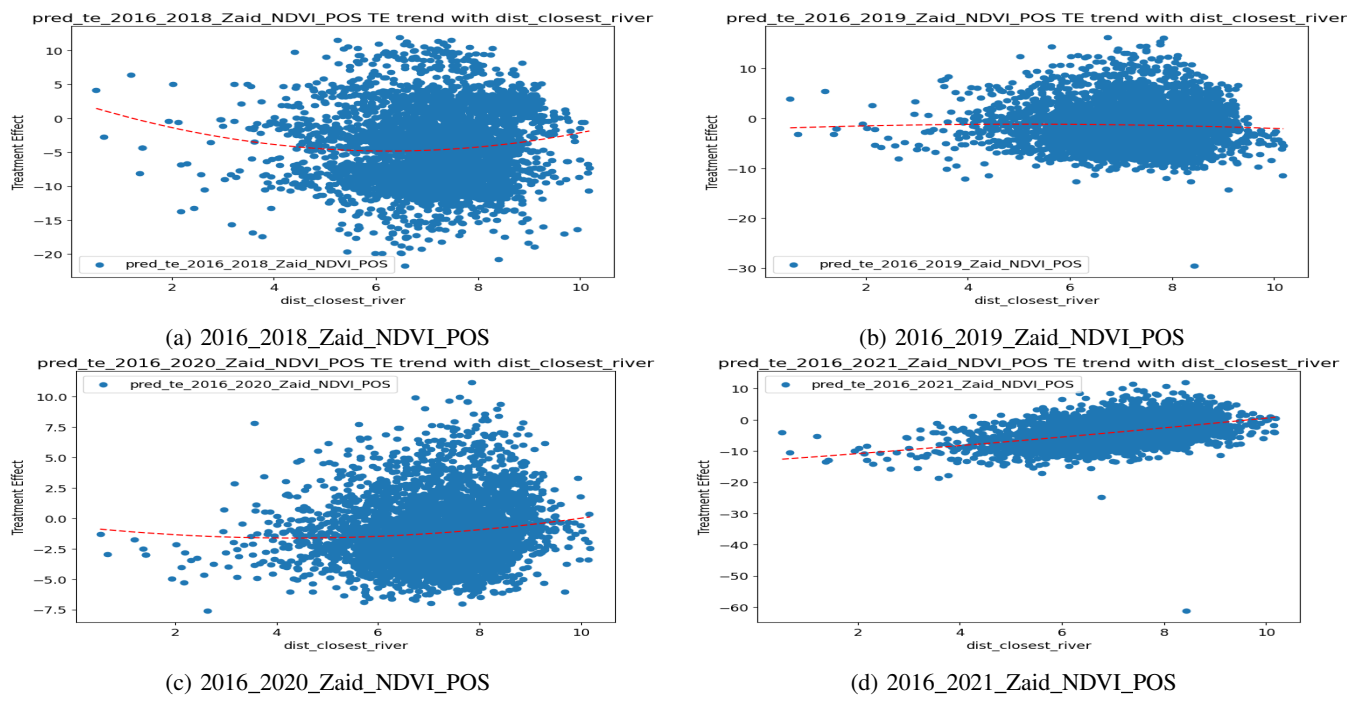


Figure 122: Trend of treatment effect (from DML) on NDVI Zaid wrt covariate dist\_closest\_river

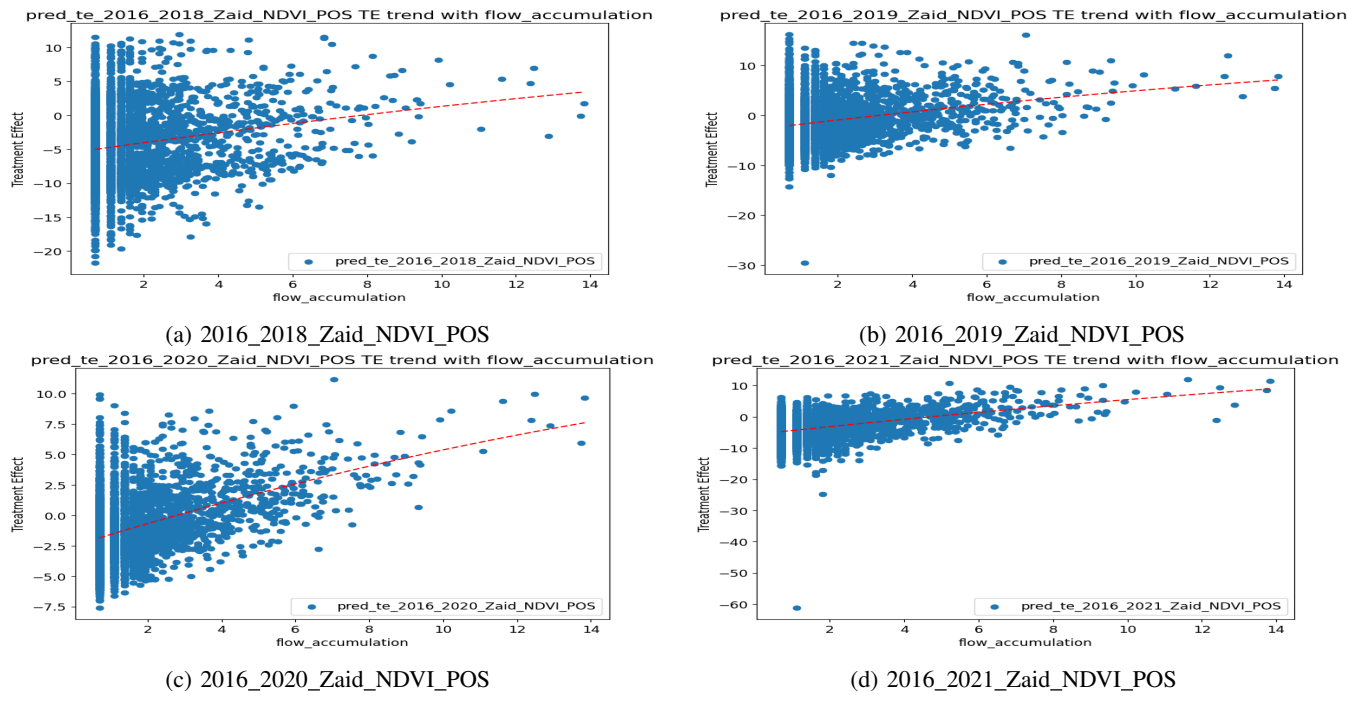


Figure 123: Trend of treatment effect (from DML) on NDVI Zaid wrt covariate flow\_accumulation

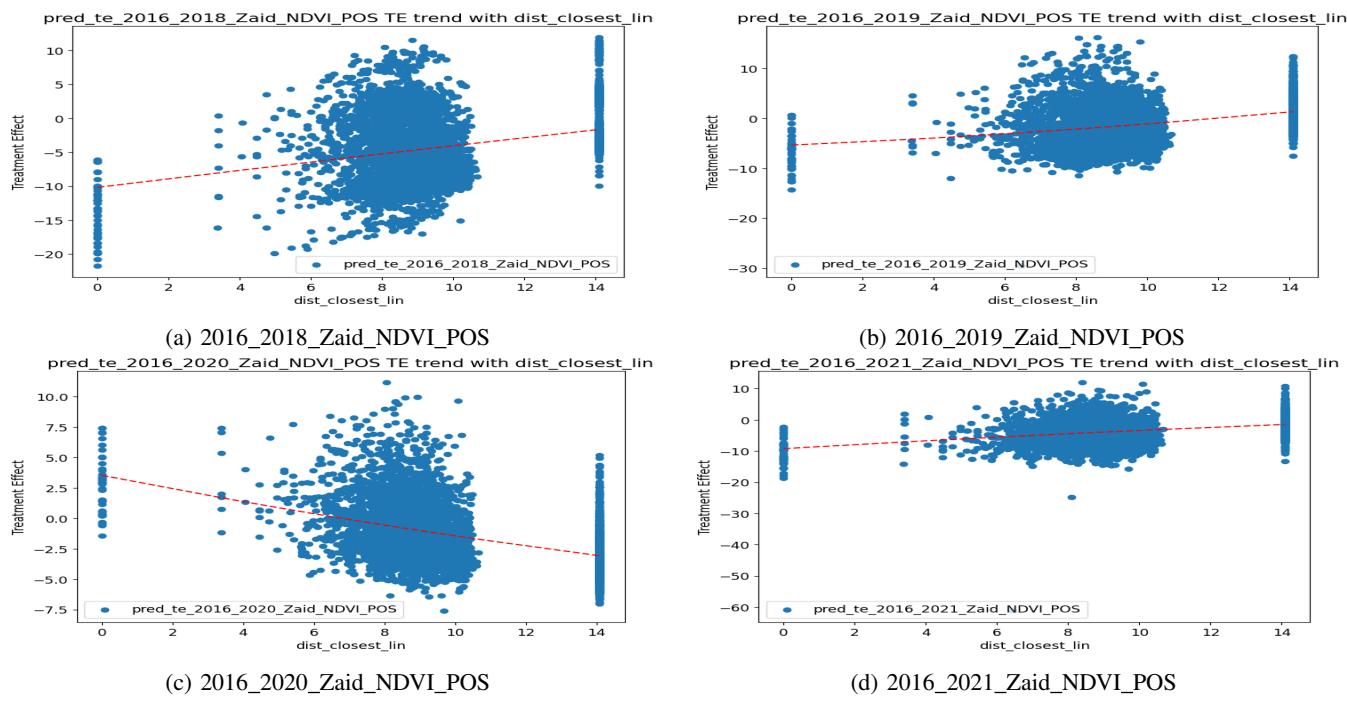


Figure 124: Trend of treatment effect (from DML) on NDVI Zaid wrt covariate dist\_closest\_lin

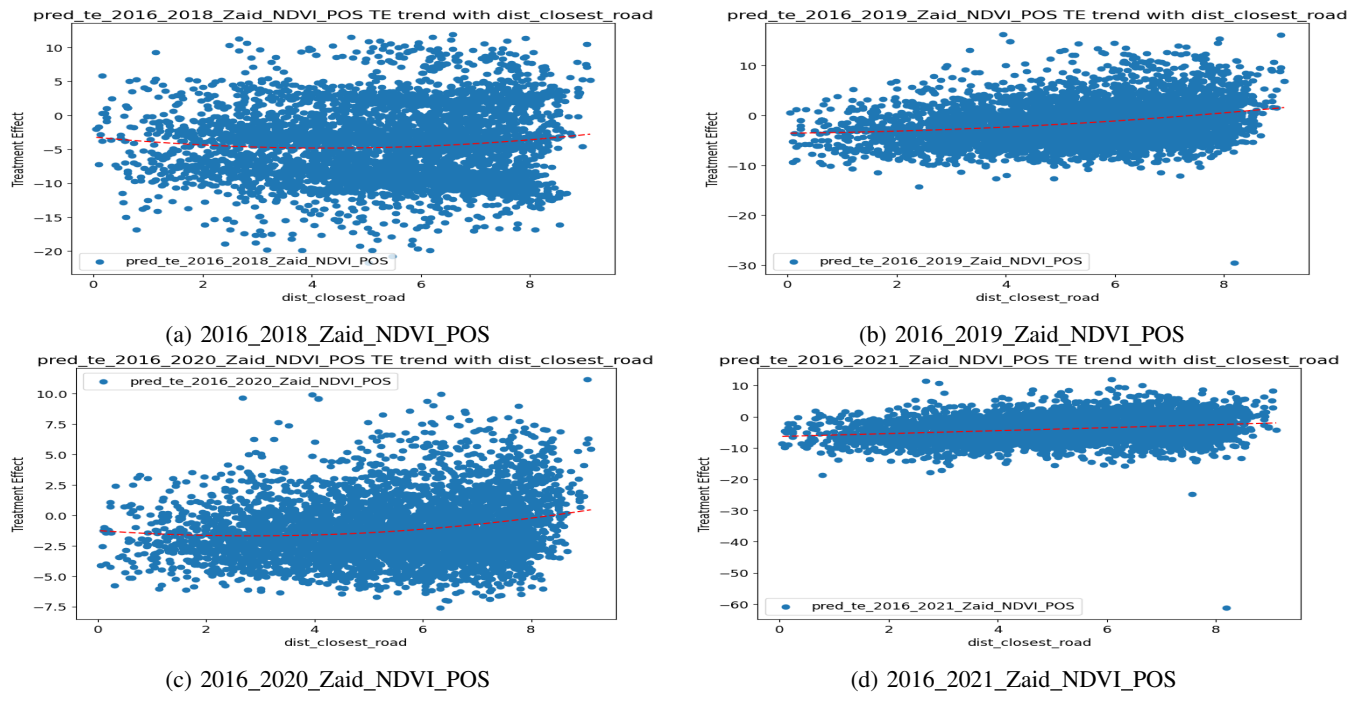


Figure 125: Trend of treatment effect (from DML) on NDVI Zaid wrt covariate dist\_closest\_road

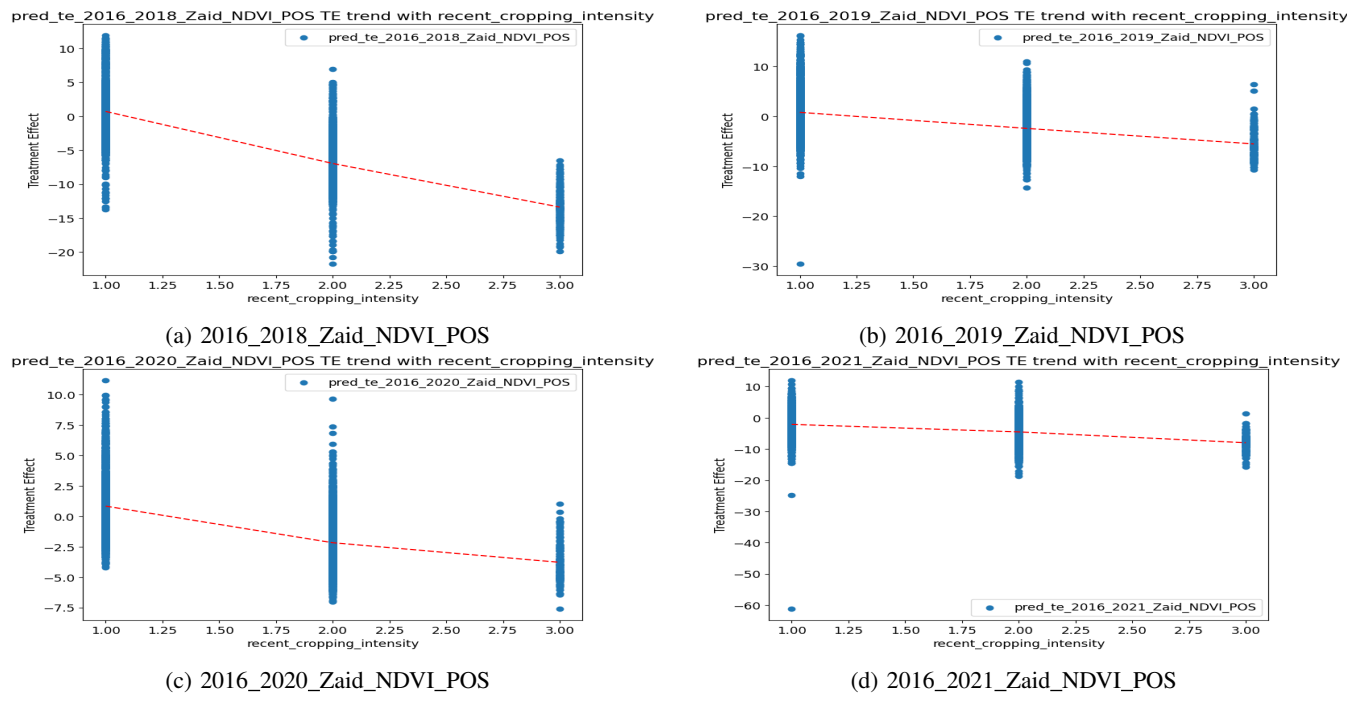


Figure 126: Trend of treatment effect (from DML) on NDVI Zaid wrt covariate recent\_cropping\_intensity

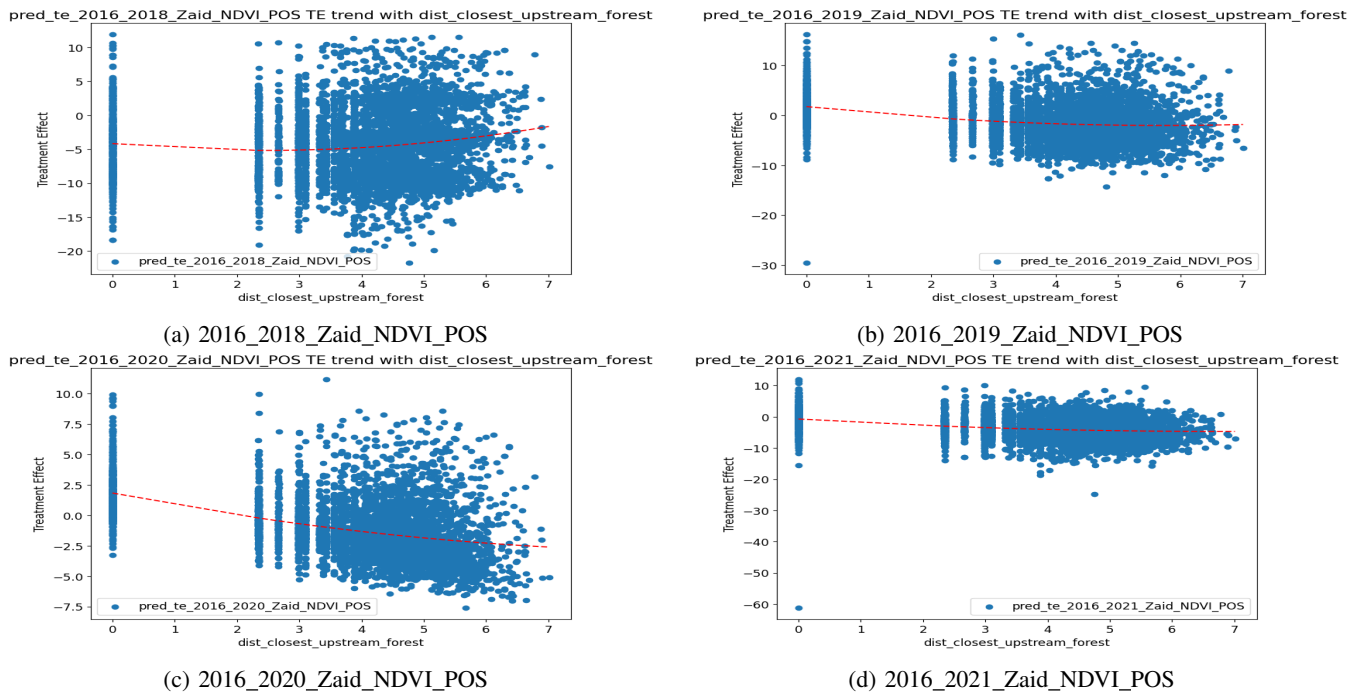


Figure 127: Trend of treatment effect (from DML) on NDVI Zaid wrt covariate dist\_closest\_upstream\_forest

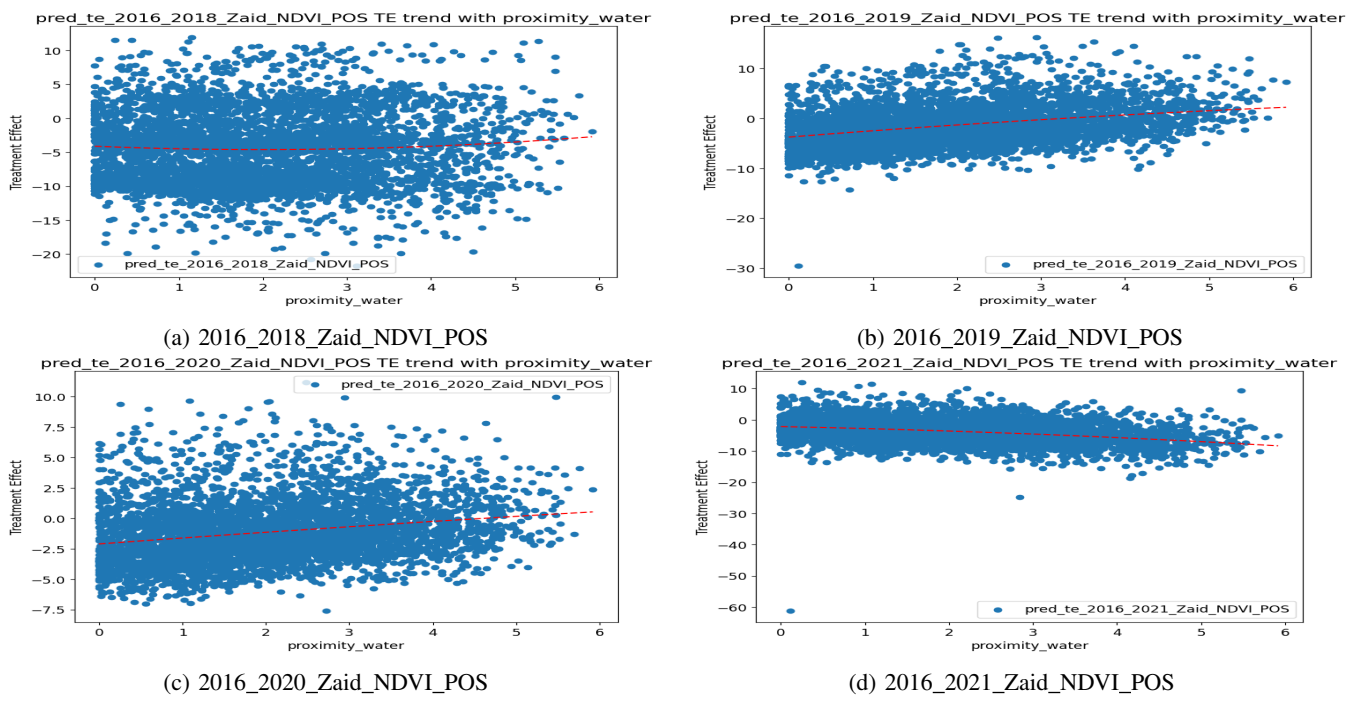


Figure 128: Trend of treatment effect (from DML) on NDVI Zaid wrt covariate proximity\_water